MATHEMATICAL MODELING OF MUTATION ACQUISITION IN HIERARCHICAL TISSUES: QUANTIFICATION OF THE CANCER STEM CELL HYPOTHESIS

by

Sara N. Gentry

A dissertation submitted in partial fulfillment
of the requirements for the degree of
Doctor of Philosophy
(Applied and Interdisciplinary Mathematics)
in The University of Michigan
2008

Doctoral Committee:

Associate Professor Trachette L. Jackson, Co-Chair
Professor Sean Morrison, Co-Chair
Professor Smadar Karni
Assistant Professor Patrick W. Nelson

ACKNOWLEDGEMENTS

I would like to thank my committee members Trachette Jackson, Sean Morrsion, Smadar Karni, and Patrick Nelson for their valuable counsel and efforts on my behalf, collaborator Rina Ashkenazi, Victoria Booth, and my professors at the University of Michigan and Washington and Lee University. I thank the people of Living Water and my friends and family for their encouragement, support, and prayers. Thank you, Brian and Mom, for helping me to stay the course and thank you, Lord, for the grace to see the finish.

TABLE OF CONTENTS

LIST OF FIGURES

Figure

LIST OF TABLES

Table

CHAPTER I

Introduction

Cancer is a disease caused by the accumulation of phenotype-altering genetic mutations in somatic cells. Malignancies exhibit different characteristics based on the specific types of mutations they have acquired, but there are commonalities found in most forms of cancer. In particular, deregulation of cell proliferation, evasion of programmed cell death, independence of growth or control signals, and increased genetic instability endow a fitness advantage in cancer cells over their normal counterparts, resulting in tumor formation.

Due to various regulatory mechanisms that preserve genomic integrity, the rate at which genetic mutations arise is very low. Furthermore, it is believed that a single mutation is not sufficient to initiate malignant growth, and thus the probability of acquiring enough mutations to initiate tumorigenesis is small. Mammalian tissues are organized in a hierarchical structure of stem, progenitor, and differentiated cells that is believed to offer additional protection against cancer. Stem cells are a small percentage of tissue cells and are long-lived with substantial proliferative potential. They often have the ability to generate all of the other cells in the tissue. In contrast, progenitors mature and lose proliferative capability as they divide, and eventually form differentiated cells that are generally short-lived and compose the majority of

the tissue. Consequently, it has been suggested stem and early progenitor cells are the only tissue cells that persist long enough to accumulate enough mutations to initiate malignancy.

Just as not every cell is capable of dividing, not all tumor cells have an equal capacity for forming new tumors. Tumor-initiating cells have qualities similar to those of stem cells, including longevity and the ability to self-renew or differentiate, albeit abnormally. Due to these parallels, tumor-initiating cells are called cancer stem cells. Cancer stem cells form as the result of mutation accumulation in stem cells or in progenitors or differentiated cells that have acquired the ability to self-renew. The cancer stem cell hypothesis suggests this population generates mutated progeny and drives tumor growth, meaning that their eradication is required to cure cancer.

In order to characterize cancer stem cells, it is necessary to know what mutations deregulate normal cell behavior. Much research has focused on identifying specific genetic transformations that initiate particular types of cancer in order to better understand the causes and driving mechanisms of these tumors. Some mutations are disease-specific, for example, the BCR-ABL fusion gene found in Chronic Myelogenous Leukemia, while others, such as the tumor suppressor, p53, have been detected in a wide variety of malignancies. In addition, investigation seeks to determine the order in which mutations are acquired, because this may influence tumor growth dynamics.

There are several challenges in cancer research, and mathematical modeling may be helpful in addressing issues that are difficult to conclude experimentally. The goal of this dissertation is to address, with the assistance of mathematical modeling, several unanswered questions surrounding the cancer stem cell hypothesis. In partic-

ular, focus is directed towards (1) investigating the sequential order of mutations that causes the most rapid tumor initiation in hierarchical tissues, (2) identifying which cellular mechanisms instigate aggressive malignancies when deregulated, and (3) examining tumor heterogeneity and composition, with specific attention to the cancer stem cell population. This will be accomplished by developing a maturity-structured mathematical model of mutation acquisition in hiearchical tissue.

Pertinent biological background information is presented in Chapter II to familiarize the reader with the biology. Specifically, hierarchical tissue, cancer stem cells, and the pathology of Chronic Myelogenous Leukemia are discussed. Chapter III reviews previously developed mathematical models that were used to simulate tissue of both normal homeostasis and cancer. In addition to highlighting the insightful conclusions derived from these models, attention is drawn to the lack of cancer models that explicitly incorporate the maturity structure of hierarchical tissue, which motivates this dissertation.

In Chapter IV, a maturity-structured model is developed and used to examine mutation acquisition in hierarchical tissue. This model has many novel features that have not previously been integrated. For instance, symmetric self-renewal, asymmetric self-renewal, and symmetric differentiation divisions are incorporated, enabling investigation of the effects on tissue homeostasis due to imbalance of the stem-cell division pattern. In addition, sequential acquisition of genetic mutations in stem, progenitor, and differentiated cells is explored. Evolving tumor composition is discussed, and the significance of genetic instability and increased symmetric self-renewal are emphasized.

Various factors influence the pattern of stem-cell division but these are not incorporated in the modeling in Chapter IV. In Chapter V, an ordinary differential

equations model is presented that incorporates regulatory mechanisms governing stem-cell division and quiescence. The model is used to simulate tissue generation and achieve homeostasis. A sensitivity analysis is conducted in Chapter VI to determine which model parameters impart the most effect on healthy tissue formation and equilibrium. Specifically, the analysis suggests that tissue equilibrium is most altered due to increased stem-cell proliferation, decreased stem-cell apoptosis, and increased symmetric self-renewal.

Chapter VII explores the deregulation of stem-cell governing mechanisms as a result of mutation acquisition. In particular, mutations increasing symmetric self-renewal in stem cells are found to cause the most aggressive forms of cancer. Furthermore, it is demonstrated that regulatory mechanisms prevent significant expansion of stem cells, but complete loss of governance can result in exponential growth.

Finally, in Chapter VIII, all of the model features from previous chapters are incorporated into one comprehensive framework. Specifically, a maturity-structured model of hierarchical tissue that incorporates stem-cell regulatory mechanisms is used to investigate mutation acquisition initiating cancer. The model structure is general enough to simulate tumorigenesis in various tissues, but as an example, the dynamics of Chronic Myelogenous Leukemia are simulated to demonstrate the model's capabilities. To conclude, the relevance and significant contributions of this modeling approach are discussed in Chapter IX, and future investigations are proposed.

CHAPTER II

Biological Background

This year, the National Cancer Institute estimates that nearly one-and-a-half million Americans will be diagnosed with cancer [93]. Although medical advances have prolonged patient survival, cures remain elusive for many forms of cancer when surgery is not enough, resulting in approximately half a million American deaths a year [93]. Based on trends established in the last five years, forty percent of people born today will develop some form of cancer in their lifetime [93]. The rate of mortality in combination with the rate of incidence makes cancer a deadly disease that affects the entire population. As a result, much research has been devoted to understanding the causes of cancer in order to develop new therapeutic treatment strategies.

The cancer stem cell hypothesis proposes that a small subpopulation of mutated cells drives malignant growth [110]. These tumor-initiating cells are called cancer stem cells because they share similar qualities with normal somatic stem cells, in particular, the ability to self-renew. Furthermore, cancer stem cells are sometimes more resistant to current methods of treatment, and their survival promotes malignant regeneration and prevents complete eradication of the tumor. In this chapter, biological background information is presented pertaining to cancer stem cells and

their contribution towards cancer development in hierarchically structured tissues.

2.1 Hierarchical Tissue Structure

Mammalian tissues are complex and composed of heterogeneous cell populations that differ in functional abilities as well as state of maturation. In many human tissues, rare and immature stem cells have been identified that are ultimately responsible for generating all tissue cells [4, 98]. Stem cells proliferate and differentiate to form progenitor cells, which are slightly more mature than stem cells. Progenitors are not fully differentiated, but they expand through several rounds of cell division and become more differentiated as they divide. When all rounds of division are completed, terminal differentiation ensures that cells reach full maturity, after which they are generally incapable of additional proliferation. Tissues often consist of several types of differentiated cells; each is necessary to perform specialized tasks. Many human tissues are formed and maintained through this hierarchical structure in which stem cells give rise to progenitor cells, which in turn give rise to differentiated cells [4].

Stem cells have several characteristics that make them unique. First, because they are naïve and multipotent, stem cells are capable of forming progeny of various lineages [63]. In contrast, as non-stem cells divide, they also become more differentiated and committed in lineage. Second, stem cells are rare within a tissue [4, 110]. Third, stem cells may enter long periods of quiescence between divisions [39, 79, 89, 104]. While it is true that a few types of differentiated cells, such as lymphocytes, can remain quiescent for an extended time between divisions, most progenitor and differentiated cells do not have a significant G_0 phase while retaining the ability to divide intermittently [61]. Fourth, stem cells have the ability to self-renew, which means that they can form daughter cells that are also stem cells [4, 110]. When non-

stem cells divide, they lose some of their proliferative potential and become more differentiated, but self-renewal allows daughter cells to retain stemness. It is this final quality that allows stem cells to live longer than other types of cells without exhausting their proliferative potential or depleting the stem-cell pool.

2.1.1 Stem-Cell Division

Stem cells are capable of both self-renewal and differentiation, which they accomplish through three different types of cell division. In a symmetric self-renewal division, the two daughter cells are also stem cells, which increases the stem-cell pool by one. Asymmetric division creates one daughter stem cell and one daughter progenitor cell that is fated to differentiate, which does not change the stem-cell pool, but increases the progenitor pool by one. Symmetric commitment occurs when both daughter cells are progenitors, which depletes the stem-cell pool by one and increases the progenitor pool by two. The three outcomes of stem cell division are depicted in Figure 2.1. In order to regulate tissue homeostasis, a balance of divisions and stem-cell apoptosis is necessary to maintain a constant number of stem cells while also generating progenitor cells [34].

Although all three types of division have been observed in various experimental settings, it is unknown which types of division occur in human tissues *in vivo* [97, 107, 125]. It is believed that stem cells possess the mechanisms to permit both symmetric and asymmetric divisions, and can switch division type based on the demands of the tissue [89, 104]. For instance, in time of injury or tissue generation, symmetric self-renewal expands the stem-cell pool to speed cell production [89]. Some hypothesize that under homeostatic conditions, asymmetric divisions occur in order to preserve stem cell numbers, but a healthy steady state could also be maintained through balanced symmetric self-renewal and differentiation divisions [34, 89].

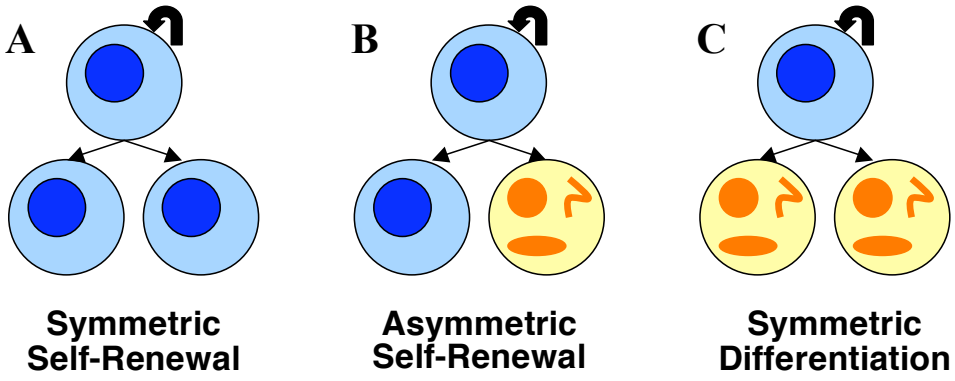

Figure 2.1: **Stem cells are capable of three kinds of division.** Stem cells may symmetrically self-renew to form two daughter stem cells (A), asymmetrically self-renew to form one stem cell and one progenitor cell (B), or symmetrically differentiate to form two progenitor cells (C).

The immortal strand hypothesis suggests that stem cells have internal mechanisms that asymmetrically cosegregate chromosomes at division ensuring the production of one stem cell and one progenitor cell [81, 107]. According to this hypothesis, the same set of chromosomes is always passed on to daughter stem cells, while the newly synthesized set is passed on to daughter progenitor cells. Thus, the immortal strand is a mechanism that assists stem cells in maintaining genetic integrity and avoiding mutation during DNA replication. Chromosomal cosegregation has been reported in a variety of mammalian adult stem cells, but experimental evidence demonstrates that murine hematopoietic stem cells do not asymmetrically segregate chromosomes [25, 64, 65, 106, 114, 115]. This finding suggests that chromosomal cosegregation is not a characteristic of all stem cells and cannot be used as a method of identifying and isolating stem cells within a tissue.

2.1.2 The Stem-Cell Niche

Because stem cells are rare and need to replenish tissue cells, they reside in niches that both protect and regulate [42]. Niches have been identified in various tissues,

including bone marrow, colon, testes, skin, hair follicle, and brain [42, 63, 97]. The stem-cell niche is defined as the microenvironment of supporting cells and chemical signals that regulates stem-cell maintenance and function [76, 97, 126]. It is believed that the niche plays a crucial role in maintaining stem-cell qualities and regulating the proliferation and differentiation of stem cells [42].

Physical interactions between stem cells and supporting cells in the niche are an important aspect of niche control [42, 97]. Adherens junctions, integrins, and contact with the extracellular matrix have all been implicated in rooting stem cells in the niche [42, 97]. Because stem cells are usually in a quiescent state, it is thought that signals in the niche inhibit differentiation [42]. Thus when a stem cell loses interaction with the niche, it may lose its stem cell characteristics and differentiate. In addition, the stem-cell niche may promote asymmetric divisions as a means of mediating homeostasis [75].

Not only are stem cells difficult to isolate from mammalian tissues, but the inability to artificially reconstruct the stem-cell niche is an additional obstacle preventing long term observation of stem cells *in vitro* [75, 95]. Consequently, it is evident that the stem-cell niche provides necessary signals to support stem cells. As more is discovered about the stem cell niche, it may be possible to more successfully observe stem cells *in vitro*, which would foster additional understanding. Furthermore, knowledge of the niche may also assist investigation regarding abnormal growth or degeneration of hierarchically structured tissues [75].

2.1.3 The Hematopoietic System

Hematopoietic stem, progenitor, and differentiated cells compose what is arguably the most understood hierarchical system. Due to the availability of data regarding blood cell production, this dissertation uses the hematopoietic system to model hi-

erarchical tissue, both in normal and cancerous situations. In order to further understand characteristics of hematopoiesis, detailed information of the hematopoietic system is now presented. Particular attention is given to cells of the granulocyte lineage as aberrant white blood cell production contributing to leukemia is discussed in Section 2.3.

Hematopoietic stem cells are responsible for generating various cell types that circulate in the blood and lymph. Differentiation of hematopoietic stem cells produces progenitor cells of either the myeloid or lymphoid lineages. Myeloid progenitors are precursors for erythrocytes, macrophages, platelets, and granulocytes, which include neutrophils, eosinophils, and basophils. Lymphoid progenitors are precursors for lymphocytes, including the T-cells and B-cells that are necessary for adaptive immunity [61, 99]. A schematic of the hierarchy of hematopoietic cells is shown in Figure 2.2.

In accordance with other types of hierarchical tissue, hematopoietic stem cells are a very small percentage of all hematopoietic cells. In murine models, stem cells comprise less than 0.01% of bone marrow cells [35, 32, 68, 80, 94]. It is difficult to purify immature cell populations and isolate stem cells, but several markers have been identified. Human hematopoietic stem cells are enriched in populations with the phenotype of $CD34^+$, $CD38^-$, Lin^-, where Lin refers to a collection of "lineage markers" that can be used to exclude differentiated cells [94]. Recently, it was demonstrated that SLAM family receptors CD150, CD244, and CD48 could be used to isolate stem and progenitor cells. Hematopoietic stem cells are purified in the population expressing $CD150^+$ $CD244^-$ $CD48^-$, transiently reconstituting multipotent myeloid progenitors express $CD244^+$ $CD150^-$ $CD48^-$, and more committed progenitors express $CD48^+$ $CD244^+$ $CD150^-$ [68]. Even with the most current isolation

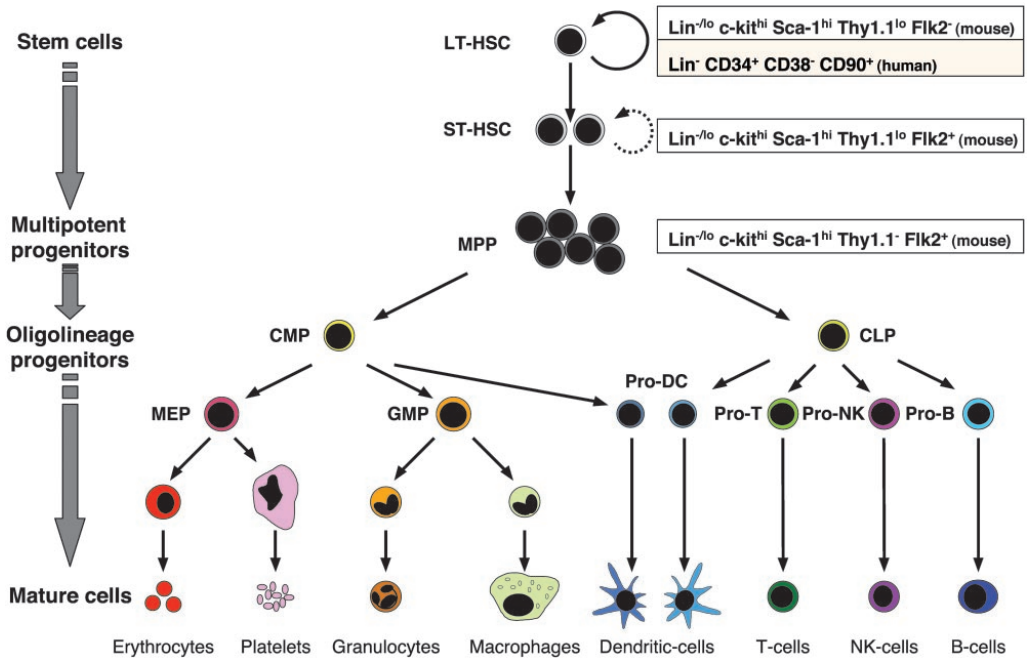

Figure 2.2: **Hierarchical structure of the hematopoietic system.** Hematopoietic stem cells form common myeloid and lymphoid progenitors, which in turn produce cells of the myeloid and lymphoid lineages. Figure from [103].

techniques, less than 50% of cells labeled as stem cells yield long-term reconstitution when transplanted into irradiated mice, implying that additional markers are needed to truly distinguish long-term reconstituting hematopoietic stem cells from the earliest progenitor cells [68].

Although there is a small number circulating in the blood, hematopoietic stem cells mainly reside in the bone marrow, where most of blood cell production takes place [103]. Progenitors expand and continue further maturation in the soft marrow in the inner bone cavity [126]. It is believed that the hard outer bone surface offers protection for immature cells while also creating a pressure gradient that pushes fully differentiated cells into the bloodstream [39, 76]. Once myeloid cells complete terminal differentiation, they no longer proliferate and are released into the blood.

Within the bone marrow, specialized niches maintain and regulate hematopoietic stem cells. It is believed that endosteal and vascular or perivascular cells each have roles in governing stem-cell behavior, as portrayed in Figure 2.3 [66]. The endosteum is the vascularized inner lining of the bone surface, including osteoblasts and osteoclasts that mediate bone formation and remodeling, respectively [66]. Although hematopoietic stem cells home near the endosteal surface, it is uncertain if endosteal cells compose the niche or instead produce signals that influence stem cells nearby [66, 68]. Recently, it was observed that nearly all hematopoietic stem cells reside within five cell diameters of sinusoids, which are specialized areas of the vasculature specially constructed to permit cells to enter the blood [67, 68]. When taken into account with the fact that hematopoietic stem cells can be mobilized quickly, this provides compelling evidence for a vascular niche [66, 72]. Experimental evidence has shown the importance of both endosteal and vascular cells in hematopoiesis, demonstrating the significance of each for blood cell production [39, 87]. Consequently,

it is likely that endosteal and vascular or perivascular cells are each significant in hematopoietic stem cell maintenance, though more detailed information regarding the contributions of these cells is needed [66].

Hematopoietic stem and progenitor cells must have high proliferative potential in order to produce the vast number of differentiated blood cells that are needed daily. The estimated blood cell daily turnover in humans includes approximately one hundred billion granulocytes, two hundred billion erythrocytes, and one hundred and fifty billion platelets [39, 78]. Most of the cell population expansion takes place in the progenitor pool, which proliferates rapidly [109]. In contrast, hematopoietic stem cells cycle less frequently, and the vast majority are in the G_0 quiescent phase [89]. In fact, approximately 70-90% of hematopoietic stem cells are quiescent at any one time [21, 39, 104]. In mice, 99% of hematopoietic stem cells have divided within 57 days [21]. Although the average division rate has not been explicitly experimentally observed in humans, it has been hypothesized that cells divide may even divide more infrequently in larger mammals, with a human hematopoietic stem cell cycling once every 25-50 weeks, on average [1, 113].

Several factors influence hematopoietic stem cell proliferation and mediate the balance between quiescence, self-renewal and differentiation. It is believed that these decisions are regulated through extrinsic and intrinsic signals, though the participating mechanisms are not fully understood [98, 108, 125]. For example, it is hypothesized that osteoblasts secrete factors that maintain quiescence, namely angiopoietin and thromboipoietin, while other factors, such as CXCL12, promote migration and localization in the bone marrow [66]. The Bmi-1, Wnt, and Sonic hedgehog (Shh) signaling pathways are involved in self-renewal [4, 57, 62, 63, 97, 108, 123]. Wnt-signaling promotes self-renewal of hematopoietic stem cells, may encourage quies-

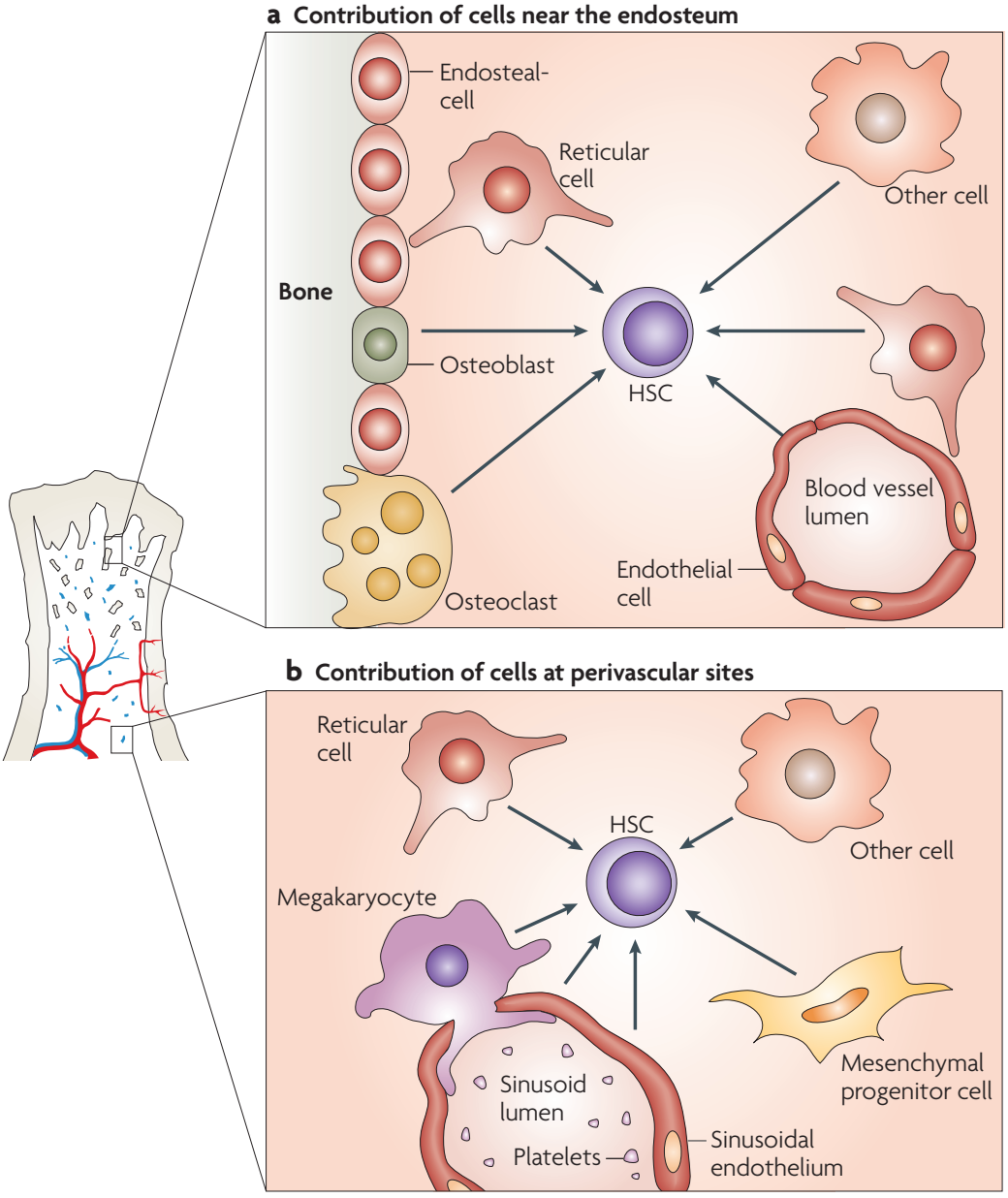

Figure 2.3: **Hematopoietic stem cell niches in bone marrow.** Hematopoietic stem cells are governed by endosteal and vascular or perivascular cells in the bone marrow. Figure from [66].

cence, and influences cell fate decisions during development [42, 63, 87, 94, 98, 110]. In addition to chemical signals influencing stem-cell division, it is hypothesized that cell-to-cell interaction and location within the niche may determine the mode of stem-cell division as the niche size dictates the size of the stem-cell pool that can be supported [33, 42, 76, 87, 97, 108]. Clearly, there are many influences governing stem-cell proliferation, many of which are not yet fully understood; however, new discoveries continue to be made.

The hematopoietic system is just one example of hiearchically structured tissue in the human body. Composed of hematopoietic stem cells, common myeloid and lymphoid progenitors, and a variety of differentiated cell types, hematopoiesis is a prime example of differentiated cell production that originates from the same population of pluripotent precursors. Hematopoietic stem cells are the most studied mammalian adult stem cells simply because of their accessibility. With new scientific advances in experimental techniques, adult stem cells in other tissues are now being studied in greater detail. Even though much has been learned, there are still many unknown characteristics of adult stem cells. In particular, understanding the mechanisms governing stem-cell self-renewal and differentiation may shed light on abnormalities in tissue regulation and maintenance.

2.2 Cancer Stem Cells

Cancer is a disease in which accumulated genetic mutations alter normal cellular characteristics. It is thought that three to ten genetic mutations are required to malignantly transform a cell [10, 50]. Although specific mutations vary from one cancer to another, there are commonalities in the types of genes they affect. In their review of cancer cells, Hanahan and Weinberg cite six characteristics that promote

aberrant growth: self-sufficiency in growth signals, insensitivity to antigrowth signals, evasion of apoptosis, limitless replicative potential, promotion of angiogenesis, and tissue invasion causing metastasis [50]. Ultimately, malignant growth requires a combination of mutations that gain cellular function in addition to those that remove tumor suppression [50].

Hierarchical tissues are not uniform in cellular composition, hence it is not surprising that the tumors arising in them are heterogeneous as well. Most notably, not all tumor cells are capable of initiating tumorigenesis [4, 12, 54, 57, 102, 110]. Tumor-initiating cells actually possess many of the same qualities as stem cells, including the ability to self-renew and differentiate into diverse cell types, significant replicative potential, and longevity [102, 110, 123]. The noted similarities between tumor-initiating cells and stem cells has led to their labeling as cancer stem cells, and the cancer stem cell hypothesis is a model explaining tumorigenesis. This hypothesis states that malignant tumors are initiated and driven by a subpopulation of cancer stem cells that promote unregulated growth [110]. It is uncertain whether or not tumorigenic cells are a small minority in all types of malignancies, and it is possible that the proportion cancer stem cells in the tumor may characterize disease aggressiveness [4].

Sometimes cancer stem cells are mutated stem cells and sometimes they arise from the mutations of progenitor or differentiated cells that have acquired the ability to self-renew extensively [4, 56, 60, 62, 102, 103, 110]. Because stem cells are are long-lived, they have more time to acquire mutations that contribute to transformation into a malignant state [28, 102, 123]. In addition, they already possess internal mechanisms enabling self-renewal and inhibiting apoptosis, so fewer mutations may be needed to initiate malignant growth [110]. In contrast, progenitors cannot limit-

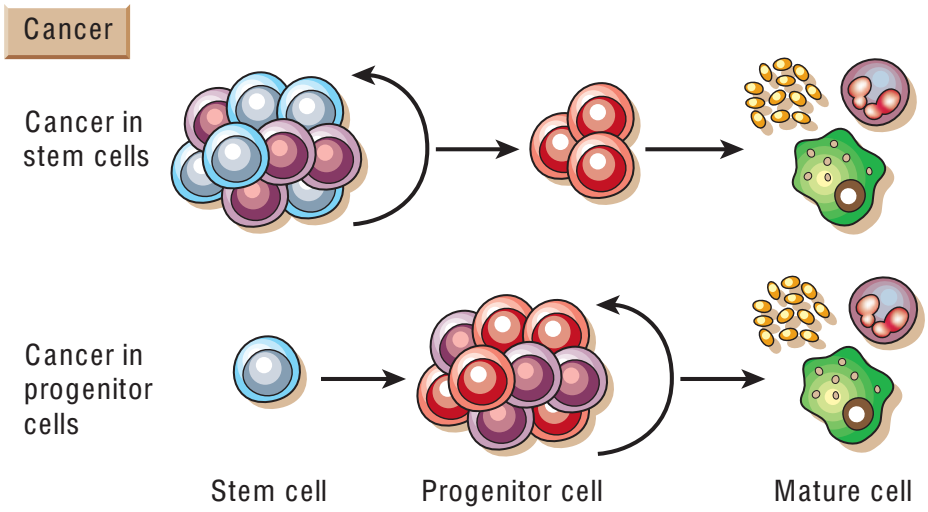

Figure 2.4: **Cellular origin of cancer stem cells.** Cancer stem cells may form as a result of either mutated stem cells or mutated progenitors that acquire the ability to self-renew. Figure from [110].

lessly self-renew even though they have high proliferative potential. Eventually they terminally differentiate and thus do not have the longevity of stem cells. However, if progenitors acquire the ability to self-renew, this permits the accumulation of additional mutations, thereby creating a cancer stem cell population [4, 60, 102, 110]. Another possibility is that some mutations could occur in stem cells that are inherited by progenitor daughter cells and thus predispose these progenitors to transformation [103, 105, 110]. Figure 2.4 schematically shows how tumor growth can be initiated in stem and progenitor cell populations. Cellular origin and order of mutation acquisition likely influence the tempo of disease progression, therefore further investigation of the pathways causing tumorigenesis may provide insight useful in preventing malignant transformation.

Aberrant self-renewal is a key component in the behavior of cancer stem cells. Deregulated pathways governing stem-cell self-renewal, such as Bmi-1, Wnt, and

Shh, contribute to tumorigenesis in various tissues [3, 12, 23, 57, 102]. Mechanisms mediating the balance between symmetric and asymmetric divisions may be potential targets for mutation as well. For example, when the machinery governing asymmetric division is deregulated, symmetrically dividing neuroblasts form tumors while the oncogene NUP98-HOXA9 that favors symmetric self-renewal in hematopoietic cells causes Acute Myelogenous Leukemia [89, 125]. It has been hypothesized that asymmetric divisions may suppress tumors, whereas increased symmetric self-renewal leads to malignancy [89]. Due to the recent findings regarding deregulated self-renewal, more attention has been focused towards understanding how balanced division is controlled.

In considering the important role that the stem-cell niche has in maintaining the homeostasis of stem cells, it is not surprising that alteration in the microenvironment may also contribute to cancer formation. First, it is thought that cancer stem cells become more independent of the niche. They may not rely on environmental cues to self-renew or proliferate and may ignore inhibitory signals [74]. Mutations may also affect receptors and molecules that bind stem cells in the niche, and loss of this control could potentially lead to metastasis [74, 105]. In addition, mutations could affect the supporting cells found in the niche rather than the stem cells themselves, thereby altering stem cell behavior. It has been demonstrated that stromal cells may be manipulated in ways that cause cancer, proving that the niche itself can become tumorigenic [16].

It is important to characterize tumor-initiating cells so that treatment successfully targets them. Unfortunately, cancer stem cells may be more resistant to therapy than other cancer cells. As shown in Figure 2.5, the cancer differentiated cells that compose the bulk of the tumor are eradicated, but cancer stem cells persist, causing

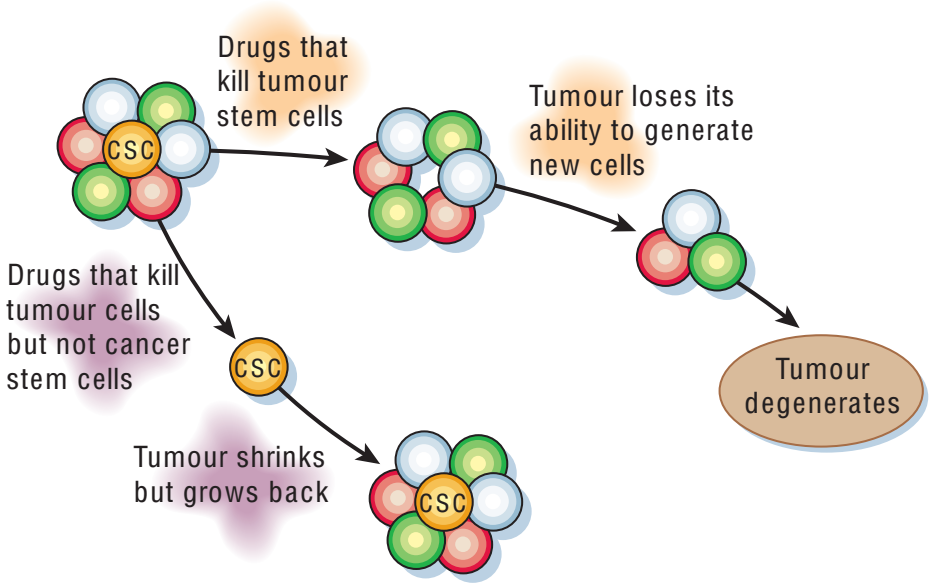

Figure 2.5: **Cancer stem cells must be targeted for disease elimination.** Tumors return when cancer stem cells persist, but are eradicated when cancer stem cells are targeted. Figure from [110].

recurrence of the disease [62, 102, 110, 123]. There are various explanations as to why cancer stem cells may be insensitive to current drug regimens. First, normal stem cells resist drug-induced apoptosis due to multidrug resistant and ATP-binding cassette transporters that pump drugs out of the cell. These could also be present in cancer stem cells [29, 55, 62, 102, 110, 123]. Second, many drugs specifically target cycling cells, but cancer stem cells may have long periods of quiescence, thereby avoiding drug sensitivity [29, 62]. Third, additional mutations may accumulate, causing drug resistance [29, 83]. Unfortunately, treatment strategies that successfully eradicate cancer stem cells may also eliminate healthy stem cells, therefore it is imperative that additional research is conducted to identify potential drug targets unique to cancer stem cells to minimize toxicity to healthy cells.

The cancer stem cell hypothesis provides a new paradigm of tumorigenesis that

accounts for heterogeneity, drug resistance, and relapse. It has reshaped the understanding of cancer and continues to influence how research is conducted. Since the cancer stem cell hypothesis was first introduced, cancer stem cells have been identified in malignancies of the blood, brain, breast, colon, and skin [40, 123]. The next section reviews a specific example of cancer that is driven by leukemic stem cells.

2.3 Chronic Myelogenous Leukemia

Chronic Myelogenous Leukemia (CML) is a form of leukemia caused by hypercellarity of cells of the granulocyte lineage. In 2008, approximately 5,000 new cases of CML will be diagnosed and 450 people will die from the disease in the United States [45, 93]. CML generally manifests in later stages of life with the median diagnosis age ranging from 45-66 years, but it can affect people of all ages [45, 93, 112]. Although it takes a relatively long time to present itself, disease progression is fairly rapid. Patients progress through three stages of disease, starting with a slow-growing chronic phase that turns into an accelerated phase and finally ends in the aggressive blast phase [41, 45, 59, 112, 120]. The whole process is fairly rapid as approximately 50% of patients die within five years of diagnosis, though survival times depend on how early disease is detected and the success of treatment [93].

Symptoms alone are not sufficient to diagnose CML since they resemble those of other diseases including weight loss, fatigue, night sweats, and enlarged spleen [45, 73]. Detection is often the result of a routine blood test due to elevated levels of white blood cells [45]. A cytogenetic analysis concludes if the patient has CML by determining the presence of the BCR-ABL fusion gene, the hallmark identifier of the disease. BCR-ABL alone cannot initiate disease, however, as it has been traced in healthy patients that do not develop CML [22, 47, 57, 60]. The mutations occurring

in CML are discussed in greater detail in Section 2.3.1.

2.3.1 Mutations Causing Chronic Myelogenous Leukemia

The Philadelphia (Ph) chromosome formed by the translocation t(9; 22)(q34; q11) is believed to be the primary source of CML [47, 103]. This mutation creates the fusion gene BCR-ABL that alters cellular kinetics that give the mutated clone growth advantage [47, 60, 119]. Many types of cancers have great variety in the mutations that cause them, but approximately 90-95% of CML patients have the Ph chromosome [41, 59, 103, 112]. Although the World Health Organization uses the Ph chromosome and BCR-ABL to diagnose CML, there are cases that are not Ph-positive, but they express a mutation whose effects are similar to those of BCR-ABL [112, 120].

The BCR-ABL mutation alters several aspects of normal cellular behavior. It inhibits apoptosis through increased survival and independence from signals that negatively regulate growth [27, 47, 48, 112]. BCR-ABL also deregulates proliferation, though there is conflicting evidence as to how this is achieved. *In vitro* data from hematopoietic precursor cells demonstrated that cycling time decreased, thereby increasing the proliferation rate, while other reports argue that leukemic stem cells retain long periods of quiescence and proliferation rates may be unaltered or even slower [48, 62, 122, 125]. Cells expressing BCR-ABL still retain the ability to differentiate, but it is hypothesized that they are able to complete extra rounds of division, increasing the number of progeny they produce and causing hypercellularity [27, 55]. Furthermore, Ph-positive cells are more susceptible to additional mutations, increasing genetic instability [47].

It is believed that CML originates in stem cells but driven by aberrant progenitor expansion [22, 47, 112]. In patients that are Ph-positive, the mutated chromosome

can be detected in stem cells as well as differentiated cells of the granulocytic, monocytic, megakaryocytic, erythroid, and occasionally lymphoid lineages, suggesting that the initial mutation occurs at the stem cell level [47, 59, 103]. It is suggested that the effects of BCR-ABL are not fully manifested in stem cells, but rather progenitors [22]. Consequently, it is likely that the progenitor population that is Ph-positive suppresses normal hematopoiesis because of its competitive growth advantage [41, 48].

The Ph chromosome alone is not sufficient to initiate CML, and additional mutations occur as the disease progresses [22, 57]. The additional expression of the anti-apoptotic protein Bcl-2 has been linked to progression into a more advanced stage [59]. In addition, mutations to tumor suppressor genes, such as p53, may also contribute to malignancy [45, 112, 122]. Deregulation of self-renewal pathways are of particular interest in monitoring the progression from chronic to blast phase. For instance, β-catenin is believed to give granulocytic progenitors self-renewal capabilities, and levels are normal in cells during the chronic phase, but increased in the later accelerated and blast phases [60]. Further investigation may determine which mutations are most significant in promoting malignant transformation.

2.3.2 Three Phases of Disease Progression

Disease progression in CML is classified into three phases: chronic, accelerated, and blast. In the chronic phase, differentiation still occurs, even in mutated cells [60]. As the disease progresses, immature leukemic cells self-renew instead of differentiating, and immature blast cells accumulate [60]. Staging is based on the percentage of immature blasts that are in the blood or bone marrow, as determined by blood tests and bone marrow aspirates. The World Health Organization classification labels the chronic phase when blasts comprise less than 10% of bone marrow or blood. Approximately 85% of diagnoses are during this stage. Accelerated phase is reached

when blasts compose 10-19% of cells. When blasts are 20% of cells, the fatal blast phase is diagnosed [120].

The chronic phase of CML is believed to be initiated by the BCR-ABL mutation. BCR-ABL deregulates cell proliferation and increases survival to cause hypercellularity, particularly in cells of the granulocytic lineage [47, 55, 59, 60]. During the chronic phase, it is thought that the hematopoietic stem cell population remains at levels comparable to those in healthy individuals [60]. In contrast, mutated progenitor and differentiated cell populations expand and suppress hematopoiesis of healthy cells due to competitive advantage [41, 60, 119].

The duration of the chronic phase ranges from 3-7 years [41, 59, 112]. During this time, mutated cells slowly take over the bone marrow, depleting Ph-negative cells [41]. Additional mutations accumulate that contribute to the progression from the chronic to accelerated and blast phases [48, 57, 59, 103]. In particular, much evidence suggests that progenitors acquire an increased capacity for self-renewal divisions that produce undifferentiated blast cells [22, 48, 60]. The immature blast population expands and differentiation ceases so that blasts compose a greater percentage of all cells, and the accelerated phase is reached when blasts comprise 10% of cells [48, 59, 60, 112, 120].

The accelerated phase is characterized by the increasing accumulation of blast cells in the blood and bone marrow. In healthy hematopoiesis, the number of precursors circulating in the peripheral blood is negligible. In contrast, blood tests from CML patients show significant amounts of immature blasts due to extensive progenitor expansion, inability to differentiate, and poor adhesion to bone marrow stroma [112]. Normal hematopoiesis is suppressed due to the dominance of the leukemic blasts, and as a result, patients may experience anemia [73]. Although not as fatal as the more

aggressive blast phase that follows, an estimated 10-20% of CML patients die in the accelerated phase [45].

Once blast phase is reached, prognosis is extremely poor, with a median survival time of five months if patients have already failed therapy with imatinib [45]. In blast phase, patients experience night sweats, fever, and bone pain as well as increased infections and bleeding as a result of lacking differentiated granulocytes and erythrocytes [45]. By this time, the leukemic clone has displaced normal hematopoiesis and granulocytic precursors are increased [59]. As portrayed in Figure 2.6, it is believed the progression to blast phase is caused by mutated progenitors that have acquired self-renewal capabilities [22, 60, 82]. Sadly, current treatment options do not eradicate leukemic stem cells, and blast accumulation persists, ultimately causing death [47, 55].

2.3.3 Treatment Options

Although prognosis is poor for patients in advanced phases of CML, the introduction of imatinib mesylate, commonly referred to as Gleevec, has demonstrated great potential and revolutionized treatment. Imatinib was first used to treat patients in 1998, and since then has become the first choice of treatment options [47]. The use of imatinib has displaced interferon-α, though the latter may be used in patients that are resistant to imatinib [45].

Imatinib is one of the more successful drugs used in fighting cancer because it successully attacks cancer cells without toxicity to healthy cells [46]. This drug inhibits ABL tyrosine kinases, which allows it to selectively target cells expressing BCR-ABL and inhibits their proliferation [55, 62]. Consequently, it is not uncommon for patients to have molecular and cytogenetic responses after treatment; that is, they have undetectable levels of BCR-ABL and the Ph chromosome, respectively [26, 47].

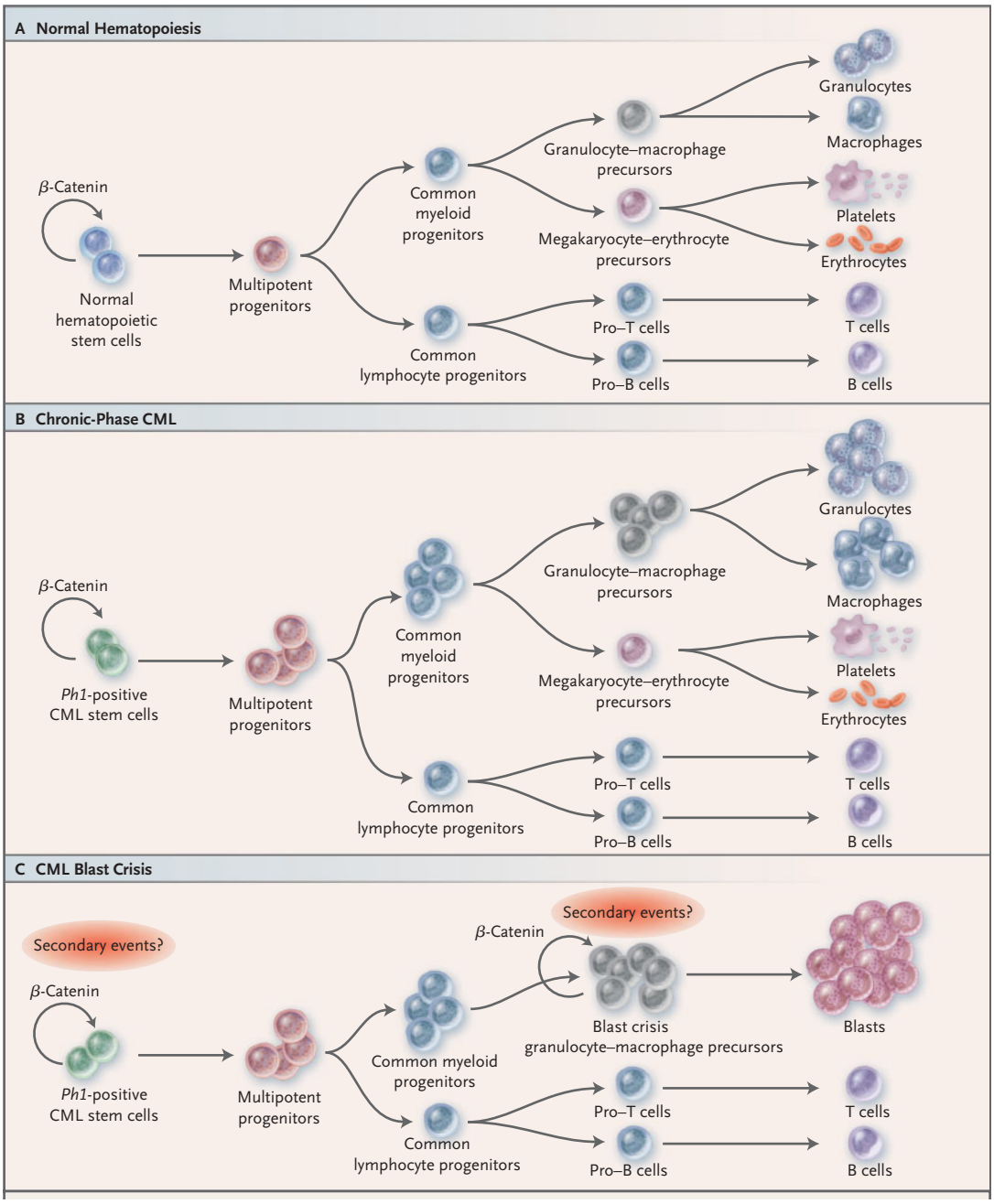

Figure 2.6: **Progression of CML.** Cells of the myeloid lineage expand during chronic phase, but differentiation still occurs. As disease progresses, progenitors acquire the ability to self-renew, causing the accumulation of immature blasts in the bone marrow and blood. Figure from [22].

If treatment is discontinued, however, relapse shortly follows, demonstrating that imatinib does not completely eliminate all leukemic cells [26, 62].

The success of imatinib demonstrates that chemotherapeutic agents may be synthesized to attack cancerous cells without also causing toxicity to healthy cells. Unfortunately, imatinib does have shortcomings in that it is not curative. One obstacle is that imatinib cannot kill quiescent cells, which allows cancer stem cells to persist and regenerate the cancer population once treatment is stopped [55]. In addition, imatinib is more successful in killing cells that are more committed, whereas primitive cells might be forced into quiescence instead of apoptosis [55]. Another challenge is one that is common in treating many forms of cancer in that cells acquire additional mutations that increase resistance to the drug [47]. For these various reasons, imatinib is unsuccessful in treating CML as it advances.

Allogeneic stem cell transplantation is the only curative treatment option known to date, but it is not considered appropriate for all cases. The percentage of patients surviving ten years ranges between 30-60%, but there is a 5-50% chance of mortality related to the procedure, which is why it is not always used as the first option of treatment [45]. Disease phase and patient age are both critical factors that determine whether or not to proceed with this treatment option. Allogeneic stem cell transplantation is generally conducted for patients in the chronic phase because survival chances decrease in more advanced stages [45]. Likewise, survival decreases as age increases, so this aggressive treatment is likely reserved for young patients in early chronic phase [45].

The progression of CML provides a perfect example of how cancer stem cells initiate and drive malignancy. The dynamics of this type of leukemia are particularly interesting because it is slow to develop but advances quickly as a result of

accumulating immature cells. Mathematical modeling can assist in gaining further understanding of this disease by examining the mutation pathways that generate disease while monitoring changes in stem, progenitor, and differentiated cell populations. The next chapter reviews previously developed mathematical models that address such issues in order to highlight areas that require additional investigation.

CHAPTER III

Mathematical Modeling of Cancer in Hierarchical Tissue

Mathematical modeling has long been utilized to supplement biological research. It can be used to interpret scientific data, make short- or long-term predictions based on recorded observations, and quantify parameters that are difficult to determine experimentally. In the area of cancer research, mathematical modeling addresses issues such as malignant growth, mutation acquisition, chemotherapy regimens, and tumor heterogeneity. The goal of this dissertation is to develop a mathematical model that investigates mutation acquisition in hierarchical tissue. In this chapter, existing relevant mathematical models are reviewed. Specifically, this chapter summarizes previous investigations of hierarchical tissue, multi-step tumorigenesis, and cancer stem cells.

3.1 Modeling Hierarchical Tissue

Most mammalian tissues are organized into a hierarchical structure consisting of stem, progenitor, and differentiated cells, and the cellular kinetics of each of these populations differs. Therefore, one cannot accurately model hierarchical tissue by assuming tissue cells are homogeneous. It is true that meaningful biological conclusions can be derived from models that simulate only one population of cells, but all of the cells must exhibit similar characteristics. For instance, it is not unreasonable

to model one cell population when all the cells are stem cells, but if differentiated cells are added to the system, then these two cell types should be separately modeled in order to capture the distinct dynamics of each population.

Stem cells generate all cells within the tissue, and under normal conditions, it is believed that the equilibrium of the stem-cell population dictates tissue homeostasis. Consequently, several mathematical models specifically focus on stem-cell regulation. In particular, the balance of self-renewal, differentiation, and apoptosis is commonly investigated. A simple time-discrete model by Hardy and Stark examined the relationship between stem and differentiated cells at steady state [51]. It was determined that stem-cell equilibrium ensured homeostasis in differentiated cells as well. Although this model simplified the mechanisms governing stem-cell division and differentiation by using constant probabilities for each, the general conclusion that stem-cell kinetics dictate tissue homeostasis is insightful.

More complicated models attempt to depict the intricate feedback regulations that govern stem-cell self-renewal, differentiation, and quiescence. For instance, Mackey introduced a model in which proliferating and quiescent stem cells were separated and the rate of self-renewal was dependent on the number of stem cells in the system [77]. By making stem-cell proliferation dependent on the number of stem cells, proliferation increases when stem cells are depleted and decreases when stem cells are numerous to prevent over-expansion, thereby incorporating negative feedback as a means of achieving and maintaining homeostasis. Further complexity was included in this model by the incorporation of a time delay that corresponded with the cycling time of proliferating cells. This feature helped to capture the dynamics of cyclical neutropenia.

Collaborators later extended Mackey's modeling framework in various ways. In

2001, Andersen and Mackey used the model to investigate chemotherapeutic effects on cancerous cells in Acute Myelogenous Leukemia [5]. Cell dynamics were modeled for both normal and malignant bone marrow cells, in order to determine the success or failure of several types of chemotherapy that target proliferating cells. To make predictions, normal and cancer cell dynamics were simulated separately, that is they did not coexist in the same tissue, with appropriate corresponding parameters. In addition, heterogeneity of bone marrow cells was not considered and mutation acquisition initiating malignancy was not discussed. However, from this model, the authors predicted that chemotherapy would not be effective, especially if tumor cells were capable of proliferating faster than normal cells.

Bernard *et al.* and Colijn and Mackey added mature cell populations to create a more comprehensive model of the hematopoietic system [13, 24]. The former considered only mature neutrophils in a model that simulated cyclical neutropenia. The latter included neutrophils, platelets, and erythrocytes to capture the cyclical dynamics of Periodic Chronic Myelogenous Leukemia. Both models incorporated negative feedback mechanisms controlling the rate of differentiation into committed lineages. As a result, regulatory mechanisms governed both stem-cell symmetric self-renewal and symmetric commitment differentiation.

The inclusion of regulatory feedback is a significant improvement in modeling tissue homeostasis. One shortcoming of the models by Mackey *et al.* is the absence of asymmetric stem-cell divisions. As a result, differentiated progeny only increase when stem-cell differentiation occurs, which depletes the stem-cell population by one. Although stem-cell loss is balanced by symmetric self-renewal divisions, the omission of asymmetric division does not permit differentiated-cell expansion without some expense to the stem-cell pool. Another limitation is the exclusion of intermediate

progenitor populations. Progenitors are not explicitly modeled but are represented in an amplification factor that incorporates precursor proliferation and apoptosis rates as well as the number of divisions that transpire between naïve stem cells and terminally differentiated cells.

Tissue hierarchy naturally lends itself to a maturity-structured mathematical framework. Several approaches have been taken in developing models that include progenitor populations. A simple structure classifies cells into stem, progenitor, and differentiated populations and model parameters are values that are averaged throughout the entire subpopulation [83, 118]. The addition of an intermediate progenitor pool more accurately simulates hierarchical tissue and may be acceptable when the characteristics of early progenitors resemble those of late progenitors. However, early progenitors often behave markedly different from progenitors later downstream, so that averaging the kinetics of all progenitors may not provide favorable results.

There are two general model structures that can capture the detailed growth dynamics in all of the intermediate progenitor populations. One discretizes maturity based on the number of divisions a cell has completed, while the other is maturity-continuous [36]. The former was conducted by Stochat *et al.* and recently in collaboration with Ashkenazi *et al.*, while the latter has been used to model hematopoiesis [7, 100, 117]. These maturity-structured models are not to be confused with age-structured models in which cell age represents progression through the cell cycle [14, 111]. Such models provide useful insight about the cycling distribution of cells within a tissue but are not within the scope of this dissertation.

When maturity is discretized, equations are created for each subpopulation. In so doing, all rates of entry or exit are specific for that cell population and need not

be uniform throughout all populations. Generally, cells of maturity i exit through apoptosis or by dividing and maturing to form cells of maturity $i+1$. If self-renewal is permitted, then the cell does not advance in maturity and remains in the i^{th} population after division. This type of structure explicitly simulates all of the dynamics of intermediate populations, but one potential drawback is the system of equations may be rather large since the number of equations in the system is often determined by the maximum number of divisions that can occur. In contrast, maturity-continuous models can capture the same dynamics as discretized models with only a few equations. A maturity variable is introduced, enabling rates to depend on cell maturity. Because maturity is continuous, smooth distribution curves can be generated that quantify the number of cells in any maturity bracket. One hindrance of this model is that it involves partial differential equations, which can be difficult to analyze theoretically.

In essence, both discretized and continuous model structures effectively capture the dynamics of hierarchical tissue, but each has its own disadvantages and advantages. A discretized approach was used in collaboration with Ashkenazi *et al.*, but in the present work, a maturity-continuous model will be developed. In particular, it will differ from previous models by including all three modes of stem-cell division and incorporating regulatory mechanisms that govern stem-cell self-renewal and differentiation.

3.2 Modeling Multi-Step Tumorigenesis

It is well known that cancer is a multi-step process in which somatic mutations accumulate to initiate malignancy [10, 50]. While it is generally accepted that mutations causing angiogenesis and metastasis occur later in development, there is much

uncertainty regarding the order of mutation acquisition in the early stages of tumorigenesis. Mathematical modeling has provided insightful information regarding these mutagenic pathways. In particular, modeling can help highlight which transformations most increase cell fitness, determine which mutations speed cancer onset and progression, and predict the order of mutation acquisition in specific malignancies. Because cancer is a result of genetic mutations, there is some degree of probability for cell transformation. Stochastic models can explore random events, while deterministic models predict the average outcome based on mutation rates and probability distribution functions. In this section, the latter are summarized.

In order to address issues of healthy cell loss that contribute both to aging and tumorigenesis, Wodarz developed a model of hierarchical tissue that modeled the degeneration of stem cells and subsequent progenitors [124]. Two scenarios of mutation accumulation were considered. When mutations did not occur during cell division, it was hypothesized that a faster rate of cell turnover protected against the mutation of normal cells. However, if mutations occurred during division, then the model predicted that faster proliferation rates promoted cancer, since cells had more opportunities to acquire mutations. This mathematical model did not explicitly include mutated cell populations, but rather investigated the loss of non-mutated cells in a hierarchical tissue.

The order of mutation acquisition likely affects the tempo of malignant growth. Spencer *et al.* developed a model of ordinary differential equations of a homogeneous tissue to address which pathway instigated the fastest tumor growth [116]. Loosely based on breast cancer data, their model predicted that evasion of apoptosis, followed by increased replication, then angiogenesis, then genetic instability constituted the fastest path to cancer. Their model, however, did not actually discriminate the se-

quential order in which mutations were acquired. For instance, cells with the ability to evade apoptosis as well as increased proliferation were collectively combined into the same subpopulation and the historical order of mutation was not distinguished. Since cells with the mutation for evasion of apoptosis surpassed all other populations expressing only one mutation, it was assumed that this was the first event in the fastest sequence. Similar calculations concluded subsequent transformations to establish the fastest path, ignoring the specific order of mutagenic events.

To specifically model mutli-step tumorigenesis in the breast, Enderling *et al.* developed a model that incorporated the multi-step approach of Spencer *et al.* for a specific mutation sequence [38]. Breast stem cells sequentially acquired two mutations to knock out one tumor suppressor gene, followed by an additional two mutations that removed a second tumor suppressor gene. Cells that had completely lost both tumor suppressor gene alleles were considered cancerous stem cells. In addition, the authors included radially symmetric spatial aspects to simulate tumor growth. As a result, non-cancerous cell populations were modeled with ordinary differential equations, while cancerous cells were modeled with a partial differential equation that was dependent both on time and a one-dimensional space variable. This model predicted that in order to generate a tumor within the clinically observed time, either mutations are acquired before puberty that make cells predisposed to accumulating additional mutations or genetic instability occurs early.

Several models have been developed that emphasize the significance of genetic instability in cancer-initiation. These models demonstrate that genetic instability promotes faster tumor growth. Beckman and Loeb used a deterministic model to figure out the probability that a cell would become cancerous based on the order in which the mutator phenotype was acquired [11]. They concluded that genetic

instability confers the greatest advantage when it occurs as the initial mutagenic event and becomes increasingly significant in highly proliferative tissues. Their results confirm those of Michor *et al.*, who established that chromosomal instability is likely an early event in the initiation of colon cancer [84, 85].

To demonstrate the competitive advantage of mutator cells over those that are not unstable, Komarova and Wodarz developed a differential equations model that contrasted the fitness of these two cell types [69]. This study hypothesized that mutator cells do not necessarily expand faster than stable cells during mutation acquisition. For instance, the magnitude of mutation rate and the extent to which apoptotic checkpoints remain in tact both influence whether the mutator or stable phenotype is favored. Therefore, they conclude genetic instability is most tumorigenic when programmed cell death is previously deregulated.

Clearly the order of mutation acquisition affects tumor dynamics. The multi-step models mentioned here were did not consider how hierarchical organization may affect the pathways to tumorigenesis. Due to the longevity and increased proliferative potential of stem cells in comparison to terminally differentiated cells, it is reasonable to propose that transformed stem cells are more capable of propagating malignancy. As a result, segregating stem, progenitor, and differentiated cells in multi-step models can generate more accurate results of mutation acquisition in hierarchical tissue.

3.3 Modeling Cancer Stem Cells

Not all mutated cells are equal in their ability to promote malignancy. It is believed that only a small percentage of tumor cells are responsible for cancer initiation and growth. These tumor-initiating cells share many qualities with stem cells, particularly the ability to self-renew and differentiate into various types of progeny, which

has led them to be called cancer stem cells [110]. Cancer stem cells are generated either as a result of mutations in stem cells that deregulate the mechanisms controlling proliferation and apoptosis, or they can arise from mutated progenitor populations that have regained self-renewal capacity [4, 22, 60, 102, 110]. The mechanisms that factor into the emergence of cancer stem cells are not fully understood. Consequently, mathematical models have been developed in order to gain insight into the dynamics of these tumorigenic cells.

Using a simple discrete mathematical model, Tomlinson and Bodmer established that mutations at the stem-cell level were most significant in promoting malignancy [118]. They argued that expansion could result from the failure of apoptosis or the block of differentiation rather than unbridled proliferation. Furthermore, they were able to demonstrate the importance of incorporating tissue hierarchy in cancer models, because mutated progenitors and differentiated cells were unable to cause exponential growth, unlike mutated stem cells. The model was first developed to simulate a normal system in homeostasis. Predictions of cancer cells were made based on the variation of model parameters, so the actual process of mutation acquisition was not studied.

One possible approach to distinguishing stem cells from differentiated cells is to classify them based on their location in the tissue. For instance, stem cells reside in the base of the colon crypt whereas differentiated progeny work their way up the crypt until they die and are removed [8, 84]. Nowak *et al.* used a linear process to simulate mutation acquisition in cells of the colon crypt [96]. Because of the way differentiated cells move up the crypt, mutations in non-stem cells are eventually removed, providing protection from cancer. A subsequent study employed the same linear structure and demonstrated that the first mutation of the tumor suppressor

APC gene must happen at the stem-cell level and predicted that a mutation causing chromosomal instability also occurred in the initial stages of colon cancer [84].

To model the cancer stem cell hypothesis in neural tumors, Ganguly and Puri created a deterministic model of tumorigenesis that compartmentalized stem, progenitor, and differentiated cells as well as their mutated counterparts [44]. In this model, stem and progenitor cells could become cancer cells through the acquisition of one mutation, so the multi-step pathways initiating cancer were not explicitly explored. The model predicted that mutations occurring in stem cells had more of an effect on tumorigenesis than mutations to progenitors. In addition, by incorporating feedback regulatory mechanisms between the various cell populations, it was suggested that repeated injury to mature cells, such as repeated radiation, could promote stem-cell proliferation, which in turn could increase mutation acquisition. This model is a good example of tumorigenesis in regulated hierarchical tissue and emphasizes the impact of mutations in stem cells, but it does not investigate the sequential order of mutation acquisition that promotes cancer.

In order to investigate what type of cell initiates blast crisis during the progression of Chronic Myelogenous Leukemia, Michor developed a model of two ordinary differential equations, one for leukemic stem cells, the other for leukemic progenitors [82]. It was argued that if leukemic stem cells promote blast crisis, then there should be no difference in the time of disease progression between patients treated with imatinib versus those that were not treated because imatinib does not kill leukemic stem cells. In contrast, if leukemic progenitors drive blast crisis, then there should be a noticeable difference between treated and untreated patients, which is indeed the case.

Mathematical models that incorporate cancer stem cells can also predict how

tissue dynamics will change as a result of treatment. In particular, cancer stem cells are not eradicated by current chemotherapeutic regimens, and therefore cause relapse by regenerating the tumor. With a simple system of ordinary differential equations, Michor *et al.* modeled the effects of imatinib administration to patients with Chronic Myelogenous Leukemia [83]. Treatment successfully killed progenitor and differentiated cells, but not all cancer stem cells. Consequently, when treatment was stopped, cancer regenerated from leukemic stem cells. In addition, the model was used to investigate the role of drug resistance in disease progression.

To further emphasize the need for therapies that target cancer stem cells, Dingli and Michor presented a simple model to investigate the effects of various treatment regimens on both normal and cancer cells [31]. The model consisted of four ordinary differential equations to simulate four distinct subpopulations in the tissue: normal stem cells, cancer stem cells, normal differentiated cells, and cancer differentiated cells. Numerical simulations started with the normal steady state values of healthy stem and differentiated cells and one cancer stem cell, and tumor generation was modeled. After cancer had reached detectable levels, various methods of treatment were simulated and it was confirmed that targeting cancer differentiated cells is insufficient to eradicate malignancy. In contrast, the model predicted that therapies either inhibiting proliferation or increasing death in cancer stem cells could eliminate cancer altogether.

Due to new discoveries of cancer stem cells, it is now more common to find mathematical models of cancer that incorporate some level of maturity-structure. To our knowledge, however, no existing mathematical model examines the sequential acquisition of mutations within hierarchically structured tissue governed by regulatory mechanisms. This dissertation aims to fulfill this lacking need in cancer modeling.

In the following chapter, mutation acquisition in hierarchical tissue is studied with a maturity-structured model. In Chapters V, VI, and VII, stem-cell governing mechanisms are discussed and their deregulation is investigated as a potential cause of cancer. Finally, in Chapter VIII, both maturity structure and regulatory mechanisms are combined into one comprehensive model, and the relevance of this model is illustrated with a simulation of mutation acquisition instigating Chronic Myelogenous Leukemia.

CHAPTER IV

A Maturity-Structured Mathematical Model of Mutation Acquisition in the Absence of Homeostatic Regulation

It is well known that mammalian tissue is not a homogeneous collection of cells, but is instead a composition of different types of cells that each have specific roles. Healthy tissue is carefully organized in a hierarchical structure consisting of stem, progenitor, and differentiated cells. Rare naïve stem are long-lived and unique in that they both self-renew and differentiate [4, 98]. Progenitor cells are more committed in lineage, but too immature to carry out specific functions. As they complete additional divisions, progenitors expand in number and become more specific, until they are fully differentiated [4]. Although differentiated cells are responsible for completing tasks that ensure the tissue functions properly, stem cells are crucial because their division kinetics ultimately maintain tissue homeostasis.

It has been suggested that the cells capable of initiating tumorigenesis share many characteristics of stem cells. Both malignant cells and normal stem cells are long-lived, evade apoptosis, have high proliferative potential, and are able to produce daughter cells of different phenotypes [4, 50, 57, 110]. Realizing these similar properties, tumor-initiating cells have been called cancer stem cells. The cancer stem cell hypothesis suggests that malignant growth is driven by a subpopulation of tumor cells that are capable of self-renewal. It is predicted that these cancer stem cells are

mutated stem cells or progenitors that have acquired stem-cell characteristics [110]. Since this cancer stem cell hypothesis originated, cancer stem cells have been identified in tumors of the breast, brain, colon, and blood, among others [4, 12, 40, 43, 57].

Due to the difficulty of isolating and studying stem cells experimentally, mathematical modeling provides further insight into the growth dynamics involved during tumorigenesis in hierarchical tissue. In order to simulate the cancer stem cell hypothesis mathematically, it is necessary to model cancer stem cells as a distinct subpopulation from other tumor cells. Furthermore, tissue hiearchy must be considered because stem, progenitor, and differentiated cells have very different properties. In this chapter, a maturity-structured mathematical model is presented that investigates mutation acquisition in stem, progenitor, and differentiated cells. The development of cancer stem cells is the focus, and mutation pathways causing the fastest emergence of disease are determined. In addition, tumor heterogeneity and composition are discussed.

4.1 A Maturity-Structured Mathematical Model of Hierarchical Tissue

Due to the varying properties of cells in hierarchical tissue, it is desirable to create a mathematical model that allows cellular kinetics to depend on cell maturity. Stem cells are the most immature cells in the tissue and they are capable of self-renewal. Though still immature, progenitors are more committed in lineage, and as they divide, they differentiate to increase cell maturity. Progenitors must complete a number of divisions to expand and generate an adequate amount of terminally differentiated cells. Therefore, the rate of proliferation must be significantly greater than the rate of apoptosis to allow expansion in this cell population. Fully mature cells are terminally differentiated, do not have any proliferative potential, and exit

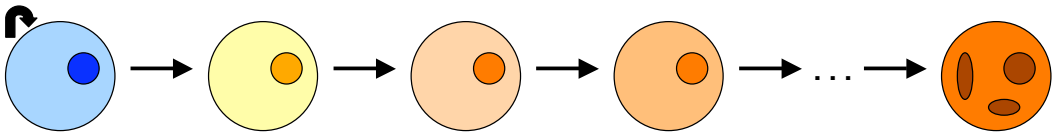

Figure 4.1: **Maturity scheme for mathematical model.** Stem cells are the most immature and can self-renew. Progenitors are more committed and differentiate as they divide. Terminally differentiated cells cannot divide and eventually die.

the tissue through cell death. Consequently, the rate of apoptosis is substantial in terminally differentiated cells. Figure 4.1 provides a schematic of the maturity progression from stem to differentiated cell.

There are various ways of explicitly modeling each of the cell subpopulations in a tissue. Some mathematical models compartmentalize stem cells, progenitor cells, and differentiated cells [5, 13, 24, 83], while others distinguish cells based on maturity, be it through discrete cell divisions [7] or continuous cell maturity level [100]. In this chapter, a differential equations model is presented in which both time and maturity are continuous. First, a model of healthy tissue will be established, and then this model will be used to investigate the process of mutation acquisition in hierarchical tissue. An ordinary differential equation is used to model the stem-cell population since it is assumed stem cells do not mature. In contrast, a partial differential equation is used for non-stem cells that is dependent on both time and maturity. To our knowledge, this is the first mathematical model that addresses the emergence of cancer stem cells within a maturity-continuous structure.

4.1.1 Model Structure

It is known that the properties of stem, progenitor, and differentiated cells are markedly different from each other. Stem cells are unique in that they are naïve and have the potential to remain in an undifferentiated state. Under homeostatic

conditions, it is thought that the majority of stem cells are in a quiescent state and divide infrequently. In contrast, progenitors eventually reach full maturity through extensive proliferation that produces differentiated progeny. As progenitors mature, their proliferative and apoptotic behavior may also change. For instance, immature myeloid precursor cells, such as myeloblasts, divide faster than more differentiated myelocytes [109]. Consequently, it is desirable to mathematically model hierarchical tissue in such a way as to allow cell kinetics to depend on cell maturity.

In 2003, Ostby *et al.* presented a continuous maturity-structured model of granulopoiesis, which simulated cells from the myeloblast stage through terminally differentiated granulocytes in a normal, healthy system [100]. Stem cells were not modeled, but rather were assumed to be at a constant level in homeostasis that fed into the progenitor population. A one-dimensional wave equation dependent on time and cell maturity was employed for progenitor cells in the bone marrow. Rates of proliferation, mobilization from the bone marrow to blood, and apoptosis were all dependent on cell maturity. Cell maturity was scaled such that the most immature cell had maturity level zero, the most mature cell had maturity level one, and the maturation rate determined how quickly cells progressed through each stage. This model assumed that cells in the blood were terminally differentiated, and thus were fully mature and did not proliferate, so that blood cells were modeled with an ordinary differential equation dependent on time only. From numerical simulations, it was suggested that progenitor apoptosis may be significant under certain assumptions. In particular, the authors determined that the significance of cell death depended on the times precursors spent in each phase and concluded that model accuracy would be improved with more reliable predictions of these transit times.

In the present work, a mathematical model is introduced that imparts a similar

maturity-continuous structure, while making various significant alterations from the Ostby model. It is important to note that the Ostby model simulated granulopoesis in homeostasis, which permitted the omission of explicitly modeling stem cells. In modeling tumorigenesis, and specifically the generation of cancer stem cells, it is essential to include an equation monitoring the dynamics of the stem-cell population. Therefore, the most significant difference between the present work and the Ostby model is the inclusion of a stem-cell equation that fosters investigation of the effects that stem cells have on tissue dynamics.

Other differences between the two models are not as striking, but still noteworthy. For instance, because the Ostby model was specifically tailored for granulopoiesis, the maturity-structured progenitor population was contained in the bone marrow, while all cells in the blood were assumed to be fully mature and thus did necessitate maturity structure in the blood compartment. Although the hematopoietic system will be simulated in this chapter as well, the mathematical model developed here is general and can be applied to any hierarchical system. The models also slightly differ in how the measurement of maturity is handled. In the Ostby model, maturity was on a scale of zero to one, and a constant maturation rate was derived from the time needed for a cell to progress from myeloblast to granulocyte. In contrast, maturity is not scaled in the current presentation, but rather progresses according to the time scale. A cell with a maturity level measured in weeks has completed an approximate number of divisions depending on the proliferation rate, which determines its progress to terminal differentiation. Therefore, the models slightly differ in how maturity is defined, but in essence are comparable since both models rely on average proliferation rates to determine maturity.

A continuous maturity-structured model is now introduced. Consider a time- and

maturity- continuous model in which time is denoted by t and the maturity of cells is denoted a. Stem cells are the most naïve cells in the system. They do not mature, and, therefore, the size of the stem cell population, denoted $S(t)$, is not dependent on a. Stem cells proliferate at rate k. Assume that each stem cell encounters one of four fates during each division: symmetric self-renewal, asymmetric self-renewal, symmetric commitment differentiation, and apoptosis. Stem cells symmetrically self-renew with probability α_S, which increases the stem cell pool by one. Stem cells asymetrically self-renew with probability α_A, which does not change the stem cell pool but increases the progenitor pool of maturity level zero by one. Stem cells symmetrically differentiate with probability α_D, which decreases the stem cell pool by one and increases the progenitor pool of maturity level zero by two. Finally, stem cells die with probability δ_S, and it follows that $\alpha_S + \alpha_A + \alpha_D + \delta_S = 1$. It is assumed in this model that stem cells only die and differentiate when dividing, though the model equations could easily be slightly modified to allow for division-independent differentiation and apoptosis.

The maturity density of differentiated cells at time t is denoted $n(t, a)$, where the number of cells between maturity level a and $a + \Delta a$ is approximately $n(t, a)\Delta a$. The proliferation rate of differentiated cells, denoted by the function $\beta(a)$, allows immature to proliferate but tends to zero as maturity is reached. The death rate of differentiated cells, given by the function $\mu(a)$, increases after full maturity. If the initial stem cell population is S_0, the initial maturity distribution of differentiating cells is given by $f(a)$, and the total number of non-stem cells in the tissue is $N(t)$, then the model equations follow:

$$
\begin{aligned}
\frac{dS}{dt} &= (\alpha_S - \alpha_D - \delta_S)kS \\
\frac{\partial n}{\partial t} + \frac{\partial n}{\partial a} &= (\beta(a) - \mu(a))n \\
n(a,0) &= f(a) \\
S(0) &= S_0 \\
\frac{\partial n}{\partial t}(0,t) &= (2\alpha_D + \alpha_A)kS \\
N(t) &= \int_0^\infty n(t,a)da.
\end{aligned} \tag{4.1}
$$

For ease of reference, this model is labeled the Maturity-Structured Model in the Absence of Homeostatic Regulation (MSMAHR). In the MSMAHR model, probabilities of stem-cell division are constant, but in the next chapter, dynamic regulatory feedback mechanisms that influence the pattern of self-renewal and differentiation will be discussed.

There are many potential functions that would be suitable choices for $\beta(a)$ and $\mu(a)$. Generally, $\beta(a)$, should be greater than $\mu(a)$ for immature cells that have not yet completed terminal differentiation in order to allow for progenitor expansion. Furthermore, as $a \to \infty$, $\beta(a) \to 0$ and $\mu(a)$ increases well beyond $\beta(a)$. By not explicitly defining functions for the proliferation and death rates of differentiating cells, the MSMAHR model remains a general enough framework to be used modeling various types of hierarchical tissue. In Section 4.1.3, specific examples are given in order to generate numerical simulations of the hematopoietic system.

4.1.2 Model Analysis

The solution of the stem-cell equation is $S(t) = S_0 e^{(\alpha_S - \alpha_D - \delta_S)kt}$. The method of characteristics may be used to solve the differentiated cell equation [92]. Assuming cell maturity is determined by time passed since a differentiated cell was formed gives

$\frac{da}{dt} = 1$, and the differentiated cell population equation is simplified to $\frac{dn}{dt} = \beta n - \mu n$. Note that $\frac{da}{dt} = 1$ implies that $a = t + C$, for some constant C. For $a > t$, $C = a_0$ and for $a < t$, $C = -t_0$.

When $a > t$, the following is true:

$$\begin{aligned}
\frac{dn}{dt} &= \beta(a)n - \mu(a)n \\
\frac{dn}{dt} &= (\beta(t + a_0)n - \mu(t + a_0))n \\
\int \frac{dn}{n} &= \int (\beta(t + a_0)n - \mu(t + a_0))dt \\
\int \frac{dn}{n} &= \int_0^t (\beta(\tau + a_0)n - \mu(\tau + a_0))d\tau \\
\int \frac{dn}{n} &= \int_{u=a_0}^{t+a_0} (\beta(u) - \mu(u))du \\
n &= K \exp\left[\int_{a_0}^{t+a_0} (\beta(u) - \mu(u))du\right] \\
n &= K \exp\left[\int_{a_0}^{a} (\beta(u) - \mu(u))du\right]. \qquad (4.2)
\end{aligned}$$

At time $t = 0$, $a = a_0$, and so $K = n(a_0, 0)$. If the initial age distribution is given by $n(a, 0) = f(a)$, then since $a_0 = a - t$,

$$\begin{aligned}
n(a,t) &= n(a_0, 0) \exp\left[\int_{a_0}^{a} (\beta(u) - \mu(u))du\right] \\
n(a,t) &= n(a - t, 0) \exp\left[\int_{a_0}^{a} (\beta(u) - \mu(u))du\right] \\
n(a,t) &= f(a - t) \exp\left[\int_{a_0}^{a} (\beta(u) - \mu(u))du\right]. \qquad (4.3)
\end{aligned}$$

Note that if $f(a) = 0$, then $n(a, t) = 0$ for $a > t$. That is, it their are no differentiating cells in the tissue at time $t = 0$, then it is impossible for the maturity level of a cell to be greater than the time that has elapsed. For instance, if $n(a, 0) = 0$, then at two weeks all differentiating cells must have maturity that is less than or equal two weeks.

When $a < t$, then the following holds:

$$\begin{aligned}
\frac{dn}{dt} &= \beta(a)n - \mu(a)n \\
\frac{dn}{dt} &= (\beta(t-t_0)n - \mu(t-t_0))n \\
\int \frac{dn}{n} &= \int (\beta(t-t_0)n - \mu(t-t_0))dt \\
\int \frac{dn}{n} &= \int_{t_0}^{t} (\beta(\tau-t_0)n - \mu(\tau-t_0))d\tau \\
\int \frac{dn}{n} &= \int_{u=0}^{t-t_0} (\beta(u) - \mu(u))du \\
\int \frac{dn}{n} &= \int_{0}^{a} (\beta(u) - \mu(u))du \\
n &= K \exp\left[\int_0^a (\beta(u) - \mu(u))du\right]. \qquad (4.4)
\end{aligned}$$

When $a = 0$, $t = t_0$, so that $K = n(0, t_0) = n(0, t)$, which in this model gives $K = (2\alpha_D + \alpha_A)kS$. Therefore, for $a < t$,

$$n(a,t) = (2\alpha_D + \alpha_A)kS(t) \exp\left[\int_0^a (\beta(u) - \mu(u))du\right]. \qquad (4.5)$$

The differentiated-cell population will go to steady state as long as the stem-cell population is in steady state, as seen in Equation 4.5. The stem-cell population is in steady state if $\alpha_S - \alpha_D - \delta_S = 0$. Otherwise, it either grows or decays exponentially, which causes the differentiated-cell population to behave accordingly. Thus stem-cell population dynamics dictate differentiated-cell population dynamics, which correlates with previous modeling results from Hardy and Stark that predicted stem-cell equilibrium determines tissue homeostasis [51].

4.1.3 Parameter Estimation

Due to the difficulty of isolating and studying stem cells *in vivo*, there are limited data for stem-cell kinetics. The hematopoietic system is perhaps the best quantified system, and as a result, parameter values for model simulations are derived from

Parameters Used			
Parameter	Biological Meaning	Value Range	Value Used
S_0	Initial number of stem cells	11,000 - 22,000 cells [1]	18,000 (cells)
α_S	Probability SSR	(derived from [125])	0.20
α_A	Probability of ASR	(derived from [125])	0.60
α_D	Probability of SD	(derived from [125])	0.15
δ_S	Probability of stem-cell death	0.05 [83]	0.05
k	Proliferation rate of stem cells	0.4043 $weeks^{-1}$ [21]	0.4043 weeks^{-1}
b	Max. prol. rate of progenitors	9.0 - 10.6 weeks^{-1} [109]	9.7 weeks^{-1}
ρ_β	Steepness of proliferation switch	No information	2
ω_β	Maturity at proliferation switch	No information	2.05 weeks
d	Max. death rate of diff. cells	15 - 18 weeks^{-1} [9, 13]	16.8 weeks^{-1}
ρ_μ	Steepness of death switch	No information	10
ω_μ	Maturity at death switch	No information	4.10 weeks

Table 4.1: Baseline parameters used to simulate the Maturity-Structured Model in the Absence of Homeostatic Regulation, found in Equations 4.1.

hematopoietic stem cells and progenitor and differentiated cells of the granulocytic lineage. The parameters used are presented in Table 4.1.3.

Although hematopoietic stem cells are better understood than stem cells in other tissues, there is still much uncertainty concerning *in vivo* measurements. Part of the discrepancy comes from the process of isolating stem cells. There are several markers that isolate immature cells from those that are more differentiated, but it can be difficult to separate stem cells from early progenitor cells. Therefore, it is not uncommon for a population of "stem" cells to also include early progenitor cells, which can taint the true measurements of stem versus early progenitor cells. As a result, the current literature includes a wide range of values regarding hematopoietic stem-cell kinetics. Because this mathematical model separates stem cells from all other cells, the parameters used here attempt to reflect the most purified stem-cell population

As cells differentiate, they lose their ability to proliferate. Stem and early progenitor cells have high proliferative potential, whereas terminally differentiated cells are unable to complete further divisions. Although some terminally differentiated cells

are long-lived, such as lymphoid cells, this model assumes that fully mature cells have a short half-life and, consequently, a significant rate of apoptosis [9, 13, 61]. In order to capture the dependence of proliferation and apoptosis on cell maturity, functions that smoothly transition between two different baseline rates are used. There are many possibilities for such functions, but for simplificity, this model assumes that the proliferation rate is approximately constant until terminal differentiation, after which it approaches zero. In contrast, the death rate is assumed to be approximately zero until terminal differentiation, after which it is approximately constant with a short half-life. Instead of incorporating step functions that introduce discontinuity, the functions used to model proliferation and death rates for non-stem cells are as follows:

$$\begin{aligned} \beta(a) &= \frac{-b}{2}\tanh(\rho_\beta(a-\omega_\beta)) + \frac{b}{2} \\ \mu(a) &= \frac{d}{2}\tanh(\rho_\mu(a-\omega_\mu)) + \frac{d}{2} + \delta_S k. \end{aligned} \tag{4.6}$$

The maximum rate of proliferation is given by b and the maximum rate of death is given by d. The maturity at which non-stem cells proliferate at half the maximum rate is ω_β, and ρ_β is the steepness of the decreasing switch. Similarly, the maturity at which non-stem cells die at half the maximum rate is ω_μ and the steepness of the increase in the switch is ρ_μ. It is also assumed that progenitors die at a rate at least as great as stem cells. The proliferation and death rate functions in Equations 4.6 are plotted in Figure 4.2.

4.1.4 Numerical Simulations and Results

In the Section 4.2, mutation pathways generating cancer in hierarchical tissue will be explored, but before this can be investigated, the steady state of healthy tissue must be first determined. In order to conduct numerical simulations, model

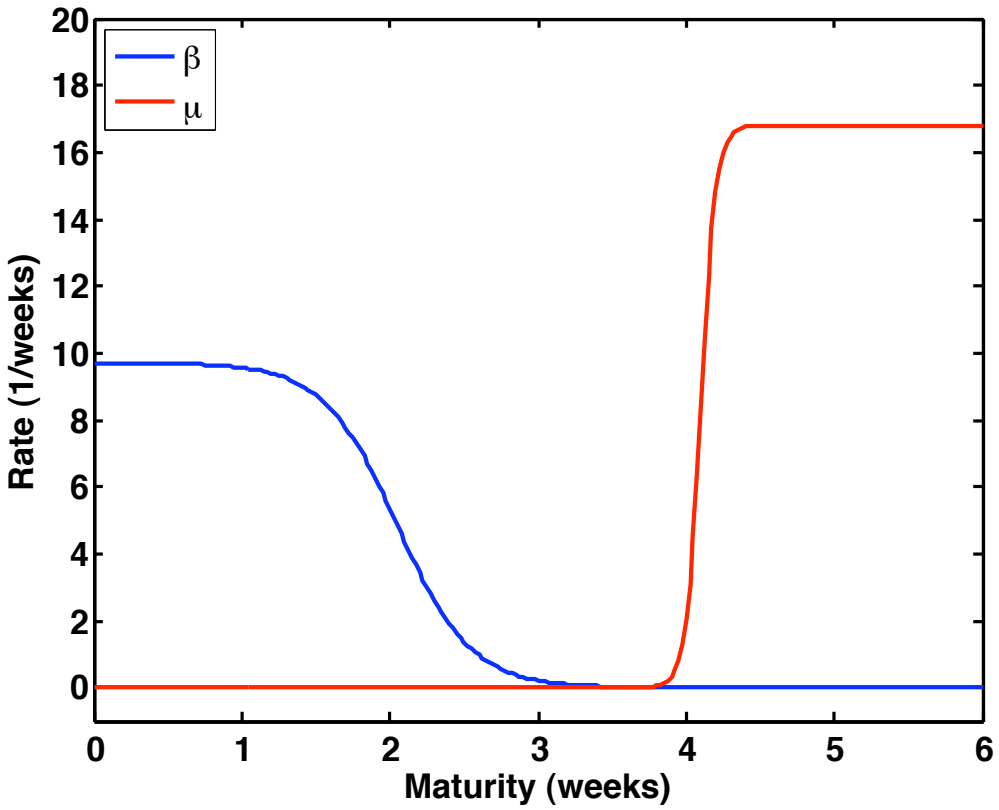

Figure 4.2: **Proliferation and death rates of differentiating cells depend on cell maturity.** The functional forms presented in Equations 4.6 are plotted versus cell maturity.

equations were discretized with the upwind method and simulations were conducted in MATLAB. Step sizes for Δt and Δa satisfy the CFL condition. For the boundary condition of differentiating cells, at the j^{th} time step, $n_0^j = (2\alpha_D + \alpha_A)\, kS^{j-1}\Delta t$.

To determine the steady state maturity-distribution of cells, it is necessary to generate the progeny resulting from a steady state of stem cells. Since hematopoietic stem cells are arguably the most observed, the hematopoietic system is used to illustrate the dynamics of hierarchical tissue. It is estimated that there are between 11,000 - 22,000 hematopoietic stem cells in an adult human [1]. In future chapters, the mechanisms regulating stem cell hematopoiesis will be discussed, so in order to correlate with following work, suppose a system is infused with 18,000 stem cells and zero progenitor and differentiated cells. Assume stem cells divide with probabilities that maintain equilibrium within the stem-cell compartment so it possible to determine the steady state maturity distribution of progenitor and differentiated cells resulting from this many stem cells. Progenitors are formed through asymmetric and symmetric commitment divisions of the existing stem cells. Progenitors proliferate and expand in number to generate fully-differentiated cells, and eventually a steady-state distribution of progenitor and differentiated cells is reached.

Figure 4.3 plots tissue dynamics as stem cells generate progenitor and differentiated cells. The maintained homeostasis of stem cells and the generation of the resulting progeny of non-stem cells is displayed in a log plot in Figure 4.3A. Initially, there is a low number of non-stem cells that are all progenitors formed from the stem-cell population. As time progresses, progenitors proliferate and expand in number as the stem-cell source continues to form early progenitors. As equilibrium is reached, the total number of non-stem cells includes all progenitors and fully-differentiated cells. Using the parameters in Table 4.1.3, the total number of non-stem cells, N,

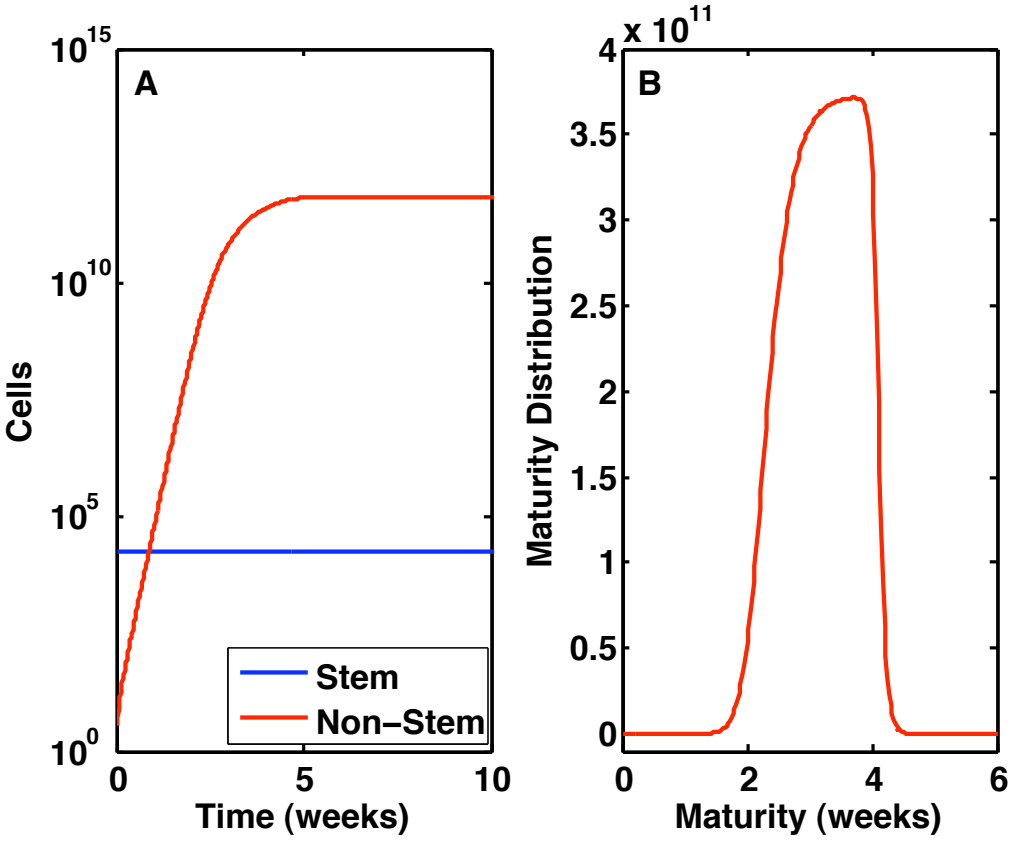

Figure 4.3: **The generation of hierarchical tissue from stem cells.** (A) A log plot of stem (blue) and non-stem (red) cells in the tissue versus time. Starting at stem-cell homeostasis, the stem-cell population remains constant over time, while the non-stem cell population expands until it reaches homeostasis. (B) The maturity distribution of non-stem cells at steady state demonstrates the majority of cells are fully mature.

reaches 6.54×10^{11} cells, which is within the range of $5 - 15 \times 11$ cells of the granulocytic lineage estimated in a human adult [52, 100, 109]. It takes approximately 4.6 weeks for N to reach 90% of its equilibrium value, though the time to constitution can be altered by the rate of proliferation in both stem and progenitor cells. In Figure 4.3B, the maturity distribution of non-stem cells at steady state demonstrates that the majority of stem cells are fully mature. At homeostasis, it is estimated that 1.3×10^{11} cells are fully differentiated, which correlates with the estimated 1.2×10^{11} granulocytes that are released from the bone marrow to the blood daily.

The proliferation and death rate functions, β and μ, respectively, are those displayed in Figure 4.2. Cells are considered to be fully mature when $\mu > \beta$, which occurs at approximately 3.8 weeks in this simulation. The cycle times of immature myeloblasts, myelocytes, and promyelocytes are estimated to be 11, 27, and 39 hours, respectively [109]. Therefore, the proliferation rate is greater for lower maturity levels, with a maximum rate of 9.7 divisions per week to correlate with the doubling time of myeloblasts. Neutrophils reside in the bone marrow for approximately 4 days after their final division before being released into the blood [39]. Once in the blood, the half-life of neutrophils is estimated at seven hours, thus the maximum of the death rate is achieved soon after cells have reached full maturity.

This section presented a maturity-structred model of hierarchical tissue that is continuous both in time and cell maturity. Mathematical analysis determined the solution for both stem and non-stem cell populations, and it was concluded that the number of progenitor and differentiated cells is directly dependent on the number of stem cells present in the system. Through numerical simulations in which cells of the granulocytic lineage were produced from an initial population of hematopoietic stem cells, it was possible to determine the steady state of non-stem cells as well as

the maturity distribution of progenitor and differentiated cells at homeostasis. These findings will be used as the baseline values of healthy hierarchical tissue in exploring the process of mutation acquisition and tumorigenesis in the next section.

4.2 Mutation Acquisition in Stem, Progenitor, and Differentiated Cells

It is believed that tumorigenesis does not result from a single mutation, but rather is a multistep process [20, 50]. Although it is known several events are needed to cause the malignant transformation of a normal cell, the order in which these mutations are acquired can affect tumor dynamics. Deregulated proliferation, evasion of apoptosis, and genetic instability are likely involved in the early stages of cancer, whereas mutations causing angiogenesis and metastasis are probably acquired in later stages, after a tumor has grown beyond a certain threshold size [50]. In this section, mutation acquisition in hematopoietic cells is investigated; consequently, angiogenesis and metastasis may be disregarded.

The hierarchical organization of most mammalian tissues may offer protection against cancer. The vast majority of tissues consist of differentiated cells that have a high rate of turnover and generally don't live long enough to accumulate enough mutations to become malignant [102, 110]. In addition, most differentiated cells do not self-renew, and when they reach full maturity, mutations are not passed on to any progeny. Generally, stem cells, or progenitors that have gained self-renewal capability, are the only tissue cells that live long enough to acquire a sufficient number of mutations and possess a sufficient proliferative potential that allows the propagation of mutations to their progeny [28, 110].

In this section, the pathways leading to tumorigenesis in hierarchical tissue are explored. This mathematical model is one of the first that permits the investigation

of sequential mutation acquisition within hierarchically structured tissue [7]. Because mutation order is monitored, it is possible to quantify the increased advantage gained through each transformation. Furthermore, tissue composition can be determined that is based on the percentages of cells with a certain number of mutations. An additional feature of this model is the explicit inclusion of all three models of stem-cell division: symmetric self-renewal, asymmetric self-renewal, and symmetric commitment differentiation. This differs from other mathematical models of cancer in which asymmetric divisions are often ignored. To our knowledge, this is the first model to incorporate all of these novel features within a maturity-continuous framework.

4.2.1 Model Structure for Mutation Acquisition

To study the process of oncogenesis in hierarchical tissue, the MSMAHR model presented in Equations 4.1 is expanded to incorporate mutation acquisition in both stem and differentiated cells. Normal stem cells, S_0, acquire their first mutation at rate m_0, at which time they are labeled as S_1. Likewise, S_1 cells acquire the second mutation at rate m_1 to become S_2 cells, and S_2 cells acquire the third mutation at rate m_2 to become S_3 cells. Stem cells with i mutations, S_i, form progenitor cells with i mutations, n_i, when they differentiate. Committed cells may also mutate as they continue to divide, and M_i is used to denote the mutation rates from n_i to n_{i+1}. It is assumed that cells may only acquire one mutation at a time. Cells with i mutations may alter any of the model parameters, depending on which mutation is acquired, thus each parameter is denoted with an i-subscript to allow these values to differ from the baseline value. A schematic diagram is displayed in Figure 4.4 and the model equations for mutation acquisition are presented below.

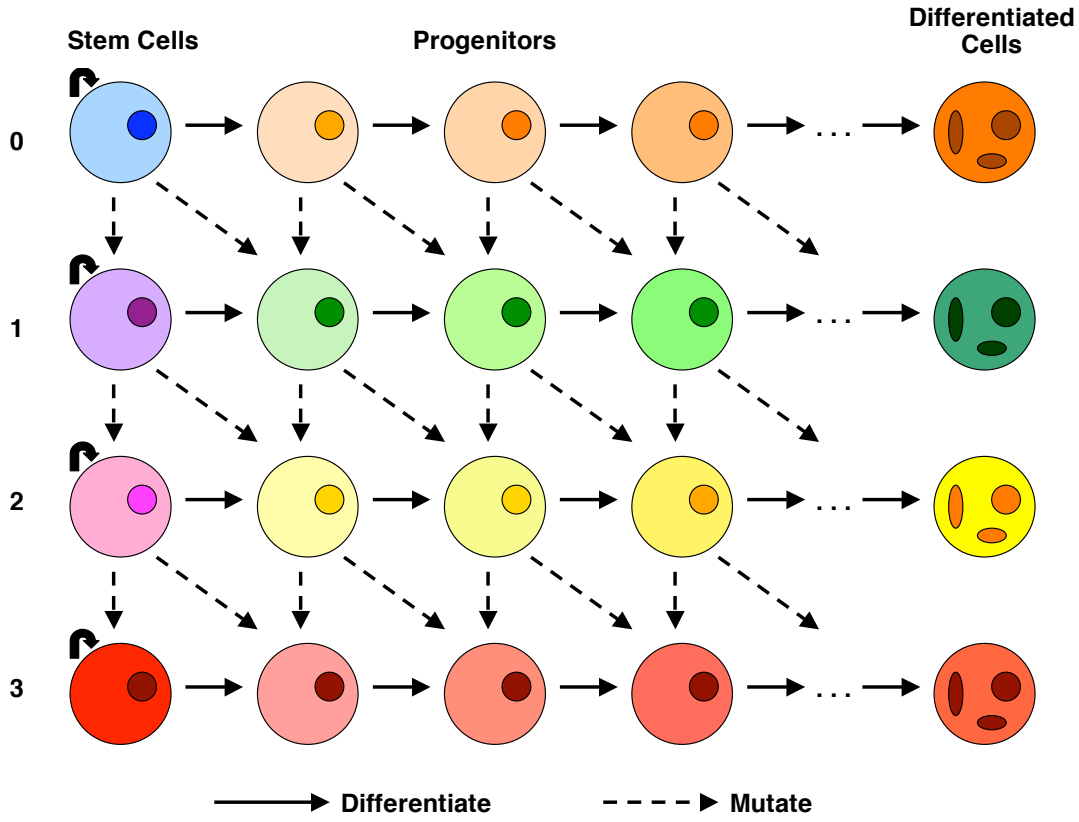

Figure 4.4: **Schematic diagram of mutation acquisition in hierarchical tissues.** Stem cells with zero, one, two, or three mutations may self-renew or differentiate to form progenitors, which in turn continue dividing and maturing. Each time cells divide, there is a small probability they will acquire a mutation. Cells can accumulate up to three mutations, at which point they are classified as cancer cells.

Stem Cells:

$$
\begin{aligned}
(4.7) \qquad \frac{dS_0}{dt} &= \left[(1-2m_0)\alpha_{S0} - m_0\alpha_{A0} - \alpha_{D0} - \delta_{S0}\right] k_0 S_0 \\
\frac{dS_1}{dt} &= \left[(1-2m_1)\alpha_{S1} - m_1\alpha_{A1} - \alpha_{D1} - \delta_{S1}\right] k_1 S_1 \\
&\quad + \left[2m_0\alpha_{S0} + m_0\alpha_{A0}\right] k_0 S_0 \\
\frac{dS_2}{dt} &= \left[(1-2m_2)\alpha_{S2} - m_2\alpha_{A2} - \alpha_{D2} - \delta_{S2}\right] k_2 S_2 \\
&\quad + \left[2m_1\alpha_{S1} + m_1\alpha_{A1}\right] k_1 S_1 \\
\frac{dS_3}{dt} &= \left[\alpha_{S3} - \alpha_{D3} - \delta_{S3}\right] k_3 S_3 \\
&\quad + \left[2m_2\alpha_{S2} + m_2\alpha_{A2}\right] k_2 S_2
\end{aligned}
$$

Differentiating Cells:

$$
\begin{aligned}
(4.8) \qquad \frac{\partial n_0}{\partial t} + \frac{\partial n_0}{\partial a} &= \left[(1-2M_0)\beta_0(a) - \mu_0(a)\right] n_0 \\
\frac{\partial n_1}{\partial t} + \frac{\partial n_1}{\partial a} &= \left[(1-2M_1)\beta_1(a) - \mu_1(a)\right] n_1 + 2M_0\beta_0(a) n_0 \\
\frac{\partial n_2}{\partial t} + \frac{\partial n_2}{\partial a} &= \left[(1-2M_2)\beta_2(a) - \mu_2(a)\right] n_2 + 2M_1\beta_1(a) n_1 \\
\frac{\partial n_3}{\partial t} + \frac{\partial n_3}{\partial a} &= \left[\beta_3(a) - \mu_3(a)\right] n_3 + 2M_2\beta_2(a) n_2
\end{aligned}
$$

Birth and Death Functions for Differentiating Cells:

$$
\begin{aligned}
(4.9) \qquad \beta_i(a) &= \frac{-b_i}{2}\tanh(\rho_{\beta i}(a - \omega_{\beta i})) + \frac{b_i}{2} \\
\mu_i(a) &= \frac{d_i}{2}\tanh(\rho_{\mu i}(a - \omega_{\mu i})) + \frac{d_i}{2}
\end{aligned}
$$

for $i = 0, 1, 2, 3$.

Initial Conditions:

$$
\begin{aligned}
(4.10) \qquad n_0(a,0) &= f(a) \\
n_{1,2,3}(a,0) &= 0 \\
S_0(0) &= S_0 \\
S_{1,2,3}(0) &= 0
\end{aligned}
$$

Boundary Conditions:

$$
\begin{aligned}
\frac{\partial n_0}{\partial t}(0,t) &= \left[2(1-m_0)\alpha_{D0} + (1-m_0)\alpha_{A0}\right] k_0 S_0 \\
\frac{\partial n_1}{\partial t}(0,t) &= \left[2(1-m_1)\alpha_{D1} + (1-m_1)\alpha_{A1}\right] k_1 S_1 \\
&\quad + \left[2m_0\alpha_{D0} + m_0\alpha_{A0}\right] k_0 S_0 \\
\frac{\partial n_2}{\partial t}(0,t) &= \left[2(1-m_2)\alpha_{D2} + (1-m_2)\alpha_{A2}\right] k_2 S_2 \\
&\quad + \left[2m_1\alpha_{D1} + m_1\alpha_{A1}\right] k_1 S_1 \\
\frac{\partial n_3}{\partial t}(0,t) &= \left[2\alpha_{D3} + \alpha_{A3}\right] k_3 S_3 \\
&\quad + \left[2m_2\alpha_{D2} + m_2\alpha_{A2}\right] k_2 S_2
\end{aligned} \tag{4.11}
$$

To easily refer to this model in subsequent discussion, it is named the Maturity-Structured Model of Mutation Acquisition (MSMMA).

4.2.2 Exploring the Pathways to Tumorigenesis

Several types of genetic transformations have been implicated in oncogenesis, but in this investigation, focus is directed towards somatic mutations that occur during DNA replication. In their review and classification of cancer cells, Hanahan and Weinberg identified commonalities in malignant cells: independence of growth signals, increased proliferation, evasion of apoptosis, insensitivity to anti-growth signals, and the abilities to promote angiogenesis and metastasize [50]. In addition, genetic instability is believed to be widespread in various cancers [15].

To examine the initiation of cancer, three mutations are considered in this work. The D mutation decreases the percentage of stem cells that go through apoptosis and decreases the maximum death rate of non-stem cells. The G mutation increases the rate at which subsequent mutations are acquired. The R mutation alters cell proliferation, by either increasing the rate of proliferation or shifting the balance of

stem-cell division to favor symmetric self-renewal. A cell is considered to be healthy and normal if it does not have any mutations and assumed to be cancerous once it has acquired all three mutations. For model simulations, all mutations are one-hit, though mutations requiring two genetic events could easily be incorporated simply by increasing the number of mutations that must occur to malignantly transform a cell. Mutations enabling angiogenesis and metastasis are not considered because model simulations are of the hematopoietic system.

The order in which mutations are acquired is noted by the order in which D, G, and R are listed. There are six possible sequences in which the mutations accumulate:

- D $\Rightarrow$ G $\Rightarrow$ R
- D $\Rightarrow$ R $\Rightarrow$ G
- G $\Rightarrow$ D $\Rightarrow$ R
- G $\Rightarrow$ R $\Rightarrow$ D
- R $\Rightarrow$ D $\Rightarrow$ G
- R $\Rightarrow$ G $\Rightarrow$ D

Tumor dynamics are compared and contrasted for all six pathways. Note that each pathway produces cancer cells that have acquired the same three mutations, but each pathway is different in the order in which mutations occur. Because a specific cancer is not being modeled, it is assumed that for each D, G, and R mutation in the model, there are approximately 100 genes that may cause transformation [116]. As a result, the mutation rate is one hundred times the suggested mutation rate of 10^{-8} per division [83, 116].

Numerical simulations were conducted using MATLAB. The upwind method was

Parameters Used			
Parameter	Biological Meaning	Normal Value	Mutated Value
S_0	Normal stem-cell homeostasis	18,000 (cells) [83]	18,000 (cells)
α_S	Probability of SSR	0.20 [125]	0.40
α_A	Probability of ASR	0.60 [125]	0.425
α_D	Probability of SD	0.15 [125]	0.15
δ_S	Probability of stem-cell death	0.05 [83]	0.025
k	Stem-cell proliferation rate	0.4043 (weeks^{-1}) [21]	0.8086 (weeks^{-1})
m	Mutation rate of stem cells	10^{-6} [6, 58, 116]	10^{-4} [58, 116]
M	Mutation rate of non-stem cells	10^{-6} [6, 58, 116]	10^{-4} [58, 116]
b	Max. progenitor proliferation rate	9.7 (weeks^{-1})	19.4 (weeks^{-1})
ρ_β	Steepness of prog. prol. switch	2	2
ω_β	Maturity at prol. switch	2.05 (weeks)	1.025 (weeks)
d	Max. differentiated cell death rate	16.8 (weeks^{-1}) [9, 13]	8.4 (weeks^{-1})
ρ_μ	Steepness of diff. cell death switch	10	10
ω_μ	Maturity at death switch	4.10 (weeks) [39]	3.075 (weeks)

Table 4.2: Parameters used for the Maturity-Structured Model of Mutation Acquisition.

used to discretize model equations, as described in Section 4.1.4. It is assumed that the hierarchical tissue begins in the healthy steady state determined by the MSMAHR model in equation set 4.1. As a result, the number of stem cells and the maturity distribution of differentiating cells for healthy tissue in homeostasis is the initial condition for simulations of tumorigenesis. Parameter values used to simulate healthy and mutated cells are presented in Table 4.2.2.

Because cancer stem cells are believed to drive tumor growth, the emergence of the first cancer stem cell establishes the onset of malignancy. As a result, the time required to generate the first cancer stem cell is recorded for each mutation pathway in order to determine which is the fastest in cancer development.

Four scenarios of mutation acquisition are investigated. In the first case, all mutations are advantageous and increase the cell's competitive advantage in some way. In the second case, mutations occurring in cells that have not yet acquired the ability to evade apoptosis are disadvantageous and increase cell death. The third case investigates the effects of a shift in the stem-cell division pattern that increases symmetric self-renewal. Finally, increased expansion in the progenitor pool due to

extra divisions is explored in the fourth case.

All Mutations are Advantageous

Consider a case in which all mutations are advantageous, which for convenience shall be referred to as Case A. In particular, suppose all mutations give the cell a specified advantage over its normal counterpart and do not cause an increase in cell death upon mutation. Specifically, the D mutation decreases the probability of stem-cell death by half and the decreases the death rate of differentiating cells by half. The G mutation augments genetic instability, increasing the rate at which mutations are acquired from 10^{-6} to 10^{-4}. The R mutation doubles the proliferation rate of both stem and progenitor cells. It is worth noting that progenitor cells with the R mutation reach full maturity in half the time of normal cells since the cells are dividing twice as fast but this mutation does not increase the number of divisions they are able to complete.

Under these conditions, genetic instability is the most significant contributor to cancer onset. The GDR and GRD pathways produce the first cancer stem cell in the shortest time, followed by the DGR and RGD pathways, and finally the DRG and RDG pathways. Figure 4.5 plots the cancer stem cells and cancer non-stem cells for each pathway over time, and illustrates that there is negligible difference between the GDR and GRD pathways, between the DGR and RGD pathways, and between the DRG and RDG pathways. Thus, it is evident that the order in which the G mutation is acquired determines the speed of cancer stem cell generation.

The fastest pathways are those in which G is acquired first, while the slowest acquire G last. The significance of the G mutation may at first seem surprising because it does not increase the cell's fitness as the D and R mutations do. In fact, the G mutation might be thought of as a silent mutation that does not appear to

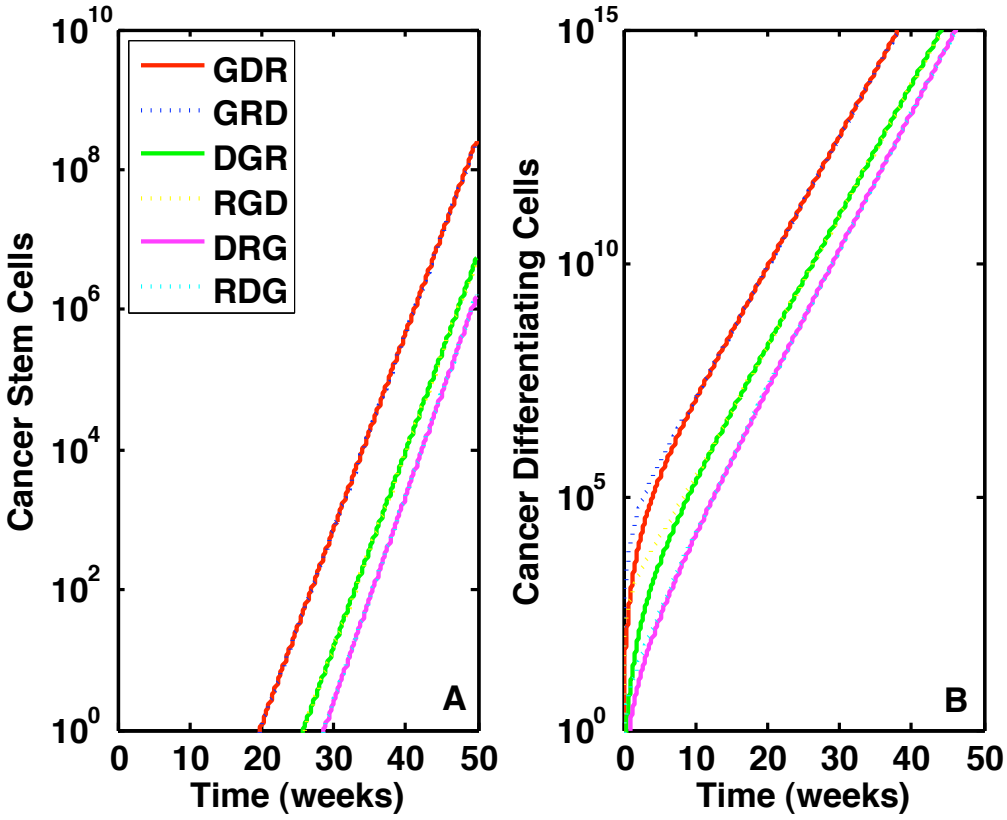

Figure 4.5: **Genetic instability determines the fastest path when all mutations are advantageous.** (A) Cancer stem cells for each pathway versus time. The order in which genetic instability is acquired has the greatest influence on determining tumor growth. Pathways in which G is acquired first are the fastest, while those that acquire G last are slowest. (B) Cancer non-stem cells reflect the behavior of cancer stem cells.

give the mutated cell any advantage. However, the acquisition of G accelerates the rate at which additional mutations are acquired, and therefore decreases the time required to generate the first cancer stem cell.

The sequential order of the G mutation is the most important in determining the fastest pathway, but no such conclusion can be made about the order of D and R mutations. Whether D or R occurs earlier in the fastest pathway depends on the amount of change between normal and mutated proliferation and death rates. For instance, using certain parameter values, GDR could be the fastest, while for others it would predict that GRD is fastest. Over a wide range of parameters, however, the impact of the G mutation is still most significant in determining the time to cancer onset. As a result, the conclusion that genetic instability dictates the time to malignancy is robust.

As shown in Figure 4.5, cancer differentiating cells are present in the tissue at early times. In fact, all pathways generate a small number of cancer differentiating cells years before the first cancer stem cell emerges. In this case it is assumed that no mutation occurs in progenitor populations that arrests differentiation. As a result, mutated differentiating cells may cause hypercellularity in the tissue, but they do not instigate malignancy because they die after completing a prescribed number of divisions. Instead, it is the emergence of the first cancer stem cell that marks the onset of disease because these cells can both self-renew to expand their number and differentiate to form mutated differentiating cells.

From Figure 4.5, one may also notice the correlation between the growth dynamics of the stem-cell population with those of the differentiating population. The model predicts that tumor growth is dependent upon the behavior of a small subpopulation of cancer cells. Therefore, under the assumptions of Case A, the model supports the

cancer stem cell hypothesis in that a select subgroup of cells promotes tumorigenesis. That is, if differentiating cells do not acquire self-renewal capability, then a small population of mutated stem cells is the driving force in tumor growth.

Death Increases Without an Anti-apoptotic Mutation

Because cell division is a tightly regulated process, the presence of mutations can force apoptosis. This defense mechanism prevents the propagation of mutations to progeny, thereby maintaining the genetic integrity of cells in the tissue. As a result, cells that have become transformed are more prone to programmed death unless they have also acquired a mutation that allows them to evade apoptosis. The next case, labeled Case B, investigates the consequences of increased death in cells that have acquired either R or G without obtaining D previously.

Suppose the mutations are defined as in Case A, with the additional condition that cells with either a G or R mutation have a higher death rate if D has not previously been acquired. The DGR and DRG pathways do not change in comparison with Case A since the D mutation is acquired first, but all other pathways are affected. Figure 4.6 demonstrates that cancer onset is delayed in pathways in which D is not acquired first. Specifically, in sequences where D is acquired second, the first cancer stem cell appears approximately ten years later than it did in case A for parameter values found in Table 4.2.2. When D is acquired last, the first cancer stem cell appears approximately twenty years later than it did for the same sequence in Case A. These results suggest that the acquisition of a mutation decreasing cell death is most advantageous in producing cancer cells if mutations are lethal. This follows from the fact that in this simulation, cells with only R and G mutations are suppressed through apoptosis, whereas cells with the D mutation can expand. For that reason, it is not surprising that the DGR pathway is the fastest, with the

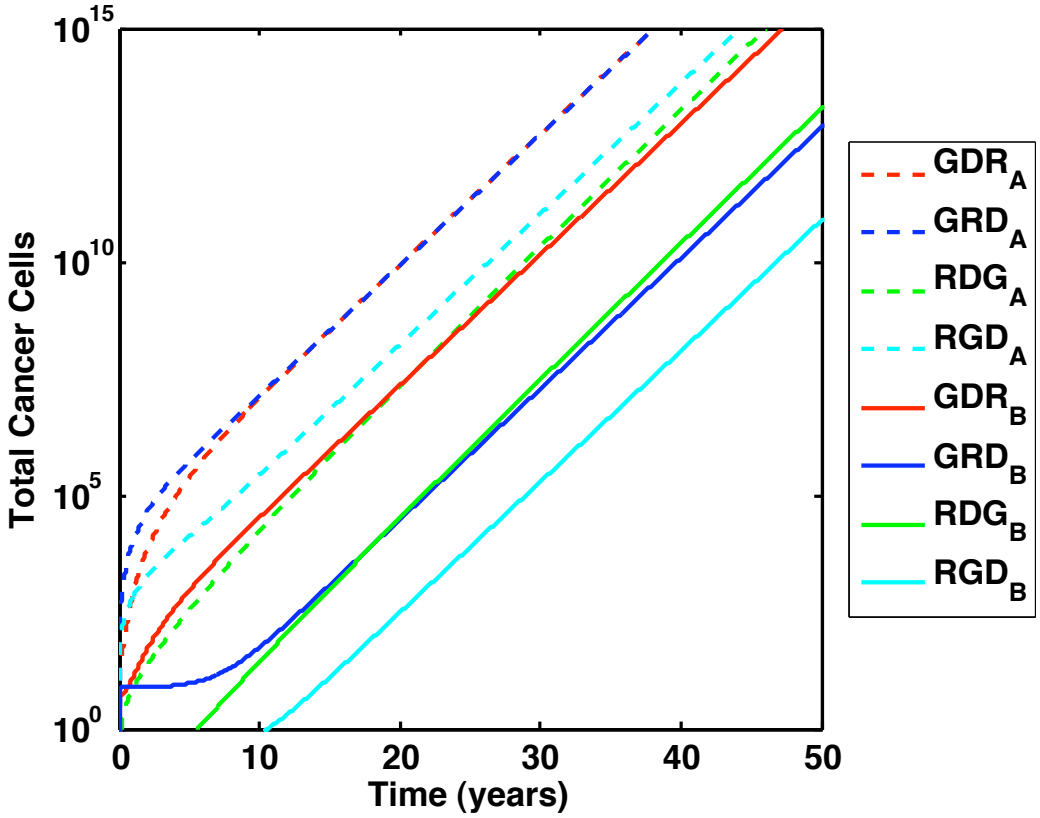

Figure 4.6: **The emergence of cancer is slowed when all mutations are not advantageous.** The emergence of cancer is delayed in pathways in which the D mutation is not acquired first. Case A is plotted with dashed lines while case B is plotted with solid lines.

first cancer stem cell appearing in 25.8 years, while the RGD pathway is slowest and produces the first cancer stem cell in 46.4 years.

The contrasting results from Case A and Case B demonstrate that the fastest pathway is dependent upon the assumptions that are made to characterize mutations. When all mutations are advantageous as in Case A, acquiring the G mutation first leads to the fastest appearance of a cancer stem cell. On the other hand, when mutated cells have increased death without the ability to evade apoptosis as in Case B, acquiring the D mutation gives rise to the first cancer stem cell. In addition, the tissue composition of the fastest pathway from Case A, denoted GDR_A, and the fastest pathway from Case B, denoted DGR_B, are notably different, as illustrated in

Figure 4.7. Following the GDR_A pathway, the majority of cells are normal for the first 28 years, after which cancer cells dominate, while cells with one or two mutations remain a small portion of the system, as shown in Figure 4.7A. Compare this with the tissue composition of the DGR_B pathway plotted in Figure 4.7B. Normal cells are the majority until 31 years, after which cells with one mutation, namely the D mutation, are most numerous. Cells with the D mutation dominate until cancer cells surpass them at 36 years. Thus the decline of normal cells in the system is comparable between the two pathways, but the system following the GDR_A pathway is usurped by cells having all three mutations, whereas the tissue following the DGR_B pathway first fills up with cells having only one mutation before being filled with cancer cells. The dominance of cancer is nearly thirteen years faster in GDR_A than in DGR_B, indicating that the disease created through the former is more aggressive than the latter.

Due to cellular machinery that arrests proliferation of mutated cells, it is likely that mutations would be detected that would force the cell into apoptosis unless the machinery itself was also erroneously transformed. Consequently, the assumptions of Case B are likely a more realistic depiction of mutation acquisition in human cells. In this case, acquiring the D mutation first bears greatest importance since it ensures the cell's survival, allowing it to accumulate further abnormalities. As in Case A, the population of cancer stem cells drives tumorigenesis and is a very small minority of all tumor cells.

Unbalanced Stem-Cell Division Pattern

Deregulation of cell proliferation can refer either to the alteration of proliferation rate or the transformation of cell division pattern. Both Cases A and B defined the R mutation as an increase in proliferation rate. Now consider Case C in which the

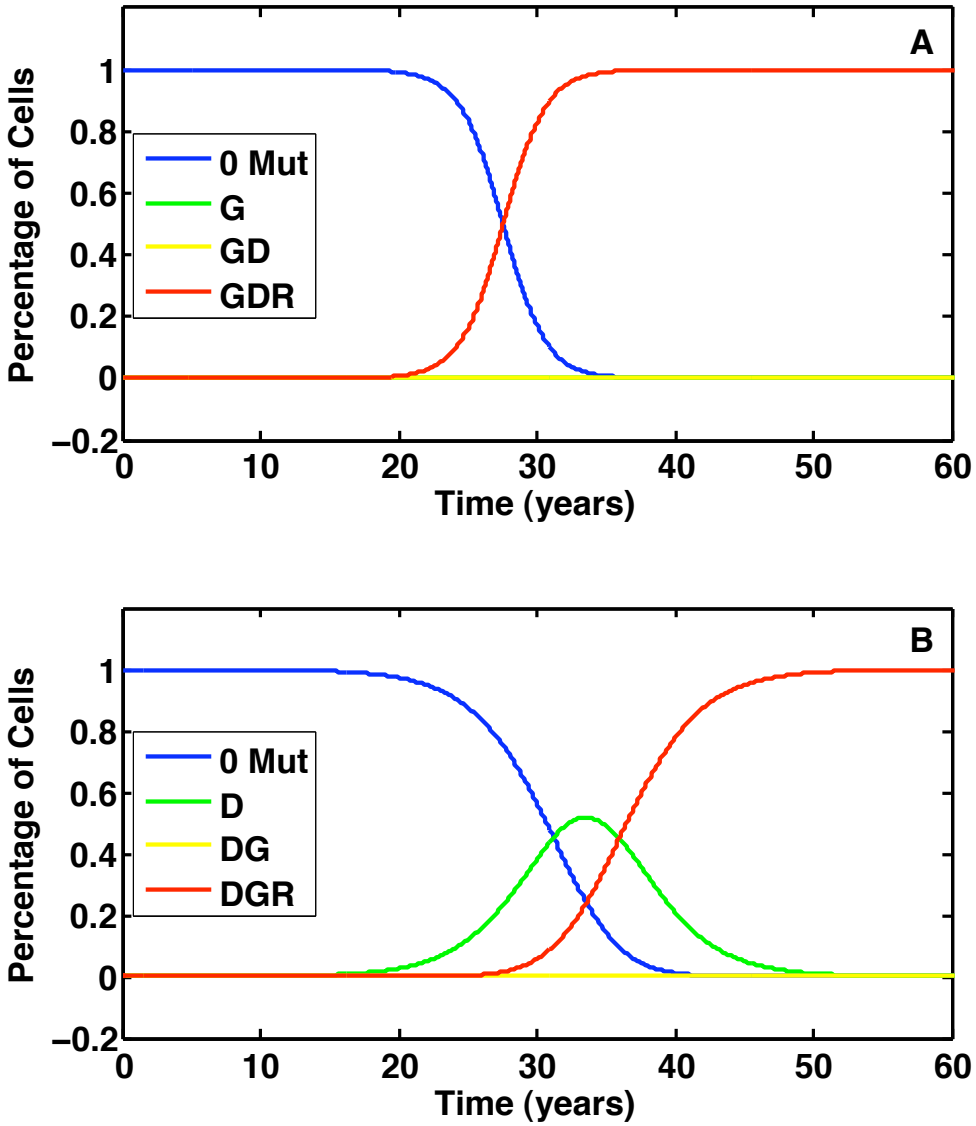

Figure 4.7: **Comparison of tissue composition for fastest paths when all mutations are advantageous versus when some are lethal.** (A) The changing tissue composition in the GDR pathway, fastest for Case A in which all mutations are advantageous. Within 28 years, cancer cells dominate the tissue. (B) The changing tissue composition for the DGR pathway, fastest for Case B in which R and G are not advantageous without D first. At approximately 31 years, cells with the D mutation are the majority, but cancer cells increase and take over the tissue in 36 years.

R mutation doubles the probability of symmetric self-renewal in stem cells, while the proliferation rate of stem cells and the division properties of progenitors are unaltered. In essence, progenitor cells with the R mutation do not behave differently than those without the R mutation, but stem cells with the R mutation are more likely to symmetrically self-renew than normal stem cells. The G and D mutations are defined as in Case A, and it is assumed that all mutations are advantageous.

Increasing symmetric self-renewal significantly quickens the pace of cancer development. In fact, all pathways have a first cancer stem cell within eight years. The fastest pathway is the GRD pathway, with the first cancer stem cell formed in 5.5 years, but the slowest pathway, DRG, is less than three years slower. Therefore, the difference between the fastest and slowest pathways is relatively insignificant, implying that increased symmetric self-renewal minimizes the impact of other mutations. In other words, when a mutation increases symmetric self-renewal, cancer stem cells rapidly emerge in all pathways so that the order of mutation acquisition does not meaningfully influence the time to first cancer stem cell.

Figure 4.8 compares the time to first cancer stem cell for each pathway in Cases A, B, and C. Cancer stem cells in Case C emerge 15 to 20 years faster than in Case A and 20 to 40 years earlier than in Case B. The speed of disease onset suggests that aberrant symmetric self-renewal may be a key contributor in aggressive forms of cancer, whereas deregulated cell proliferation may be characteristic of diseases that progress more slowly. Furthermore, increased symmetric self-renewal appears to diminish the impact of genetic instability because the difference between slowest and fastest pathways is relatively insignificant.

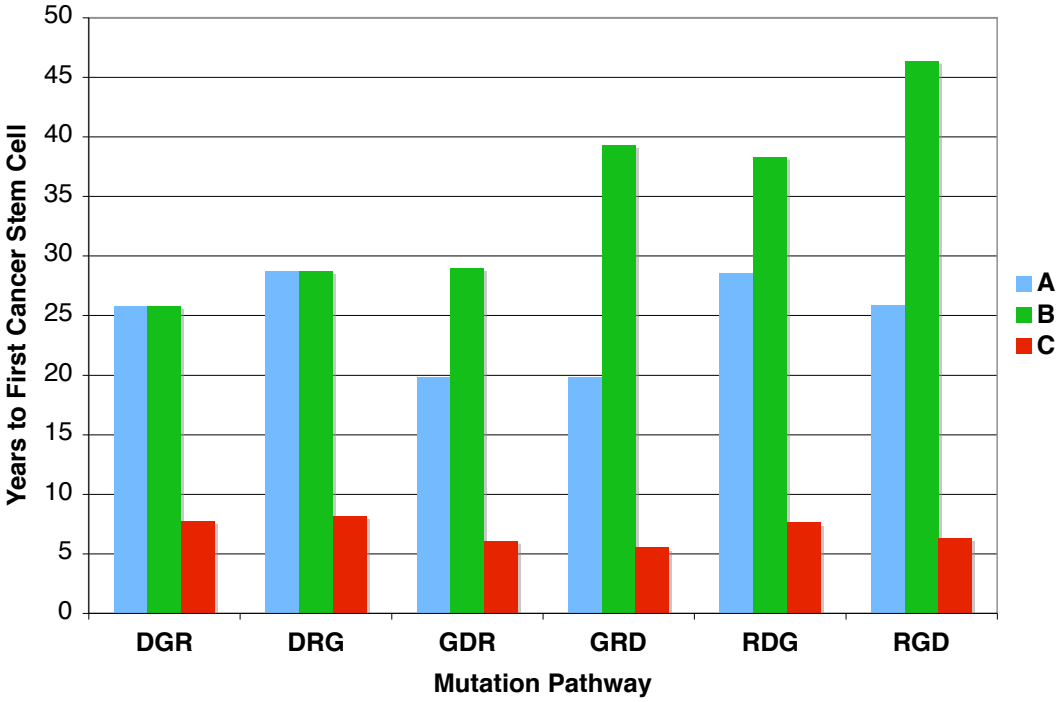

Figure 4.8: **Unbalanced symmetric self-renewal significantly decreases the time to cancer.** When stem-cell division pattern is unbalanced with an increase in symmetric self-renewal, cancer stem cells rapidly develop.

Progenitors Complete Additional Divisions

It is unknown if cancer stem cells are mutated stem cells or mutated progenitor cells that have gained stem-cell characteristics, particularly the ability to self-renew. To address this issue, Case D assumes the R mutation affects the proliferation of progenitor cells by increasing the number divisions before terminally differentiating. Stem cells may acquire the R mutation, though it does not alter the stem-cell kinetics and therefore acts as a pre-cancerous mutation that later manifests in progeny that are more differentiated. The proliferation rate of both stem and non-stem cells does not increase with the R mutation so that this mutation only increases the number of progenitor divisions. As in Cases A, B and C, the D mutation decreases apoptosis, the G mutation increases the mutation rate. In addition, it is assumed that all mutations are advantageous.

The time to first cancer stem cell is slower for all six pathways than in the previous cases because mutated stem cells do not proliferate faster or symmetrically self-renew more than normal stem cells. However, progenitor and differentiated populations expand due to the extra divisions completed by progenitors, as shown in Figure 4.9A. The percentage of tissue cells having one mutation is plotted in Figure 4.9B. The DGR pathway, in which R is acquired last, is the only pathway in which a majority of tissue cells have one mutation over time. As demonstrated in Figure 4.9C, the majority of tissue cells following the DRG and RDG pathways have two mutations, D and R. All other pathways are taken over by cells with all three mutations, as shown in Figure 4.9D. The hypercellularity resulting from the D and R mutations alone could lead to death as the tissue reaches a fatal burden of cells as in the DRG and RDG pathways. However, tissues following these pathways are primarily composed of cells with the D and R mutations that might be more reactive to treatment since

genetic instability has not been acquired. If treatment successfully targets cells that have not acquired all three mutations, then pathways generating tumors mainly composed of cells with all three mutations are more problematic.

Unlike Cases A, B, and C, the composition of non-stem cells in the tissue does not mirror the composition of stem cells because the R mutation only manifests itself in progenitor cells. Consider the GDR pathway, which is the first pathway to have a cancer stem cell in this case. Figure 4.10A plots the composition of the stem-cell pool over time. Normal stem cells dominate for the first forty-nine years, after which the majority of stem cells have the G and D mutations. There are a small number of cancer stem cells, and although they exceed normal stem cells in 57 years, they do not surpass those with only two mutations. In contrast, the composition of differentiated cells is markedly different, as plotted in Figure 4.10B. Cells with all three mutations take over the non-stem cell pool within 34 years, while cells with one or two mutations remain a small percentage of progenitor and differentiated cells. The contrast between stem-cell and non-stem cell compositions proves that cancer growth is due to expansion in the progenitor pool, not the stem-cell pool.

Because mutated differentiating cells continue to mature and have not acquired the ability to limitlessly self-renew, it is still the small percentage of cancer stem cells that drives tumorigenesis. Without the self-renewing cancer stem cell population, mutated differentiating cells would cause hypercellularity but ultimately reach a state of homeostasis, even though elevated. It should be noted that the R mutation is what causes significant expansion in progenitors, and the growth of cell populations with the R mutation may cause proliferative disorders, even if all three mutations have not been acquired.

This case in which R extends proliferation of progenitors without affecting stem

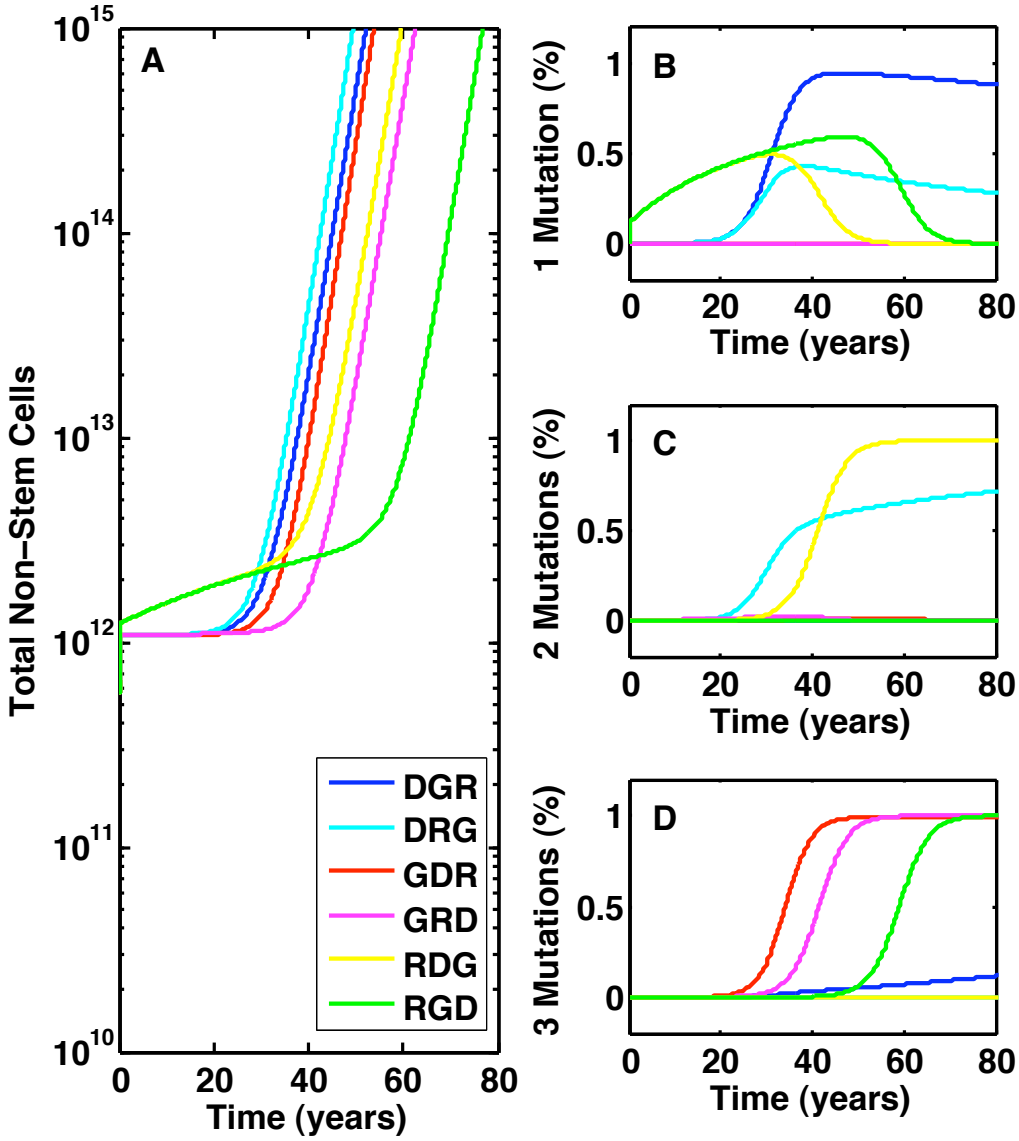

Figure 4.9: **Progenitor and differentiated cells accumulate due to extra progenitor divisions.** (A) The total non-stem cell population for each pathway. The DRG pathway generates hypercellularity the fastest. However, most of these cells only have 2 mutations. (B) The percentage of progenitor and differentiated cells that have one mutation. DGR is the only pathway dominated by cells with one mutation. (C) The percentage of progenitor and differentiated cells that have two mutations over time. Tissues following the DRG and RDG pathways are mainly composed of cells with both the D and R mutations. (D) The percentage of progenitor and differentiated cells with three mutations over time. Tissues following GDR, GRD, and RGD are eventually taken over by cancer cells.

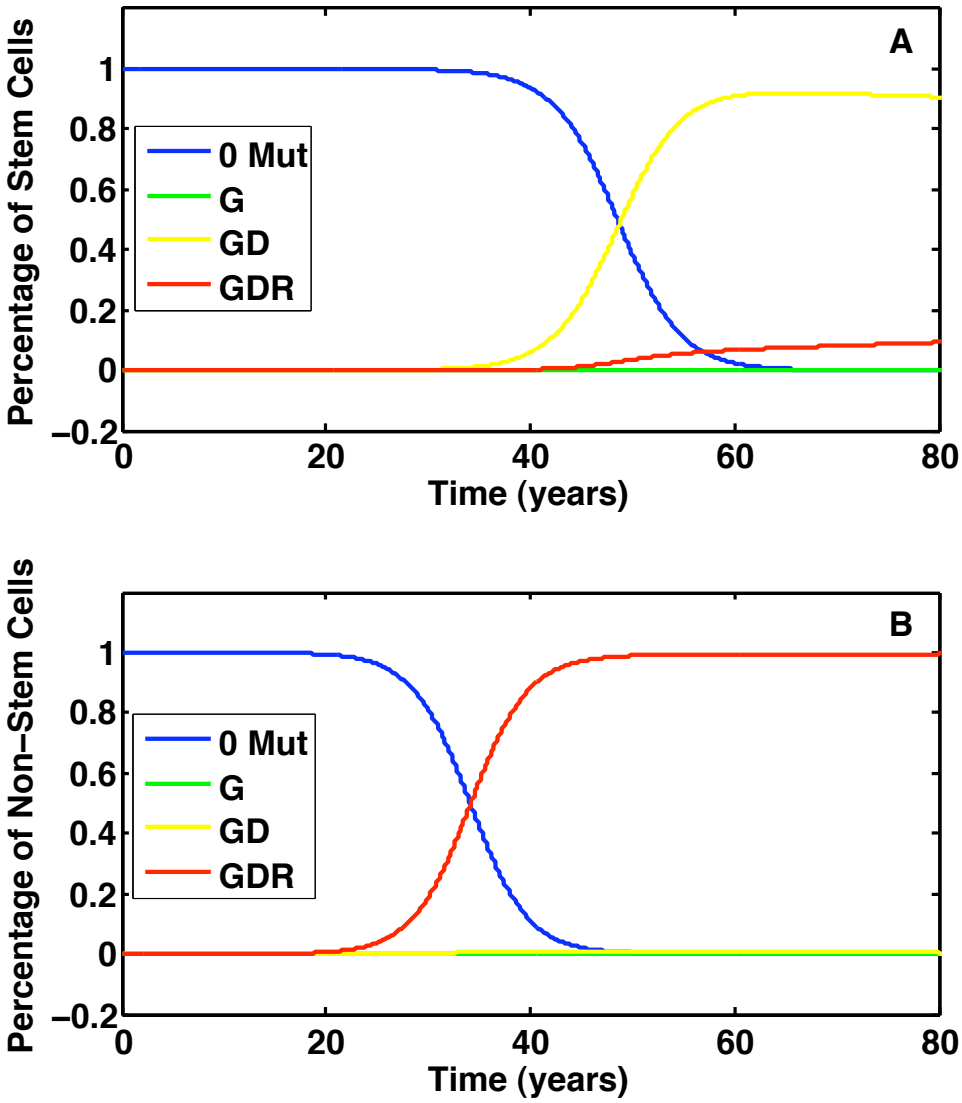

Figure 4.10: **Comparison of stem cell composition and non-stem cell composition for the GDR pathway in case D.** (A) The percentage of stem cells with 0, 1, 2, or 3 mutations over time. After 30 years, the majority of stem cells have only the D mutation. (B) The percentage of non-stem cells with 0, 1, 2, or 3 mutations. After 20 years, the majority of non-stem cells have all 3 mutations due to the extra division and amplification of progenitor cells that have acquired the R mutation.

cells is unique in that the system may reach a fatal level of cancer cells before any cancer stem cells are formed. By increasing the number of divisions progenitors complete before terminal differentiation, there is a massive expansion in mutated progenitor and differentiated cell populations and may be indicative of a myeloproliferative disease. However, this type of R mutation is not sufficient in causing cancer without pre-cancerous mutations occurring in the stem-cell pool, which is illustrated in Figure 4.11. If stem cells are capable of acquiring one, two, or three mutations, then the cancer cell population grows due to the exponential growth of mutated stem cell populations. In contrast, if stem cells do not acquire any mutations, then cancer progenitor and differentiated cells remain at low, undetectable levels because cancer progenitors eventually reach terminal differentiation and die, thereby preventing expansion. Therefore, at least one mutation must occur in stem cells that initiates exponential growth in order to generate malignancy.

These results indicate that unless progenitor cells acquire a mutation that permits them to self-renew and prevent maturation as stem cells normally do, stem-cell mutations are critical in promoting tumorigenesis. However, the model predictions from Case D demonstrate the substantial impact that extra progenitor divisions have on tissue hypercellularity. As a result, it is hypothesized that progenitor self-renewal would generate an even greater increase in tissue mass and would be a more aggressive disease. Such a mutation is believed to facilitate the transition between chronic to blast phase in Chronic Myelogenous Leukemia. As a result, the possibility of progenitors gaining limitless self-renewal potential will be investigated later in Chapter VIII, where a mathematical model is presented that simulates disease progression in Chronic Myelogenous Leukemia.

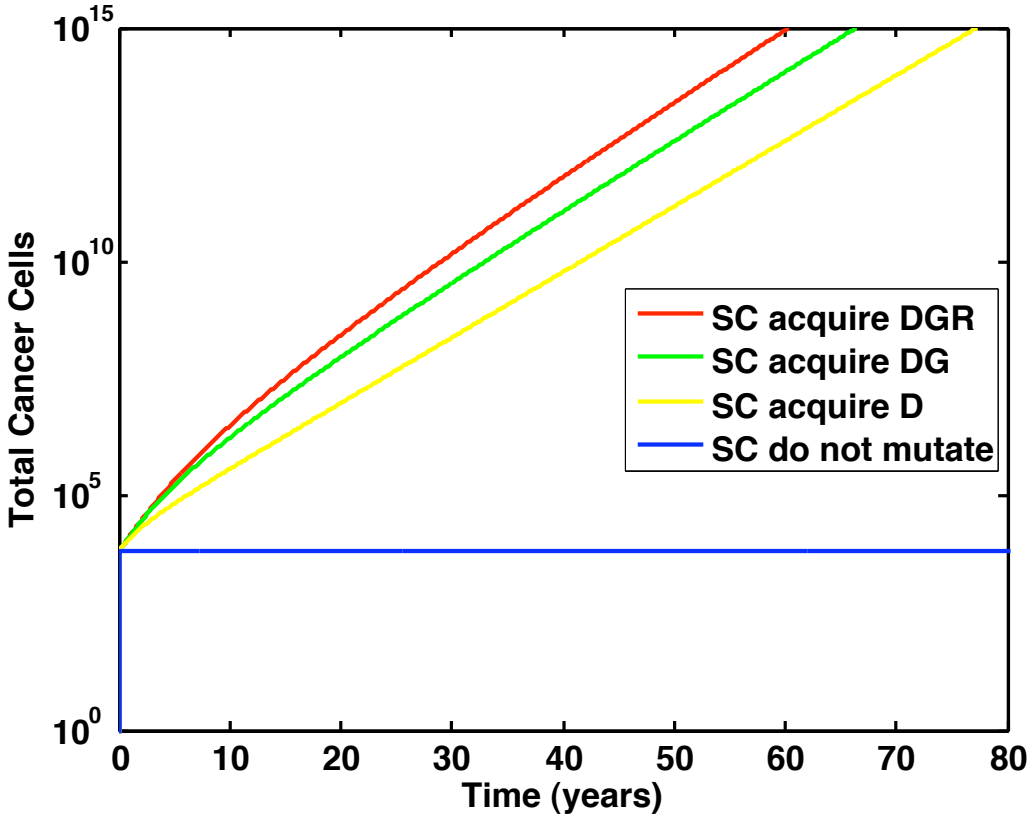

Figure 4.11: **At least one mutation is needed in stem cells for malignant tumor growth.** Cancer growth is fastest when stem cells acquire all three mutations, but cancer growth still occurs when one or two mutations may be acquired at the stem cell level. When stem cells do not mutate, increased progenitor expansion alone is not sufficient to cause malignant growth.

4.3 Conclusions

Although many types of mutations have been identified in cancer cells, it is difficult to determine the order in which they were acquired that led to malignancy. In this chapter, mutation acquisition in hierarchical tissue has been examined with a maturity-structured mathematical model in order to investigate the impact that mutation order has on tumor dynamics. In particular, the sequential accumulation of somatic mutations was modeled to examine the multi-step process that initiates cancer. Importantly, it was concluded that the order in which mutations are acquired does affect the tempo of tumorigenesis. In addition, tumor composition varies for different mutation pathways, so that some sequences generate tumors that are dominated by cancerous cells, while others are primarily comprised of cells with only one or two mutations.

For each mutation pathway considered, the time to first cancer stem cell determined the onset of malignancy, so that the fastest pathway could be established. If all mutations are advantageous, genetic instability is the key determining factor for the emergence of cancer stem cells, and this result is robust for a wide range of parameters. The fastest pathways acquired genetic instability first, which agrees with the results of Michor *et al.*, who predicted that chromosomal instability was an early event in colon cancer [84]. This result differs from the work by Spencer *et al.*, who predicted that the fastest pathway to cancer ends with genetic instability. Rather than following the particular order in which mutations accumulate, however, Spencer *et al.* did not distinguish the chronological order of mutations that generated cells with a particular phenotype. In contrast, the predictions presented in this chapter suggest that the specific sequential order of mutation acquisition decisively

influences tumor dynamics.

In addition to the importance of mutation sequence, model predictions indicate that certain types of mutations are more significant than others in dictating cancer onset. For instance, when all mutations are advantageous, acquiring genetic instability first leads to the fastest path. In contrast, if mutations are lethal when evasion of apoptosis has not yet been acquired, then the fastest pathways are initiated with mutations decreasing cell death. Particularly significant are mutations that cause the stem-cell division pattern to be unbalanced in the favor of symmetric self-renewal. Increased symmetric self-renewal significantly quickens cancer onset and progression because it rapidly expands the cancer stem cell population. Furthermore, it diminishes the importance of all other mutations in that cancer stem cells emerge in all pathways within a relatively short time of each other.

When mutations affect stem and progenitor cells similarly, the model predicts that the dynamics of the differentiating-cell population are dictated by the dynamics of the stem-cell population. As a result, the cancer stem cell population is the driving force of tumor growth. However, if a mutation is acquired in stem cells, but is not manifested until inherited in a progenitor, then the dynamics of stem cells and non-stem cells do not closely correlate. For example, a mutation that increases the number of progenitor divisions contributes to hypercellularity and tumorigenesis, even before the formation of cancer stem cells. Yet, if progenitor and differentiated cells do not acquire limitless self-renewal potential, malignancy does not form unless some initial mutations occur in the stem-cell population. This result demonstrates the driving force of cancer stem cells in tumor formation and disease progression. Furthermore, the model predicts that the cancer stem cell population is a small minority of tumor cells for all cases discussed in this chapter. Because differentiation

pathways are not disabled, mutated progeny continue to expand and mature, forming cancerous differentiated cells that significantly outnumber stem cells. According to model results, it is predicted that the percentage of tumor cells that are cancer stem cells significantly increases only if differentiation is somehow inhibited.

The mathematical model presented in this chapter provides a general framework that could be used to investigate tumorigenesis in any hierarchical tissue. To demonstrate the usefulness of this model, simulations of mutation acquisition in hematopoietic cells were conducted, but the model structure is general enough to be adapted to other tissues and include any number of mutations. The maturity structure offers unique insight into the maturity distribution of tumor cells, which may be beneficial for studying malignancies in which the distribution of stem, progenitor, and differentiated cells is significantly altered. Another novel feature of this model is the incorporation of all three modes of stem-cell division, which makes it possible to determine the effects on tumor dynamics when the balance is deregulated. In this model, it is assumed the probabilities of symmetric self-renewal, asymmetric self-renewal, and symmetric commitment differentiation are constant and regulatory mechanisms governing stem-cell division pattern are not incorporated. There are many factors that influence self-renewal and differentiation, however, which motivates the investigation of stem-cell regulation in the next chapter.

CHAPTER V

Regulatory Mechanisms in Hierarchical Tissue

The previous chapter introduced a mathematical framework for hierarchical tissue in which stem cells were modeled with an ordinary differential equation while differentiating cells were modeled with a maturity-structured partial differential equation. The Maturity-Structured Model in the Absense of Homeostatic Regulation (MSMAHR) presented in Equations 4.1 used constant probabilities to determine the outcomes of stem-cell division. Although useful information about tumorigenesis can be obtained by starting with such a model, cellular growth dynamics in hierarchical tissue are more accurately modeled when regulatory factors governing stem-cell division are incorporated. In particular, the stem-cell niche and chemical signaling can influence both self-renewal and differentiation to promote tissue homeostasis. When constant probabilities of stem-cell division are employed, there are three possible scenarios of tissue dynamics: cell populations may exponentially grow without bound, cell populations may decline to elimination, or cell populations may remain in steady state for all time. While homeostasis is likely most common in healthy individuals, clearly there are times when tissue expansion is needed, such as in tissue generation or reconstitution after injury, and others when suppression is required, such as when correcting hypercellularity. Because cellular kinetics can adjust in accordance with

tissue demands, the MSMAHR model is insufficient in capturing the intricacies of feedback regulations acting within hierarchical tissue. Rather, probabilities of stem-cell self-renewal and differentiation are likely dependent upon the number of stem and differentiated cells within the tissue, thereby necessitating a non-linear model.

It is not surprising that abnormalities in tissue regulation can potentially instigate tumor formation. Therefore, mathematical investigation of feedback interactions may highlight the types of genetic mutations that cause greatest malignancy within hierarchical tissue. However, in order to understand how irregularities contribute to tumorigenesis, it is necessary to first validate a model that accurately simulates healthy tissue. This chapter incorporates mechanisms that regulate stem-cell division and quiescence in order to mathematically simulate homeostasis of the hematopoietic system. First, biological background of regulatory mechanisms is reviewed. Then, an introductory mathematical model is developed to fit experimental data of the stem-cell division pattern. Subsequently, cycling and quiescent stem cells and differentiated cells are incorporated into a non-linear model of ordinary differential equations, which is then used to simulate tissue generation. In contrast with the MSMAHR model, intermediate classes of differentiating cells are not explicitly modeled, thereby removing the maturity-structured partial differential equation modeling non-stem cells. Instead, terminally differentiated cells are assumed to have reached full maturity and are modeled with an ordinary differential equation. This was done to focus more on regulatory mechanisms governing the stem-cell population without added complexities from the maturity structure. In Chapter VIII, a model will be introduced that incorporates both regulatory mechanisms in stem cells and a maturity-structured population of differentiating cells. Finally, this chapter concludes by discussing the significance of feedback regulations contributing to tissue

homeostasis.

5.1 Regulation of Tissue Homeostasis

The proliferation of stem cells is a tightly regulated, yet responsive, process, controlled by various mechanisms that are not fully understood. For instance, certain chemical signals may promote stem-cell self-renewal, while others initiate differentiation in response to a need for additional mature cells [89, 125]. Furthermore, environmental cues also influence stem-cell division [125]. Changes in the microenvironment have the ability to alter stem-cell function and in some cases, could lead to malignancy, so it is important to understand how interactions within the surrounding microenvironment affect stem cells [2].

5.1.1 The Stem-Cell Niche

Because the percentage of stem cells in healthy tissues is very small, these cells must be protected and maintained through tight regulation. It is believed that the stem cell niche is crucial in both aspects [42, 95, 126]. The niche is the microenvironment composed of neighboring cells and cytokines that surround the stem cells in a tissue [126]. One of the obstacles in stem-cell research is the inability to scientifically reconstruct niches, which makes it difficult to maintain stem cells *in vitro* because signals from the niche affect stem-cell survival, proliferation and differentiation [42, 95, 126].

In recent years, researchers have investigated the importance of the stem-cell niche in various tissues such as bone marrow, testis, hair follicle, colon, ovary, and brain [42]. The mathematical model presented in this chapter investigates tissue homeostasis in the hematopoietic system, therefore the bone marrow niche of hematopoietic stem cells (HSCs) is now discussed. The bone marrow is composed

of red and yellow marrow. Fatty cells constitute yellow marrow, while red marrow is responsible for blood cell production [39]. Soft bone marrow and blood vessels comprise the inner bone cavity, while the rigidity of the outer bone capsule provides external protection and maintains the balance of pressure needed to release appropriate amount of new blood cells into circulation [39, 126]. Many details regarding the hematopoietic stem cell niche remain uncertain, but it is believed that endosteal, vascular, and perivascular cells may all play a role [66].

The stem-cell niche also includes cytokines that are found in the microenvironment. Several proteins are associated with stem-cell maintenance and differentiation, and scientists have recently begun identifying these molecules and their functions. For instance, the expression of Notch, a transmembrane protein used in cell-to-cell communication, may promote stem-cell quiescence, and integrins may affect the interactions between stem cells and the extracellular matrix [42]. The growth-promoting Wnt family of proteins are prevalent during embryogenesis and may play a role in cell proliferation and differentiation [42]. Independence from the control of niche signaling leads to cancer, which is further evidence that the niche is crucial in maintaining tissue balance. Loss of tumor suppressor Pten causes HSC mobilization and leukemia [76]. Alteration in the balance between the anti-growth bone morphongenic protein, BMP, and Wnt signaling promotes tumorigensis [74, 76]. Therefore, it is clear that signaling pathways in the niche mediate tissue homeostasis.

It is known that a small number of hematopoietic stem cells circulate in the blood, but their function remains a mystery [70]. Stem cells may temporarily leave the niche and maintain stemness through mobilization, and return to the niche in a process known as homing [70, 126]. Stem-cell mobilization and homing are crucial for successful stem-cell transplantation, and will only occur if the niche is intact [39]. While

all of the mechanisms involved in mobilization and homing are not fully understood, it is known that the niche significantly impacts the maintenance and growth of stem cells.

5.1.2 Signals Promoting Differentiation

Within hierarchically structured tissues, immature progenitors are responsible for expanding and eventually differentiating into fully mature cells that carry out specific functions for the tissue. Hematopoietic stem cells are precursors for all types of blood cells including lymphocytes, macrophages, erythrocytes, platelets, and granulocytes. Chemical signaling may influence the proliferation and differentiation of stem cells into different progeny types as demanded. Several colony-stimulating factors have been identified in the hematopoietic system that impact stem and progenitor cell behavior. Interleukin-3, IL-3, has been used as part of stem-cell mobilization regimens and promotes the survival and proliferation of progenitors to increase production of various differentiated progeny including macrophages, granulocytes, mast cells, megakaryocytes, and erythrocytes [9, 86]. Macrophage colony-stimulating factor, M-CSF, and granulocyte colony-stimulating factor, G-CSF, promote survival, proliferation, and differentiation of mature and precursor macrophages and granulocytes, respectively [9, 30].

Additional knowledge of the role of G-CSF is of particular interest in developing a mathematical model of stem cells and neutrophils. G-CSF is the primary signal involved in promoting the survival, proliferation, and differentiation cells within the neutrophil lineage, and it is essential for terminal differentiation of mature neutrophils [9]. In an immune response, G-CSF is produced by monocytes and macrophages. It then binds to cells expressing the G-CSF receptor, which are primarily neutrophils and their precursors [9]. It is interesting to note that G-CSF

receptors are not expressed by cells of the erythroid or megakaryocytic lineage [30]. Thus G-CSF binding is a mechanism specifically used to maintain homeostasis of granulocytic cells in that its presence promotes differentiation and ensures a sufficient neutrophil response, but its absence prevents hypercellularity by inhibiting surplus production [9].

5.2 Stem-Cell Division Pattern

It is believed that stem cells are capable of three types of division: symmetric self-renewal (SSR), asymmetric self-renewal (ASR), and symmetric commitment differentiation (SCD). It is difficult to determine the mode of stem-cell division experimentally, but current investigation continues to identify potential signals that promote self-renewal and differentiation. In a recent experiment, Wu *et al.* used time-lapse imaging techniques to record the divisions of murine hematopoietic precursor cells *in vitro*. Immature cells were isolated by expression of the GFP marker, which is downregulated as cells differentiate. Over the course of three days, GFP+ cell division was recorded to investigate the effects of both extrinsic and intrinsic cues on cell proliferation and self-renewal [125]. Although *in vitro* observations cannot possibly mirror *in vivo* human hematopoietic stem cell kinetics perfectly, the experimental data quantifies all three types of stem-cell division in mammals and provides an opportunity to determine appropriate parameter values, which will be useful in subsequent modeling investigations.

5.2.1 Mathematical Modeling of Feedback Mechanisms Governing Stem-Cell Division

The *in vitro* experiment by Wu *et al.* is certainly a simplification of the behavior of stem and progenitor cells *in vivo*, but it provides rare data on the division pattern of stem cells. Unfortunately, scientists are currently unable to monitor stem-cell kinetics

and division patterns *in vivo*, which makes it difficult to create a mathematical model that accurately simulates *in vivo* behavior. Modeling these *in vitro* results may assist in quantifying parameters that would otherwise be unattainable. Consequently, a simplified model of stem and early progenitor cells is now used to investigate stem-cell division patterns.

The experimental data may be modeled with a system of differential equations for two types of cells, GFP+ and GFP-. The GFP+ cell population, denoted S, contains the most immature cells, including stem cells, while the GFP- cell population, denoted N, consists of cells more differentiated. Every successful GFP+ division results in one of three fates: symmetric self-renewal (SSR) with probability α_S, asymmetric self-renewal (ASR) with probability α_A, and symmetric commitment differentiation (SCD) with probability α_D. Therefore, $\alpha_S + \alpha_A + \alpha_D = 1$. Furthermore, GFP+ cells divide at rate k and die with rate δ_S, and GFP- cells die with rate δ_N. GFP- cells are formed through asymmetric and differentiation divisions of the GFP+ population. The amplification factor, A, incorporates the average number of progeny resulting from the differentiation of a precursor cell as well as the rate of division for GFP- cells, which was not directly measured in the experiment. Using an amplification factor to eliminate the need for explicitly modeling all intermediate cellular populations has been done in various mathematical models of hematopoiesis [13, 24, 83]. The resulting model is a system of two ordinary differential equations:

$$\begin{aligned} \frac{dS}{dt} &= \left[k\left(\alpha_S - \alpha_D\right) - \delta_S\right] S \\ \frac{dN}{dt} &= \left(2\alpha_D + \alpha_A\right) kAS - \delta_N N \end{aligned} \tag{5.1}$$

where

$$\begin{aligned} \alpha_S(S) &= (1-\delta_S)\left(\frac{\theta_S^n}{\theta_S^n + S^n}\right) \\ \alpha_A(S) &= 1 - \alpha_S(S) - \alpha_D. \end{aligned}$$

Symmetric self-renewal of stem cells may be controlled by both extrinsic and intrinsic chemical signaling. Certain environmental cues may promote self-renewal, while others promote differentiation. Similarly, proteins produced within the cell affect how a stem cell divides. The Hill function $\left(\frac{\theta_S^n}{\theta_S^n+S^n}\right)$ in α_S has been used in previous mathematical models of hematopoiesis and is derived from receptor-ligand binding kinetics [5, 13]. As the number of stem cells, S, approaches zero, the probability of symmetric self-renewal based on chemical signaling approaches the maximum value of one. The parameter θ_S may be interpreted as the number of stem cells at which the probability of symmetric self-renewal based on chemical signaling is equal to one-half. Higher values of the exponent $n > 0$ increase the sensitivity of GFP+ cells to the chemical signaling for symmetric self-renewal. Because the cells are monitored for three days, it is assumed that progeny cells do not reach full maturity, and thus there is no feedback of differentiated cells to affect the probability of symmetric commitment differentiation. Therefore, α_D is approximately constant over the course of three days. The model terms are summarized in Table 5.1.

5.2.2 Environmental Effects on Stem-Cell Division Pattern

To test the role of the extrinsic signaling on proliferation and division pattern, GFP+ cells were plated in two different environments. Both groups of cells exhibited similar rates of proliferation and cell death, but the pattern of GFP+ cell division was markedly different. The OP9 medium, composed of stroma cells capable of maintaining hematopoietic stem cells *in vitro*, promoted symmetric self-renewal. In

Term	Definition
S	Number of GFP+ cells
N	Number of GFP- cells
$\alpha_S(S)$	Proportion of GFP+ cells that symmetrically self-renew $= (1-\alpha_D)\left(\frac{\theta_S^n}{\theta_S^n+S^n}\right)$
α_D	Proportion of GFP+ cells that symmetrically differentiate
$\alpha_A(S)$	Proportion of GFP+ cells that asymmetrically self-renew $= 1-\alpha_S(S)-\alpha_D$
θ_S	Switch parameter of symmetric self-renewal
n	Exponent that determines sensitivity for symmetric self-renewal
k	Proliferation rate of GFP+ cells
δ_S	Death rate of GFP+ cells
A	Amplification factor
δ_N	Death rate of GFP- cells

Table 5.1: Definitions of terms used in modeling experimental data from Wu *et al* [125].

contrast, the 7F2 medium, composed of osteoblastic cells from mice, promoted differentiation and asymmetric self-renewal. It was thus concluded that environmental cues can affect the outcome of stem cell division[125].

Experimental Procedure and Results

In the experiment performed by Wu *et al.*, 5000 GFP+ cells were plated on either a 7F2 or OP9 feeder layer. Over the course of three days, division modes were observed. At the end of three days, the number of GFP+ and GFP- cells were recorded along with the average percentage of all three types of GFP+ cell division that occurred over the three days. The 7F2 feeder layer promoted asymmetric self-renewal. Of all GFP+ cell divisions, only 33% resulted in symmetric self-renewal, whereas 50% were asymmetric divisions and 17% were differentiation divisions. In contrast, the OP9 feeder layer promoted symmetric self-renewal over differentiation. Of all GFP+ cell divisions observed for three days, 60% resulted in symmetric self-renewal divisions, whereas 26% were asymmetric, and 14% were differentiation. The death rate and division rate of GFP+ cells did not vary significantly between the two different feeder layers. The different environments, however, altered the death

rate of GFP- cells. In the 7F2 medium, it was estimated that the death rate of GFP- cells was approximately twice that of GFP+ cells, while in the OP9 medium, it was estimated that the death rate of GFP- cells was approximately three to four times that of GFP+ cells [125].

Model Simulations of Experimental Data

Due to the lack of published data on the three potential outcomes of stem-cell division, these experimental results provide a rare opportunity to quantify mathematical parameters used to model regulatory mechanisms. Many of the model parameters may be determined directly from the experimental data. Specifically, the division rate of GFP+ cells, k, death rate of GFP+ cells, δ_S, probability of symmetric commitment differentiation, α_D, and death rate of GFP- cells, δ_N, were recorded experimentally. The Hill function parameters, θ_S and n, and amplification factor, A, are determined to fit the experimental results. In Table 5.2, we present the parameters used in the mathematical simulations.

For numerical simulations, the ordinary differential equation solver *ode15s* in MATLAB was used. Using the experimental initial condition of 5000 GFP+ cells and zero GFP- cells, the number of GFP+ and GFP- cells was modeled for a time span of three days. The average occurrence of each division type was found by calculating the average of the functions for α_S, α_A, and α_D over the three-day span. As demonstrated in Table 5.2, the model predictions are in coherence with the experimental data. Over the course of three days on the 7F2 feeder layer, the experimentalists found that the fraction of GFP+ cells undergoing symmetric self-renewal, asymmetric self-renewal, and differentiation was 33%, 50%, and 17%, respectively. With parameter values $\theta_S = 4,300$, $n = 2$, and $A = 1.3$, the model derives the same division fractions and predicts the three-day cell count total of 5,666 GFP+ cells

Model Comparisons with Experimental Data				
	7F2 Param. Range	7F2 Model	OP9 Param. Range	OP9 Model
k (per day) *	0.6238-0.9935	0.8087	0.6469-0.9242	0.7856
θ_S (cells) +	4,100-4,600	4,300	11,000-14,800	13,000
n +	2-4	2	2-5	2
δ_S (per day) *	0.0662-0.0959	0.0828	0.0622-0.0786	0.0744
δ_N (per day) *	$2\delta_S$	0.1756	$4\delta_S$	0.2976
A +	1.0-1.6	1.3	0.7-1.0	1.0
GFP+ cells +	N/A	5,666	N/A	12,617
GFP+ cells (%) *	$34\% \pm 5\%$	33%	$65\% \pm 5\%$	61%
GFP- cells +	N/A	11,400	N/A	8,129
GFP- cells (%) *	$66\% \pm 5\%$	67%	$35\% \pm 5\%$	39%
GFP-:GFP+ cells *	1.56-2.45	2.01	0.43-0.67	0.64
α_S (%) *	32-34%	33%	61-67%	65%
α_A (%) *	47-53%	50%	19-25%	23%
α_D (%) *	16-18%	17%	11-14%	12%
Parameters with * are experimentally determined				
Parameters with + are mathematically determined				

Table 5.2: A comparison of the experimental data with the predicted model values. Cell numbers are determined at the end of the three-day experiment. Division percentages are average values figured over the course of the experiment.

and 11,400 GFP- cells. For the OP9 feeder layer, the experimental data concluded that the fraction of GFP+ cells undergoing symmetric self-renewal, asymmetric self-renewal, and differentiation was 65%, 25%, and 10% respectively. With $\theta_S = 13,000$, $n = 2$, and $A = 1$, the model achieves these results for division pattern and predicts a three-day cell count of 12,617 GFP+ cells and 8,129 GFP- cells. A comparison of the experimental data with model predictions is presented in Table 5.2.

Figure 5.1 plots the growth dynamics of the cells in the 7F2 medium in A and B, and the dynamics of the OP9 medium in C and D. There are striking differences in both cellular composition and mode of GFP+ cell division when the 7F2 medium is contrasted with the OP9 medium. GFP+ cells plated in the 7F2 medium favor asymmetric self-renewal over other division outcomes. Consequently, the GFP+ population grows minimally whereas the GFP- cell population experiences significant expansion, as seen in Figure 5.1A. In particular, GFP- cells surpass GFP+

cells in approximately 1.3 days and by the end of the three-day experiment, GFP- cells compose 67% of all cells. In contrast, GFP+ cells plated in the OP9 medium favor symmetric self-renewal over both asymmetric and commitment differentiation divisions. As a result, it is not surprising that the GFP+ population expand considerably and remain the majority of cells over the three-day experimental course, as shown in Figure 5.1C.

The properties of cells in the 7F2 and OP9 environments are alike for proliferation and death of GFP+ cells, but the division pattern is significantly different. Therefore, it is not surprising that the majority of parameters are comparable between both cases while the switch parameter affecting symmetric self-renewal, θ_S, differs significantly. The value used for θ_S in the OP9 environment is more than three times that of the 7F2 environment. In the 7F2 environment, the probability of symmetric self-renewal due to chemical signaling is 50% when there are 4,300 GFP+ cells, but since 5,000 GFP+ cells are initially plated, throughout the three-day experiment the probability of symmetric self-renewal divisions is less than 50%, and asymmetric division is dominant. In contrast, in the OP9 environment, 13,000 GFP+ cells are needed before the GFP+ cell division mode switches from symmetric to asymmetric self-renewal, so symmetric division is dominant during the experiment. Therefore, knowing the value of θ_S is crucial in determining the balance between symmetric and asymmetric self-renewal divisions. Although this particular experimental procedure focused on the division pattern of GFP+ cells, thereby highlighting the significance of θ_S in the mathematical model, the effects of other model parameters are better understood through a sensitivity analysis.

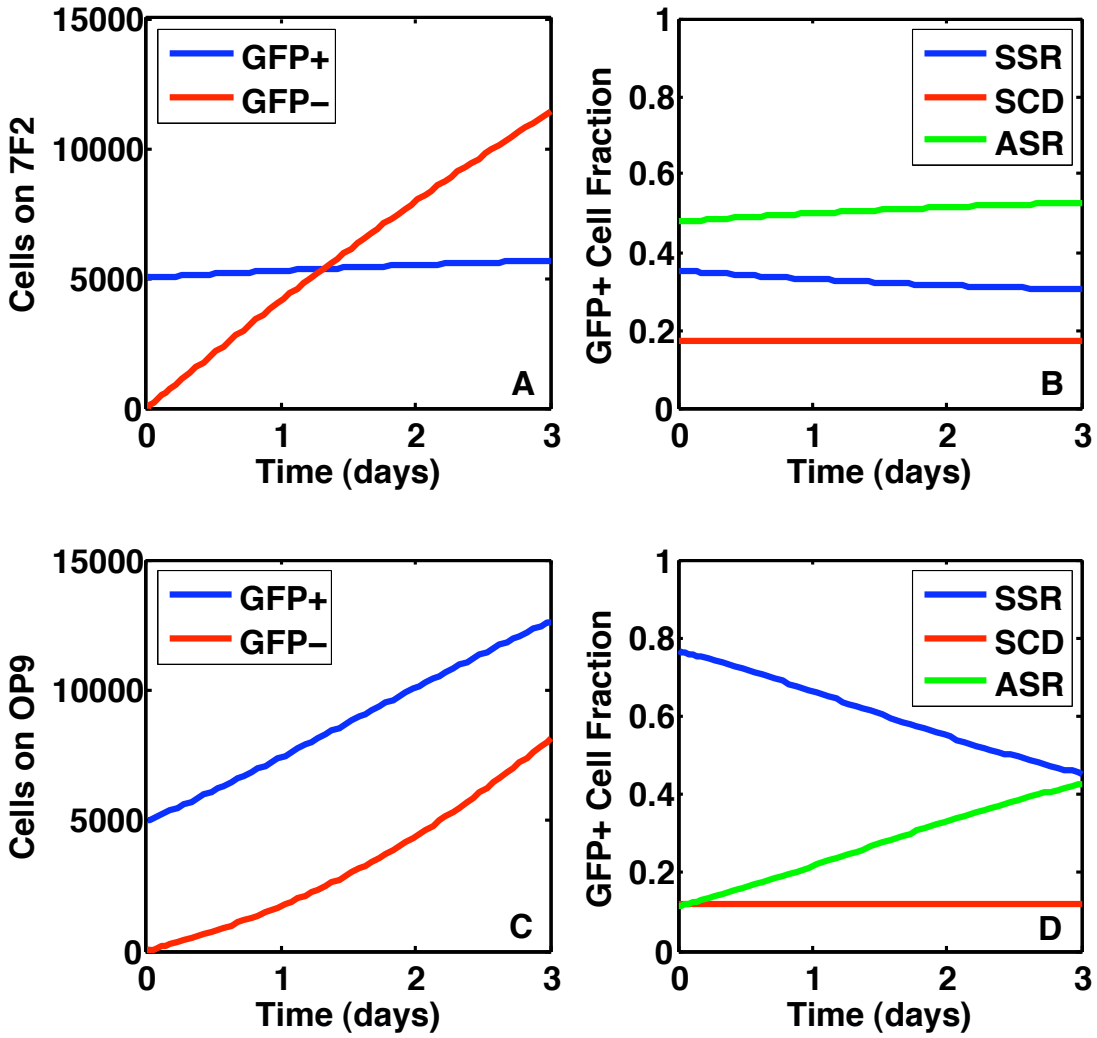

Figure 5.1: **Growth dynamics of GFP+ cells in 7F2 and OP9.** (A) GFP+ and GFP- cells in 7F2 versus time. (B) Asymmetric division is favored in 7F2. (C) GFP+ and GFP- cells in OP9 versus time. (D) Symmetric self-renewal is favored in OP9.

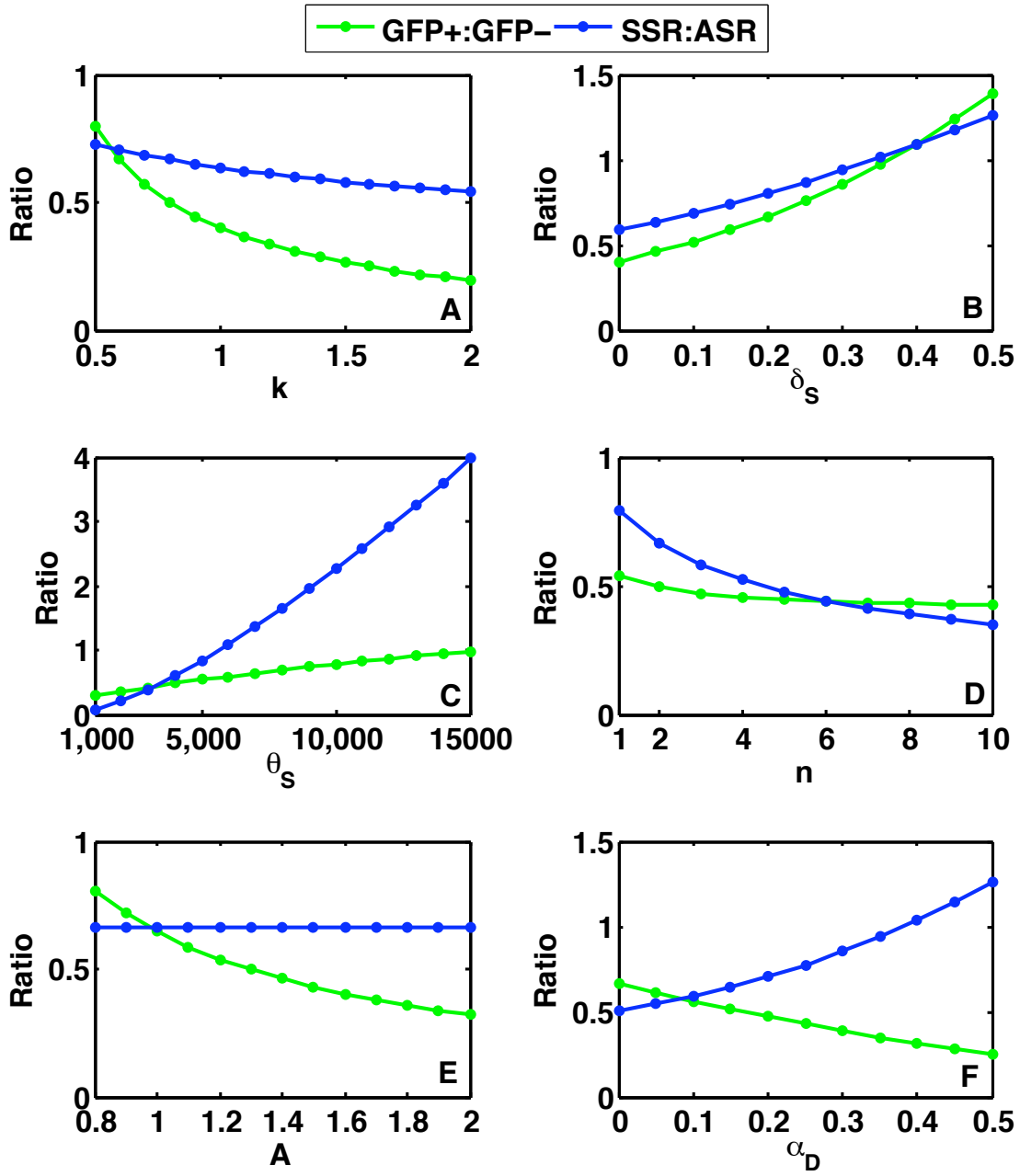

Figure 5.2: **Sensitivity Analysis.** The ratio of the number GFP+ cells to GFP- cells (green) and the ratio of symmetric self-renewal to asymmetric division (blue) are plotted as each parameter varies. Baseline parameters are taken from the 7F2 model set in Table 5.2.

Parameter Sensitivity Analysis

A sensitivity analysis can be used to determine the effects of parameter changes on the model. The sensitivity analysis was conducted for parameters used for 7F2 as opposed to OP9 because the 7F2 medium is believed to be more representative of the hematopoietic stem-cell environment for an adult human. Using the parameter values determined for the 7F2 medium, Figure 5.2 plots the ratio of GFP+ cells to GFP- cells as well as the ratio of symmetric self-renewal to asymmetric self-renewal divisions as the specified parameter varies. Cell counts and division averages are determined at the end of a three-day period of observation and then compared to the data from modeling the original experimental results.

As shown in Figure 5.2A, increased GFP+ cell proliferation decreases the ratio of GFP+ to GFP- cells. Recalling that asymmetric divisions are dominant in the 7F2 environment, increasing the proliferation rate increases the number of asymmetric divisions more than the number of symmetric self-renewal divisions, thereby increasing the GFP- cell population in comparison with GFP+ cells. Doubling the rate of GFP+ cell proliferation decreases the ratio of GFP+:GFP- cells from approximately 1:2 to 1:4, because an increase in k does not affect GFP+ steady state, but greatly increases GFP- cells. In addition, the frequency of symmetric self-renewal decreases in relation to asymmetric division. Increasing the rate of proliferation switches off symmetric self-renewal faster, thereby decreasing the three-day average. However, the ratio of divisions does not decrease as quickly as the ratio of cells. In contrast, increasing GFP+ cell death increases both ratios, as demonstrated in Figure 5.2B. An increase in δ_S decreases the number of GFP+ cells, which increases symmetric self-renewal. If $\delta_S > 0.35$, symmetric division is favored over asymmetric division, as stem cells divide symmetrically to avoid elimination. The increase in symmetric

self-renewal subsequently decreases asymmetric and differentiation divisions, which decreases the number of GFP- cells as compared to GFP+ cells.

Figures 5.2C and D plot the model sensitivity to the Hill function parameters, θ_S and n. The switch parameter θ_S has more effect on GFP+ division pattern than any other parameter. Doubling θ_S from 5,000 to 10,000 cells more than doubles the ratio of symmetric self-renewal to asymmetric self-renewal. The increase in symmetric self-renewal increases the number of GFP+ cells, which in turn increases the ratio of GFP+ cells to GFP- cells. Increasing the Hill function exponent, n, does not significantly decrease the ratio of GFP+ to GFP- cells, but rather has more impact on decreasing the frequency of symmetric self-renewal. Increasing n sharpens the switch for symmetric self-renewal so that when $S > \theta_S$, the probability of SSR approaches zero faster. Since the initial condition of 5,000 plated GFP+ cells is greater than the baseline parameter value of $\theta_S = 4,300$, the probability of SSR decreases for higher values of n. Although n affects the division pattern, it has minimal impact on the steady state of the system, suggesting that there are several values that could fit this parameter.

Figure 5.2E demonstrates that the amplification factor, A, does not affect the ratio of cell division, but decreases the ratio of GFP+ to GFP- cells. It does not alter the steady state of GFP+ cells, but increasing A does increase the steady state of GFP- cells, thereby increasing the number of GFP- cells for every GFP+ cell. Figure 5.2F plots the model sensitivity to the frequency of symmetric differentiation. As expected, increasing the probability of symmetric differentiation increases the frequency of SSR as GFP+ cells must symmetrically self-renew to compensate for GFP+ cells lost through differentiation. In addition, the number of GFP- cells increases as differentiation increases, decreasing the ratio of GFP+ to GFP- cells.

Although the experiment is only run over the course of three days, long-run predictions may be made through a steady state analysis. The steady states of the system are the elimination state $(0,0)$ and a positive steady state (S^*, N^*) corresponding to healthy tissue containing both stem and mature cells, where

$$\begin{aligned} S^* &= \theta_S \left(\frac{k\left(1-2\alpha_D\right)-\delta_S}{k\alpha_D+\delta_S} \right)^{\frac{1}{n}} \\ N^* &= \frac{\left(2\alpha_D+\alpha_A\right)kA}{\delta_N} S^* \\ &= \frac{\left(k-\delta_S\right)A}{\delta_N} S^*. \end{aligned} \tag{5.2}$$

Specifically, when $n = 2$,

$$\begin{aligned} S^* &= \theta_S \sqrt{\frac{k\left(1-2\alpha_D\right)-\delta_S}{k\alpha_D+\delta_S}} \\ N^* &= \frac{\left(k-\delta_S\right)A\theta_S}{\delta_N} \sqrt{\frac{k\left(1-2\alpha_D\right)-\delta_S}{k\alpha_D+\delta_S}}. \end{aligned} \tag{5.3}$$

For biological parameter values, θ_S, k, α_D, δ_S, A, and δ_N are non-negative. When $k < \frac{\delta_S}{(1-2\alpha_D)}$, the healthy tissue steady state does not exist and the elimination state is stable. The positive steady state exists when $k > \frac{\delta_S}{(1-2\alpha_D)}$ and it is stable. Careful consideration of the parameters shows that the latter case holds true for biologically relevant values.

The steady state analysis proves that the relationship between GFP+ cell proliferation, k, symmetric differentiation, α_D, and the death rate of GFP+, δ_S determines the existence of a healthy tissue steady state as well as the instability of the elimination state. Bifurcation diagrams of GFP+ cell steady state as dependent on the rates of GFP+ proliferation, differentiation, and death are presented in Figure 5.3. As expected, increasing symmetric differentiation or GFP+ cell death decreases the steady state until the positive solution is eliminated completely and the elimination state becomes stable. Increasing the GFP+ cell proliferation rate increases the

steady state of GFP+ cells, but the change in steady state is small in comparison with changes in k. This corresponds with the sensitivity analysis, which concluded that increasing GFP+ cell proliferation had greater impact on the steady state of GFP- cells than GFP+ cells.

Although stability does not depend on θ_S, A, and δ_N, each of these parameters is important in determining the actual value of the steady state of the system. First, observe that N^* is linearly dependent on S^*, so the parameters that most greatly affect the steady state of stem cells will similarly affect differentiated cells. Note S^* depends linearly on θ_S. Thus, increasing θ_S and thereby increasing the probability of symmetric self-renewal has a greater impact on increasing GFP+ cells than does increasing the GFP+ cell proliferation rate, k. Although a large increase in k may result in minor GFP+ cell increase, it is important to note that N^* is linearly dependent on $(k - \delta_S)$, so that large increases in k significantly increase GFP- cells. In addition, N^* is linearly dependent on the amplification factor, A, which means that extra divisions during maturation contribute to an elevated level of GFP- cells. From this analysis, we conclude that the number of GFP+ cells is most affected by θ_S, and the number of GFP- cells is most affected by θ_S, k, and A.

By studying each parameter's effects on model outcomes, it is possible to predict how mutations might alter the growth dynamics of both the GFP+ and GFP- cell populations. Clearly, mechanisms controlling the balance between asymmetric and symmetric self-renewal could be potential targets for oncogenesis, as demonstrated by the impact of the parameter θ_S. Mutations increasing the GFP+ proliferation rate or increasing the amplification factor may not significantly contribute to the accumulation of GFP+ cells, but may lead to hypercellularity of differentiated cells. Although this in itself may be problematic, it is likely less pathologically aggressive

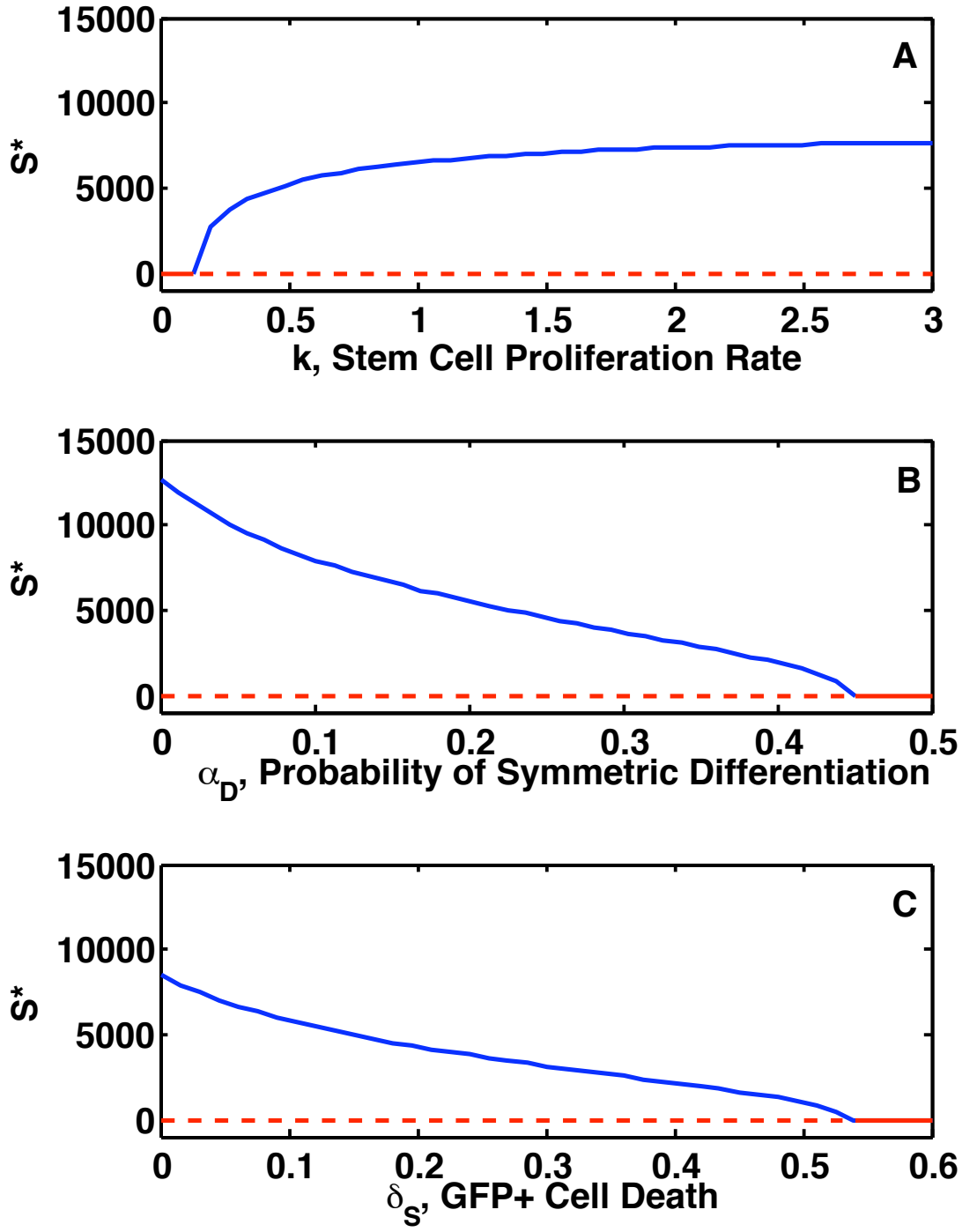

Figure 5.3: **Stability and existence of the positive steady state.** The existence and stability of the positive steady as well as the stability of the elimination steady state depends on the GFP+ cell proliferation rate (A), the probability of GFP+ cell symmetric differentiation (B), and the GFP+ cell death rate (C).

than the accumulation of GFP+ cells because current treatment regimens are often able to eliminate differentiated cells but are unsuccessful in targeting naïve stem cells. These issues were addressed in an additional experiment in which Wu *et al.* investigated the mechanisms of two specific mutations that are known to cause very different forms of leukemia.

5.2.3 Intrinsic Properties Affect Cellular Proliferation

Both extrinsic and intrinsic signals contribute to the regulation of the many proteins and signaling pathways involved in cellular proliferation and maintenance. The different GFP+ cell division patterns of cells on 7F2 versus OP9 media prove that environmental cues are capable of altering cellular signaling. To demonstrate how mutated proteins contribute to oncogenesis by way of intrinsic signals, Wu *et al.* tested the effects of BCR-ABL and NUP98-HOXA9 in murine hematopoietic cells [125]. Both mutations are found in hematopoietic precursor cells and are causes of leukemia, but each leads to the development of very different forms of disease. Therefore, by investigating the cellular properties that are deregulated by each protein, it is possible to gain further understanding regarding the causing mechanisms and progression of disease.

Although other mutations are involved in the development of Chronic Myelogenous Leukemia (CML), expression of the BCR-ABL fusion protein is the primary marker used for diagnosis of the disease [17, 22, 120]. Caused by the translocation t(9; 22)(q34; q11) in hematopoietic precursor cells, BCR-ABL inhibits apoptosis and enables additional cellular divisions [27, 46]. It is believed that BCR-ABL-positive cells suppress normal hematopoiesis by creating a dominant clone that hinders the differentiation of non-mutated progenitors [48]. BCR-ABL does not, however, block differentiation altogether, and the initial chronic phase of CML is characterized by

an increase of both progenitor and mature cells [55].

In contrast, the fusion protein NUP98-HOXA9 caused by the translocation t(7; 11)(p15; p15) is expressed in cells of patients with Acute Myelogenous Leukemia (AML) and blast crisis CML [37, 88]. It is believed NUP98-HOXA9 expression increases self-renewal in myeloid progenitor cells, contributing to an increased number of immature blast cells of the myeloid lineage [88]. Furthermore, in patients expressing NUP98-HOXA9, both erythroid and myeloid differentiation is inhibited [88]. Therefore, this mutation shifts the balance of stem-cell division mode in favor of symmetric self-renewal.

Experimental Procedure and Results

In order to investigate how these mutations affect cell proliferation and death, three thousand GFP+ cells were infected with BCR-ABL, three thousand GFP+ cells were infected with NUP98-HOXA9, and then compared to three thousand non-infected GFP+ cells in a control group. Cell divisions, pattern of division, and death were monitored in each group over three days *in vitro*. The data suggests that BCR-ABL has greater impact on the cell proliferation rate and survival, while NUP98-HOXA9 alters the pattern of cell division. In three days, GFP+ cells completed an average of 2.7 divisions in the control group, 6.5 divisions in BCR-ABL cells, and 3.5 divisions in NUP98-HOXA9 cells, corresponding to the derived proliferation rates of 0.6238 per day, 1.5018 per day, and 0.8087 per day, respectively. The percent of GFP+ cells lost to apoptosis was 14% in the control cells, 7% in the BCR-ABL cells, and 12% in NUP98-HOXA9 cells. Consequently, the death rate was 0.0503 per day in the control cells, 0.0242 in BCR-ABL cells, and 0.0426 in NUP98-HOXA9 cells. In the control group, the frequency of symmetric self-renewal (SSR), asymmetric self-renewal (ASR), and symmetric commitment differentiation (SCD) was 42%, 48%,

Parameter	Control		BCR-ABL		NUP98-HOXA9	
	Exper.	Model	Exper.	Model	Exper.	Model
$k(day^{-1})$	0.6238	0.6238	1.5018	1.5018	0.8087	0.8087
$\delta_S(day^{-1})$	0.0503	0.0503	0.0242	0.0242	0.0426	0.0426
$\theta_S(cells)$	n/a	3,200	n/a	4,900	n/a	7,300
$\delta_N(day^{-1})$	0.1006	0.1006	0.0484	0.0484	0.0852	0.0852
A	n/a	1.3	n/a	1.4	n/a	1.4
GFP+ cells	n/a	4,385	n/a	8,210	n/a	7,698
GFP- cells	n/a	5,758	n/a	28,086	n/a	9,653
GFP-:GFP+	n/a	1.31	3.45	3.42	1.22	1.25
Avg. SSR (%)	42	41	45	45	62	62
Avg. ASR (%)	48	49	42	42	25	25
Avg. SCD (%)	10	10	13	13	13	13

Table 5.3: Parameter values, experimental observations, and model predictions for mutated cells [125].

and 10%, respectively. In BCR-ABL cells, SSR was slightly greater with 45%, ASR slightly less with 42% and SCD slightly greater with 13%. In NUP98-HOXA9 cells, SSR increased to 62%, ASR decreased to 25%, and SCD was 13% [125].

Model Simulations of Experimental Data

The mathematical model presented in Equations 5.1 can also be used to simulate the growth dynamics of BCR-ABL and NUP-HOXA9 infected cells. Table 5.3 presents the model parameters and a comparison of experimental data with model predictions. With an initial condition of 3,000 uninfected GFP+ and zero GFP- cells, mathematical modeling predicts the control GFP+ population grows to 4,461 cells and the control GFP- population grows to 5,752 cells. The average frequency of SSR is 41%, ASR is 49%, and SCD is 10%, in accordance with 42%, 48%, and 10% experimentally recorded.

Model predictions for the BCR-ABL group are compared with the control group. Both are plotted in Figure 5.4A-B, where BCR-ABL curves are solid, and control curves are dashed. With the initial condition of 3,000 BCR-ABL-infected GFP+ cells and zero GFP- cells, the model predicts GFP+ growth to 8,210 cells and GFP-

growth to 28,086 cells. The ratio of GFP- cells to GFP+ cells is 3.42, which is more than 2.6 times that of the non-infected cells, demonstrating that cell differentiation is successful, and cell accumulation occurs from increased proliferation and survival. In the BCR-ABL group, the GFP- population surpasses the GFP+ population by day one, which is less than half the time needed in the control group. However, the average frequency of SSR is 45%, ASR is 42%, and SCD is 13%, which is not significantly different from measurements of the control group. Therefore, BCR-ABL causes disease by accumulating cells through increased proliferation and decreased apoptosis.

Similarly, in Figure 5.4C-D, model predictions for the NUP98-HOXA9 group are plotted with solid lines and compared to the control group plotted with dashed lines. With the initial condition of 3,000 NUP98-HOXA9-infected GFP+ cells and zero GFP- cells, the model predicts that over three days, the GFP+ population grows to 7,698 cells and the GFP- population grows to 9,653 cells. In comparison to the non-mutated control group, the ratio of GFP- cells to GFP+ cells decreased slightly to 1.25, demonstrating the preference for symmetric divisions of immature cells over differentiation. In contrast, the percentage of cells symmetrically self-renewing is markedly different from those in the control group. In NUP98-HOXA9 cells, the average frequencies of SSR, ASR, and SCD are 62%, 25%, and 13%, as compared with 42%, 48%, and 10%, respectively. In the control group, the switch from symmetric to asymmetric self-renewal occurs within a half day, but in the NUP98-HOXA9 group, the switch does not occur until two-and-a-half days, indicating the dominance of symmetric self-renewal in mutated cells. It may be concluded that NUP98-HOXA9 causes disease through abnormal symmetric self-renewal, which increases immature blast cells and prevents the formation of differentiated cells, thereby inhibiting the

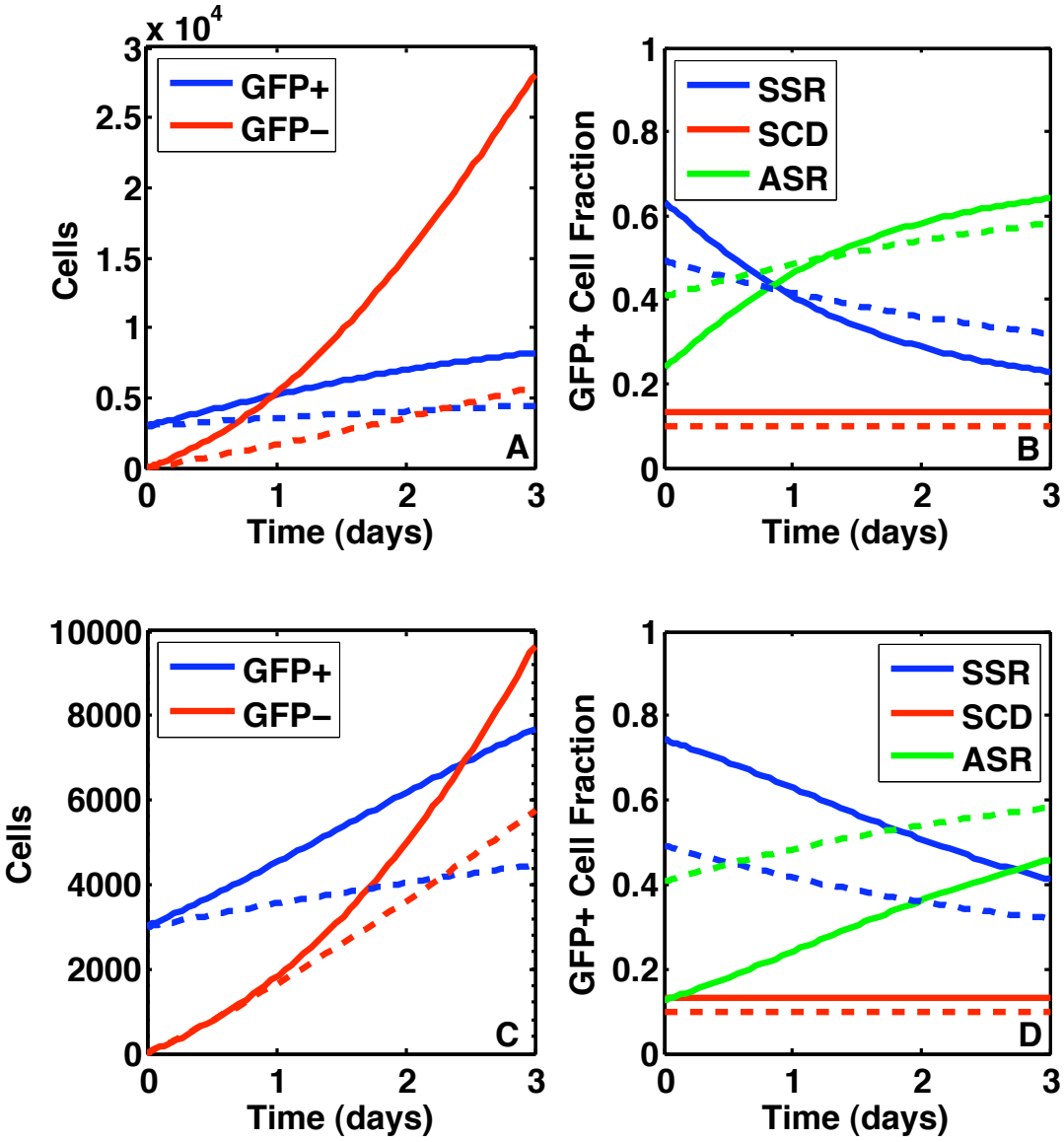

Figure 5.4: **BCR-ABL and NUP98-HOXA9 promote cancer growth through different mechanisms.** (A) BCR-ABL (solid) expression increases proliferation and decreases apoptosis, causing greater expansion of both cell types, but particularly GFP- cells, compared to control cells (dashed). (B) The mode of GFP+ cell division in cells infected with BCR-ABL is comparable to uninfected cells. (C) GFP+ cell proliferation and death rates of cells infected with NUP98-HOXA9 (solid) are not significantly different from those in control cells (dashed), but the ratio of GFP- cells to GFP+ cells is slightly decreased in comparison with control cells due to increased SSR. (D) NUP98-HOXA9 shifts the mode of GFP+ cell division to favor symmetric self-renewal.

daily functions performed by mature blood cells.

5.2.4 Conclusions

The experiments conducted by Wu *et al.* employ time-lapse imaging to demonstrate that mammalian hematopoietic precursor cells can complete three types of division: symmetric self-renewal, asymmetric self-renewal, and symmetric commitment differentiation. In addition, their results confirm that both external environmental cues and internal cellular signals may affect cell division pattern and proliferation rate. A mathematical model was created that accurately captures the experimental data. Further investigation determined that mutations affecting the GFP+ cell proliferation rate, k, and the symmetric self-renewal switch parameter, θ_S, have the most potential in causing abnormal growth, though each instigates different forms of disease. Increased GFP+ cell proliferation contributes to the hypercellularity of GFP- cells, whereas increased symmetric self-renewal increases the fraction of primitive cells. The former is observed in Chronic Myelogenous Leukemia, but the latter found in the more aggressive Acute Myelogenous Leukemia, which suggests that deregulation of symmetric self-renewal may be involved in speeding disease progression.

Although this *in vitro* experiment cannot fully characterize hematopoietic stem cells, the conclusions derived from this model may be usefully employed in creating a mathematical model of the hematopoietic system *in vivo*. It is accepted that stem cells are capable of three types of division, but there is minimal data quantifying the proportions of division type because mammalian stem cells are difficult to isolate, maintain, and observe experimentally. Of the cells and environments used in these experiments, the non-mutated GFP+ cells in the 7F2 environment most resemble hematopoietic stem cells *in vivo*. This environment favors asymmetric division, and

if the plated cells reached steady state, the probabilities of symmetric self-renewal, asymmetric self-renewal, and symmetric differentiation would be approximately 20%, 65%, and 15%. While it is certainly possible for other division patterns to occur in human hematopoietic stem cells, it is currently impossible to conclusively determine these probabilities *in vivo*. Because this division pattern is determined from experimental data that can be referenced, this estimation of division pattern will be used is subsequent modeling of hematopoiesis.

5.3 Cycling and Quiescent Stem Cells

The use of regulatory mechanisms to influence stem-cell division pattern is one way that homeostasis is maintained. Another is through mechanisms that govern the transition between quiescence and cycling in the stem-cell population. The ability to remain quiescent for long periods of time is one of the major differences of stem-cell behavior *in vivo* versus *in vitro* [63]. In adults, it has been estimated that 5-25% of hematopoietic stem cells are actively cycling [21, 90, 104]. Consequently, under homeostatic conditions, the majority of hematopoietic stem cells are quiescent, resting in the G_0 phase of the cell cycle. However, the percentage of cycling stem cells is not static throughout the life of the host. For instance, in tissue generation, a larger proportion of stem cells actively divide in order to expand cell number [89]. If the majority of cells remained quiescent, the tissue would never expand or could even be eliminated. Yet stem cells could not perpetually sustain an elevated amount of cycling or the tissue would exponentially grow without bound. Clearly, there are mechanisms in place that control the balance between cycling and quiescent stem cells, and these regulations likely depend on the number of cells in the system.

Due to the difficulty of reproducing stem cell niches *in vitro*, it is challenging to

experimentally quantify the kinetics of the interchange between the quiescent and cycling stem-cell compartments. Mathematical modeling enables theoretical investigation of the interactions between cycling and quiescent stem cells. In addition, predictions may be made pertaining to how the balance between quiescent and cycling cells subsequently effects the growth dynamics of the tissue. In this section, a mathematical model is presented that incorporates regulatory mechanisms governing stem-cell division pattern similar to those discussed in Section 5.2 while also including mechanisms that mediate the balance between cycling and quiescent stem cells.

5.3.1 Incorporating Cycling and Quiescent Stem-Cell Compartments

To accurately model tissue generation followed by maintenance *in vivo*, it is necessary to separate stem cells into cycling and quiescent compartments. In doing so, it is possible to capture the initial stages of expansion, followed by tapering growth leading to homeostasis. In contrast with the model presented in Section 5.2.1, the stem-cell population is divided into quiescent stem cells, Q, and cycling stem cells, C. Mature differentiated cells are denoted N. At this time, intermediate progenitor cells are not explicitly modeled, however, an amplification factor is included, denoted A. Quiescent stem cells enter the cycling compartment at maximum rate p and cycling cells enter the quiescent compartment at maximum rate q. The probability that a quiescent cell will enter cycling is Φ and the probability that a cycling cell will go into quiescence is Ψ. Cycling cells proliferate with rate r. Once in the cycling compartment, stem cells complete one of four processes during the division process: symmetric self-renewal, asymmetric self-renewal, symmetric differentiation, or apoptosis. The proportions of stem cells that symmetrically self-renew, asymmetrically self-renew, symmetrically differentiate, and die are given by α_S, α_A, α_D,

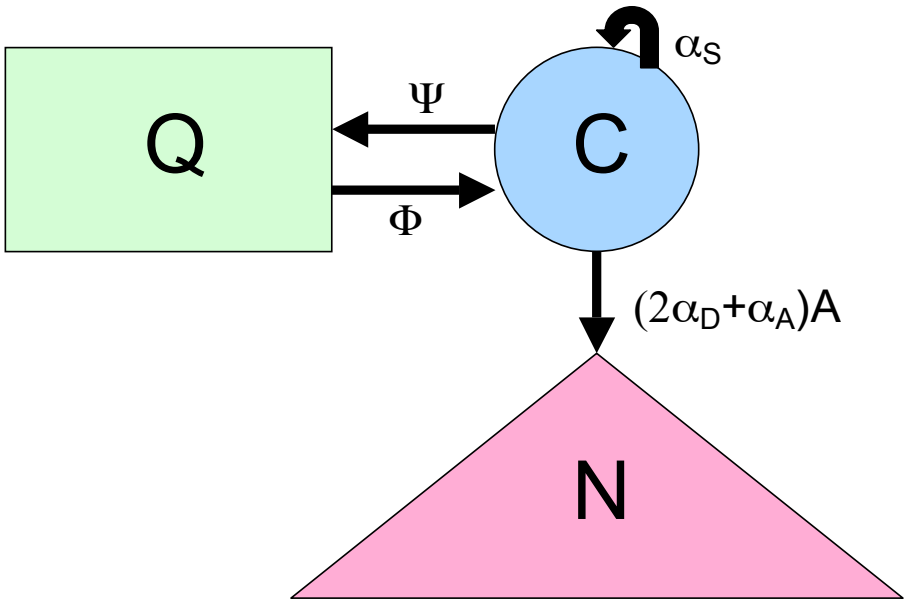

Figure 5.5: **Schematic diagram of quiescent and cycling stem cells and differentiated cells.** Stem cells enter cycling and quiescent compartments with probabilities that are dependent on stem-cell numbers. Cycling stem cells are capable of three types of divisions. Differentiated cells are formed through asymmetric and symmetric commitment differentiation divisions.

and δ_S, respectively. Cycling stem cells are the source for the mature differentiated-cell population. Differentiated cells are formed through symmetric differentiation or asymmetric divisions of a cycling stem cell, and differentiated cells die with rate δ_N. A schematic diagram of the flow of cells between quiescent, cycling, and differentiated compartments is presented in Figure 5.5.

In contrast with Equations 5.1, the number of terminally differentiated cells in the tissue influences the probability of symmetric commitment differentiation in stem cells, which was previously irrelevant in modeling experimental data due to the short time frame. It should also be noted that this model differs from others in which differentiation occurs after division. In such models, cycling cells always self-renew and progeny enter the quiescent compartment. Stem cells exit the quiescent pool by differentiating, dying, or entering the cycling pool to self-renew [13, 24]. Instead,

this model employs the recent observations of Wu *et al.* that suggest symmetric differentiation can occur at the time of division [125].

Regulatory mechanisms that control the transition between cycling and quiescent stem cells are poorly understood. However, it is known that in times of stress or tissue generation, quiescent stem cells may enter the cycling compartment to promote expansion. The interchange of quiescent and cycling cells is likely dependent on chemical signaling. The probability that a quiescent cell enters cycling is given by $\Phi(C) = \frac{\sigma_C^2}{\sigma_C^2+C^2}$, where σ_C is the number of cells in the cycling compartment at which the probability that a quiescent cell enters cycling is 50%. A higher number of cycling cells yields a lower probability that a quiescent cell will enter the cycling compartment. Cycling cells are forced into quiescence when a sufficient number of cells are cycling. The probability a cycling cell enters quiescence is given by $\Psi(C) = \frac{C^2}{\sigma_Q^2+C^2}$, where σ_Q is the number of cycling cells at which the probability of a cycling cell entering quiescence is 50%. As cycling cells approach zero, Ψ approaches zero so that the few cycling cells do not become quiescent. As cycling cells increase, Ψ approaches one.

Because stem cells are long-lived and tightly regulated, it is assumed stem-cell death only occurs due to errors in the division process. Therefore, death of quiescent stem cells is negligible and the small constant probability that a cycling stem cell goes through apoptosis during division is denoted δ_S. The probabilities of division outcomes of cycling stem cells adhere to the condition $\alpha_S + \alpha_A + \alpha_D + \delta_S = 1$. The proportion of cycling stem cells that symmetrically self-renew, denoted α_S, is dependent on stem-cell chemical signaling as well as the physical size of the stem-cell niche, K_S. Specifically,

$$\alpha_S(C,Q) = (1-\delta_S)\left(\frac{\theta_S^2}{\theta_S^2+C^2}\right)\left(1-\frac{C+Q}{K_S}\right), \tag{5.4}$$

where the Hill function is described in Section 5.2.1 and was used in previous modeling by Mackey *et al.* [13, 24, 77]. Stem-cell interaction with the niche is necessary for maintaining stemness, thus the logistic term $\left(1 - \frac{C+Q}{K_S}\right)$ demonstrates the physical restraint of the niche size on symmetric self-renewal due to limited available space for stem-cell sustenance [124]. Note that symmetric self-renewal cannot exceed $(1 - \delta_S)$, since it is assumed that stem cells die with constant probability.

To further illustrate why both chemical signaling and niche control are found in the functional form for symmetric self-renewal, consider the function $f(x) = g(x)h(x)$, where $g(x) = \left(\frac{a^2}{a^2+x^2}\right)$ and $h(x) = \left(1 - \frac{x}{c}\right)$, where a and c are arbitrary positive constants. Note that α_S resembles $f(x)$, the chemical signaling function shares the form of $g(x)$, and the niche control function is similar to $h(x)$. Let $c = 1$ for the purpose of this example. Figure 5.6 displays two examples for $f(x)$ with different a values. In Figure 5.6A, symmetric self-renewal is more restricted by chemical signaling than the niche, whereas the converse is true in Figure 5.6B. In both cases, $f(x)$ captures key components of both the Hill function and the logistic function. Note that $f(x)$ is zero when the niche is full, which is $x = 1$ in this example, but it also follows the qualitative behavior of the Hill function due to chemical signaling. As a result, both functional forms are incorporated into α_S in order to capture both traits.

The proportion of cycling stem cells that divide into differentiated cells is given by

$$\alpha_D(C, Q, N) = (1 - \delta_S)\left(\frac{\theta_N}{\theta_N + N}\right)\left(\frac{C+Q}{K_S}\right). \tag{5.5}$$

The Hill function $\left(\frac{\theta_N}{\theta_N+N}\right)$ reflects the effects of chemical signaling that promote or suppress differentiation depending on the existing population of mature cells and

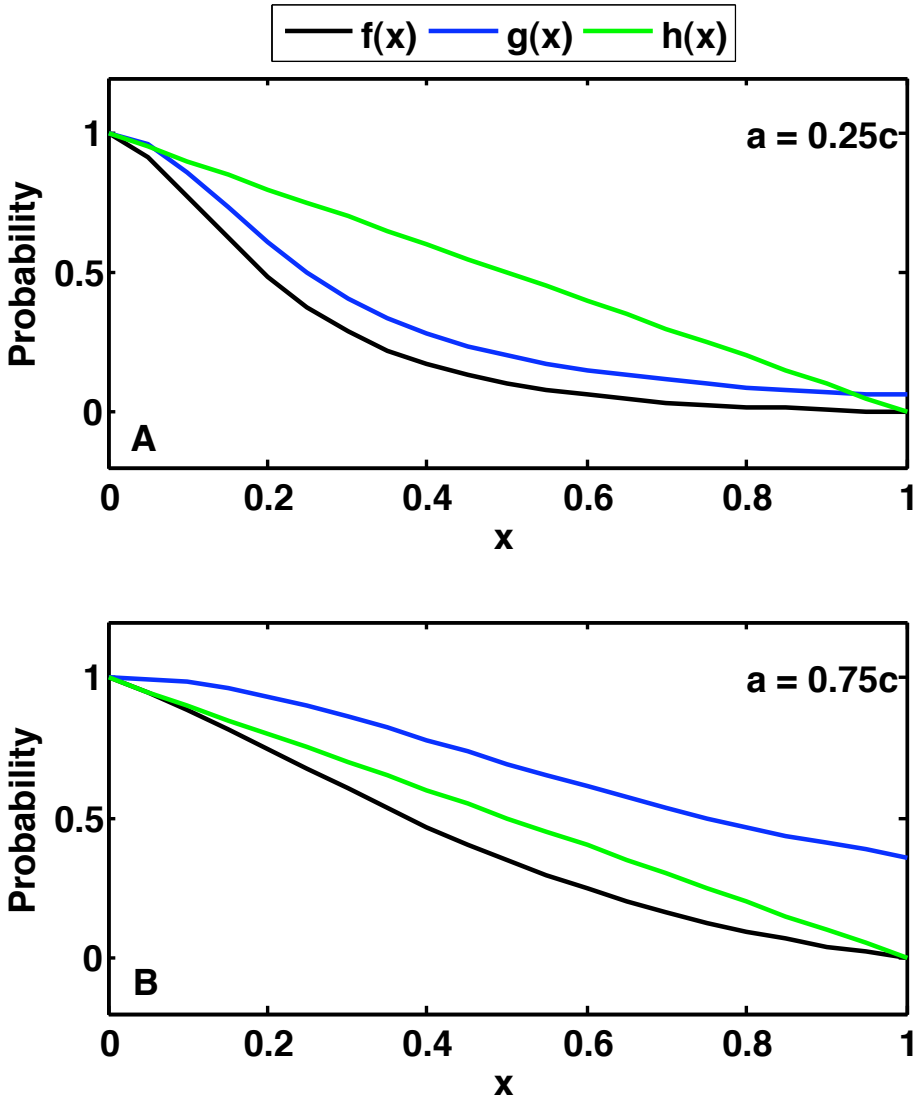

Figure 5.6: **Functional forms used to determine the probability of symmetric self-renewal.** The probability of symmetric self-renewal follows that of function f(x), which takes into account both chemical interactions and niche control. Probability based solely on chemical signaling is given by function g(x), and probability based solely on niche control is given by function h(x).

has been used in previous models [13, 24]. In addition, the term $\left(\frac{C+Q}{K_S}\right)$ ensures preference is given to self-renewal division over differentiation in cases where both stem and differentiated cells are depleted so the system is not compromised and extinguished [117].

The proportion of cycling stem cells that asymmetrically self-renew is determined by

$$\alpha_A(C,Q,N) = 1-\alpha_S(C,Q)-\alpha_D(C,Q,N)-\delta_S. \tag{5.6}$$

It is important to note that the model does not discriminate based on the mechanism by which asymmetric division is achieved. The asymmetric division term can encompass divisions that occur by the immortal-strand hypothesis or divisions in which two identical cells determine their fates from cues after division. The stem-cell division types are merely classified by the state of the two daughter cells at the time of their subsequent division. The system of differential equations for the model under the presented assumptions is as follows:

$$\begin{aligned} \frac{dQ}{dt} &= -p\Phi Q + q\Psi C \\ \frac{dC}{dt} &= p\Phi Q - q\Psi C + r\left[\alpha_S - \alpha_D - \delta_S\right]C \\ \frac{dN}{dt} &= \left(2\alpha_D + \alpha_A\right)ArC - \delta_N N. \end{aligned} \tag{5.7}$$

For ease, this model is labeled the ODE Model of Tissue Generation (ODEMTG) when referenced in subsequent text. The model terms and definitions are summarized in Table 5.4.

Definition of Model Terms	
C	Cycling stem cells
Q	Quiescent stem cells
N	Differentiated cells
$\Phi(C)$	The probability quiescent cells enter the cycling compartment $= \frac{\sigma_C^2}{\sigma_C^2+C^2}$
σ_C	Number of cells at which quiescent cells enter cycling at 50%
$\Psi(C)$	The probability at which cycling cells become quiescent $= \frac{C^2}{\sigma_Q^2+C^2}$
σ_Q	Number of cells at which cycling cells enter quiescence at 50%
r	The division rate of cycling stem cells
p	The rate at which quiescent cells enter cycling
q	The rate at which cycling stem cells enter quiescence
$\alpha_S(C,Q)$	The proportion of cycling cells that symmetrically self-renew $= (1-\delta_S)\left(\frac{\theta_S^2}{\theta_S^2+C^2}\right)\left(1-\frac{C+Q}{K_S}\right)$
θ_S	Number of cells at which SSR due to signaling occurs at 50%
$\alpha_D(C,Q,N)$	The proportion of cycling cells that differentiate $= (1-\delta_S)\left(\frac{\theta_N}{\theta_N+N}\right)\left(\frac{C+Q}{K_S}\right)$
θ_N	Number of cells at which SCD due to signaling occurs at 50%
$\alpha_A(C,Q,N)$	Proportion of stem cells that renew asymmetrically $= [1-\alpha_S(C,Q)-\alpha_D(C,Q,N)-\delta_S]$
δ_S	The proportion of cycling stem cells that go through apoptosis
K_S	Carrying capacity of all stem cells, determined by the niche
A	Amplification factor
δ_N	Death rate of differentiated cells

Table 5.4: The biological meaning of the model terms used in the ODE Model of Tissue Generation.

5.3.2 Steady States and Stability Analysis

The steady states of the model include an elimination state whose eigenvalues correspond to the solutions for λ in the polynomial

$$-\lambda^3 + (r(1-2\delta_S) - q)\lambda^2 + (p+\delta_N)(r(1-2\delta_S) - q)\lambda + p\delta_N r(1-2\delta_S) \;=\; 0.$$

All parameters are measurements of biological qualities and therefore cannot be negative. When $\delta_S < \frac{1}{2}$, according to Descartes' Rule of Signs, there exists at least one positive eigenvalue, and therefore the solution is unstable. Furthermore, when $\delta_S > \frac{1}{2}$, all roots for λ are negative, so the elimination is stable. In other words, when stem cells die with at least 50% probability, the tissue is eliminated, which is sensible considering that stem cells are the source of all other cells in the tissue.

Non-zero steady states may be found by noting that at equilibrium,

$$\begin{aligned} Q &= \frac{q\Psi}{p\Phi}C \\ N &= \frac{(2\alpha_D + \alpha_A)rA}{\delta_N}C, \end{aligned} \tag{5.8}$$

which leads to the condition

$$\alpha_S - \alpha_D - \delta_S = 0.$$

Therefore, steady states may be determined by solving for roots of the seventh-degree polynomial

$$P_7C^7 + P_6C^6 + P_5C^5 + P_4C^4 + P_3C^3 + P_2C^2 + P_1C + P_0 = 0$$

with the following coefficients:

$$\begin{aligned}
P_7 &= -(1-\delta_S)\delta_N\theta_N q \\
P_6 &= -(1-\delta_S)\theta_S^2(1-2\delta_S)rAq \\
P_5 &= -(1-\delta_S)\theta_S^2\delta_N\theta_N q - (1-\delta_S)\delta_N\theta_N\left(q\theta_S^2 + (p+q)\sigma_C^2\right) \\
&\quad -K_S p\sigma_C^2\delta_S(1-2\delta_S)rA \\
P_4 &= -(1-\delta_S)\theta_S^2(1-2\delta_S)rA\sigma_C^2(p+q) - K_S p\sigma_C^2\delta_S\delta_N\theta_N \\
P_3 &= (1-\delta_S)\theta_S^2\sigma_C^2\left((1-2\delta_S)rApK_S - \delta_N\theta_N(p+q)\right) \\
&\quad -(1-\delta_S)\delta_N\theta_N\sigma_C^2\left(\theta_S^2(p+q) + p\sigma_Q^2\right) \\
&\quad -K_S p\sigma_C^2\delta_S(\theta_S^2+\sigma_Q^2)(1-2\delta_S)rA \\
P_2 &= (1-\delta_S)\theta_S^2 p\sigma_C^2(\delta_N\theta_N K_S - (1-2\delta_S)rA\sigma_Q^2) \\
&\quad -K_S p\sigma_C^2\delta_S(\theta_S^2+\sigma_C^2)\delta_N\theta_N \\
P_1 &= (1-\delta_S)\theta_S^2 p\sigma_C^2\sigma_Q^2\left((1-2\delta_S)rAK_S - \delta_N\theta_N\right) \\
&\quad -(1-\delta_S)\delta_N\theta_N\theta_S^2 p\sigma_C^2\sigma_Q^2 - K_S p\sigma_C^2\delta_S\sigma_Q^2\theta_S^2(1-2\delta_S)rA \\
P_0 &= K_S p\sigma_C^2\sigma_Q^2\delta_S\theta_S^2\delta_N\theta_N(1-2\delta_S).
\end{aligned}$$

By Descartes' Rule of Signs, there exists at least one positive steady state (Q^*, C^*, N^*) since $P_7 < 0$ and $P_0 > 0$ for all positive parameter values with $\delta_S < \frac{1}{2}$. In particular, when using the parameters given in Table 5.5, there is only one positive steady state at $(Q^*, C^*, N^*) = (1.52e4, 2.75e3, 2.62e10)$ and it is stable, with eigenvalues $\lambda_{1,2,3} = -0.0151, -0.6296, -2.7420$.

5.3.3 Numerical Simulations of Tissue Generation

There is little conclusive data regarding the *in vivo* cellular kinetics of stem cells. The hematopoietic system is the most studied, but there are still many unknown behaviors, particularly regarding the interchange between quiescent and cycling stem

Parameters		
Term	Value Range	Used Value
r	0.002 - 0.6931 (1/day) [1, 21]	0.2310 (1/day)
p	No Information	0.4620 (1/day)
q	No Information	0.2310 (1/day)
σ_C	No Information	750 (cells)
σ_Q	No Information	1,500 (cells)
θ_S	No Information	3,000 (cells)
θ_N	No Information	1×10^{10}(cells)
δ_S	0.05 (calculated from [83])	0.05
K_S	15,000 - 1,000,000 (cells) [1, 83]	3×10^4(cells)
A	No Information	1.1×10^8
δ_N	2.4 (1/day) [9, 13]	2.4 (1/day)
Model Steady State Predictions		
C	5-25% of stem cells [21, 90, 104]	2,750 (cells)
Q	75-95% of stem cells [21, 90, 104]	15,200 (cells)
N	$2 - 6 \times 10^{10}$ (cells) [9, 100]	2.62×10^{10}
Ψ	No Information	0.7701
Φ	No Information	0.0694
α_S	0.1850 - 0.2760 (derived from [125])	0.2073
α_A	0.5540 - 0.7150 (derived from [125])	0.5853
α_D	0.1000 - 0.1700 (derived from [125])	0.1573

Table 5.5: Parameter values for the ODE Model of Tissue Generation are from *in vivo* hematopoietic cells when possible.

cells. Furthermore, there is some discrepancy in the classification of long-term versus short-term stem cells and early progenitor cells, making it difficult to isolate parameter values for a pure stem-cell population. The following simulations use the parameter values presented in Table 5.5, measured in hematopoietic cells when possible. The differential equation solver *ode15s* in MATLAB was used to run numerical simulations.

By separating cycling and quiescent stem cells into two compartments, it is possible to investigate stem-cell dynamics during tissue generation. For instance, consider the case in which one stem cell must generate additional stem cells and neutrophils until homoestasis is reached. As seen in Figure 5.7A-B, one stem cell is capable of generating enough progeny to achieve a healthy steady state. Initially, the majority of stem cells are cycling, but as the system is reconstituted, most become quiescent

and at steady state, 85% of stem cells are quiescent, while 15% are cycling. With an initial condition of one cycling stem cell and zero quiescent stem cells and differentiated cells, it takes 7.25 weeks to reach 10^{10} differentiated cells, bringing the system out of neutropenia, and 22.55 weeks weeks to reach 90% of the steady state of differentiated cells. The corresponding probabilities for stem-cell transition between quiescence and cycling and division outcomes are plotted in Figure 5.7C-D. When the system begins to regenerate, no cycling cells enter quiescence, but at steady state, 77% of cycling cells enter quiescence. In contrast, the probability that quiescent cells enter cycling is initially the maximum 100%, but this decreases to approximately 7% at steady state. Stem-cell division patterns also change throughout the time of generation. Symmetric self-renewal first expands the cycling pool of stem cells, then asymmetric and differentiation divisions create differentiated cells. Initially, 95% of all stem-cell divisions result in symmetric self-renewal, but as steady state is achieved, this decreases to about 21%, and the probabilities of symmetric differentiation and asymmetric division increase from 0% to 16% and 59%, respectively.

Such dynamics of tissue generation could not be studied with a model using constant probabilities of cycling and stem-cell division. Note that in this model, 100% of stem cells are initially cycling, and they self-renew with 95% probability and die with 5% probability. With a stem-cell proliferation rate of 0.231 per day, the net growth rate of stem cells is 0.207 per day. If constant division probabilities were used, the stem-cell population would exponentially grow. One stem cell proliferating at a rate of 0.207 per day would expand into a population that would surpass the niche size of 30,000 cells within 50 days, and in the meantime, zero differentiated cells would be formed due to the lack of differentiation. On the other hand, at homeostasis, the net growth rate of the stem-cell population is zero, and it would be

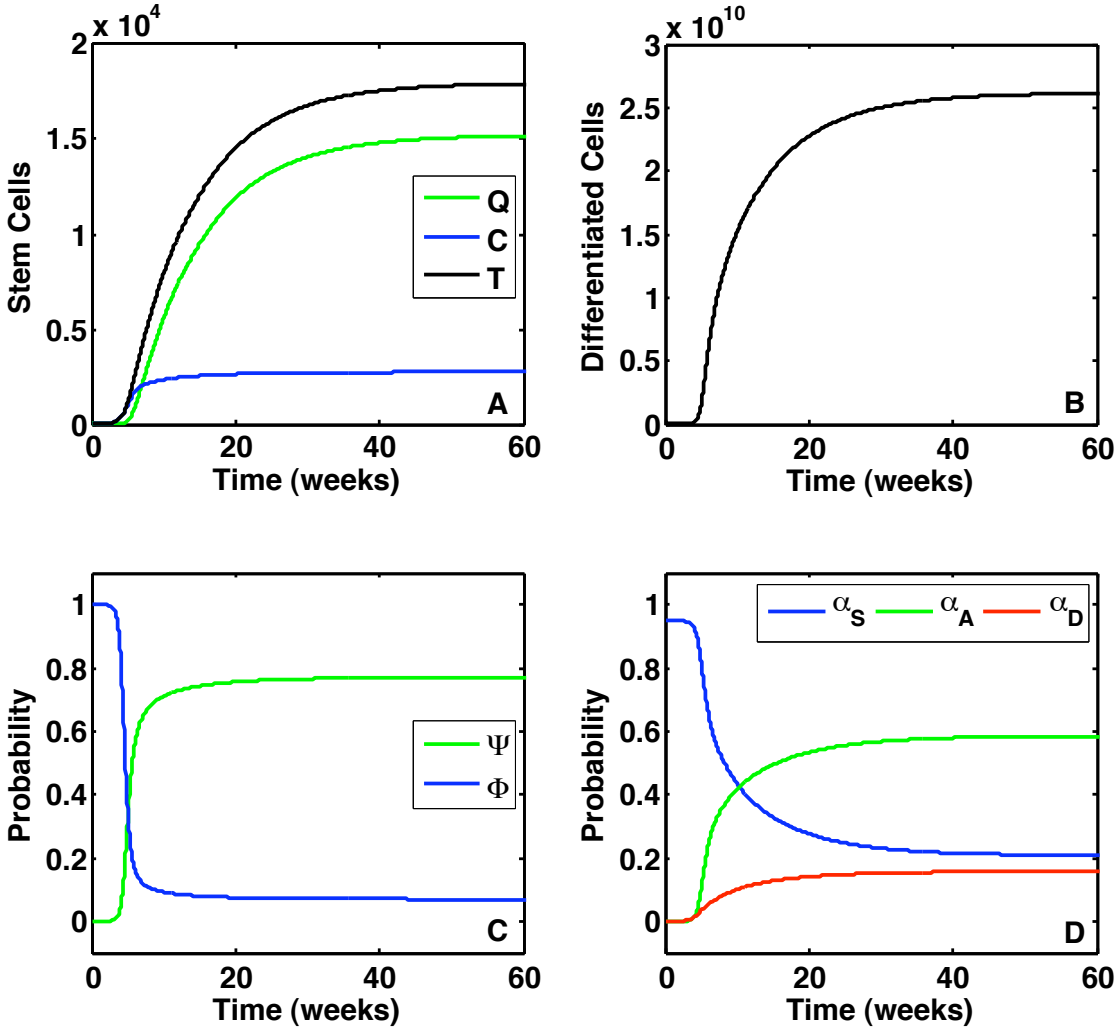

Figure 5.7: **Tissue generation from one cycling stem cell.** (A) Quiescent stem cells, Q, cycling stem cells, C, and total stem cells, T, are plotted versus time for 60 weeks as a system is generated by one cycling stem cell. (B) Differentiated cells reach 90% of the steady state in 22.6 weeks. (C) The probability that cycling cells enter quiescence, increases from 0 to 77% while the probability that quiescent cells enter cycling, decreases from 100 to 7%. (D) Symmetric self-renewal decreases from 95 to 21%, while asymmetric and symmetric differentiation increase from zero to 59% and 16%, respectively.

impossible for one stem cell to expand and generate an entire tissue. It is therefore evident that a mathematical model incorporating feedback regulatory mechanisms is preferable when investigating hierarchical tissue.

5.4 Conclusions

In order to accurately capture characteristics found in hierarchical tissue, a mathematical model has been presented that incorporates feedback mechanisms between stem- and differentiated-cell populations. A three-compartment mathematical model of quiescent stem cells, cycling stem cells, and differentiated cells may be used to study generation or reconstitution of normal tissue. Furthermore, it permits investigation of the balance between cycling and quiescent stem cells as well as the three modes of stem-cell division involved in hematopoiesis. The parameters used in numerical simulations were derived from the hematopoietic system, but the model could easily be adapted to gain insight into other types of tissue by changing appropriate parameter values.

Accurately modeling healthy tissue enables the study of mutation acquisition in cells within a hierarchical structure. In particular, it fosters investigation of aberrant feedback mechanisms that contribute to abnormal tissue growth. The balance between symmetric self-renewal, symmetric differentiation, and asymmetric self-renewal divisions is especially important in achieving and maintaining homeostasis, which implies that disturbing this balance is a potential cause of malignancy. Subsequent work will further examine these effects to indicate the types of mutations that are most problematic, but before mutation acquisition is addressed, a sensitivity analysis of the ODEMTG model is presented in the next chapter in order to investigate the significance of parameters on homeostasis.

CHAPTER VI

Modeling the Regulation of Tissue Homeostasis

The preceding chapter introduced a mathematical model of hierarchical tissue that enabled investigation of the mechanisms governing stem-cell division pattern and the transition of stem cells between quiescence and cycling. This model was used to simulate tissue generation and to establish homeostasis. In this chapter, the sensitivity of model parameters is discussed in further detail in order to highlight the regulatory aspects that have the greatest effect on tissue generation and equilibrium. First, a differential sensitivity analysis is conducted that quantifies the change in cell populations during tissue generation due to parameter perturbations. Next, a system of two ordinary differential equations is derived from the reduction of the ODE Model of Tissue Generation (ODEMTG) system in Equations 5.7 to model tissue homeostasis. Finally, a principle component analysis is conducted in order to determine parameter combinations that significantly impact equilibrium solutions.

6.1 Differential Sensitivity Analysis

Tissue generation is a dynamical process likely influenced by several aspects of cellular kinetics. For instance, the stem-cell proliferation rate determines the speed at which daughter cells can be produced, affecting the time required to reach full constitution. In addition, the mechanisms regulating the pattern of stem-cell division

can factor into tissue composition by controlling the ratio between stem cells and differentiated cells. In this section, a sensitivity analysis of the ODEMTG model in equation 5.7 is conducted in order to quantify the effects of parameter perturbations on tissue generation.

6.1.1 Sensitivity Equations

Following the techniques outlined by Bortz and Nelson, sensitivity equations are generated by differentiating model equations with respect to the parameter in question [18]. Thus the sensitivity equations are partial derivatives of the solution curves, and interpret how parameter changes alter solutions over time. For any arbitrary parameter ρ, the sensitivity functions are defined as

$$\begin{aligned} C_\rho(t) &= \frac{\partial}{\partial \rho} C(t,\rho) \\ Q_\rho(t) &= \frac{\partial}{\partial \rho} Q(t,\rho) \\ N_\rho(t) &= \frac{\partial}{\partial \rho} N(t,\rho). \end{aligned} \tag{6.1}$$

For example, to investigate the effects of the stem-cell proliferation rate, r, the three equations in the ODEMTG model are differentiated with respect to r, resulting in the following system:

$$\begin{aligned} \dot{Q}_r &= -p\Phi Q_r - pQ\Phi_r + q\Psi C_r + qC\Psi_r \\ \dot{C}_r &= p\Phi Q_r + pQ\Phi_r - q\Psi C_r - qC\Psi_r + r\left(\alpha_S - \alpha_D - \delta_S\right) C_r \\ &\quad + C\left[r\left(\alpha_{Sr} - \alpha_{Dr}\right) + \left(\alpha_S - \alpha_D - \delta_S\right)\right] \\ \dot{N}_r &= \left(2\alpha_D + \alpha_A\right) ArC_r + AC\left[r\left(2\alpha_{Dr} + \alpha_{Ar}\right) + \left(2\alpha_D + \alpha_A\right)\right] - \delta_N N_r. \end{aligned} \tag{6.2}$$

The sensitivity solutions can be analyzed in two ways. Semi-relative sensitivity solutions can be computed by multiplying the parameter of interest by the sensitivity equations, for example, rC_r, rQ_r, and rN_r. Solving the resulting system quantifies

how solutions change when a parameter is varied by a factor of choice. For instance, it is often of interest to know how solutions behave when the sensitivity parameter is doubled. Semi-relative solutions have the same units as the original model solutions; that is, the units of rC_r are those of C, which in this case is cycling stem cells.

Logarithmic sensitivity solutions are computed by multiplying the parameter of interest by the sensitivity equations and dividing by the baseline solutions. For instance, the logarithmic sensitivity solutions with respect to r are $\frac{r}{C}C_r, \frac{r}{Q}C_r$, and $\frac{r}{N}C_r$. The logarithmic name derived from the equality $\frac{\partial \log(C)}{\partial \log(r)} = \frac{r}{C}C_r$. In contrast to semi-relative solutions, logarithmic sensitivity solutions are dimensionless and determine the percentage change of solutions according variation in the parameter of choice. Although useful information is obtained from both types of sensitivity solutions, only logarithmic solutions are presented in this chapter.

6.1.2 Logarithmic Sensitivity Solutions

The system of differential equations needed to produce sensitivity solutions were analytically derived for each of the eleven parameters in the ODEMTG model. Sensitivity solution curves were produced using the *ode15s* solver in MATLAB. In order to visually manage all of the corresponding sensitivity solution curves, parameters are classified into three groups. The first group consists of parameters found in the functional forms governing stem-cell transition between quiescent and cycling pools: p, q, σ_C, and σ_Q. The second group of parameters are involved in regulating stem-cell division probabilities: θ_S, K_S, θ_N, and δ_S. The third group is composed of the parameters most significantly affecting the number of differentiated progeny in the system: r, A, and δ_N.

First, the parameters involved in stem-cell transition between quiescence and cycling are studied. Specifically, the logarithmic sensitivity solutions with respect to

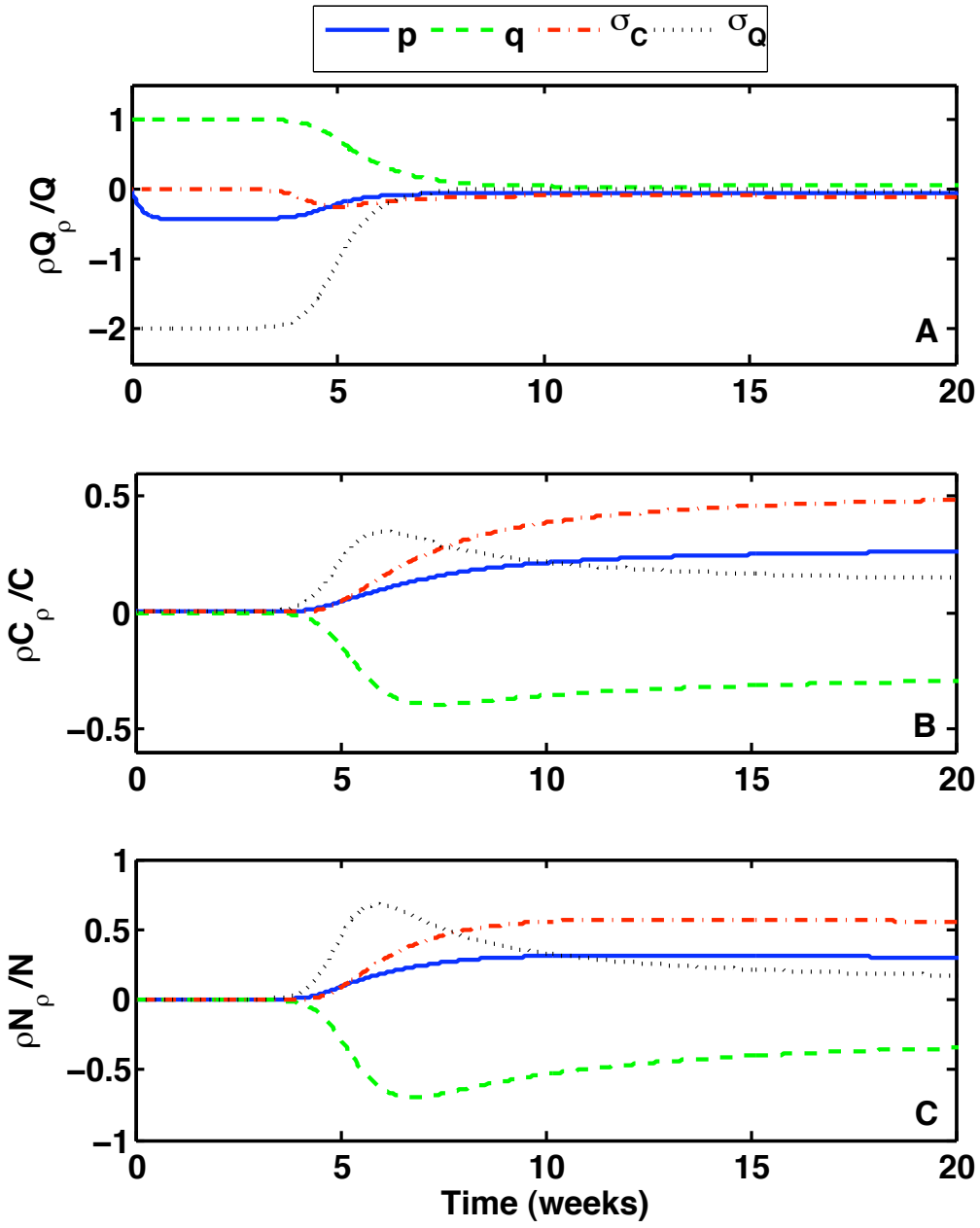

Figure 6.1: **Sensitivity of parameters affecting stem-cell transition.** Parameters controlling the transition between quiescence and cycling have little effect on homeostasis.

the parameters p, q, σ_C, and σ_Q are plotted in Figure 6.1. Recall that p is the maximum rate at which quiescent stem cells enter cycling and q is the maximum rate at which cycling stem cells enter quiescence. Parameters σ_C and σ_Q are found in the functional forms for $\Phi(C)$ and $\Psi(C)$, the probabilities at which stem cells enter the cycling and quiescent compartments, respectively. The solution curves in Figure 6.1 may be interpreted as the percentage change to the solutions for quiescent stem cells, cycling stem cells, and differentiated cells due to the doubling of the parameter in question. This type of analysis gives insight into the temporal changes in solution curves due to the variation of a parameter. For instance, according to Figure 6.1A, at time $t = 0$, the solutions generated by doubling q increase baseline solutions by approximately 100%, but as time progresses, the logarithmic sensitivity solution approaches zero, suggesting that q has minimal effect on homeostasis of quiescent cells.

Interestingly, doubling any of the parameters involved in stem-cell transitioning does not significantly change homeostatic population levels. While at first this may seem surprising, one must remember that regulatory mechanisms such as symmetric self-renewal and symmetric differentiation remain intact that control any increase or decrease in cycling stem cells, thereby minimizing extreme expansion or depletion of all populations. Although each cell population is fairly robust to changes in these parameters over the long term, there are short-term effects that are worth noting. In particular, perturbations to the rate at which cycling cells enter quiescence, q, and the parameter σ_Q have significant effect on the quiescent stem-cell compartment during the initial stages of tissue generation. Increasing σ_Q increases the number of cells needed in the cycling compartment before cycling cells enter quiescence with 50% probability. Therefore, doubling σ_Q decreases the number of quiescent stem

cells at the start of tissue generation by 200% because less cells exit the cycling compartment. On the other hand, doubling the maximum rate at which cells enter quiescence, q, causes an initial 100% increase of quiescent cells at the start of tissue generation. As homeostasis is reached, however, perturbations in both σ_Q and q are negligible.

Next, the parameters found in the functional forms governing stem-cell division are investigated. The ODEMTG model in Equations 5.7 incorporates feedback mechanisms that regulate four possible outcomes of stem-cell division. Parameters θ_S and θ_N respectively determine how many stem or differentiated cells are needed for symmetric self-renewal or commitment differentiation to occur with 50% probability due to chemical signaling. The size of the stem cell niche, K_S, also contributes to the probability of symmetric self-renewal and symmetric commitment differentiation. Finally, the probability of stem-cell death, δ_S, also influences the outcome of stem-cell division. The logarithmic sensitivity solutions with respect to θ_S, θ_N, δ_S, and K_S are plotted in Figure 6.2.

Perturbations to the size of the stem-cell niche, K_S, have the greatest long-term effects on tissue homeostasis. Doubling the niche increases the cycling stem-cell and differentiated-cell populations at homeostasis by approximately 30%, but increases the number of quiescent stem cells by approximately 100%. This implies that if other regulatory mechanisms remain unaltered, a larger niche supports a greater number of stem cells, but favors these additional cells in quiescence. Doubling the parameters θ_S, θ_N, and δ_S has less effect on homeostatic population levels, but variation in δ_S significantly alters all of the cell populations in the initial stages of tissue generation. Since tissue generation is initiated with one cycling stem cell, a significant increase in the probability of stem-cell death will negatively impact the cycling population of

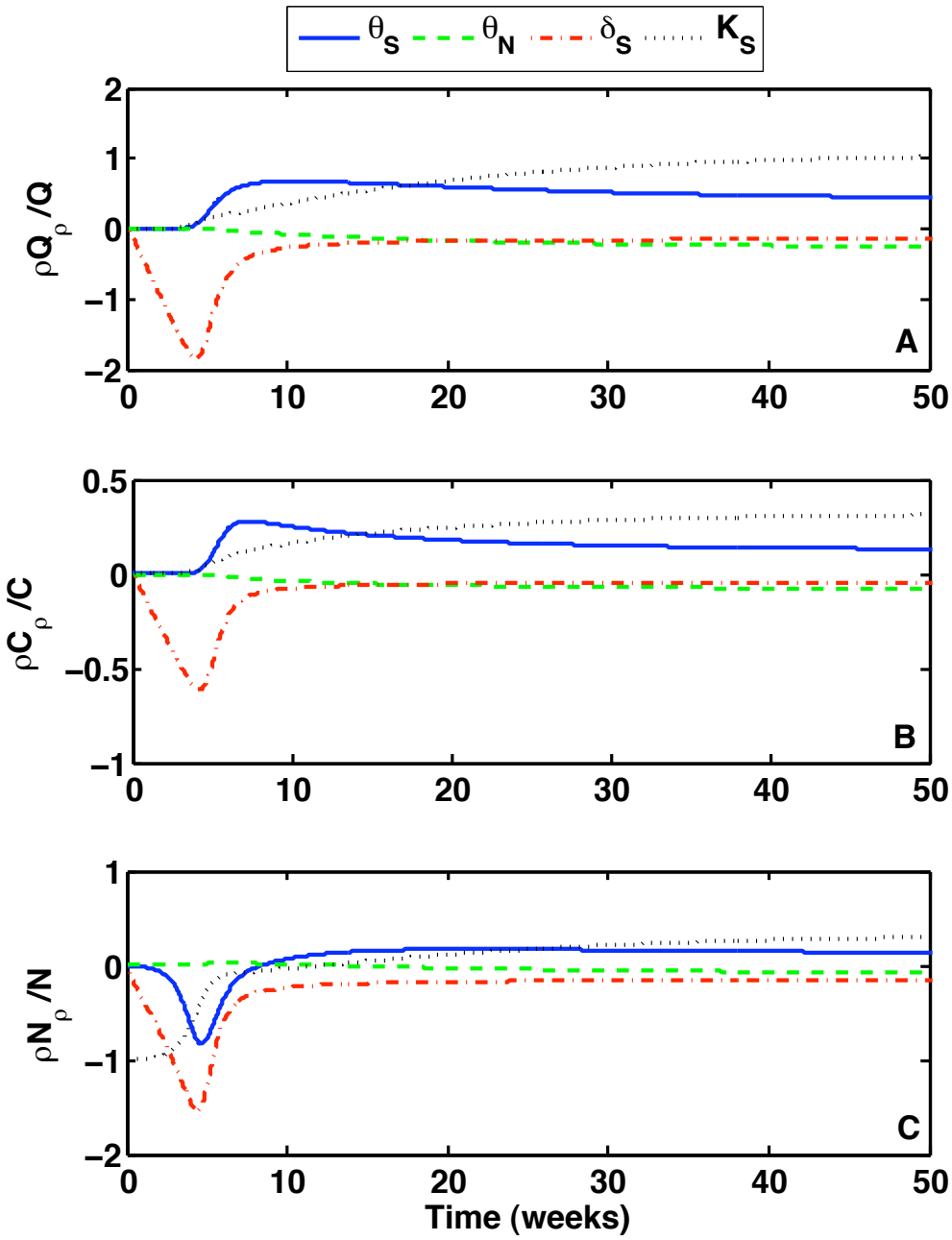

Figure 6.2: **Sensitivity of parameters involved in determining stem-cell division mode.** The size of the stem-cell niche is most significant in a long-term increase of quiescent stem cells. The probability of stem-cell death significantly impacts all cell populations early in tissue generation, but the effect is neutralized within ten weeks.

stem cells, which in turn diminishes the number of cells able to enter quiescence as well as the potential for producing differentiated progeny. These effects are contained within the first 10 weeks of tissue generation, however, and do not radically alter homeostasis.

The final group of parameters features those most directly affecting the number of differentiated cells in the system. The stem-cell proliferation rate, r, is the rate at which cycling stem cells divide. The amplification factor, A, accounts for the expansive cell divisions of intermediate progenitors that produce the necessary number of differentiated cells. Lastly, δ_N is the death rate of terminally differentiated cells. Since this last group of parameters each appear linearly in the model equation for differentiated cells, it is expected that doubling the stem-cell proliferation rate or amplification factor leads to a 100% increase in differentiated cells, whereas increasing differentiated cell death rate leads to a 100% decrease in differentiated cells. Furthermore, neither of these parameters affects the long-term equilibrium of the cycling or quiescent stem-cell populations. Because perturbations of the amplification factor and differentiated cell death rate do not cause significant temporal changes during the early stages of tissue generation, these are not explicitly plotted. However, perturbation of the stem-cell proliferation rate has a major impact on generation time, and as a result, the final plot focuses on this parameter, and only plots the logarithmic sensitivity solutions with respect to r in Figure 6.3.

It is particularly important to highlight the short-term impact of increasing the stem-cell proliferation rate. If cycling stem cells proliferate faster in the initial stages of tissue generation, then it takes less time to reach homeostasis as all cell populations expand more quickly. Perturbation of stem-cell proliferation realizes its maximal effect approximately four weeks after the start of tissue generation. At this time,

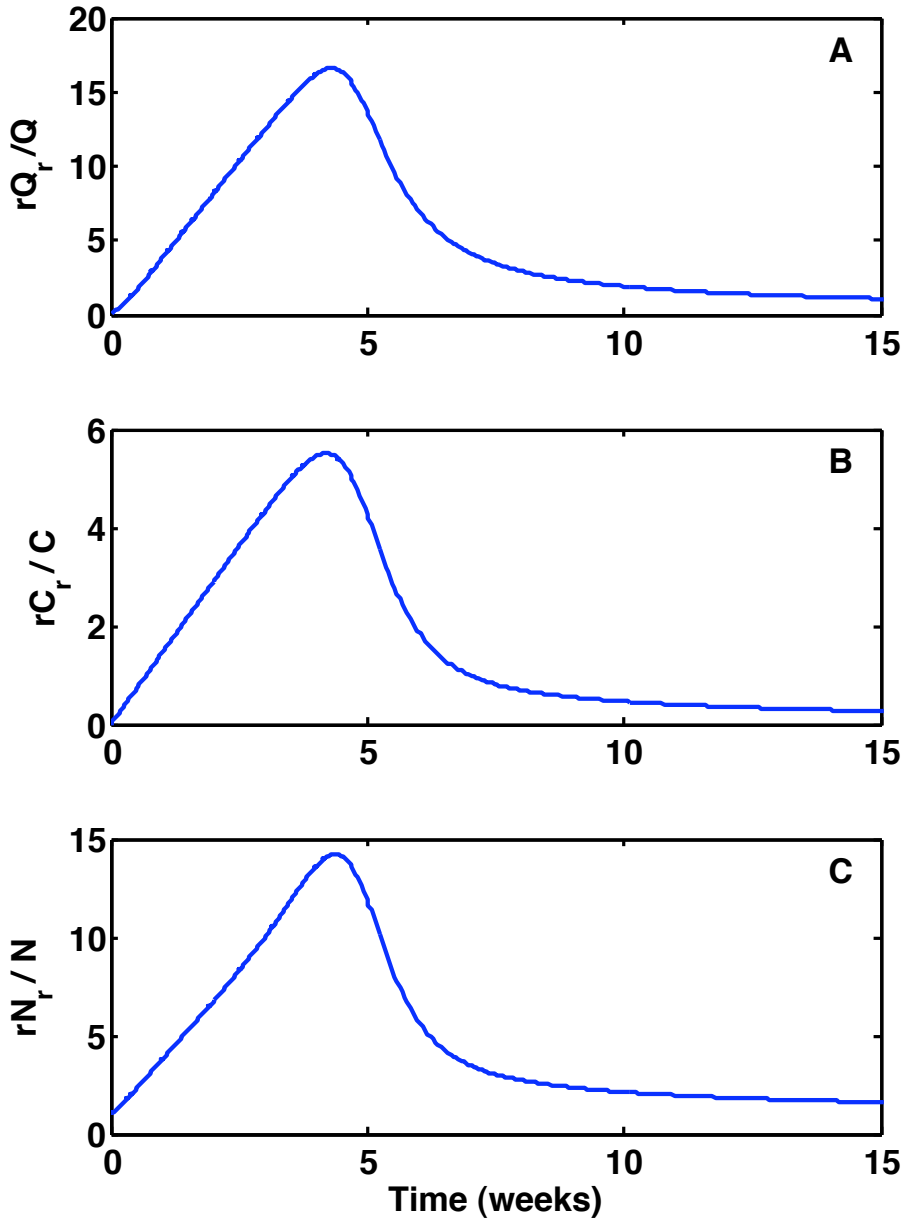

Figure 6.3: **Sensitivity of the stem-cell proliferation rate.** The stem-cell proliferation rate dramatically increases all cell populations early in tissue generation. In addition, it significantly affects the homeostatic level of differentiated cells, but does not alter the equilibrium of both stem-cell populations.

the doubling of r increases the quiescent stem-cell population by 17-fold, the cycling compartment by approximately 5.5-fold, and the differentiated-cell population by nearly 15-fold. Clearly the rate at which cycling stem cells divide is an important factor in determining how long it takes for tissue to be generated. Since increasing the stem-cell proliferation does not alter the steady state of stem cells in homeostasis, the dramatic temporal variation due to increased stem cell proliferation would not have been detected without conducting this type of sensitivity analysis.

6.1.3 Discussion

In comparing and contrasting the sensitivity solutions for each of the model parameters, it is evident that some parameters have significant effects on the long-term outcome of homeostatic solutions, while others have an immediate, but short-lived effect during the initial stages of tissue generation. The stem-cell proliferation rate, r, is unique in that it impacts both long-term and short-term dynamics considerably. Variations in this parameter cause the greatest effect during the initial stages of generation in comparison with all other parameters. Increasing the stem-cell proliferation rate increases the number of stem cell divisions that occur in a given time frame, promoting faster expansion in all cell populations. These effects do not persist over time in the stem cell populations, however, as the number of quiescent and cycling stem cells at homeostasis remains unaltered due to a balanced pattern of stem-cell division. In contrast, long-term effects are realized in the differentiated-cell population due to the increased number of stem-cell divisions producing differentiated progeny through asymmetric and commitment differentiation divisions. Homeostatic solutions of the differentiated-cell population are also significantly altered by the amplification factor, A, and differentiated-cell death rate, δ_N. Specifically, the differentiated cell population increases by 100% when A is doubled, and decreases

by 100% when δ_N is doubled, but this is expected.

There are other parameters that cause significant variation in the the initial stages of tissue generation. The maximum rate at which cells enter quiescence, q, and the switch parameter at which cycling cells enter quiescence with 50% probability, σ_Q, notably alter the solution of quiescent stem cells at the beginning of tissue formation, but these effects diminish after five weeks. This result implies that alterations in the rate and probability at which cycling cells enter quiescence have greater significance in earlier stages of tissue growth rather than the later period of homeostasis. Similarly, the probability of stem-cell death, δ_S, initially impacts both quiescent stem cells and differentiated cells negatively, decreasing these solutions by approximately 180% and 150%, respectively, but as tissue continues generating, the percentage change at homeostasis diminishes.

Although various parameters have significant short-term effects during tissue generation, the change in solutions is normalized over the long run due to regulatory mechanisms that control tissue homeostasis. Parameters q, σ_Q, δ_S and particularly r all significantly affect tissue dynamics early, but do not maintain their influence as time progresses and tissue equilibrium is reached. Consequently, single parameter perturbations may influence the pace of tissue generation, but are held in check by regulatory mechanisms that govern tissue dynamics.

The sensitivity solutions for the size of the stem-cell niche, K_S reveal several details regarding the importance of this parameter. First, it is the most important parameter in determining the number of stem cells at homeostasis. Although the long-term solution of cycling cells does increase, a greater percentage change occurs in the quiescent population. Specifically, doubling the size of the stem-cell niche increases the number of cycling stem cells by 30% and quiescent cells by 100%. In

addition, doubling the niche initially decreases the solution of differentiated cells by 100%, though this variation goes to zero in approximately five weeks. When the niche is increased and there are few stem cells in the system, as at the start of tissue generation, symmetric self-renewal is favored over the other types of stem-cell division, which inhibits the production of differentiated cells. As the stem-cell population expands and the niche is filled, however, symmetric self-renewal decreases and differentiation proceeds. The logarithmic sensitivity solution of the differentiated cell population with respect to K_S is unique in that it is the only one in which the initial percentage change is negative while the change at homeostasis is positive. This is explained by the fact that the larger niche supports a greater number of stem cells in the long-run, which in turn produces more differentiated cells at homeostasis.

One may notice that with the exception of the initial spike caused by increasing the stem-cell proliferation rate, all other sensitivity solutions for cycling stem cells have percentage changes of magnitude less than 100%. Even more telling is the observation that no parameter alters the long-run solution of cycling stem cells by more than 50%. Therefore, the doubling of a single parameter is not sufficient to greatly change the homeostasis of cycling stem cells. This implies that the regulatory mechanisms governing the cycling compartment compensate for considerable parameter perturbations. It is possible that a combination of parameters could impact the solution at homeostasis, but before this type of analysis is discussed in section 6.3, the next section will present a reduced model that effectively models tissue after completed generation.

6.2 Mathematical Modeling of Homeostatic Tissue

In Chapter V, the ODEMTG model was introduced in Equations 5.7 to simulate generation of hierarchical tissue. The previous section discussed the sensitivity of each of the parameters in this three-equation model. It was determined that perturbations in parameters associated with stem-cell transitioning between cycling and quiescent populations could affect the number of cells during the initial stages of tissue formation, but did not significantly impact tissue homeostasis in the long-run. This observation suggests that the interplay between quiescence and cycling does not noticeably alter the composition of the total stem-cell population at homeostasis. Consequently, the ODEMTG model can be reduced into a system of two ordinary differential equations by combining the quiescent and cycling populations into one stem-cell pool, and this model can be used for tissues that have completed generation.

6.2.1 Model of Homeostatic Tissue Regulation

In this section, the ODEMTG three-equation model is reduced to a system of two ordinary differential equations by combining quiescent and cycling stem cells into one population. Let S be the total number of stem cells and note that $S = Q + C$ and $\frac{dS}{dt} = \frac{dQ}{dt} + \frac{dC}{dt}$. Therefore, according to Equations 5.7,

$$\begin{aligned} \frac{dS}{dt} &= (\alpha_S - \alpha_D - \delta_S)\, rC \\ \frac{dN}{dt} &= (2\alpha_D + \alpha_A)\, rAC - \delta_N, \end{aligned} \tag{6.3}$$

where

$$\begin{aligned}
\alpha_S &= (1-\delta_S)\left(\frac{\theta_S^2}{\theta_S^2+C^2}\right)\left(1-\frac{S}{K_S}\right) \\
\alpha_D &= (1-\delta_S)\left(\frac{\theta_N}{\theta_N+N}\right)\left(\frac{S}{K_S}\right) \\
\alpha_A &= 1-\alpha_S-\alpha_D-\delta_S.
\end{aligned}$$

If ξ is the percentage of stem cells that are cycling at homeostasis, then $C = \xi S$, which gives

$$\frac{dS}{dt} = (\alpha_S - \alpha_D - \delta_S)\, r\xi S$$

and

$$\alpha_S = (1-\delta_S)\left(\frac{\theta_S^2}{\theta_S^2+(\xi S)^2}\right)\left(1-\frac{S}{K_S}\right).$$

By making the substitutions $\bar{\theta_S} = \frac{\theta_S}{\xi}$ and $k = r\xi$ and dropping the bar on $\bar{\theta_S}$ for convenience, the final reduced system of equations is

$$\begin{aligned}
\frac{dS}{dt} &= (\alpha_S - \alpha_D - \delta_S)\, kS \\
\frac{dN}{dt} &= (2\alpha_D + \alpha_A)\, rAS - \delta_N
\end{aligned} \tag{6.4}$$

with

$$\begin{aligned}
\alpha_S &= (1-\delta_S)\left(\frac{\theta_S^2}{\theta_S^2+S^2}\right)\left(1-\frac{S}{K_S}\right) \\
\alpha_D &= (1-\delta_S)\left(\frac{\theta_N}{\theta_N+N}\right)\left(\frac{S}{K_S}\right) \\
\alpha_A &= 1-\alpha_S-\alpha_D-\delta_S.
\end{aligned}$$

For ease of referral in subsequent discussion, Equations 6.4 is called the Model of Homeostatic Tissue Regulation (MHTR).

6.2.2 Analysis of Tissue Equilibrium

System equilibrium is achieved when either $S = 0$ or $(\alpha_S - \alpha_D - \delta_S) = 0$. The elimination state corresponds to a system with zero stem cells and zero differentiated

cells. This steady state has eigenvalues $\lambda_1 = k(1 - 2\delta_S)$ and $\lambda_2 = -\delta_N$. Therefore, the elimination state is stable if and only if $\delta_S > \frac{1}{2}$. In other words, the elimination state is stable when the probability of stem-cell death is greater than 50%, and unstable otherwise. In healthy tissue, it is assumed that stem-cell death occurs with small probability during division, specifically 5% as derived from the suggested proliferation and death rates of hematopoietic stem cells, rendering the elimination state unstable [21, 83].

A positive steady state exists when $(\alpha_S - \alpha_D - \delta_S = 0)$ is satisfied. Under this condition, the steady state of differentiated cells is linearly dependent upon the stem-cell population such that

$$N = \frac{(1 - 2\delta_S)kA}{\delta_N} S. \tag{6.5}$$

By substituting this equality for N into $(\alpha_S - \alpha_D - \delta_S) = 0$, the steady state of stem cells can be derived by solving for the roots of the third-degree polynomial

$$P_3 S^3 + P_2 S^2 + P_1 S + P_0 = 0,$$

where

$$\begin{aligned}
P_3 &= -\delta_S K_S (1 - 2\delta_S) kA - (1 - \delta_S)\delta_N \theta_N \\
P_2 &= -(1 - \delta_S)(1 - 2\delta_S)\theta_S^2 kA - \delta_S K_S \delta_N \theta_N \\
P_1 &= -2(1 - \delta_S)\theta_S^2 \delta_N \theta_N - \theta_S^2 K_S (1 - 2\delta_S)^2 kA \\
P_0 &= (1 - 2\delta_S)\delta_N \theta_N \theta_S^2 K_S.
\end{aligned}$$

If $\delta_S < \frac{1}{2}$, then according to Descartes' Rule of Signs, there is exactly one positive solution for tissue homeostasis. Using the parameters presented in Table 6.1, numerical derivation finds the equilibrium solution to be 1.80×10^4 stem cells and 2.62×10^{10}

Parameters		
Term	Value Range	Used Value
r	0.002 - 0.6931 (1/day) [1, 21]	0.2310 (1/day)
ξ	0.05 - 0.25 [21, 90, 104]	0.1528
k	ξr	0.035 (1/day)
θ_S	$\frac{3{,}000}{\xi}$	19,600 (cells)
θ_N	No Information	1×10^{10}(cells)
δ_S	0.05 (calculated from [83])	0.05
K_S	15,000 - 1,000,000 (cells) [1, 83]	3×10^4(cells)
A	No Information	1.1×10^8
δ_N	2.4 (1/day) [9, 13]	2.4 (1/day)

Table 6.1: Parameter values for the Model of Homeostatic Tissue Regulation are from *in vivo* hematopoietic cells when possible.

differentiated cells. The eigenvalues of this equilibrium solution are $\lambda_1 = -2.71$ and $\lambda_2 = -0.02$, demonstrating that the solution is stable.

The probability of stem-cell death, δ_S is the only bifurcation parameter for the MHTR model presented in Equations 6.4. This implies that stem-cell apoptosis is the key factor in determining whether a healthy tissue homeostasis may be reached. If dividing stem cells die with probability greater than 50%, then the stem-cell population declines to zero, subsequently decreasing differentiated progeny until all cells are eliminated. However, if less than 50% of dividing stem cells go through apoptosis, then the tissue reaches a positive equilibrium state. Figure 6.4 plots the bifurcation of solution stability as dependent on δ_S.

This two-equation model of stem and differentiated cells provides an appropriate framework for capturing the important dynamics of a generated tissue in homeostasis. Although parameters involved in transitioning stem cells between quiescence and cycling are eliminated, these have a small impact on tissue equilibrium as confirmed by the sensitivity analysis from Section 6.1. Importantly, the MHTR model retains parameters from the ODEMTG model that had long-term effect, particularly the stem-cell niche and stem-cell proliferation rate. By reducing the number of equations, there are less parameters, which makes it simpler to now investigate which

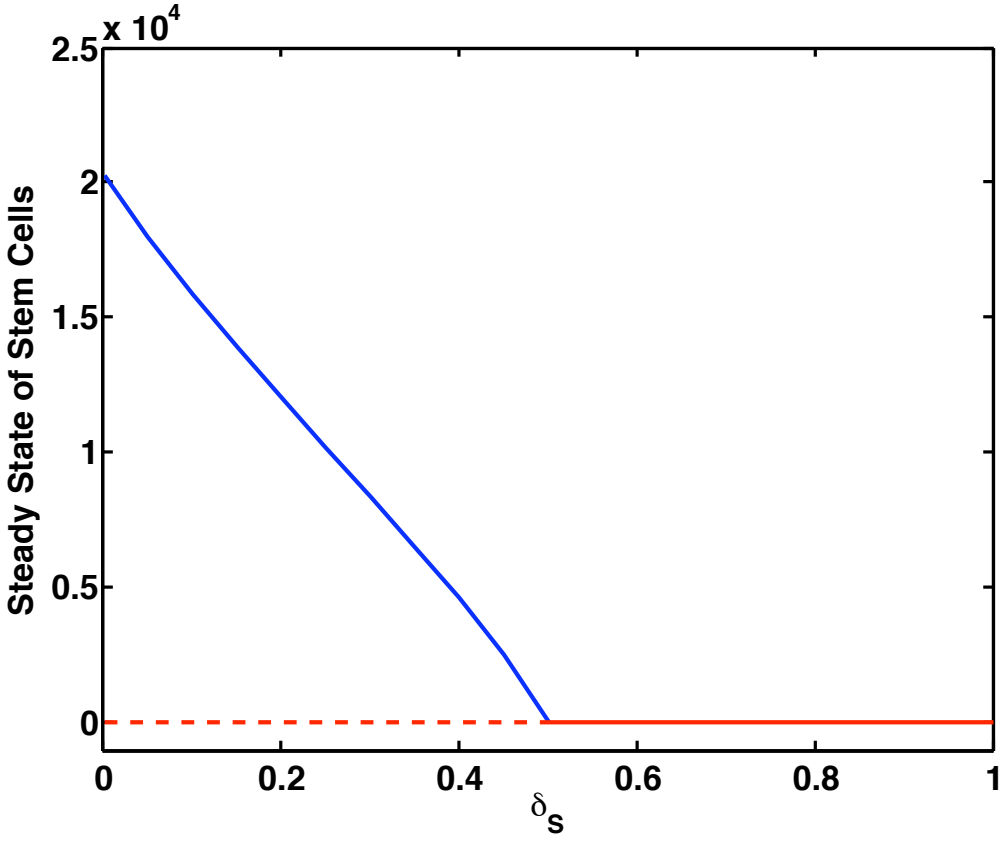

Figure 6.4: **The probability of stem-cell death is the only bifurcation parameter for the Model of Homeostatic Tissue Regulation.** When less than half of the stem-cell division outcomes result in apoptosis, a positive equilibrium solution exists and it is stable. When the probability of stem-cell death is greater than 50%, the elimination state is stable.

combinations of parameters cause significant variations in solutions homeostasis.

6.3 Principal Component Analysis

Principal component techniques are often employed in statistical analysis in order to highlight important combinations of variables in a system. The theory of principal component analysis (PCA) may likewise be applied to a model's parameter space to determine solution effects based on changes to more than one parameter. Differential sensitivity analysis, as presented in Section 6.1, is useful in identifying which individual parameters cause the greatest variation. In a dynamical system, it is possible that alterations in more than one parameter could negate any effects resulting in little deviation from the baseline solution. On the other hand, some parameter combinations could amplify solution differences more when varied jointly rather than separately. It is therefore beneficial to conduct a principal component analysis to determine the key groupings of parameters that most significantly alter solutions.

6.3.1 Theory of Principal Component Analysis

In order to familiarize the reader with PCA theory, an outline of the analysis is now presented as is relevant to analyze the MHTR model [18]. Let x be the two dimensional vector $x = [S(t,\rho), N(t,\rho)]$ of the solutions of stem cells, S, and differentiated cells, N, evaluated at time t for the parameters ρ. If ρ^* denotes the baseline parameters, then the least squares function is defined

$$J(\rho) = \int_{t_0}^{t_f} R(\rho;t)^T R(\rho;t) dt, \tag{6.6}$$

where

$$R(q;t) = [r_1(t,\rho,\rho^*), r_2(t,\rho,\rho^*)] \tag{6.7}$$

and

$$r_i(t,\rho,\rho^*) = \frac{x_i(t,\rho)-x_i(t,\rho^*)}{x_i(t,\rho)}. \tag{6.8}$$

Taylor series can be used to make the approximation

$$J(\rho) \approx (\Delta\rho)^T \left\{ \int_{t_0}^{t_f} R'(\rho^*;t)^T R'(\rho^*;t)dt \right\} (\Delta\rho), \tag{6.9}$$

where

$$R'_{(i.j)}(\rho^*;t) = \frac{1}{x_i(t,\rho)} \frac{\partial x_i(t,\rho)}{\partial \rho_j}|_{\rho=\rho^*}. \tag{6.10}$$

Because the solutions of the system are numerically derived, the time interval $[t_0, t_f]$ may be partitioned into ν subintervals such that

$$J(\rho) \approx \frac{(t_f-t_0)}{\nu}(\Delta\rho)^T \mathbf{S}_\rho^T \mathbf{S}_\rho (\Delta\rho) \tag{6.11}$$

where the sensitivity matrix

$$\mathbf{S}_\rho^T = \left[R'(\rho;t_1), R'(\rho;t_2), \ldots, R'(\rho;t_\nu)\right]. \tag{6.12}$$

The maximum of J occurs when the change in parameters, that is $\Delta\rho$, is in the direction of the eigenvector corresponding to the largest eigenvalue of $\mathbf{S}_\rho^T\mathbf{S}_\rho$, whereas the minimum occurs in the direction corresponding the the smallest eigenvalue. Therefore, matrix $\mathbf{S}_\rho^T\mathbf{S}_\rho$ can be calculated, and its eigenvalues determined in order to determine the direction in which maximum and minimum change occurs. When the eigenvectors are primarily in the directions of the parameter axes, it suggests that the parameters act independently of each other. When eigenvectors are skewed from the parameter axes, however, then it implies that there is some correlation between the two parameters that leads to maximal change.

6.3.2 Numerical Results

To determine which parameter pairings can cause the greatest effects on model solutions, a PCA was conducted for each of the potential couplings of the seven parameters in the MHTR model. When the directions incurring maximum and minimum change are nearly horizontal and vertical in correlation with the axes, the parameters act independently of each other, so it is important to identify those groups of parameters in which the axes are rotated since it implies some level of dependence. In other words, when there is parameter dependence, a change in one parameter may be compensated by a corresponding change in the other parameter in order to maintain the solution derived when using the baseline parameters ρ^*.

Of all the pairings taken from the seven MHTR parameters, only two couplings exhibit dependence, and the directions causing maximum and minimum effect are plotted in Figure 6.5. The first pair consists of the stem-cell proliferation rate, k, and the probability of stem-cell death, δ_S, as shown in Figure 6.5A. Perturbations local to ρ^* have maximal effect in the direction given by the line

$$k = -1.03\delta_S + 0.299. \tag{6.13}$$

and minimal effect along

$$k = 0.969\delta_S + 0.199 \tag{6.14}$$

This result may be interpreted by saying that an increase in stem-cell proliferation accompanied with a decrease in stem-cell death in the direction of Equation 6.13 will cause the greatest increase of cells in the system. On the other hand, an increase in stem cell death an increase in stem-cell proliferation combined with an increase of stem-cell apoptosis in the direction of Equation 6.14 will cause minimum change to the system.

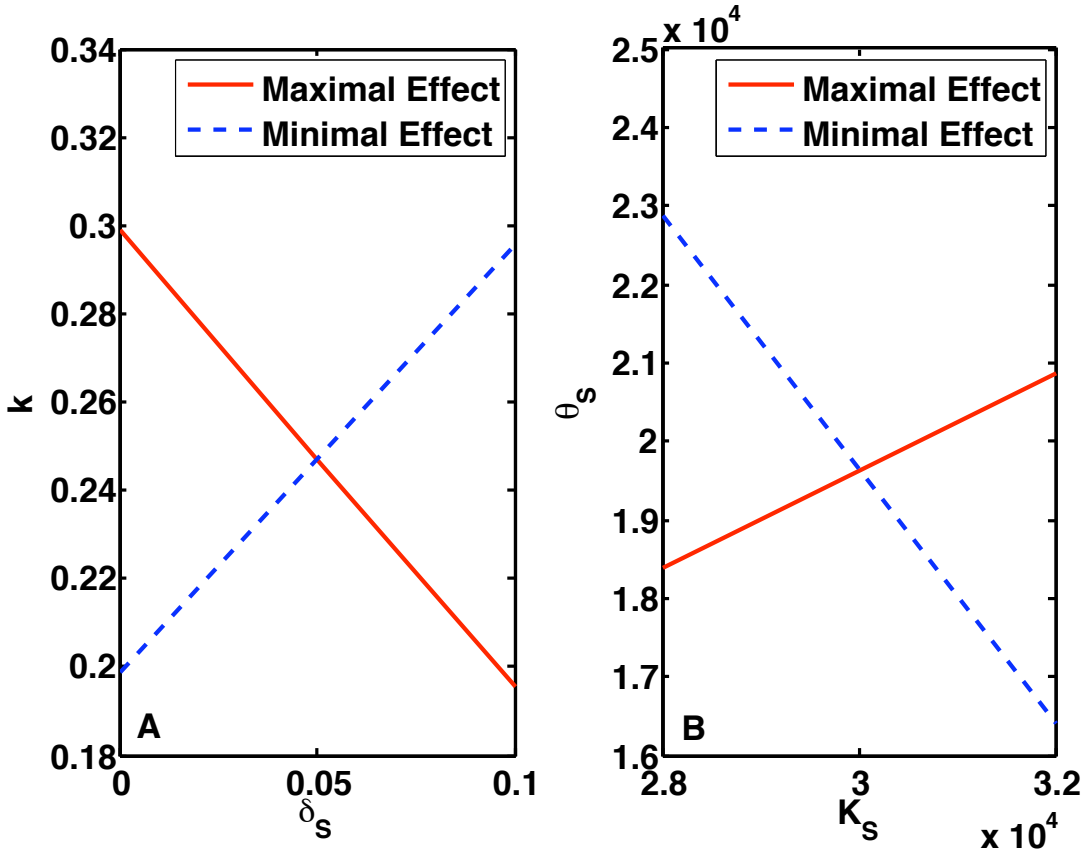

Figure 6.5: **Significant parameter pairings according to Principal Component Analysis.** Two pairings demonstrate significant correlation: the stem-cell proliferation rate and stem-cell death rate (A), and the two key parameters involved in symmetric self-renewal of stem cells (B).

The second pairing, shown in Figure 6.5B, includes θ_S and K_S, which both contribute to the probability of symmetric self-renewal in stem cells. Perturbations local to ρ^* have maximal effect in the direction of

$$\theta_S = 0.619K_S + 1080 \tag{6.15}$$

and minimal effect along

$$\theta_S = -1.62K_S + 68,100. \tag{6.16}$$

In other words, maximal effect occurs when both θ_S and K_S increase in the direction of equation 6.15. In contrast, if perturbation increases the size of the niche, then a decrease of the chemical signaling switch parameter, θ_S, in the direction of equation 6.16 may compensate for minimal change.

This principal component analysis suggests that variation to two pairs of parameters could significantly alter tissue homeostasis: (i) k, the stem-cell proliferation rate, and δ_S, the probability of stem-cell death, and (ii) θ_S, the parameter determining symmetric self-renewal based on signaling, and K_S, the size of the stem-cell niche. Specifically, increased stem-cell proliferation coupled with reduced apoptosis contributes to maximal change from equilibrium. In addition, the increase of symmetric self-renewal of stem cells due to increased signaling and niche availability causes maximal effect on the state of the tissue.

It is interesting to note that deregulated proliferation, apoptosis, and self-renewal have all been implicated in tumorigenesis [50]. Therefore, it is not surprising that variation in these model parameters greatly disturb tissue homeostasis. In particular, increased proliferation and decreased cell death cause hypercellularity in differentiated cells with little long-term effect on stem cells, whereas unbalanced symmetric self-renewal significantly expands stem cells, which in turn increases the number of

differentiated cells as well. These results are consistent with the findings of Wu *et al.* [125]. Specifically, they hypothesize that BCR-ABL increases cell prolfieration and inhibits apoptosis to cause cancer that exhibits a high ratio of differentiated to immature cells. In contrast, NUP98-HOXA9 deregulates the balance of symmetric self-renewal, and causes a form of malignancy that is more aggressive because it expands the number of cancer stem cells. The next chapter will address the acquisition of these types of mutations and determine the effects that stem-cell deregulation has on tumor initiation.

CHAPTER VII

Deregulation of Tissue-Governing Mechanisms

The Maturity-Structured Model of Mutation Acquisition (MSMMA) presented in Chapter IV investigated tumorigenesis in hierarchical tissue and predicted that unbalanced stem-cell division pattern is potentially a main cause of malignancy. In order to further investigate mechanisms that control the stem-cell division pattern, the Ordinary Differential Equations Model of Tissue Generation (ODEMTG) was presented in Chapter V. In that model, symmetric self-renewal, asymmetric self-renewal, and symmetric commitment differentiation divisions critically depended on both stem-cell and differentiated-cell populations. Chapter VI discussed the sensitivity of the ODEMTG model, and simplified the system from three equations to two. It was argued that the two-equation model, called the Model of Homeostatic Tissue Regulation (MHTR), could be used to simulate tissue that has achieved homeostasis following generation. In the present chapter, this MHTR model is used to address how deregulation of the mechanisms preserving stem-cell homeostasis contributes to cancer.

7.1 Model Structure

Just as hierarchical structure influences the multi-step process of tumorigenesis, mechanisms governing tissue homeostasis may also significantly impact cancer

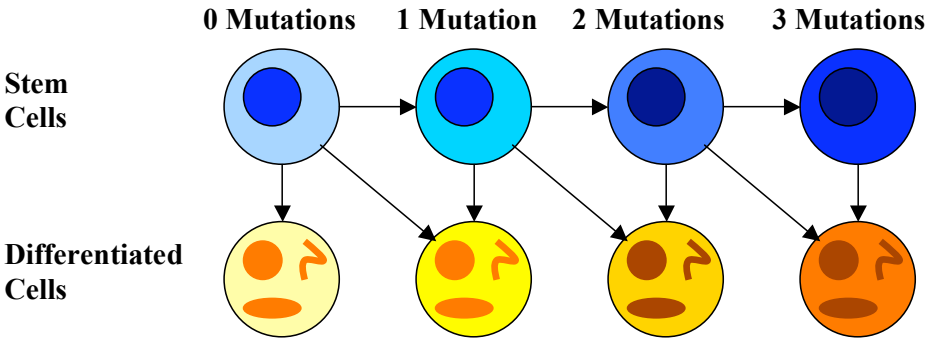

Figure 7.1: **Mutation acquisition in stem cells and the formation of abnormal progeny.** Stem cells acquire mutations with small probability during each division and pass on mutations to their progeny. Terminally differentiated cells are fully mature, and therefore, do not divide and acquire additional mutations.

growth dynamics. In order to investigate the sequential acquisition of mutations that initiate cancer in regulated tissue, the MHTR model is now extended in order to incorporate mutated cell populations. Stem and differentiated cells with i mutations are denoted S_i and N_i, respectively. Specifically, $i = 0, 1, 2, 3$ because three mutations are considered: decreased cell death, genetic instability, and deregulated proliferation. Stem cells mutate with probability m_i during division. Stem cells are the source for differentiated cells through asymmetric and symmetric differentiation divisions. Unlike the model presented in Chapter IV, intermediate populations of progenitors are omitted, and since terminally differentiated cells cannot complete further divisions and mutate, stem cells are the only cells that can acquire additional mutations. A schematic of the flow of cells from one population to another is shown in Figure 7.1.

The mathematical model consists of eight ordinary differential equations. The parameters of the non-mutated stem cells, S_0, and non-mutated differentiated cells, N_0, are as defined in Chapter VI, Table 6.1. Original model equations are presented in Chapter VI, Equations 6.4. Parameters alter depending on which mutations have

been acquired; hence, each parameter is also denoted with the subscript i to denote that it corresponds to the population of cells with i mutations. The model equations are as follows:

$$
\begin{aligned}
(7.1)\qquad \frac{dS_0}{dt} &= \left[(1-2m_0)\,\alpha_{S0} - (1-m_0)\,\alpha_{A0} - \alpha_{D0} - \delta_{S0}\right] k_0 S_0 \\
\frac{dS_1}{dt} &= \left[(1-2m_1)\,\alpha_{S1} - (1-m_1)\,\alpha_{A1} - \alpha_{D1} - \delta_{S1}\right] k_1 S_1 \\
&\quad + \left[2m_0\alpha_{S0} + m_0\alpha_{A0}\right] k_0 S_0 \\
\frac{dS_2}{dt} &= \left[(1-2m_2)\,\alpha_{S2} - (1-m_2)\,\alpha_{A2} - \alpha_{D2} - \delta_{S2}\right] k_2 S_2 \\
&\quad + \left[2m_1\alpha_{S1} + m_1\alpha_{A1}\right] k_1 S_1 \\
\frac{dS_3}{dt} &= \left[\alpha_{S3} - \alpha_{D3} - \delta_{S3}\right] k_3 S_3 + \left[2m_2\alpha_{S2} + m_2\alpha_{A2}\right] k_2 S_2 \\
\frac{dN_0}{dt} &= \left[2\,(1-m_0)\,\alpha_{D0} + (1-m_0)\,\alpha_{A0}\right] A_0 k_0 S_0 - \delta_{N0} N_0 \\
\frac{dN_1}{dt} &= \left[2\,(1-m_1)\,\alpha_{D1} + (1-m_1)\,\alpha_{A1}\right] A_1 k_1 S_1 - \delta_{N1} N_1 \\
&\quad + \left[2m_0\alpha_{D0} + m_0\alpha_{A0}\right] A_0 k_0 S_0 \\
\frac{dN_2}{dt} &= \left[2\,(1-m_2)\,\alpha_{D2} + (1-m_2)\,\alpha_{A2}\right] A_2 k_2 S_2 - \delta_{N2} N_2 \\
&\quad + \left[2m_1\alpha_{D1} + m_1\alpha_{A1}\right] A_1 k_1 S_1 \\
\frac{dN_3}{dt} &= \left[2\alpha_{D3} + \alpha_{A3}\right] A_3 k_3 S_3 - \delta_{N3} N_3 + \left[2m_2\alpha_{D2} + m_2\alpha_{A2}\right] A_2 k_2 S_2
\end{aligned}
$$

with the probabilities of stem-cell division defined as

$$
\begin{aligned}
\alpha_{S0} &= (1-\delta_S)\left(\frac{\theta_S^2}{\theta_S^2 + (S_0+S_1+S_2)^2}\right)\left(1 - \frac{S_0+S_1+S_2+S_3}{K_S}\right) \\
\alpha_{D0} &= (1-\delta_S)\left(\frac{\theta_N}{\theta_N + (N_0+N_1+N_2)}\right)\left(\frac{S_0+S_1+S_2+S_3}{K_S}\right) \\
\alpha_{A0} &= 1 - \alpha_S - \alpha_D - \delta_S.
\end{aligned}
$$

The functional forms of division probabilities were explained in Chapter V, Section 5.3.1. It is assumed that cancer cells with all three mutations, denoted S_3, do not produce signals to inhibit symmetric self-renewal, and thus they are omitted

from the Hill function in α_S. Likewise, cancer differentiated cells do not influence symmetric differentiation. Cancer cells do take up space within the stem-cell niche, and as a result, all stem cells are incorporated in the logistic term. For ease of future discussion, the model presented in Equations 7.1 is called the Model of Mutation Acquisition in Regulated Tissue (MMART).

The mutation pathway is the order in which mutations occur. All mutation pathways are compared and contrasted in order to determine which sequences generate cancer cells fastest. As in Chapter IV, three mutations are considered that are believed to be involved in the initial stages of tumorigenesis. The D mutation decreases the death rate in both stem and differentiated cells. The G mutation increases genetic instability by increasing the rate at which additional mutations are acquired. The R mutation alters proliferation characteristics of stem cells, by increasing either the proliferation rate or the probability of symmetric self-renewal. The various possibilities for the R mutation will each be examined separately in different cases. The parameter values for both normal and mutated cells are presented in Table 7.1. Although values are derived from the hematopoietic system, the model can be easily applied to other tissues by using appropriate parameter values.

7.2 Increased Stem-Cell Proliferation

The sensitivity analysis conducted in Chapter VI suggested that the stem-cell proliferation rate is a key parameter in determining tissue generation, and when combined with changes in stem-cell death, it has a big effect on homeostasis. Proliferation is increased in various forms of cancer. For instance, overexpression of the potassium channel TREK-1, the androgen receptor, and cyclin D1 have each been implicated in increased proliferation in prostate cancer cells [49, 53, 121]. It has also

Parameter	Value Used	Mutated Value
c*	0.1528	
r*	$\frac{7\ln(2)}{3}$ (weeks^{-1})	
k	$rc = 0.2471$ (weeks^{-1})	$2k$ (weeks^{-1}) @
θ_S	$\frac{3e3}{c} \approx 1.96e4$ (cells)	$2\theta_S$ (cells) !
K_S	3e4 (cells)	$2K_S$ (cells) $
θ_N	1e10 (cells)	
δ_S	0.05	$0.5\delta_S$
A	1.1e8	
δ_N	16.8 (weeks^{-1})	$0.5\delta_N$ (weeks^{-1})
m	10^{-6}	10^{-4}
* parameter from Chapter Six needed to determine parameters		
@ only used when proliferation rate increases		
! only used when chemical signals are deregulated		
$ only used when the niche capacity increases		

Table 7.1: Parameter values of non-mutated cells and mutated cells for the Model of Mutation Acquisition in Regulated Tissue. The D mutation alters death terms, the G mutation alters the mutation rate, and the R mutation may increase the stem-cell proliferation rate, or terms increasing symmetric self-renewal.

been suggested that BCR-ABL, which is expressed in CML patients, increases the rate at which hematopoietic cells divide [125].

According to the sensitivity analysis in Section 6.1.2, increasing the stem-cell proliferation rate alone has minimal effect on the homeostasis level of stem cells. Rather, it increases the number of divisions that stem cells complete, which offers more opportunity to gain additional mutations. It should be noted that as long as symmetric self-renewal and symmetric commitment differentiation are balanced, then the stem-cell population reaches equilibrium, even if the rate of proliferation increases. The number of differentiated progeny significantly increases because of the increased number of asymmetric self-renewal and symmetric commitment differentiation stem-cell divisions, but also reaches equilibrium due to stem-cell homeostasis.

When the R mutation doubles the stem-cell proliferation rate, three sub-cases may be considered. In the first case, all mutations are advantageous and give the mutated cell added benefits over normal cells. In the second case, mutated cells that have acquired G and/or R mutations without a previous D mutation have

increased cell death. In the third case, cells with G and/or R are penalized without the D mutation with the added assumption that cancer cells do not retain feedback regulatory mechanisms. Specifically in this case, the probabilities of stem-cell division are constant in cells with all three mutations. For each of these sub-cases, the pathway that causes the fastest emergence of the cancer stem cell population is determined, and the change in tissue composition over time is discussed.

7.2.1 All Mutations are Advantageous

Consider a case in which every mutation gives advantage to the cell. That is, each mutation increases the cell's fitness and cell death does not increase in attempting to eliminate the mutated cell. Under such conditions, the pathways that acquire G first are the fastest, concurring with the results from Section 4.2.2. Genetic instability predisposes the cells to accumulating additional mutations, which quickens the time in forming the first cancer stem cell. The GDR and GRD pathways are fastest, with the first cancer stem cell forming in 19 years and the slowest pathway, DRG, is nearly nine years slower. Cancer stem cells and cancer differentiated cells of all pathways are plotted versus time in Figure 7.2A-B, respectively.

The MSMMA model in Chapter IV did not incorporate feedback regulations governing stem-cell division, and as a result, the system did not adjust to the increasing number of mutated cells in the tissue. Normal cells remained in homeostasis, while all mutated populations expanded without bound. With the inclusion of feedback in the present model, mutated cells do not grow exponentially for all time, but instead displace non-mutated cells, until healthy cells diminish from the system entirely. The tissue composition of the fastest pathway, GDR, is plotted in Figure 7.2C. Non-mutated cells dominate the tissue for approximately thirty years, after which cancer cells are the majority. In contrast, when following the slowest pathway, DRG, cells

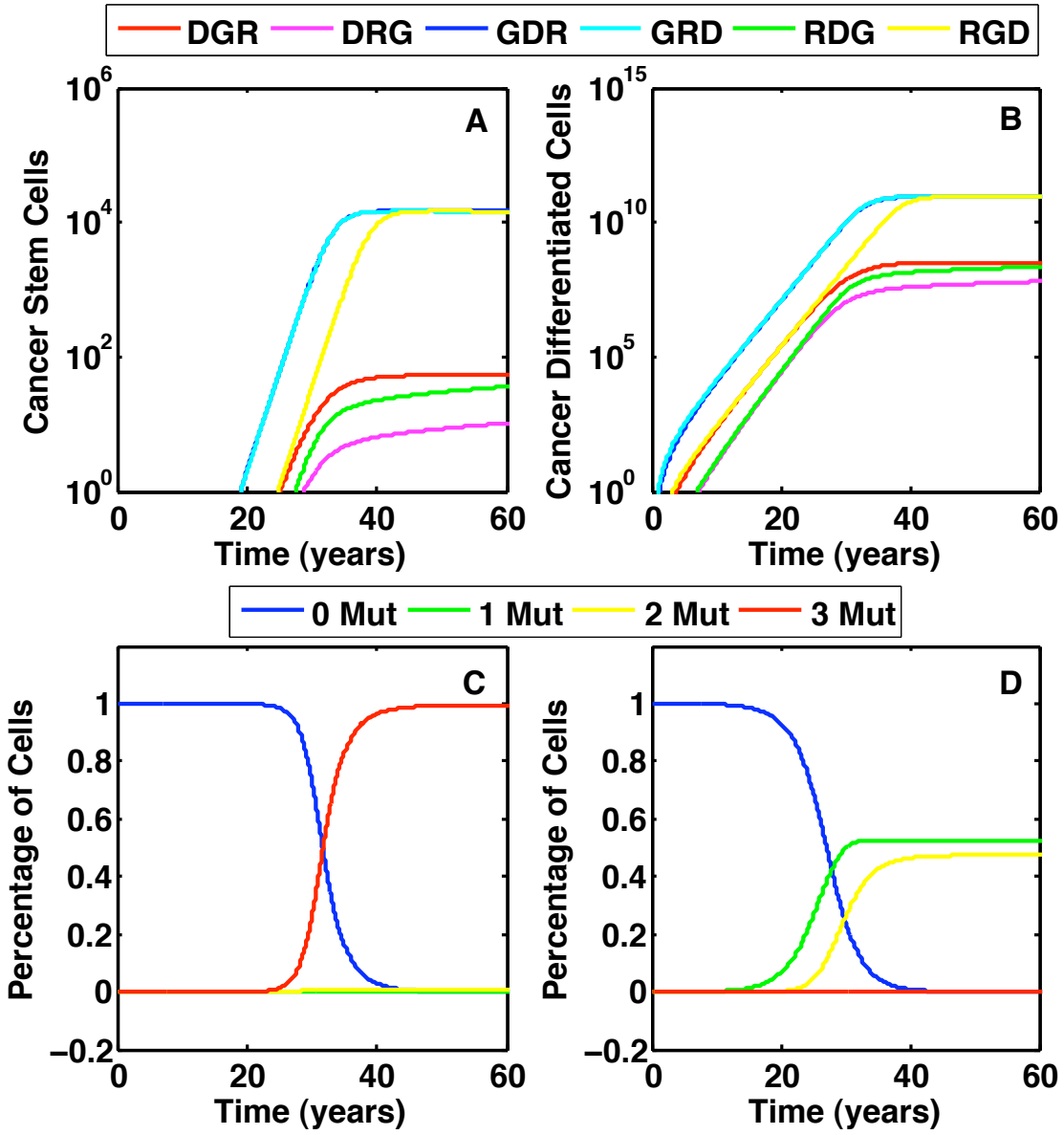

Figure 7.2: **Comparison of pathways when all mutations are advantageous.** The order in which the G mutation is acquired determines the fastest paths. (A) Cancer stem cells formed in each pathway are plotted versus time. The GDR pathway has the first cancer stem cell, followed closely by the GRD pathway. (B) Differentiated cancer cells are plotted versus time for each pathway. The growth of differentiated cancer cells mirrors the growth of cancer stem cells in each pathway. (C) Tissue composition for the fastest pathway, GDR, versus time. (D) Tissue composition for the slowest pathway, DRG, versus time.

with only one and two mutations eventually take over the tissue and cancer cells remain a small percentage, as demonstrated in Figure 7.2D. Therefore, not only does the time to form the first cancer stem cell vary between various pathways, but the order in which mutations are acquired also determines the dominance of cancer cells within the tissue.

Model predictions for fastest pathway are consistent with results from Chapter IV. This implies that the significance of genetic instability is not diminished in tissues that are regulated by governing mechanisms. There is one important difference between current MMART model predictions in comparison with MSMMA predictions. Advantageous mutations in tissues that are not governed by regulatory mechanisms, as in the MSMMA model, automatically cause exponential growth. In contrast, when regulatory mechanisms are incorporated, exponential tumor growth does not occur if these governing factors are still in place. Rather, an elevated equilibrium is approached, and cancer results from the displacement of normal cells. This implies that exponential cancer growth can only occur in the absence of feedback regulation.

7.2.2 Lethal Mutations

Now a case is investigated in which every mutation does not give the cell added advantage, but can instead increase cell death as a result of cellular machinery recognizing the mutation and forcing the cell into apoptosis. The D, G, and R mutations are defined as in Section 7.2.1, but it is assumed that cells that have acquired either the G and/or R mutation without the D mutation have an increased rate of apoptosis such that the probability of stem-cell death is 0.95 during division. For example, in the GRD pathway, cells with the G mutation only obtain the ability of mutate faster but they also have a higher death rate. Cells that are able to acquire the next mutation, R, have both genetic instability as well as increased proliferation, but cell

death remains high since apoptosis is favored due to the recognition of mutation. Once D is acquired, then the cell has increased its ability to evade apoptosis, which lowers the death rate, and the advantages gained in the previous G and R mutations remain.

Unlike the findings in Section 7.2.1, the order in which genetic instability is acquired is not important in determining the pace in which cancer is initiated. To illustrate this conclusion, consider the DGR and RGD pathways. Both pathways acquire G second, but DGR is the fastest pathway while RGD is the slowest. Therefore, the significance of genetic instability is minimized when it is lethal mutation. Instead, if the probability of cell death increases in mutated cells that cannot already evade apoptosis, then acquiring the D mutation first contributes to the fastest emergence of cancer stem cells. Once cells obtain the D mutation, then all subsequent mutations are advantageous, which is not true if either G or R is acquired first.

Not only does the fastest pathway change under the assumption of advantageous versus lethal mutations, but the tissue compositions of the fastest pathways are contrasting. Figure 7.3 compares the tissue composition between the fastest pathway in Section 7.2.1, GDR, and the fastest pathway under the assumption of lethal mutations, DGR. In the GDR pathway, cancer cells take over the tissue in thirty years. In stark contrast, cells with only one mutation, namely the D mutation, eventually dominate tissue following the DGR pathway. Therefore, it could be argued that the all-advantageous sequence GDR is a more aggressive form of disease.

The initiation of cancer is delayed 10-20 years in pathways for which D is not first. Furthermore, the tissue composition for each pathway resembles the pathway's composition under the assumption that all mutations are advantageous, but the dominance of mutated subpopulations is delayed. For example, in the pathway

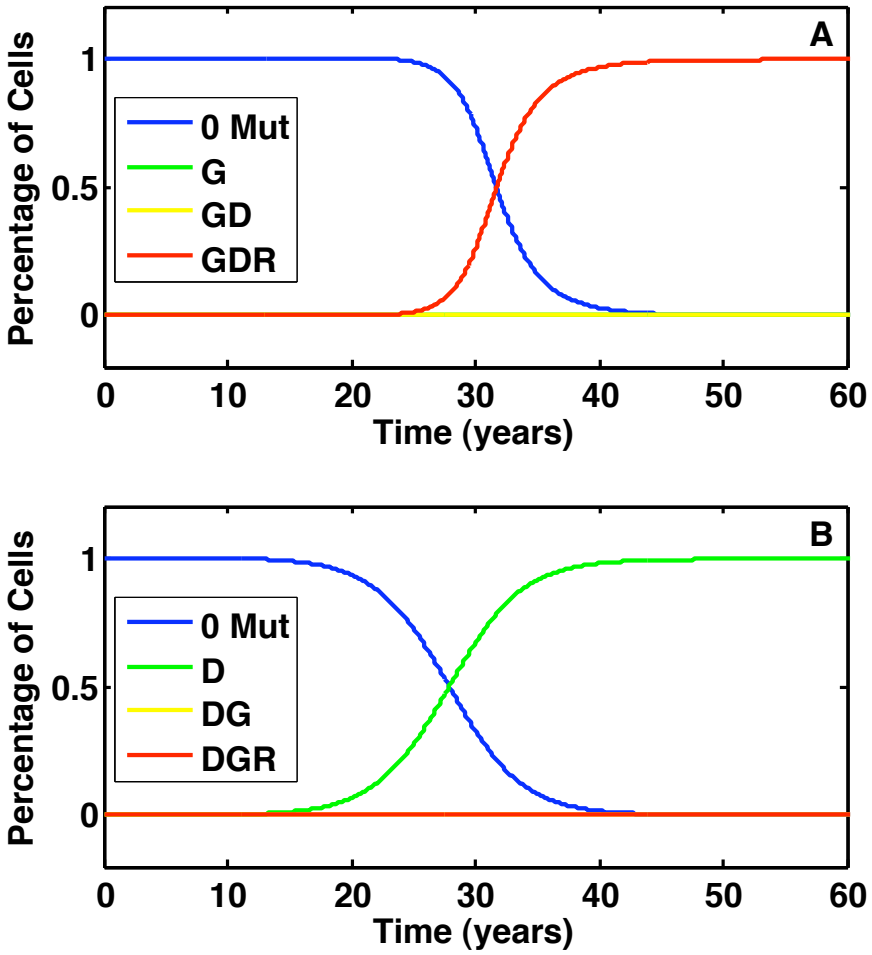

Figure 7.3: **Comparison of tissue composition in fastest pathways when all mutations are advantageous versus when some are lethal.** (A) The tissue composition of the fastest pathway, GDR, when all mutations are advantageous. The majority of tissue is eventually comprised of cells with all three mutations. (B) The tissue composition of the fastest pathway, DGR, when some mutations are lethal. Its tissue composition is strikingly different in that the majority of cells eventually have only one mutation and cancer cells are a small percentage of the tissue.

GDR in which G is lethal without D, cancer cells still eventually dominate the tissue, though it is ten years later than when all mutations are advantageous. The prevalence of cancer cells in the tissue implies that this pathway simulates a disease that progresses quickly, even though it takes longer to initiate than the DGR pathway. In contrast, the DGR pathway produces a tumor that primarily consists of cells with one mutation. The D mutation is the only mutation that can directly increase the steady state of stem cells, while both the G and R mutations affect how quickly cells move from one mutated population to the next. As a result, when D is acquired first, stem cells with one mutation outnumber normal cells, and this advantage for expansion allows the clone with the D mutation to dominate the tissue.

Once again, model predictions are consistent with the results presented in Chapter IV. Specifically, in the event that mutations are lethal without a previously acquired ability to evade apoptosis, the fastest pathway begins with the D mutation. Similar with the simulations in Section 7.2.1, regulatory mechanisms remain intact, so cell populations do not grow exponentially. The two cases explored thus far demonstrate that unrestricted growth is not possible in tissues that maintain some level of regulation. Hypercellularity can occur, but some level of equilibrium is achieved, even if it is abnormal. The next section will consider the effects on tumor dynamics when regulatory mechanisms are removed in cancerous cells.

7.2.3 Cancer Cells Lose Regulatory Mechanisms

In the two cases presented thus far, mutations have affected death, genetic instability, and proliferation of stem cells, but the regulatory mechanisms governing stem-cell division pattern have remained intact. As recorded in Chapter IV, without feedback mechanisms in place that attempt to regain tissue homeostasis, the cancer population grows exponentially over time. In stark contrast, the results from Sec-

tions 7.2.1 and 7.2.2 demonstrate that if the stem-cell population does not completely lose regulatory mechanisms, then even the cancer cell populations can be contained. In addition, recall that in Chapter IV simulations, non-mutated cells maintained homeostasis while mutated populations grew exponentially. Cancer dominance was a result of an increased number of mutated cells that vastly outnumbered non-mutated cells, not the loss of healthy cells. Conversely, in regulated tissue, non-mutated cells diminish because mutated cells have a competitive advantage and displace healthy cells.

Because cancer cells can become independent in providing their own growth signals, it is not unreasonable to suggest that cancer cells could lose control from regulatory mechanisms [50]. To investigate this possibility, assume that the D, G, and R mutations are defined as in Section 7.2.2, so that G and R are not advantageous without D. In addition, assume that cells that have acquired both the D and R mutations become independent of niche signaling and lose feedback interactions that dictate the mode of stem-cell division. In other words, the probabilities of stem-cell division become constant for cells that have acquired both D and R mutations, equating to some self-reliance in growth signals and evasion of apoptosis.

To determine the constant probabilities of symmetric self-renewal, asymmetric self-renewal, and symmetric commitment differentiation, the functional forms of α_S, α_A, and α_D are evaluated at the initial starting time, using mutated parameter values. For example, at $t = 0$, the initial probability of symmetric self-renewal in cancer cells to be $\alpha_{SC} = 0.21$, when using the mutated parameter value δ_{SC}. Likewise, the probability of symmetric differentiation in cancer cells would initially be $\alpha_{DC} = 0.16$. With the probability of apoptosis as $\delta_{SC} = 0.025$ in D-mutated cells, the remainder of the divisions are asymmetric, giving a probability of $\alpha_{AC} = 0.60$. Thus, there is a

slight imbalance in symmetric divisions and death of stem cells, causing exponential growth of cancer cells that is maintained over time since feedback mechanisms are not in place to decrease symmetric self-renewal or increase symmetric commitment differentiation. As the cancer population grows without bound, the total stem-cell population can surpass the size of the niche because cancer cells do not have this restraint. It is assumed that when the total stem-cell population exceeds the niche size, the probability of symmetric self-renewal in regulated cells is zero, and the probability of symmetric differentiation is determined by $\alpha_D = (1-\delta_S)\frac{\theta_N}{\theta_N+(N_0+N_1+N_2)}$ to ensure that the probabilities of stem-cell division are contained between zero and one. In other words, the influence of the stem-cell niche on division pattern is removed in cells with both the D and R mutations.

When the D and R mutations enable unrestricted growth, the initial stages of tumorigenesis do not greatly differ from those determined in Section 7.2.2, but over time, the differences between these cases are noteworthy. Figure 7.4 plots the total number of cancer cells that result from the fastest pathways. Let Case A be the case in which all mutations are advantageous presented in Section 7.2.1, Case B represents lethal mutations as in Section 7.2.2, and Case C is for unregulated division in this section. Recall the GDR pathway was fastest when all mutations were advantageous, while the DGR pathway was fastest if lethal mutations were considered. When cancer cells are independent of regulation, the DGR pathway is fastest, and the first cancer stem cell is formed merely 0.3 years faster than when regulation is maintained. However, unlike previous cases, the cancer population not only displaces non-mutated cells, but continues to expand and eventually overtakes the number of cancer cells in both other cases.

The loss of governing mechanisms is not mandatory for the emergence of cancer

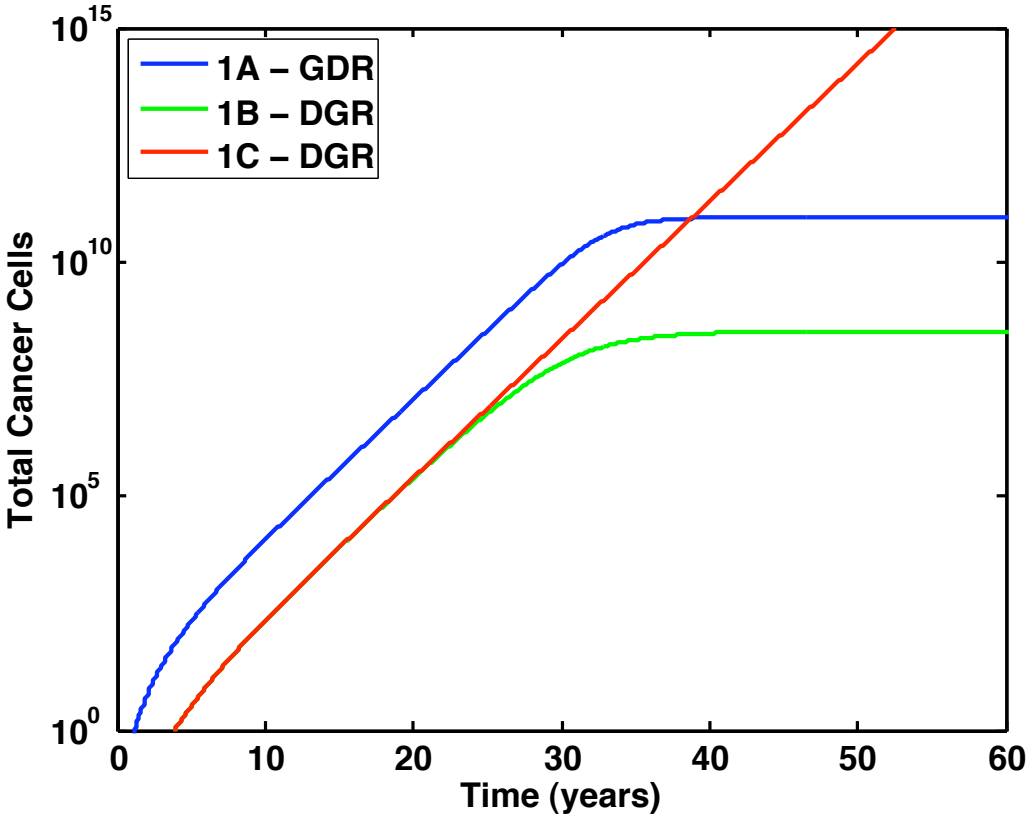

Figure 7.4: **Comparison of fastest pathways for all cases in which stem-cell proliferation is increased.** GDR is the fastest pathway in Case A (blue). DGR is the fastest pathway in Case B (green). DGR is also the fastest in Case C, but if cancer cells lose feedback regulation, then cancer stem cells grow exponentially (red).

stem cells, as confirmed by the results in Sections 7.2.1 and 7.2.2. Cancer dominates tissue in which governing mechanisms continue to be maintained due to competitive advantage over healthy cells. In such circumstances, disease can result from the elimination of healthy cells that have been replaced with mutated cells that do not properly function. However, when mutated cells are also independent of regulation, not only do cancer cells displace non-mutated cells, but exponential growth causes the cancer population to expands uncontrollably. These results imply that tumors composed of cells that have lost tissue-governing mechanisms are more malignant than tumors in which some semblance of regulation is maintained.

7.3 Unbalanced Pattern of Stem-Cell Division

It has been suggested that an unbalanced symmetric self-renewal divisions in stem cells may contribute to certain forms of cancer [4, 12, 20, 23]. For instance, the Wnt/β-catenin signaling pathway that is important in stem-cell self-renewal has also been implicated in cancer [23]. Furthermore, mutations that increase the probability of symmetric self-renewal may even cause more aggressive forms of disease than those that merely quicken proliferation. For example, consider Chronic and Acute Myelogeous Leukemia (CML and AML). Patients with CML express BCR-ABL, which increases proliferation, whereas AML patients express NUP98-HOXA9, which increases self-renewal in hematopoietic stem cells and causes a more malignant form of leukemia [125].

Clearly, the mechanisms that govern stem-cell self-renewal are of great interest when investigating the emergence of cancer stem cells. The mathematical model in Chapter IV did not account for the dynamic regulation of stem-cell division as dependent upon tissue status. Now that feedback mechanisms have been incorpo-

rated, it is possible to examine the impact of mutations that affect stem-cell division properties. Specifically, alteration of θ_S and K_S, will be addressed since these two parameters determine the probability of symmetric self-renewal. In this section, the R mutation will increase one of these parameters, thereby increasing symmetric self-renewal, while the rate of proliferation will remain unaltered. As before, the D mutation decreases death and the G mutation increases genetic instability.

7.3.1 All Mutations are Advantageous

Again consider the case in which all mutations are advantageous. That is, cell death does not increase in mutated cells, and mutated cells have competitive advantage over non-mutated cells. The D mutation decreases the probability of stem-cell death and the differentiated cell death rate by half. The G mutation increases the probability at which mutations are acquired from 10^{-6} to 10^{-4}. The R mutation doubles the value of θ_S, which increases the initial probability of symmetric self-renewal by approximately 10%.

In correlation with the conclusions in Section 7.2.1, the earlier genetic instability is acquired, the faster cancer stem cells are formed. However, increasing symmetric self-renewal through the doubling of the parameter θ_S significantly decreases the time to the first cancer stem cell in all pathways. The fastest pathway is GRD, with the first cancer stem cell formed in 8.4 years, nearly eleven years earlier than the appearance of the first cancer stem cell in Section 7.2.1. In agreement with model predictions in Chapter IV, genetic instability is less significant when symmetric self-renewal mutations are considered than when the rate of proliferation increases, as all pathways develop cancer stem cells quickly.

The growth dynamics of the stem- and differentiated-cell populations for the GRD pathway are plotted in Figure 7.5A-B. As illustrated in Figure 7.5C, the probabilities

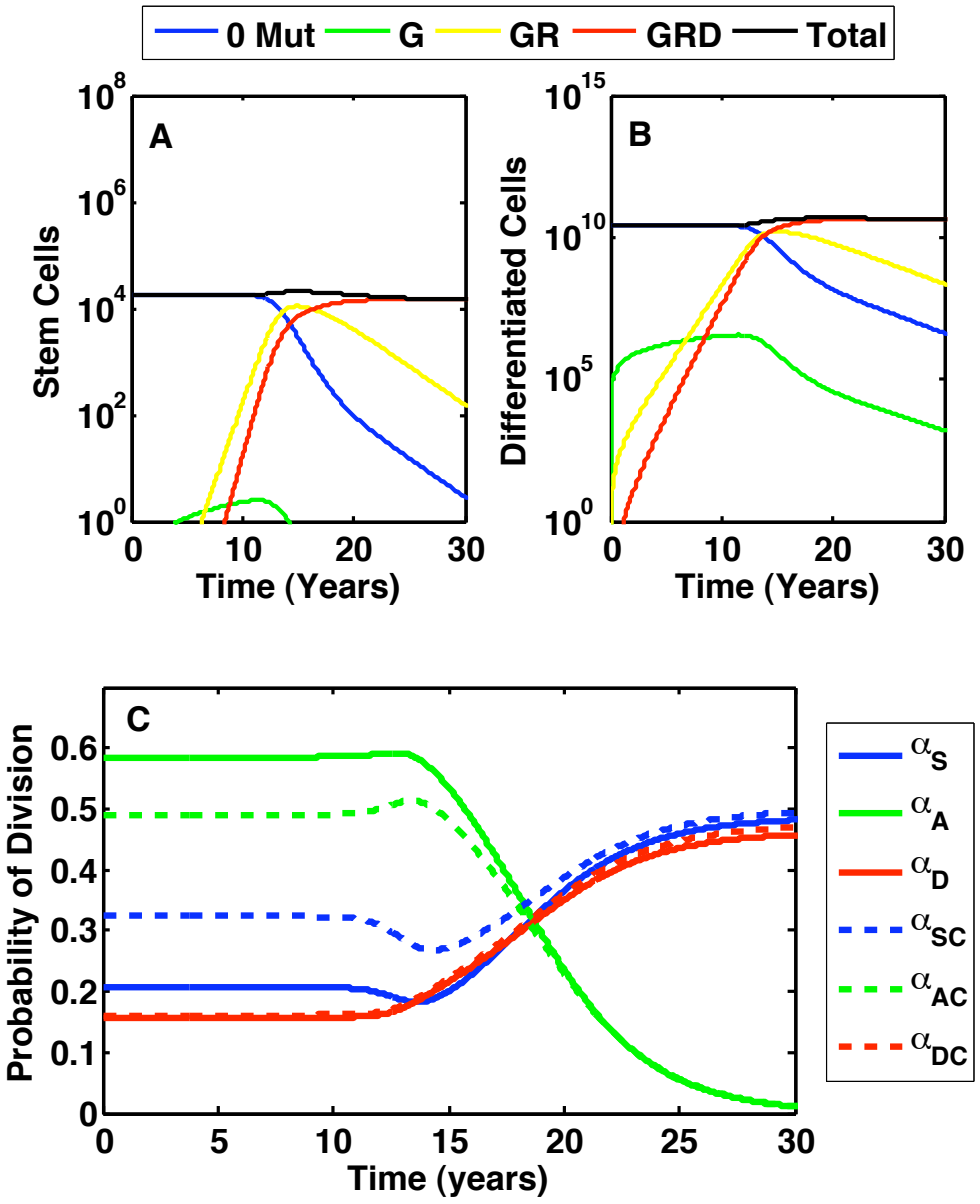

Figure 7.5: **Growth dynamics for the fastest pathway when the R mutation increases symmetric self-renewal.** When all mutations are advantageous and the R mutation increases symmetric self-renewal, the GRD pathway is fastest. (A) Stem cells versus time. The first cancer stem cell is formed in 8.44 years. (B) Differentiated cells versus time. (C) The probabilities for each type of stem cell division versus time. Probabilities for non-mutated cells are plotted with solid lines, cancer cells with dashed lines.

of stem cell-division shift over time to favor symmetric divisions. Doubling θ_S increases the initial probability of symmetric self-renewal from 0.21 to 0.32, which consequently decreases the probability of asymmetric division. As cancer cells displace non-mutated cells, the Hill functions in both symmetric self-renewal and symmetric commitment differentiation tend to one. In both non-mutated and cancer stem cells, the probability of symmetric self-renewal goes to 0.5, the probability of symmetric commitment differentiation goes to 0.475, and the probability of asymmetric division goes to zero.

An imbalance in favor of symmetric self-renewal causes rapid expansion in mutated cells and quickly displaces healthy cells. In approximately 15 years, cancer dominates the tissue. Although the probability of symmetric self-renewal is initially increased in cells with the R mutation, regulatory mechanisms were not completely eliminated. As a result, the initial rapid expansion is eventually controlled, preventing unrestricted tissue growth. This implies that altered regulations may still be capable of mediating homeostasis, even if it is abnormally controlled.

7.3.2 Lethal Mutations

As in Section 7.2.2, suppose that G and R mutations are not advantageous in cells that have not previously acquired the D mutation. In stem cells that have either G and/or R but not D, the probability of death is 0.95. Under these assumptions, the DGR is the fastest pathway, but the first cancer stem cell forms in 11.7 years, less than half of the time required by the same pathway when proliferation is altered rather than symmetric self-renewal. In fact, a cancer stem cell is formed in all pathways within 18 years. This is remarkable because the slowest pathway initiates cancer before even the fastest pathway in Section 7.2.1, in which all mutations are advantageous.

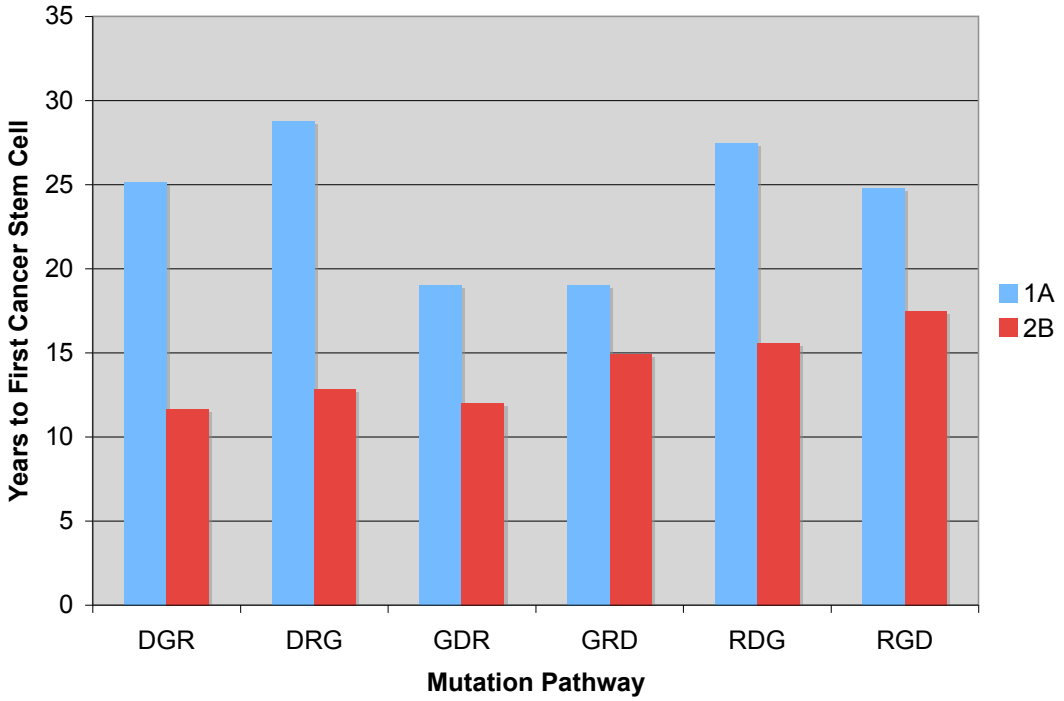

Figure 7.6: **Increased symmetric self-renewal speeds cancer onset more than increased proliferation rate.** The time to first cancer stem cell is faster for increased symmetric self-renewal when all mutations are not advantageous even when compared to the case where all mutations are advantageous with increased proliferation rate.

Figure 7.6 compares the time to first cancer stem cell for each pathway when all mutations are advantageous and R increases the proliferation rate versus those in which R increases symmetric self-renewal and G and R are lethal. Increasing symmetric self-renewal approximately 10% by doubling θ_S dramatically decreases the time to first cancer stem cell in comparison with increasing the rate of stem-cell proliferation. It is therefore suggested that increasing unbalanced symmetric divisions causes malignancies to develop quicker than increasing the rate of division. Furthermore, symmetric self-renewal minimizes the differences in cancer initiation when comparing all pathways. As a result, unbalanced symmetric self-renewal dictates a faster pace of cancer development, regardless of the sequential order of mutations.

7.3.3 Cancer Cells Lose Regulatory Mechanisms

The last two cases demonstrate that cancer cells can emerge from increased symmetric self-renewal, even if regulatory mechanisms are not completely lost. Based on the conclusions that unbalanced symmetric divisions speed the onset of cancer more than increased stem-cell proliferation, one would predict that unregulated symmetric divisions would be additionally problematic. Indeed, if stem cells with both the R and D mutations become independent of division regulation and governing mechanisms are lost, the cancer stem-cell population emerges quickly and grows exponentially.

To emphasize the significance increasing symmetric self-renewal on cancer stem-cell dynamics, the cancer stem-cell population of the fastest pathways from each of the six cases discussed thus far are plotted in Figure 7.7. Case 1 denotes all the simulations in which the R mutation doubles the proliferation rate of stem cells, while Case 2 denotes the simulations in which the R mutation doubles θ_S and increases symmetric self-renewal. All mutations are advantageous in Cases 1A and 2A, G and R mutations are not advantageous without D in Cases 1B and 2B, and stem-cell division regulation is lost in cells with D and R mutations in Cases 1C and 2C.

The fastest pathways in which R increases symmetric self-renewal are significantly faster than the pathways in which R increases the stem-cell proliferation rate. This only emphasizes our previous results from Chapter IV that predicted aberrant symmetric self-renewal can be an important factor in determining cancer initiation. In addition, when comparing Cases 1C and 2C in which the cancer stem-cell population grows exponentially, the rate at which cancer grows is markedly increased in the latter case. Therefore, deregulated unbalanced symmetric self-renewal quickly initiates tumorigenesis and continues to promote cancer expansion through an elevated growth rate if regulatory mechanisms are lost.

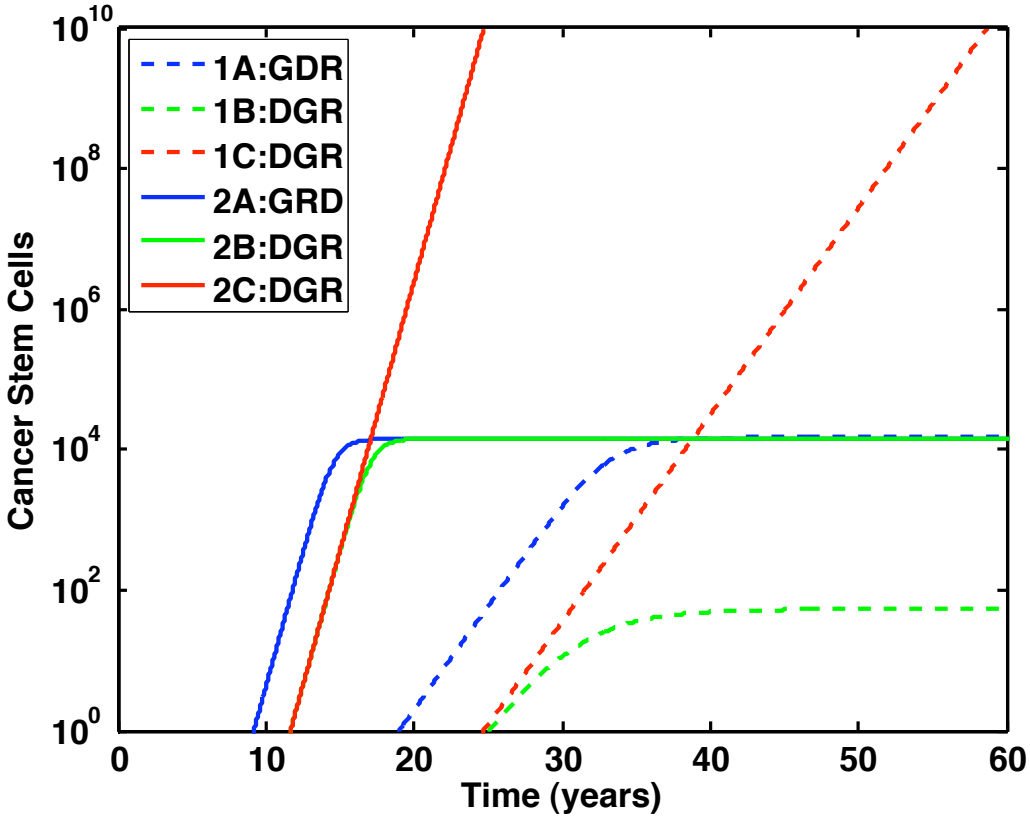

Figure 7.7: **Complete loss of regulation enables malignant growth.** Case One simulations, in which stem-cell proliferation is increased, are plotted with dashed lines. Case Two simulations, in which symmetric self-renewal is increased, are plotted with solid lines. The first cancer stem cell is formed via the GDR pathway when symmetric self-renewal is increased and all mutations are advantageous. The most malignant growth is formed through the DGR pathway, when stem cells have increased symmetric self-renewal and have also lost feedback regulation.

7.3.4 Increased Stem Cell Niche

It has been suggested that cancer stem cells are not as dependent on the stem-cell niche as normal stem cells [74, 76]. As a result, cancer stem cells are not as restricted by the physical carrying capacity of the niche. In Sections 7.2.3 and 7.3.3, all control from the stem-cell niche was removed, and cancer stem cells grew exponentially. Now a case is considered in which cancer stem cells are still restricted by the niche, but the niche controlling mutated cells is larger since it is assumed mutated cells have more freedom in where they reside. Due to the results of the sensitivity analysis in Chapter VI, Section 6.1.2, it is predicted that increasing the niche will have a major impact on tumor growth, since it was the only model parameter that significantly altered long-term homeostasis of stem cells. In the following simulations, the R mutation doubles the size of the stem-cell niche, K_S, but does not change the proliferation rate, k, or θ_S. As in Sections 7.2.2 and 7.3.2, the D mutation decreases the death rate, the G mutation increases the mutation rate, and it is assumed that the G and R mutations are not advantageous unless D has been acquired.

The results of Section 7.3.2 demonstrated that increasing θ_S increases symmetric self-renewal, but it is now suggested that doubling K_S causes a greater increase in symmetric self-renewal divisions. In addition, increasing K_S also decreases the probability of symmetric commitment differentiation. The combination of the increase in symmetric self-renewal and decrease in symmetric commitment differentiation creates an even larger imbalance of symmetric divisions than doubling θ_S. Consequently, it is not surprising that a mutation increasing the stem-cell niche causes the fastest cancer onset. The DGR pathway is fastest, forming the first cancer stem cell in 6.65 years, though all pathways have a cancer stem cell in under ten years.

There is an additional interesting aspect of the growth dynamics caused by this

mutation. The increased niche capacity for R-mutated stem cells give them a significant competitive advantage other cells. As mutated cells fill up the niche, feedback regulation forces symmetric self-renewal of normal cells to go to zero since the system does not want to add more stem cells. In addition, symmetric commitment differentiation of normal cells goes to its maximum value of $(1 - \delta_S)$ in order to push cells out of the niche. In so doing, the normal cell population differentiates more than it self-renews, which in turn causes the forced rapid extinction of normal cells.

Figure 7.8 compares the probabilities of stem-cell division that occur in a system following the DGR pathway for when symmetric self-renewal increases due to increasing θ_S, as in Section 7.3.2 as opposed to when it increases because of the niche. When symmetric self-renewal is increased by doubling θ_S, all cells continue to be regulated by the same size niche. As time progresses, non-cancer cells diminish, which forces the chemical signaling term $\frac{\theta_S^2}{\theta_S^2+(S_0+S_1+S_2)^2}$ to one, and symmetric self-renewal in both normal and cancer cells goes to 50%, as demonstrated in Figure 7.8A. The other 50% of divisions result in symmetric commitment differentiation and apoptosis. In contrast, when the R mutation doubles the niche, the signaling term also goes to one as time progresses, but because cancer cells fill up the niche and can in fact surpass the niche, symmetric self-renewal in normal cells diminishes while symmetric commitment differentiation goes to 95%. Cancer cells do not have the same division probabilities as normal stem cells in the long run due to the increased niche capacity; cancer stem cells symmetrically self-renew at 50% and symmetrically differentiate at 47.5%, as plotted in Figure 7.8B. In summary, a mutation that increases the cell's self-reliance apart from the niche, thereby increasing the potential niche capacity in which the cell may reside, creates a considerable imbalance in stem-cell division probabilities while also promoting extensive differentiation and loss of normal cells.

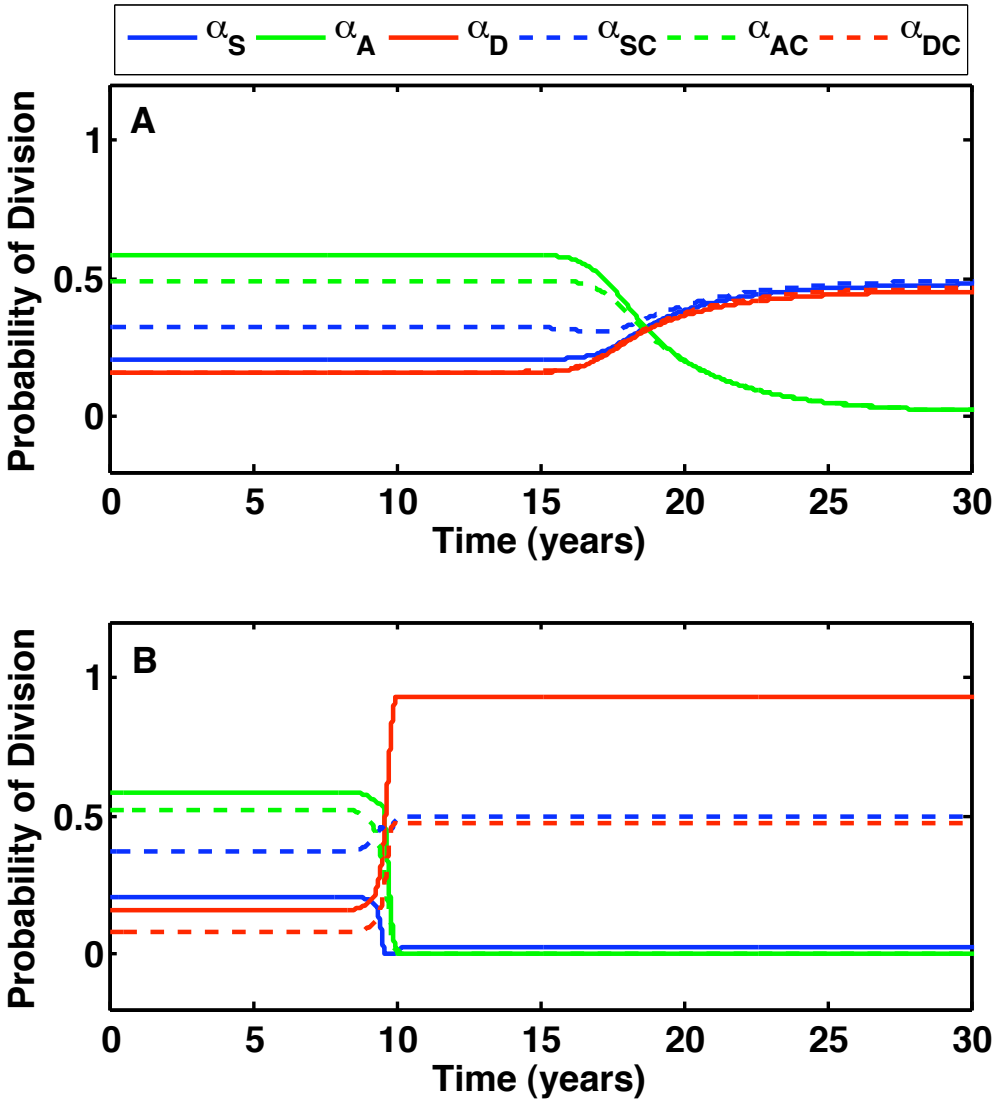

Figure 7.8: **Comparison of stem-cell division probabilities for mutations that increase symmetric self-renewal.** The fastest pathway of both cases is DGR, but the probabilities of stem-cell division are markedly different. Values for non-mutated cells are plotted with solid lines, cancer cells are plotted with dashed lines. (A) The probabilities of stem cell division when the R mutation doubles the switch parameter. Both mutated and healthy cells approach balanced division patterns in the long run. (B) The probabilities of stem cell division when the R mutation doubles the niche size. Normal cells are forced to differentiate due to crowding from the niche.

7.4 Conclusions

This chapter focused on investigating mutation acquisition in hierarchical tissue in which stem-cell division is governed by regulatory mechanisms. The order of mutations that causes the fastest formation of a cancer stem cell was determined under various conditions. Several results from this chapter coincide with predictions from the Maturity-Structured Model of Mutation Acquisition in Chapter IV. In particular, when all mutations are advantageous, the sequential order in which genetic instability is acquired crucially determines the time to cancer onset. Although pathways beginning with genetic instability are fastest for both types of R mutations, its effects are significantly diminished when symmetric self-renewal is increased, demonstrating that aberrant symmetric self-renewal may instigate aggressive malignancies. Over all, mutations that disturb the balance between symmetric self-renewal and symmetric commitment differentiation divisions cause initiate cancer faster than mutations increasing stem-cell proliferation rate.

Although many of the model predictions in this chapter reflect those discussed in Chapter IV, there are many aspects of tumor dynamics that can be investigated to a greater extent with the incorporation of regulatory mechanisms. For instance, with the inclusion of feedback mechanisms that govern stem-cell division, cancer cells do not necessarily grow exponentially as seen in the results from Chapter IV. Rather, if regulation remains in tact, even though it may be abnormal, a new equilibrium is achieved. Furthermore, unlike the predictions of the MSMMA model in Chapter IV, healthy cells diminish due to the displacement by mutated cells that have a competitive advantage in the niche.

In the event that all regulation is lost in cancer cells, exponential growth of the

cancer population occurs in addition to the depletion of normal cells. Therefore, the model predicts that stem-cell governing mechanisms maintain system homeostasis under healthy conditions and cancer is easily initiated when they are lost. Consequently, feedback regulation controlling stem-cell self-renewal and differentiation can prevent exponential growth due to perturbations, but complete loss initiates unrestricted expansion in cancerous populations. In this chapter, the populations of progenitors were not explicitly modeled, and thus did not determine the effects of deregulation on intermediate populations. The following chapter will more closely examine the effects of tissue deregulation on all tissue cells by incorporating the regulatory mechanisms outlined in this chapter with the maturity structure defined in Chapter IV.

CHAPTER VIII

Mathematical Modeling of Homeostatic Deregulation Instigating Chronic Myelogenous Leukemia

In previous chapters, the process of mutation acquisition was investigated in hierarchical tissue through the use of two different mathematical models. In Chapter IV, a maturity-structured model of stem, progenitor, and differentiated cells was used to monitor the initiation of cancer stem cells and the growth of progeny cancer cells, but this model did not include regulatory mechanisms that preserve homeostasis. In order to incorporate these tissue-governing mechanisms, an ordinary differential equations model was developed in Chapters V and VI in which stem-cell division probabilities were dependent on stem and differentiated cell populations. This ODE model was used in Chapter VII to investigate the consequences of acquired mutations that transform the mechanisms regulating the balance of stem-cell division pattern. In order to obtain a comprehensive modeling framework for theoretical investigation of cancer initiation in hierarchical tissue, a model is now presented that incorporates both the maturity-structure from Chapter IV with the regulatory feedback mechanisms examined in Chapters V, VI, and VII. The tissue of choice is the blood and this new model is first developed to describe a healthy hematopoietic system. Then, the model is used to investigate the growth dynamics of Chronic Myelogenous Leukemia (CML). To our knowledge, this is the first presentation of a cell maturity-structured

model that incorporates (1) the sequential acquisition of phenotype altering mutations, (2) tissue hierarchy, and (3) internal feedback regulation of homeostasis.

8.1 Mathematical Modeling of Granulopoiesis

The hematopoietic system is composed of stem cells and a variety of progenitor and differentiated cells in the lymph and blood systems. Hematopoietic stem cells are precursors for cells of both the lymphoid and myeloid lineages. Lymphocytic progenitors differentiate into B cells, T cells, and NK cells, all of which are necessary components of the immune system. Myeloid progenitors differentiate to form platelets, macrophages, etrythrocytes, and granulocytes, which include eosinophils, basophils and neutrophils [99].

The majority of hematopoietic stem cells reside in the bone marrow, though some have also been detected in the spleen and blood [9, 71, 91]. The bone marrow is also the location for the expansion and maturation of progenitors and differentiating cells. Once myeloid cells reach full maturity, they are released into the bloodstream. Terminally differentiated cells in the blood do not complete additional divisions and have a short half-life. Therefore, the bone marrow is the site of proliferation, expansion, and differentiation, while blood circulation transports fully mature cells to meet tissue demands throughout the body.

In this chapter, a maturity-structured mathematical model is presented that focuses on granulopoiesis, that is, the process by which granulocytes are formed. Granulocytes are crucial for an innate immune response. The primary function of these cells is to remove pathogens, and their continuous production is characteristic of a healthy immune system [61]. Hematopoietic stem cells, precursor myeloblasts and myelocytes, and fully-differentiated granulocytes, specifically neutrophils, are con-

sidered. Unlike the models presented in previous chapters, cells reside in one of two compartments, namely, the bone marrow or the blood. It is assumed that, under normal conditions, stem, progenitor, and differentiating cells remain in the bone marrow while terminally differentiated cells mobilize into the blood. Although it is true that stem cells can circulate in the blood, it is assumed that their number is negligible in comparison with all the other cells. By distinguishing between cells that are in the blood as opposed to the bone marrow, it is possible to determine the distribution of cell maturity in each tissue, which will later enable investigation of immature blast accumulation that is associated with the progression of CML.

8.1.1 Model Structure

The model uses the maturity-structure of Chapter IV while also incorporating the stem-cell division regulatory mechanisms of Chapters V and VI. Stem cells, S, divide at rate k, and with each division, stem cells either symmetrically self-renew with probability α_S, asymmetrically self-renew with probability α_A, symmetrically differentiate with probability α_D, or die with probability δ_S. Progenitor cells are formed through asymmetric and differentiation divisions. Although it is known that a small number of stem cells circulate the blood through the process of mobilization [71], it is assumed that stem cells and immature progenitors reside in the bone marrow, while fully mature cells are released into the blood, as depicted in Figure 8.1. Cells of maturity level a at time t in the bone marrow and the blood are denoted $w(a,t)$ and $n(a,t)$, respectively. The net growth rate of cells in the bone marrow, given by $\beta(a)$, the mobilization rate of cells from the bone marrow into the blood, given by $\gamma(a)$, and the death rate of cells in the blood, given by $\mu(a)$, are dependent on cell maturity. The system of model equations is as follows:

$$
\begin{aligned}
\frac{dS}{dt} &= (\alpha_S - \alpha_D - \delta_S)\, kS \\
\frac{\partial w}{\partial a} + \frac{\partial w}{\partial t} &= (\beta(a) - \gamma(a))\, w \\
\frac{\partial n}{\partial a} + \frac{\partial n}{\partial t} &= \gamma(a) w - \mu(a) n
\end{aligned} \tag{8.1}
$$

with initial and boundary conditions

$$
\begin{aligned}
S(0) &= S_0 \\
w(a,0) &= f(a) \\
n(a,0) &= g(a) \\
\frac{\partial w}{\partial t}(0,t) &= (2\alpha_D + \alpha_A)\, kS \\
\frac{\partial n}{\partial t}(0,t) &= 0.
\end{aligned} \tag{8.2}
$$

The total number of cells in the bone marrow and blood at time t are respectively defined as

$$
\begin{aligned}
W(t) &= \int_0^\infty w(a,t)da \\
N(t) &= \int_0^\infty n(a,t)da.
\end{aligned} \tag{8.3}
$$

For ease of referral in subsequent discussion, the model presented in Equations 8.1, 8.2, and 8.3 is called the Maturity-Structured Model Incorporating Regulatory Feedback Mechanisms (MSMIRFM).

The functional forms for the probabilities of stem-cell division are as defined in Chapters V, VI, and VII. Specifically,

$$
\begin{aligned}
\alpha_S(S) &= (1-\delta_S)\left(\frac{\theta_S^2}{\theta_S^2 + S^2}\right)\left(1 - \frac{S}{K_S}\right) \\
\alpha_D(S,N) &= (1-\delta_S)\left(\frac{\theta_N}{\theta_N + N}\right)\left(\frac{S}{K_S}\right) \\
\alpha_A(S,N) &= 1 - \alpha_S(S) - \alpha_D(S,N) - \delta_S.
\end{aligned}
$$

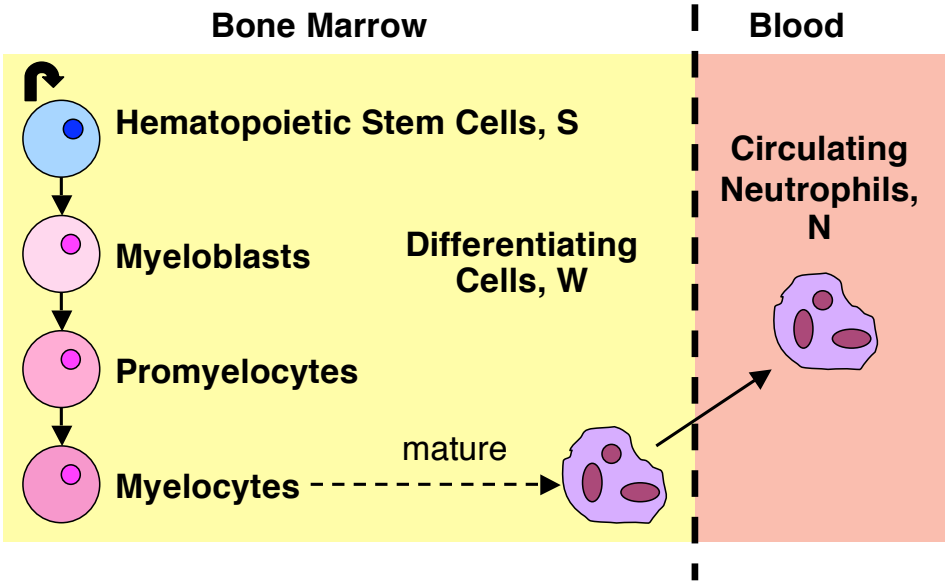

Figure 8.1: **Cells are divided into bone marrow and blood compartments.** Hematopoietic stem cells and progenitor cells reside in the bone marrow while terminally differentiated neutrophils are in the blood circulation.

The growth rate and death functions, $\beta(a)$ and $\mu(a)$ are those defined in Chapter IV. The release of differentiated cells into the blood must compensate for the death of circulating terminally differentiated cells. The mobilization entry rate, $\gamma(a)$, is also switch function, with a maximum rate that is derived from the estimated turnover of granulocytes in the blood. The functional forms are as follows:

$$\begin{aligned} \beta(a) &= \frac{-b}{2}\tanh(\rho_\beta(a-\omega_\beta)) + \frac{b}{2} \\ \gamma(a) &= \frac{g}{2}\tanh(\rho_\gamma(a-\omega_\gamma)) + \frac{g}{2} \\ \mu(a) &= \frac{d}{2}\tanh(\rho_\mu(a-\omega_\mu)) + \frac{d}{2} + \delta_S k. \end{aligned} \tag{8.4}$$

The model terms and parameter values are presented in Table 8.1.

8.1.2 Numerical Simulations of Granulopoietic Homeostasis

Model equations were discretized with the upwind method, and numerical simulations were conducted using MATLAB. The initial condition of 1,000 stem cells and

Term	Biological Meaning	Value Used
S	hematopoietic stem cells	11,000-22,000 (cells) [1]
W	precursors in bone marrow	$5 - 15 \times 10^{11}$ (cells) [1, 52, 100, 109]
N	neutrophils in blood	$2 - 6 \times 10^{10}$ (cells) [9, 100, 101]
$\alpha_S(S)$	probability of SSR	0.20 (from Chapter V) [125]
$\alpha_D(S,N)$	probability of SCD	0.15 (from Chapter V) [125]
$\alpha_A(S,N)$	probability of ASR	0.60 (from Chapter V) [125]
k	stem-cell proliferation rate	0.247 (weeks^{-1}) [21]
θ_S	switch parameter for SSR	19,600 (cells)
K_S	stem-cell niche capacity	30,000 (cells)
θ_N	switch parameter for SCD	1×10^{10} (cells)
δ_S	probability of stem-cell death	0.05 [83]
$\beta(a)$	progenitor net growth rate	
b	maximum growth rate	9.7 (per week) [100, 109]
ρ_β	steepness of β switch	2
ω_β	maturity at β switch	2.05 (weeks)
$\gamma(a)$	entry rate into blood	
g	maximum blood entry rate	4.2 (per week)
ρ_γ	steepness of γ switch	10
ω_γ	maturity at γ switch	4.05 (weeks)
$\mu(a)$	differentiated-cell death rate	
d	neutrophil death rate	16.8 (per week) [9, 13, 39]
ρ_μ	steepness of μ switch	10
ω_μ	maturity at μ switch	4.10 (weeks) [39]

Table 8.1: Parameter values for the Maturity-Strucutred Model Incorporating Regulatory Feedback Mechanisms.

zero progenitor and differentiated cells was used to generate the hierarchical tissue and determine the homeostasis steady states and maturity distributions of the system. It should be noted that the model does not segregate cycling and quiescent stem cells, but instead monitors the total stem-cell population. Following the results acquired from numerical simulations of hematopoietic tissue generation in Chapter V, it is assumed that approximately 15% of all stem cells are cycling during the entire generation period. Although tissue generation is more accurately modeled by separating cycling and quiescent stem cell populations so the percentage of cycling stem cells can vary depending on tissue status, reconstitution is not the primary focus of these simulations. Rather, the purpose is to establish the steady state maturity distribution of cells in the bone marrow and blood compartments that will be used as the initial conditions in the mutation acquisition model, because these distributions cannot be solved analytically.

Figure 8.2 plots the growth of each of the cell populations during generation. The stem-cell population is plotted in Figure 8.2A. The system begins with 1,000 stem cells, growing to a steady state of approximately 18,360 stem cells, which is within the predicted range of 11,000-22,000 hematopoietic stem cells in adult humans [1]. The total number of differentiating cells in each the bone marrow and the blood is plotted in Figure 8.2B. Initially there are no cells in both the bone marrow and blood. As the system is generated, it reaches a steady state of approximately 7.28×10^{11} cells in the bone marrow and 2.97×10^{10} cells in the blood. Neutrophils have a short half-life and high rate of turnover, but they need a few days to fully mature in the bone marrow before being released into the the blood. Therefore, the total number of cells in the bone marrow is far greater than the number of cells in the blood. Figure 8.2C shows the maturity distributions of cells in the bone marrow as well as

the blood. The majority of cells in the bone marrow are near full maturity, ready for release into the blood, while the majority of cells in the blood are fully mature.

The functions determining cell division and death rates are plotted in Figure 8.3. The probabilities for each type of stem-cell division, shown in Figure 8.3A, change over time in reaction to the generation of additional stem and differentiated cells. Initially, symmetric self-renewal dominates, but as the system approaches homeostasis, asymmetric divisions comprise 60% of stem-cell divisions, while symmetric self-renewal and differentiation account for 20% and 15% of stem-cell divisions, respectively. The maturity-dependent growth, release, and death rates are plotted versus maturity level a in Figure 8.3B. Myeloblasts have a cycling time of 11-24 hours, thus the maximum rate of proliferation is determined from this doubling time [100, 109]. Cell cycle times increase as cells mature, thus the proliferation rate approaches zero as cells mature. Upon completing the final division, cells require 3-4 days to achieve full maturity, after which they are released into the blood. In the bone marrow, the number of non-proliferating cells of the granulocyte lineage ranges from $2.7 - 6.6 \times 10^{11}$ cells, and it is estimated that 1.2×10^{11} granulocytes are released into the blood every day [39, 109]. Consequently, the estimated release from the bone marrow occurs at a maximum rate of 0.2-0.6 per day, or 1.4-4.2 per week. The maximum release rate is approached after bone marrow cells reach full maturity, which is assumed to occur when $\gamma > \beta$; or when baseline parameters are used, as in this simulation, approximately 3.8 weeks. Cells have a short half-life in the blood, thus accounting for the high death rate of differentiated cells quickly after release.

The proliferation rate of differentiating cells in the marrow, given by the maturity-dependent function $\beta(a)$, is helpful in determining the composition of cells in the bone

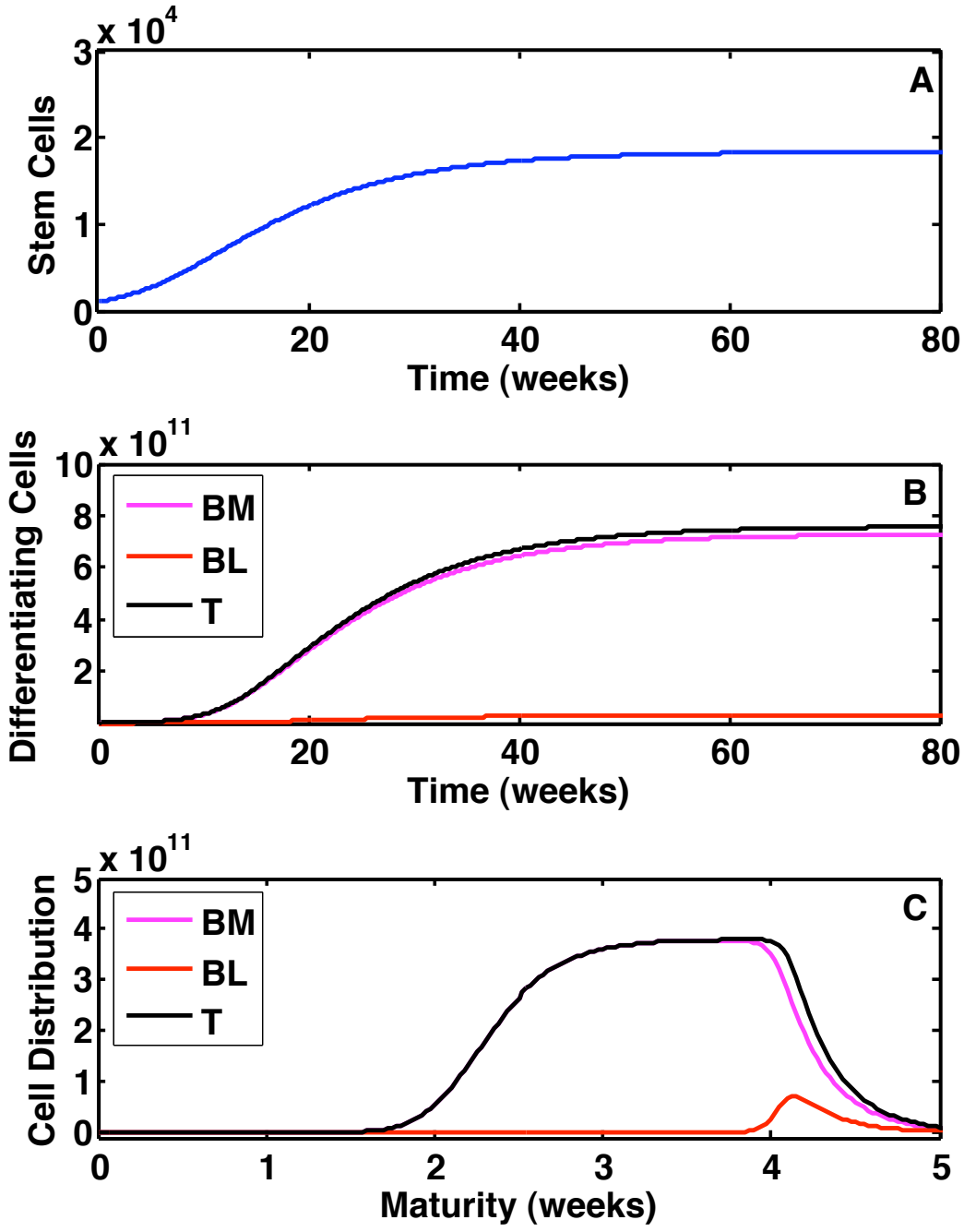

Figure 8.2: **Hierarchical tissue reaching homeostasis.** (A) Stem cells versus time. (B) Total differentiating cells (black) as found in the bone marrow (magenta) and blood (red). (C) Maturity distribution of cells in the bone marrow (magenta) and the blood (red).

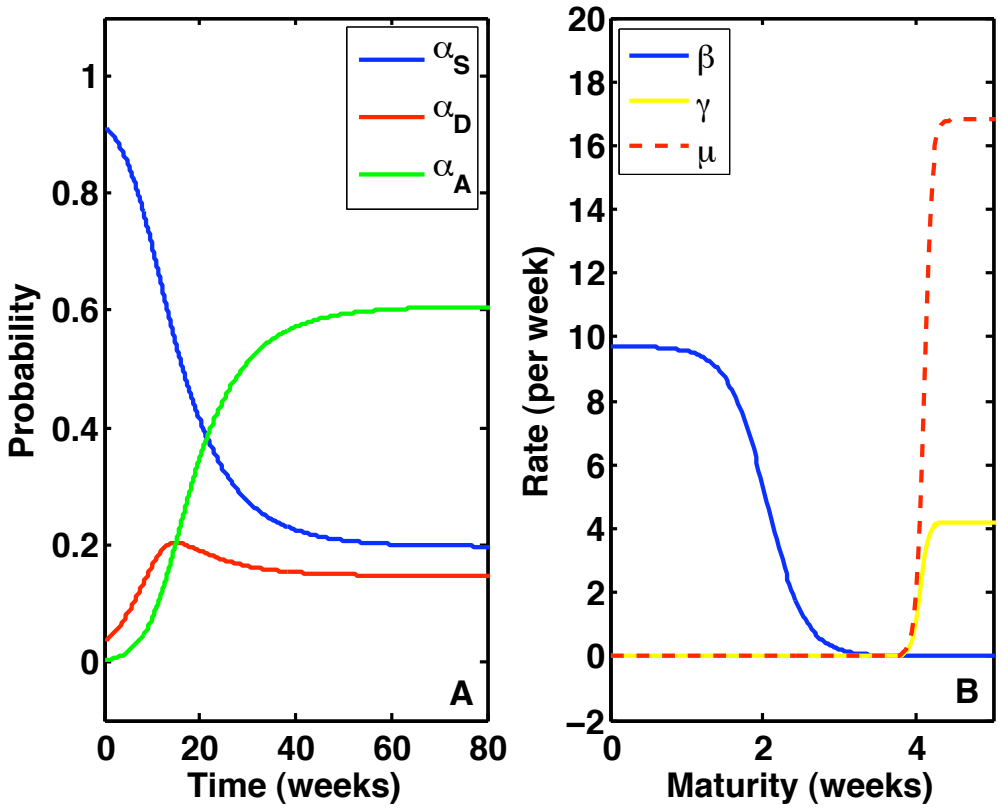

Figure 8.3: **Probabilities of stem-cell division, and rates for proliferation, mobilization, and apoptosis in differentiating cells.** (A) Probabilities of stem-sell division versus time. As the system is generated, symmetric self-renewal, symmetric differentiation, and asymmetric self-renewal approach 20%, 15%, and 60%, respectively. (B) The proliferation, blood-entry, and death rates of progenitor and differentiated cells are dependent on cell maturity.

marrow. The estimated doubling time of precursor cells in the bone marrow is 11-24 hours for myeloblasts, 20-42 hours for promyelocytes, and 39-57 for myelocytes [52, 100]. These cycling times correspond with weekly proliferation rates of 4.85-10.6 in myeloblasts, 2.77-5.82 in promyelocytes, and 2.04-2.99 in myelocytes. Therefore, bone marrow cells of maturity a can be classified based on their corresponding value of $\beta(a)$. When the baseline parameters in Table 8.1 are used, there are approximately 1.39×10^{10} myeloblasts, 3.03×10^{10} myelocytes, and 1.39×10^{11} promyelocytes, and 5.44×10^{11} maturing neutrophils, of which 1.83×10^{11} are fully mature. According to these cell counts, the composition of granulocytic precursors in the bone marrow consists of approximately 2% myeloblasts, 4% promyelocytes, 19% myelocytes, and 75% maturing cells; approximately 25% of bone marrow cells are fully mature. These results are comparable with recorded scientific data of bone marrow composed of 2.5-3% myeloblasts, 3-5% promyelocytes, 22-26% myelocytes, and 66-72% maturing cells [52, 100, 109].

8.1.3 Conclusions

In this section, a mathematical model was presented that incorporated both maturity-structure and regulatory feedback mechanisms governing stem-cell division pattern in order to simulate healthy homeostasis of granulocytes and their precursors. To our knowledge, this is the first mathematical model of hierarchical tissue that incorporates both maturity structure and feedback mechanisms in its framework. Numerical simulations of tissue generation were conducted, and tissue homeostasis was investigated to determine the number and maturity-distribution of granulocytic cells in equilibrium in both blood and bone marrow. Using experimentally measured parameter values, model predictions were in coherence with recorded cell counts and tissue composition based on cell maturity.

The MSMIRFM model presented in equations 8.1 differs from the MSMAHR model presented in Equations 4.1 due to the inclusion of regulatory mechanisms that govern the balance of stem-cell divisions. The main distinction between the model predictions is in the dynamics regarding stem-cell division. In the MSMAHR model, the probabilities of symmetric self-renewal, asymmetric self-renewal, and symmetric commitment differentiation remain constant and do not change, regardless of tissue dynamics. Stem cells remain in equilibrium as long as the division pattern is balanced. Consequently, the MSMAHR model cannot capture both the expansion that initially occurs during tissue generation as well as the maintenance of homeostasis. In contrast, the MSMIRFM model allows the probabilities of stem-cell division pattern to adjust according to the status of the tissue.

The MSMIRFM model employs the same regulatory feedback mechanisms as the MHTR model in equations 6.4, but unlike the MHTR model, captures the dynamics of intermediate progenitor populations. The MHTR model accurately simulates equilibrium of stem cells and terminally-differentiated cells, but does not explicitly model progenitors. Therefore, it is impossible to determine the maturity-distribution of tissue cells with the MHTR model. The MSMIRFM model, on the other hand, includes all tissue cells on the maturity spectrum, from the most naïve stem cells to progenitors to terminally differentiated cells.

The mathematical model presented in this section combines the novel features of the models presented in Chapters IV, V, and VI. By doing so, this inclusive model captures all aspects of hierarchically structured tissue dynamics. Specifically, this model integrates tissue hierarchy, regulatory mechanisms governing homeostasis, and maturity-dependent cell proliferation, mobilization, and death into one comprehensive framework. This model will be utilized in the next section in order to investigate

the sequential acquisition of deregulating mutations causing the accumulation of immature blast cells that contribute to disease progression in Chronic Myelogenous Leukemia.

8.2 Mathematical Modeling of Chronic Myelogenous Leukemia

Chronic Myelogenous Leukemia (CML) is merely one of the blood and bone marrow disorders that deregulates healthy hematopoiesis. Specifically, CML is a myeloproliferative disorder in which cells of the myeloid lineage expand [23, 59]. The National Cancer Institute estimates that 4,830 new cases of CML will be diagnosed and 450 people will die from the disease in 2008. The rate of incidence in males is nearly double that of females, with 1.9 per 100,000 men and 1.1 per 100,000 women having the disease [93]. Although CML affects adults and children, the median age of patients at diagnosis ranges between 45-66 years [45, 93]. Treatment has been more successful in the last few years with the introduction of Gleevec, the drug specifically tailored to attack the mutated cells causing this disease, but the overall survival rate is still poor and approximately 50% of CML patients will die within five years of diagnosis [93].

One of the obstacles of treating CML is that current chemotherapy regimens successfully target differentiated cells but are unsuccessful in killing cancer stem cells [22]. By not eradicating cancer stem cells, the source of cancer is able to survive and continues to proliferate and expand, thereby regenerating disease even after times of remission. In CML, It is unclear if these cancer stem cells are mutated stem cells that become deregulated or if progenitor cells have acquired mutations that allow them to self-renew, though mounting evidence suggests the latter [22, 60]. Either way, the resulting malignant cells have similar qualities of survival and self-renewal

as stem cells and are thus termed cancer stem cells.

As demonstrated in Chapter VII, mathematical modeling can be a useful tool in investigating mutation acquisition contributing to the emergence of cancer stem cells. Additionally, it is possible to deduce how deregulated cells alter the dynamics of the whole tissue. In this section, the maturity-structured model presented in Section 8.1.1 is extended to include mutation acquisition that instigates CML. First, the types of mutations found in CML cells are classified and the pathology of tri-phasic disease progression are reviewed. Next, the mathematical framework is presented. Finally, the results of numerical simulations are discussed.

8.2.1 Biology of Mutated Cells and Pathology of CML

The Philadelphia (Ph) chromosome, formed from the translocation t(9; 22)(q34; q11), is detected in 95% of CML patients, which has subsequently made it the trademark mutation associated with the disease [47, 59, 103, 120]. It is unknown how the Ph chromosome is initially formed, but it is believed that its formation leads to the chronic phase of CML [47]. The Ph chromosome produces the oncoprotein BCR-ABL, which is one of few mutations that incurs several effects on a cell. BCR-ABL has been linked to deregulated proliferation, decreased apoptosis, decreased adherence, and increased genetic instability [27, 47].

The Ph chromosome has been found in cells of the granulocytic, erythroid, lymphoid, monocytic, and megakaryocytic lineages, suggesting that the initial mutation occurs at the stem cell level but manifests itself in progeny downstream, particularly in cells of the granulocytic lineage [59, 103]. Although the Ph chromosome is used to diagnose CML, it has also been detected at low levels in the blood of healthy people, suggesting that additional mutations are needed to actually cause disease [17, 22, 47, 59]. Furthermore, it is believed that Ph-positive progenitors ac-

quire mutations that promote self-renewal, such as β-catenin, which leads to a more aggressive form of leukemia and initiates the transition from the chronic to blast phase [48, 60].

Patients with CML are classified into three phases that are determined by the percentage of blasts in the bone marrow or blood. Under normal conditions, myeloblasts compose approximately 2.5-3% of the bone marrow, and are generally absent from peripheral circulation [52, 100, 109]. According to the World Health Organization classification, the chronic phase is when blasts compose less than 10% of cells in the bone marrow or periipheral blood, the accelerated phase is when blasts compose 10-19%, and the most aggressive phase, the blast phase, is determined when blasts compose 20% or more [120]. In the chronic phase, mutated cells still differentiate, preventing the accumulation of mutated progenitors. As the disease progresses, it is believed that additional mutations enable progenitors to self-renew and prevent differentiation [48, 60]. The progression through chronic, accelerated, and blast phases is caused by deregulated proliferation, increased survival, and inhibited differentiation of leukemic blasts that expand and displace normal hematopoiesis, eventually resulting in fatality.

8.2.2 A Mathematical Model of Blast Accumulation in CML Progression

Because the progression of CML is characterized by the accumulation of undifferentiated blast cells, a maturity-structured model of hematopoietic cells is needed to fully capture the dynamics of this form of cancer. In order to simulate the acquisition of mutations in hematopoietic cells that lead to CML, the MSMIRFM model presented in Equations 8.1 is now extended such that stem, progenitor, and differentiated cells may have zero, one, two, or three mutations. In contrast to the mutation acquisition models presented in Chapters IV and VII, this model is specifically tai-

lored to the mutations observed in CML. In particular, BCR-ABL and a mutation promoting self-renewal in progenitors are considered.

There is little evidence that other mutations occur prior to the formation of the Ph chromosome, therefore, it is assumed that this is the first mutation [47]. In particular, BCR-ABL has been associated with deregulated proliferation, increased survival, and increased genetic instability. Since the Ph chromosome alone is insufficient to cause disease, it is assumed that these advantages are not fully manifested until the second mutation is acquired [17, 22, 47, 112]. However, because BCR-ABL increases survival, it is assumed that acquiring this mutation is not a lethal mutation, and therefore, the death rate of cells with only one mutation does not increase. When the second mutation is acquired, cells are phenotypically altered by a change in proliferation, decrease in apoptosis, and increase in genetic instability. Thus, cells with either one or two mutations are BCR-ABL-positive, but it is the cells with two mutations that initiate the chronic phase of CML. Lastly, it is believed that blast crisis develops as progenitor cells acquire the ability to self-renew [48, 60]. Self-renewal in essence freezes the maturation of cells. Consequently, this model assumes that cells with three mutations do not continue maturation, and thus are removed from the maturity-structured partial differential equation and instead modeled with an ordinary differential equation, similar to the stem cell populations. A schematic diagram of the model is shown in Figure 8.4. The model equations are as follows:

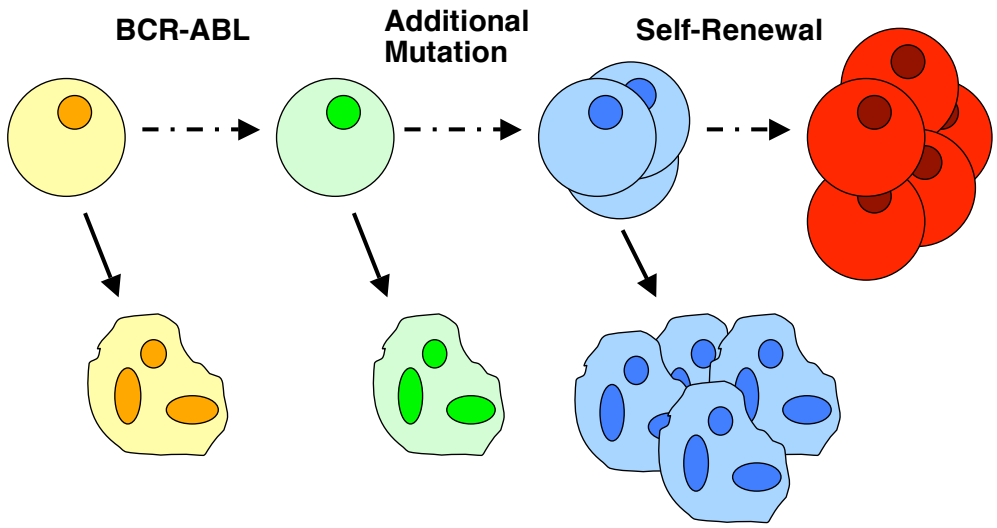

Figure 8.4: **Schematic diagram of the mathematical model for CML.** Progenitor and stem cells first acquire the mutation for BCR-ABL, though it is insufficient alone to change cellular characteristics. After a second mutation is acquired, cells have proliferative advantage, increased survival, and increased genetic instability. Differentiation remains in tact in clones with one or two mutations. The third mutation may only be acquired in stem cells and early progenitors. It causes unregulated self-renewal and blocks differentiation, thereby creating a population of blast cells.

Stem Cells:

$$
\begin{aligned}
\frac{dS_0}{dt} &= \left((1-2m_0)\alpha_{S0} - m_0\alpha_{A0} - \alpha_{D0} - \delta_{S0}\right) k_0 S_0 \\
\frac{dS_1}{dt} &= \left((1-2m_1)\alpha_{S1} - m_0\alpha_{A1} - \alpha_{D1} - \delta_{S1}\right) k_1 S_1 \\
&\quad + \left(2\alpha_{S0} + \alpha_{A0}\right) m_0 S_0 \\
\frac{dS_2}{dt} &= \left((1-2m_2)\alpha_{S2} - m_0\alpha_{A2} - \alpha_{D2} - \delta_{S2}\right) k_2 S_2 \\
&\quad + \left(2\alpha_{S1} + \alpha_{A1}\right) m_1 S_1 \\
\frac{dS_3}{dt} &= \left(\alpha_{S3} - \alpha_{D3} - \delta_{S3}\right) k_3 S_3 + \left(2\alpha_{S2} + \alpha_{A2}\right) m_2 S_2
\end{aligned} \tag{8.5}
$$

where

$$
\alpha_{Si} = (1-\delta_{Si}) \left(\frac{\theta_{Si}^2}{\theta_{Si}^2 + (S_0+S_1+S_2)^2} \right) \left(1 - \frac{S_T}{K_{Si}} \right) \tag{8.6}
$$

$$
\alpha_{Di} = (1-\delta_{Si}) \left(\frac{\theta_{Ni}}{\theta_{Ni} + (N_0+N_1+N_2)} \right) \left(\frac{S_T}{K_{Si}} \right) \tag{8.7}
$$

$$
\alpha_{Ai} = 1 - \alpha_{Si} - \alpha_{Di} - \delta_{Si} \tag{8.8}
$$

for $i = 0, 1, 2, 3$ and $S_T = S_0 + S_1 + S_2 + S_3$.

Bone Marrow Cells:

$$
\begin{aligned}
\frac{\partial w_0}{\partial a} + \frac{\partial w_0}{\partial t} &= ((1 - 2M_0)\beta_0(a) - \gamma_0(a))\, w_0 \\
\frac{\partial w_1}{\partial a} + \frac{\partial w_1}{\partial t} &= ((1 - 2M_1)\beta_1(a) - \gamma_1(a))\, w_1 \\
&\quad + 2M_0\beta_0(a)w_0 \\
\frac{\partial w_2}{\partial a} + \frac{\partial w_2}{\partial t} &= ((1 - 2M_2)\beta_2(a) - \gamma_2(a))\, w_2 \\
&\quad + 2M_1\beta_1(a)w_1 \\
\frac{dW_3}{dt} &= (2\alpha_{D3} + \alpha_{A3})\, k_3 S_3 + (2\alpha_{D2} + \alpha_{A2})\, m_2 k_2 S_2 \\
&\quad + 2M_2\beta_2(a)w_2 + (\beta_3 - \gamma_3)\, W_3
\end{aligned} \tag{8.9}
$$

where

$$W_i(t) = \int_0^\infty w_i(a,t)da \tag{8.10}$$

$$\beta_i(a) = \frac{-b_i}{2}\tanh(\rho_{\beta i}(a - \omega_{\beta i})) + \frac{b_i}{2} \tag{8.11}$$

$$\gamma_i(a) = \frac{g_i}{2}\tanh(\rho_{\gamma i}(a - \omega_{\gamma i})) + \frac{g_i}{2} \tag{8.12}$$

for $i = 0, 1, 2$, and β_3 and γ_3 are constants.

Blood Cells:

$$
\begin{aligned}
\frac{\partial n_0}{\partial a} + \frac{\partial n_0}{\partial t} &= \gamma_0(a)w_0 - \mu_0(a)n_0 \\
\frac{\partial n_1}{\partial a} + \frac{\partial n_1}{\partial t} &= \gamma_1(a)w_1 - \mu_1(a)n_1 \\
\frac{\partial n_2}{\partial a} + \frac{\partial n_2}{\partial t} &= \gamma_2(a)w_2 - \mu_2(a)n_2 \\
\frac{dN_3}{dt} &= \gamma_3 W_3 - \mu_3 N_3
\end{aligned} \tag{8.13}
$$

where

$$N_i(t) = \int_0^\infty n_i(a,t)da \tag{8.14}$$

$$\mu_i(a) = \frac{d_i}{2}\tanh(\rho_{\mu i}(a-\omega_{\mu i})) + \frac{d_i}{2} \tag{8.15}$$

for $i = 0, 1, 2$ and μ_3 is constant.

Initial Conditions:

$$\begin{aligned} S_0(0) &= S_0 \\ S_{1,2,3}(0) &= 0 \\ w_0(0) &= f(a) \\ w_{1,2}(0) &= 0 \\ W_3(0) &= 0 \\ n_0(0) &= g(a) \\ n_{1,2}(0) &= 0 \\ N_3(0) &= 0 \end{aligned} \tag{8.16}$$

Boundary Conditions

$$\begin{aligned} \frac{\partial w_0}{\partial t}(0,t) &= \left(2(1-2m_0)\alpha_{D0} + (1-m_0)\alpha_{A0}\right) k_0 S_0 \\ \frac{\partial w_1}{\partial t}(0,t) &= \left(2(1-2m_1)\alpha_{D1} + (1-m_1)\alpha_{A1}\right) k_1 S_1 \\ &\quad + \left(2\alpha_{D0} + \alpha_{A0}\right) m_0 k_0 S_0 \\ \frac{\partial w_2}{\partial t}(0,t) &= \left(2(1-2m_2)\alpha_{D2} + (1-m_2)\alpha_{A2}\right) k_2 S_2 \\ &\quad + \left(2\alpha_{D1} + \alpha_{A1}\right) m_1 k_1 S_1 \\ \frac{\partial n_{0,1,2}}{\partial t}(0,t) &= 0 \end{aligned} \tag{8.17}$$

For ease of discussion, this model is now referred to as the Mathematical Model of Blast Accumulation (MMBA).

8.2.3 Numerical Simulations for the Onset and Progression of CML

Although it is known that the BCR-ABL fusion gene is the major contributor in the onset of CML, there are many unanswered questions regarding disease progression. For instance, it is unknown if both stem cells and progenitor cells acquire mutations that upregulate self-renewal and cause the accumulation of blast cells [22]. There is also discrepancy in the literature about how BCR-ABL affects cellular kinetics. Some data suggests that BCR-ABL increases the proliferation rate in both stem and progenitor cells [83, 125]. In direct contrast, other data implies that BCR-ABL does not increase the rate of dividing cells, but rather increases the number of divisions before reaching full maturity [19, 27, 48, 122]. It is also possible that stem cells can acquire this mutation, but that it does not become advantageous until inherited in progenitors [22, 103]. In this section, model predictions are presented in order to address these issues.

To execute numerical simulations, model equations were discretized with the upwind method and solved in MATLAB. Two primary sets of parameters were used. The first, recorded in the Mutated Value (1) column in Table 8.2, assumes a doubled proliferation rate, halved apoptosis rate, and increased genetic instability in stem and differentiating cells with two mutations. The second, recorded in Table 8.2 under the column Mutated Value (2), also assumes an increase in genetic instability, but the kinetics for apoptosis and proliferation are quite different from the first case. In the second case, the anti-apoptotic quality in cells with two mutations is manifested as a decreased probability of apoptosis in stem cells and an increased length of survival in differentiating cells, which enables additional progenitor divisions but does not alter the rate of proliferation.

Cells with all three mutations are blast cells and do not mature. It is assumed

Term	Baseline Value	Mutated Value (1)	Mutated Value (2)
k (weeks^{-1})	0.247	0.494	0.247
θ_S (cells)	19,600	19,600	19,600
K_S (cells)	30,000	30,000	30,000
θ_N (cells)	1×10^{10}	1×10^{10}	1×10^{10}
δ_S	0.05	0.025	0.025
b (weeks^{-1})	9.7	19.4	9.7
ρ_β	2	2	2
ω_β (weeks)	1.7	0.85	2.4
g (weeks^{-1})	4.2	4.2	4.2
ρ_γ	10	10	10
ω_γ (weeks)	3.7	2.85	4.4
d (weeks^{-1})	16.8	8.4	16.8
ρ_μ	10	10	10
ω_μ (weeks)	3.75	2.90	4.45
β_3 (weeks^{-1})		4.215	4.215
γ_3 (weeks^{-1})		4.2	4.2
μ_3 (weeks^{-1})		8.4	8.4
$m_{0,1}$		10^{-8}	10^{-8}
$M_{0,1}$		10^{-8}	10^{-8}
m_2		10^{-6}	10^{-6}
M_2		10^{-6}	10^{-6}

Table 8.2: Parameter values for Mathematical Model of Blast Accumulation simulations.

that these cells are leukemic stem cells because they have acquired the ability to self-renew. The rates of proliferation, mobilization, and cell death are constant in blast cells because their cell machinery does not respond to regulatory mechanisms. Because leukemic stem cells do not mature, the model permits blast cells to exit the bone marrow at a constant rate. The proliferation rate determines how quickly the blast population expands. In order to estimate the net growth rate of blasts, the estimated time of disease progression is considered. Specifically, three to seven years are required for the transition from chronic phase to blast phase, during which the number of blasts dramatically increases. It is not unreasonable to suggest blasts increase by a factor of 20 during this time, which translates into a weekly net growth rate of 0.008 to 0.02 per week. Consequently, the proliferation of blasts is assumed to satisfy the condition $0.008 < \beta_3 - \gamma_3 < 0.02$. Finally, blasts die at a rate that is half the apoptotic rate of non-mutated differentiated cells. All model parameters are

summarized in Table 8.2.

The symptoms of patients with CML is rather vague, and diagnosis sometimes is made from the results of routine blood tests [45]. In order to identify the time at which a person might present with CML, the earliest diagnosis time is when the number of neutrophils in the blood surpasses the maximum normal count of 6×10^{10} cells. In all likelihood, this diagnosis estimation is an underestimate, as the patient can be diagnosed in the chronic phase as long as the bone marrow or blood compartments have less than 10% blasts. Accelerated phase begins when either the bone marrow or blood contains 10% blasts, and blast phase is similarly determined for the composition of 20% blasts. These times are recorded for each of the conducted simulations in order to directly compare and contrast model predictions.

Tissue Dynamics Resulting from Increased Proliferation Rate

According to the observations in a recent experiment that recorded the division of immature hematopoietic precursors, BCR-ABL does not influence the division pattern, but increases the rate at which cells divide [125]. Therefore, the first case of mutation acquisition contributing to CML is based on the following assumptions: (1) the first mutation generates BCR-ABL but does not increase cell fitness, (2) the second mutation doubles the proliferation rates in both stem and progenitor populations, decreases the rate of apoptosis by half in all cells, and increases genetic instability, and (3) the third mutation promotes self-renewal and blocks differentiation. Because the proliferation rate is doubled in progenitors, it doubles the number of divisions that are completed in a certain time; therefore, the maturity at which the $\beta(a)$ function switches off is decreased by half in order to preserve the number of divisions that occur in the progenitor population. In addition, it should be noted that this simulation portrays a worst case scenario in the fact that all differentiating

cells may acquire the third mutation that upregulates self-renewal. It is likely that only early progenitors could acquire self-renewal properties, and this case will be discussed later. The parameters used in for this simulation are listed in the Mutated Value (1) column of Table 8.2.

Under these assumptions, the model predicts disease onset and time needed for progression from chronic to blast phase within the recorded median ranges. Blood cellularity is doubled in 40.5 years, but at this time bone marrow cells have not yet doubled. At 51.4 years, the bone marrow and blood each contain approximately 5% leukemic blasts. The number of cells in the bone marrow is approximately 7.5 times the maximum number of cells in healthy marrow, while cells in the blood are increased by 15-fold, which correlates with reported estimates of 5-10-fold increase in total cell mass during the chronic phase of CML [27]. The accelerated phase begins at 52.1 years and is shortly followed by the blast phase at 52.9 years. Assuming the diagnosis of chronic phase would occur some time between 40.5-51.4 years, this progression time is in agreement with the estimated 3-7 years required for the transition from chronic to blast phase. Figure 8.5 plots healthy and mutated cell populations over time as well as the composition of cells in the bone marrow and the blood.

It is generally believed that chronic phase CML is initiated by mutations at the stem-cell level, but it is unknown if the mutation increasing self-renewal in progenitors, which is the third mutation in model simulations, must also be acquired in stem cells [22]. In order to address this issue, consider the case in which stem cells do not acquire the third mutation so that $m_2 = 0$. Surprisingly, the model predicts that times for disease onset and progression do not greatly alter from those in which stem cells do accumulate all three mutations, though there is a difference in tissue dynamics. If stem cells acquire all three mutations, then the final muta-

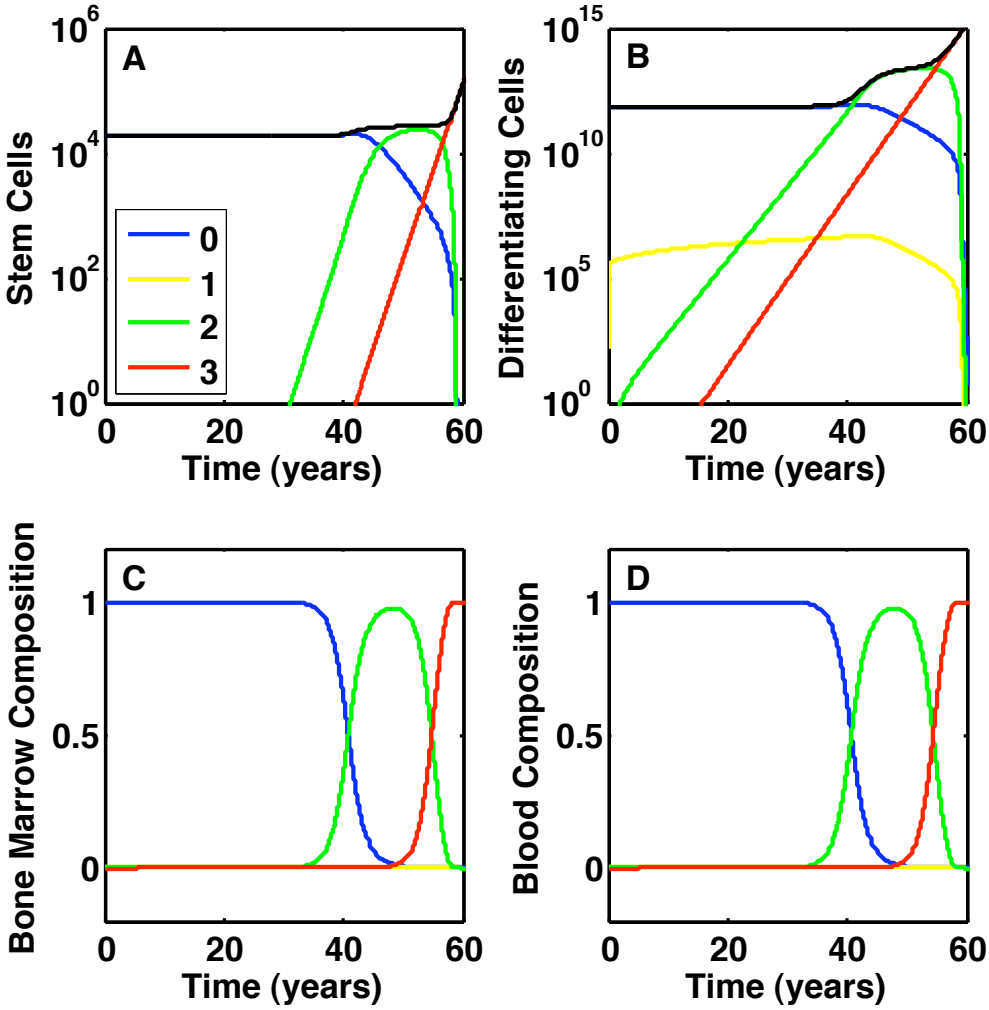

Figure 8.5: **Tissue dynamics resulting from increased stem-cell and progenitor proliferating rates.** (A) Stem cells with 0, 1, 2, and 3 mutations versus time. (B) Differentiating cells with 0, 1, 2, and 3 mutations versus time. (C)-(D) The evolving composition of cells in the marrow and blood, respectively.

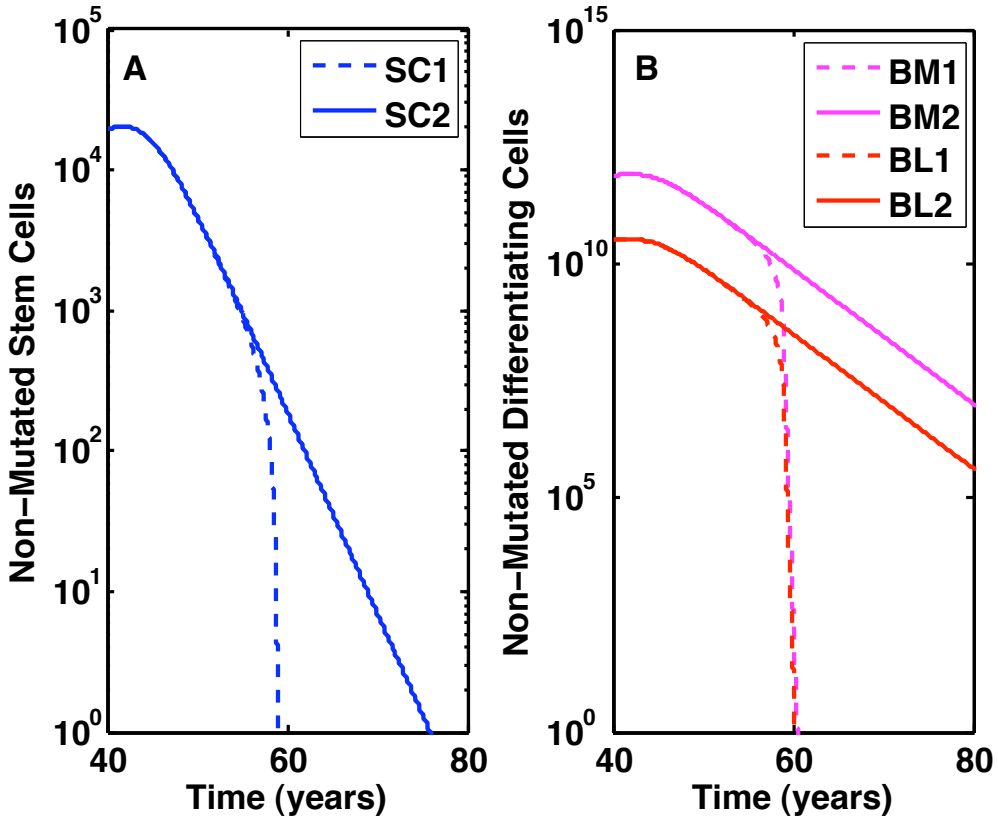

Figure 8.6: **Healthy granulopoiesis is displaced less quickly when stem cells do not mutate to form cancer stem cells.** (A) Non-mutated stem cells are displaced less quickly when stem cells do not acquire the third mutation (solid line SC2) than when stem cells can mutate into cancer stem cells (dotted line SC1). (B) The corresponding non-mutated populations of differentiating cells in the bone marrow and blood depending on whether or not stem cells acquire the third mutation.

tion enables ungoverned self-renewal, which promotes expansion of cancer stem cells. These leukemic stem cells take over the niche, forcing non-mutated stem cells into differentiation. Consequently, the tissue is rapidly depleted of non-mutated stem and differentiating cells. In contrast, when stem cells do not acquire the third mutation, stem cells with two mutations dominate non-mutated stem cells, but the total number of stem cells does not exceed niche control. Therefore the decline of non-mutated stem cells and thus healthy granulopoiesis is slower when stem cells do not acquire the third mutation, as demonstrated in Figure 8.6.

Model simulations predicting slower displacement of non-mutated cells agree more with scientific observations. It has been noted that Ph-positive stem cells displace normal hematopoiesis but do not completely destroy normal stem cells [47]. In addition, it is thought that the total number of hematopoietic stem cells does not significantly increase as disease progresses [22, 60]. Both observations are more accurately captured by the model when stem cells do not acquire the third mutation. Therefore, model predictions concur with recent findings that suggest the mutation deregulating self-renewal in progenitors is acquired in progenitors and not stem cells [22, 60].

It is unlikely that fully mature cells can reacquire the properties necessary for limitless self-renewal capability because they lose much of their proliferative potential as they divide. As a result, it is reasonable to assume that differentiating cells may only acquire the third mutation in earlier progenitor phases. Suppose that stem cells do not acquire the third mutation, and progenitors may only acquire the third mutation if their maturity level is less than 0.5 weeks, which corresponds to having completed approximately nine divisions. As predicted, this slows the expansion of the leukemic blast population, which subsequently delays disease progression. It does not affect the amount of hypercellularity due to expansion of cells with two mutations, as the blood surpasses the maximum healthy level in 40.5 years. However, accelerated phase begins at 67.7 years, and blast phase at 68.8 years, approximately 16 years later than when all differentiating cells acquire self-renewal capability. Depending on when the disease is first diagnosed, the length of progression under these assumptions may be longer than reported values.

One final scenario is yet considered under the assumption that BCR-ABL increases the rate of proliferation. There are contrasting views as to whether BCR-ABL acts the same way in both stem and progenitor cells. Suppose that BCR-ABL

does not alter stem-cell proliferation, but only increases the rate at which progenitors divide. Specifically, stem cells with two mutations die with smaller probability and have increased genetic instability but have a normal rate of proliferation. In contrast, differentiating cells with two mutations proliferate twice as fast as their normal counterparts. Furthermore, assume that the third mutation is only acquired in committed progenitors of maturity less than 0.5 weeks. While the model predicts that malignancy results from this pathway of mutation acquisition, the tissue dynamics do not reflect those of CML. In particular, there is no hypercellularity of the Ph-positive clone, which is shown in Figure 8.7. Under these assumptions, mutated stem cells gain very little advantage over their non-mutated counterparts. As a result, very few mutated stem cells exist in the tissue and an increased rate of progenitor division alone does not increase the number of differentiating cells. Cells with two mutations, namely, the cells that should initiate the chronic phase of CML, do not even comprise 1% of all cells and are surpassed by blast cells before they are probably detected. Based on model simulations of this scenario, results suggest that if BCR-ABL imparts proliferative advantage by way of increasing the proliferation rate, then the proliferation rate of stem cells must also be increased to reflect observations of CML.

Each of the model simulations presented thus far has used the assumption that BCR-ABL increases the rate of proliferation. According to model predictions, this type of proliferative advantage does give rise to mutated populations of stem and differentiating cells that are similar to those observed in CML, but under certain conditions. In particular, it is hypothesized that if BCR-ABL increases the rate of proliferation, then it must do so in both stem and progenitor populations in order to generate dynamics that correlate with CML. Although malignancy can occur

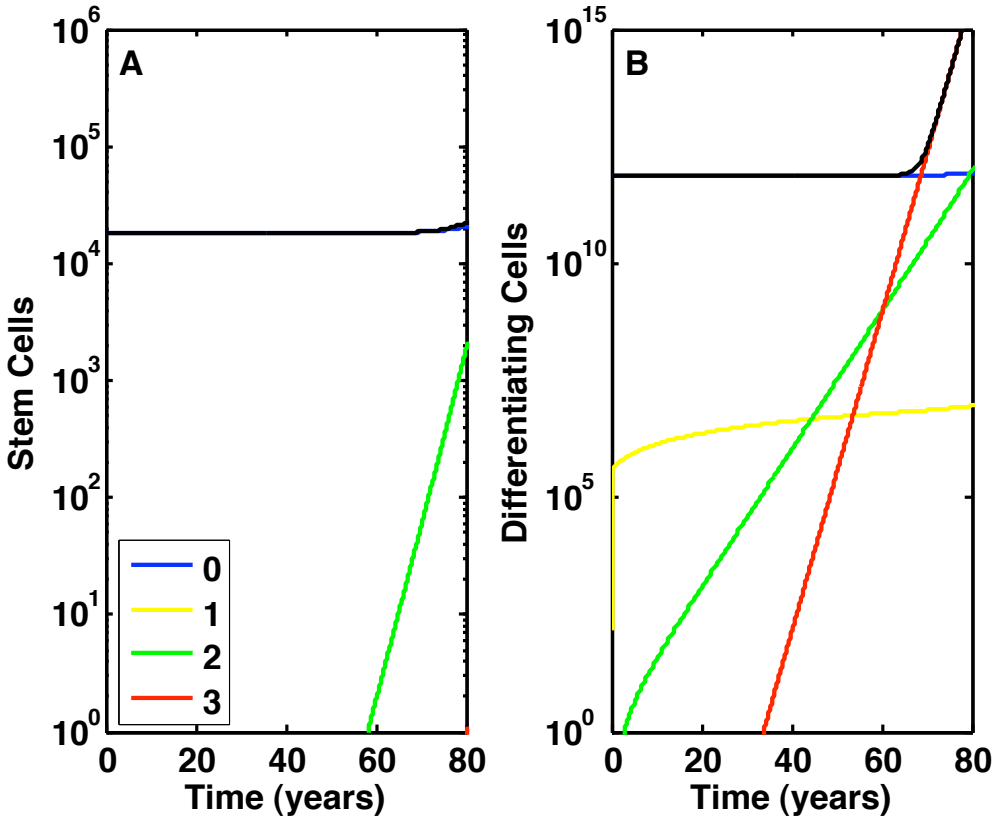

Figure 8.7: **Increased proliferation in progenitors, but not stem cells, does not generate tissue dynamics representative of CML.** (A) Stem cell populations with 0, 1, and 2 mutations are plotted versus time. Without proliferative advantage, mutated stem cells do not expand significantly. (B) An increased rate of proliferation followed by acquisition of self-renewal capability does cause malignancy, but the tissue dynamics do not reflect those of CML. Hypercellularity is not experienced until the tissue is dominated by blast cells.

from self-renewing progenitors, the disease does not resemble CML, and may be indicative of another disorder. Furthermore, the model suggests that if leukemic stem cells grow exponentially due to the loss of regulation, normal hematopoiesis is displaced quicker than if governing mechanisms remain in tact to control the size of the stem-cell population.

Simulations in which early committed progenitors are the only cells able to acquire the mutation that upregulates self-renewal exhibit particularly close coherence with the median times reported for CML diagnosis. The onset of the accelerated phase occurs more quickly if all differentiating cells have equal opportunity to acquire the ability to self-renew. Consequently, one of the factors that may influence the tempo of disease progression may lie in the capacity of downstream progenitors to acquire self-renewal capability.

This section has explored various scenarios of mutation acquisition, under the assumption that BCR-ABL increases the rate of proliferation, to determine if any of these cases generate disease that exemplifies CML. There is some disagreement on how BCR-ABL gives mutated cells a proliferative advantage, however. Next, the model will be used to investigate the other view, which suggests that BCR-ABL does not increase proliferation rate, but rather increases survival, thereby increasing the number of progenitor divisions.

Tissue Dynamics Resulting from Extra Progenitor Divisions

Some researchers believe that the proliferative advantage gained with BCR-ABL is not due to an increased rate of division, but rather through increased survival that permits extra divisions to occur in progenitor stages [19, 27, 48, 122]. In order to consider this possibility, the second scenario of the initiation and progression of CML is based on the following assumptions: (1) cells with the first mutation are BCR-

ABL-positive but do not exhibit increased fitness over non-mutated cells, (2) cells with two mutations have increased survival that decreases apoptosis in stem cells and permits extra rounds of division in progenitors, and (3) cells with three mutations can self-renew and do not mature. Specifically, progenitors survive for an additional 0.7 weeks, which enables them to complete six to seven extra divisions before reaching full maturity. Although the second mutation is acquired in stem cells, the proliferative advantage is not realized in stem cells but downstream progeny. Furthermore, it is assumed that stem cells acquire the third mutation and differentiated cells can only accumulate the self-renewal mutation if their maturity is less than $a = 0.5$ weeks. The parameters used for this simulation are listed in the Mutated Value (2) column of Table 8.2.

Based on these assumptions and parameter values, the model predicts that blood cellularity is doubled in 63.7 years and tissue is composed of 5% leukemic blasts in 70.1 years. It is hypothesized that diagnosis would occur some time in this time frame. The accelerated phase begins at 71.7 years, followed by the blast phase at 73.5 years. Therefore, it takes an estimated 3.4 to 10 years from the time of diagnosis for disease to develop into the blast phase. The first mutated differentiating stem cells are formed within weeks, but it is the emergence of the two-mutation stem cell that truly marks disease onset. Mutated differentiating cells continue to mature and eventually die, but this clone is sustained once mutated stem cells form. The first stem cell with two mutations is formed in 58.1 years. Six years later, cells with two mutations dominate the system, which correlates with scientific observations that estimate Ph-positive cells displace normal hematopoiesis in approximately eight years [47].

Even though stem cells may acquire the third mutation in this simulation, cancer

stem cells do not emerge from the stem cell population, which is quite different from results of the previous section. Stem cells with two mutations have an increased rate of genetic instability and increased survival expressed through a diminished probability of apoptosis, but proliferative behavior of stem cells is unaltered. As a result, stem cells with two mutations have a slight increase of fitness in comparison to normal stem cells, but the mutated clone does not overtake normal hematopoietic stem cells. In fact, when 5% of blasts are detected in the blood, only 75 mutated stem cells exist and all express two mutations. The number of mutated stem cells increases to 246 by the time blast phase is diagnosed, but all of these only express two mutations. It has been suggested that non-mutated cells are more frequent in less mature cell populations than fully differentiated cells [48]. The model predicts that less than one percent of stem cells are Ph-positive throughout disease progression, even though mutated progeny overtake normal granulopoiesis.

The model predicts hypercellularity results from extra rounds of division in mutated progenitors. Furthermore, each subsequent division compounds on the previous so that the effects are more apparent downstream in the lineage, particularly in the early stages of disease. Figure 8.8 records the percentage of cells that are proliferating and those that have completed divisions at four distinct times during progression: the times at which (A) blood exceeds normal cell counts, (B) 5% of cells are blasts, (C) the accelerated phase begins, and (D) the blast phase begins. As cells acquire self-renewal capabilities and the blast population expands, hypercellularity of immature cells is more noticeable. This prediction is consistent with the observation that the suppression of normal hematopoiesis by CML cells is more prominent in cells of greater maturity [48]. Furthermore, the blast population accounts for an increasing percentage of all proliferating cells as disease progresses. Therefore, by assuming

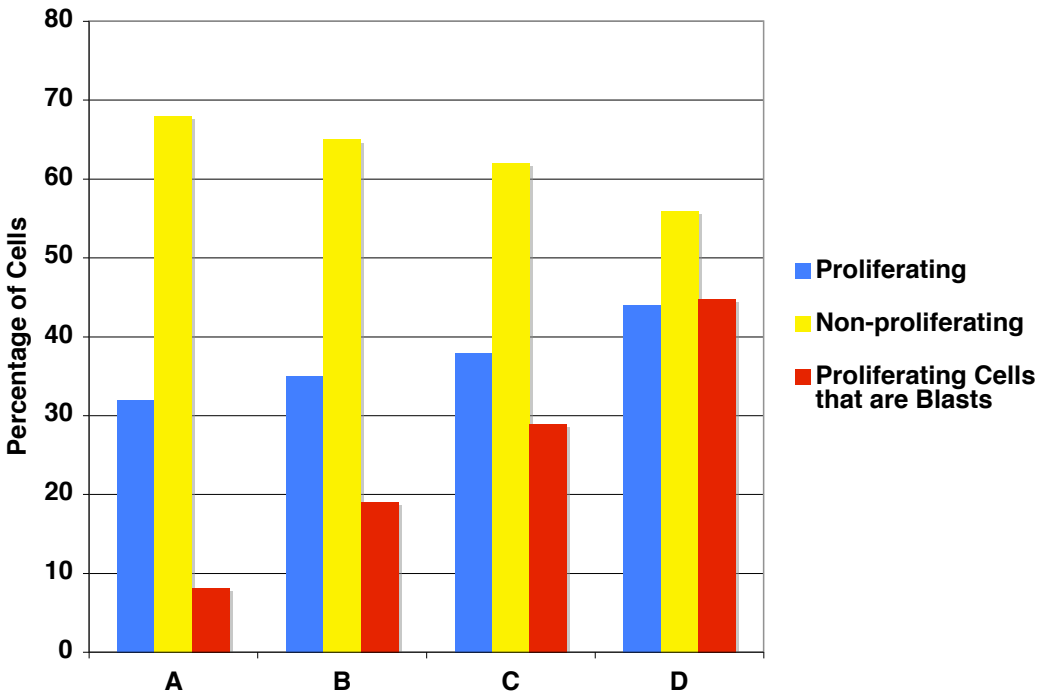

Figure 8.8: **Immature cells increase in frequency as disease progresses.** Proliferating cells include stem cells, myeloblasts, promyelocytes, myelocytes, and blasts. Non-proliferating cells are those that have completed the final division. The blast column shows what percentage of proliferating cells are blast cells. (A) The time at which cells in the blood exceeds normal counts. (B) The time at which five percent of cells are blasts. (C) The start of the accelerated phase. (D) The start of the blast phase.

proliferative advantage enables additional progenitor divisions, model simulations closely correlate with recorded diagnosis times and reflect evolving tissue dynamics commonly observed in CML.

BCR-ABL Alone is Inadequate for Malignancy

Lastly, model simulations are used to confirm that the BCR-ABL mutation is insufficient to generate malignancy. Suppose that stem and differentiating cells acquire two mutations: the BCR-ABL mutation and another mutation that enables increased fitness due to BCR-ABL. In this case, progenitors do not acquire stem-cell like properties, in particular, the ability to self-renew and inhibit differentiation. Two cases are considered. In the first case, stem and differentiating cells with two

mutations have an increased rate of proliferation and a decreased rate of apoptosis. In the second, it is assumed that BCR-ABL increases survival of all cells, which enables additional divisions in progenitors and decreases the probability of apoptosis in stem cells.

The model predicts that hypercellularity ensues from BCR-ABL, but is insufficient to promote malignancy. In this simulation, no cells exhibit deregulated self-renewal. Under the assumption that BCR-ABL does not inhibit the mechanisms governing stem-cell self-renewal, the total number of stem cells is maintained by the niche, as shown in Figure 8.9A and C. In Figure 8.9B and D, it is evident that added divisions increase the total number of differentiating cells, but because these cells do not acquire the ability to self-renew, they reach full maturity and eventually die. Therefore, there is no long-term expansion of mutated cells, so the model predictions concur with the widely accepted belief that deregulated self-renewal is the key mutation that drives malignancy and advances disease progression in CML. It should be noted that fatality could result depending on the magnitude of cell increase, but due to the success of treating BCR-ABL-expressing cells with the drug imatinib, it is theorized that this type of hypercellularity could be treated, even if never fully eradicated.

It is hypothesized that expansion of BCR-ABL-expressing cells is due to selective advantage of Ph-positive stem cells. The Ph chromosome has been detected in various lineages of hematopoietic stem cells, suggesting that this mutation occurs at the stem-cell level [59, 103]. In order to determine if hypercellularity results when mutations only occur in differentiating progeny, suppose the stem-cell mutation rate is zero. The model predicts that BCR-ABL-expressing cells do form as a result of progenitor mutations, but in the absence of a self-renewing mutated source, these mutated cells reach full maturity and die so that mutated cells comprise no more than 0.001% of

the overall tissue, as demonstrated by the dashed line comparisons in Figure 8.9. Therefore, unless BCR-ABL is able to impart some capacity of self-renewal, disease does not form if this mutation does not occur at the stem-cell level.

Another potential way in which BCR-ABL could lead to life-threatening disease is if hypercellularity forces immature cells from the marrow into the blood before they are terminally differentiated. This could result in an insufficient number of differentiated cells that are needed to perform specific tasks or could problematically increase blood density. Ph-positive cells do not bind to stromal cells as well as Ph-negative cells, so it is not unreasonable to assume that the mobilization of cells with two mutations increases as the bone marrow cavity is filled. There are various ways in which this could be addressed mathematically in the model. To illustrate one possibility, suppose that the mobilization rate of cells with two mutations, $\gamma_2(a)$ shifts up by G, where G depends on the fullness of the bone marrow at that time. Since normal bone marrow cell counts range from 5×10^{11} to 1.5×10^{12} cells of the granulocytic lineage, suppose that the marrow capacity is approximately 10^{13}. As an example, consider $G = \frac{\xi W(t)}{10^{13}}$, where $W(t)$ is the total number of cells in the bone marrow at time t, and ξ is the factor that determines how much mobilization increases in mutated cells. Suppose for simplicity that $\xi = 1$. At homeostasis, $G = 0.08$, which increases the mobilization of BCR-ABL expressing cells by approximately 2% more than the rate of non-mutated cells. Obviously, mobility could be increased more with a greater value for ξ, but this is sufficient for this illustration.

As time progresses and the marrow fills, G increases, which increases the rate at which cells mobilize into the blood. Whereas non-mutated cells have a negligible mobilization rate until they reach full maturity, cells with two mutations can mobilize into the blood at all maturity levels due to the shift in the mobilization curve.

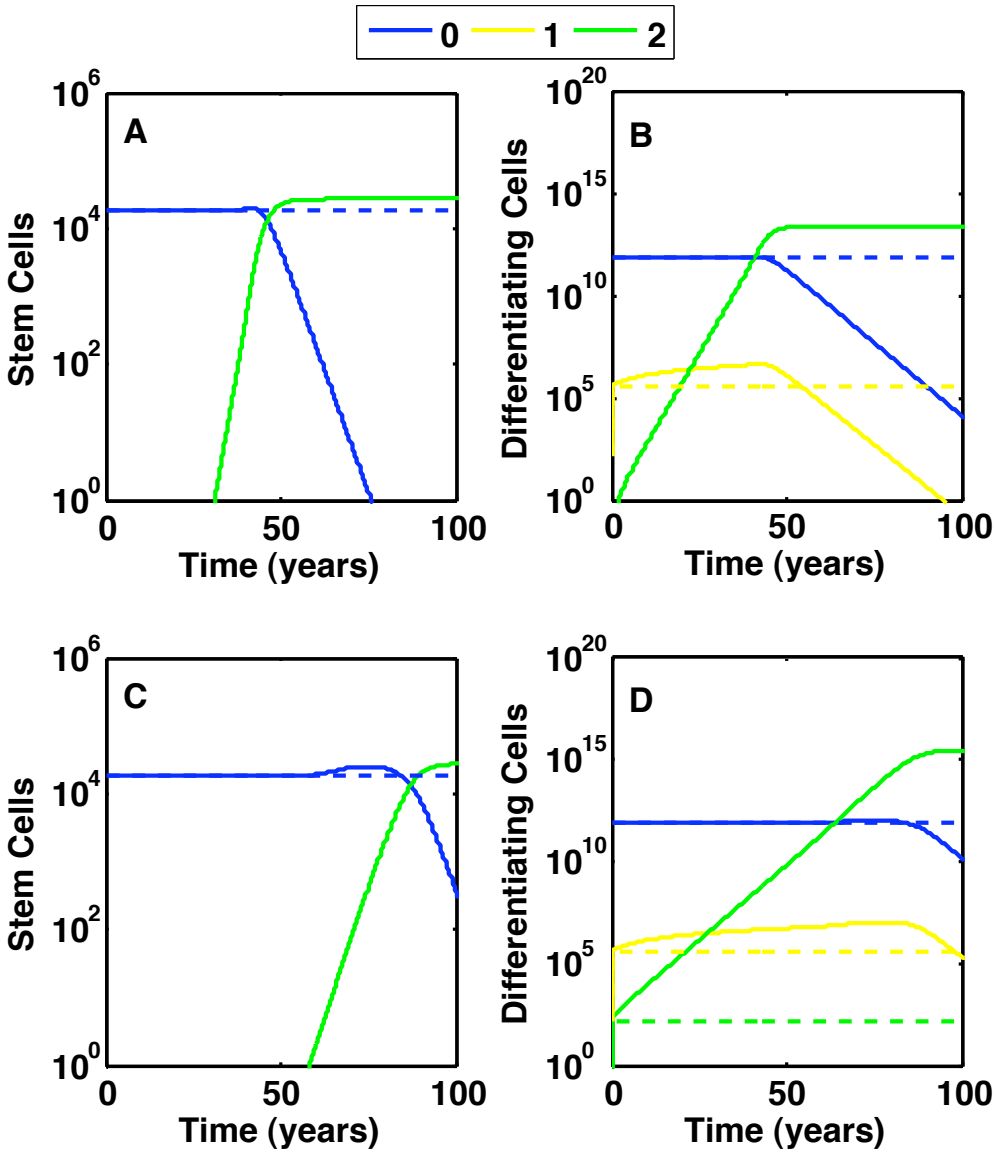

Figure 8.9: **BCR-ABL alone causes hypercellularity but not malignancy.** (A)-(B) The stem- and differentiating-cell populations when BCR-ABL increases the rate of proliferation. Solid lines show the in which stem cells acquire mutations, while dashed lines show what happens when stem cells do not mutate. (C)-(D) Tissue dynamics when BCR-ABL increases the survival of progenitors, thereby increasing the number of permitted divisions.

Consequently, immature mutated cells are released into the blood before they are fully differentiated. Over time, as mutated cells expand and overcrowd the bone marrow, more and more immature cells accumulate in the blood, which is depicted in Figure 8.10. The healthy maturity-distribution of cells in homeostasis is shown in Figure 8.10A. The blood consists of fully mature cells and the majority of bone marrow cells are in the final stages of differentiation. Figure 8.10B plots the maturity distribution in 35 years, which is not significantly altererd. However, by 70 years, hypercellularity is accompanied by the appearance of immature cells in the blood, as demonstrated in the maturity distribution of Figure 8.10C. As time progresses to 100 years, more immature cells are released into the blood, distorting the healthy distribution even further, which is finally shown in Figure 8.10D.

This illustration suggests that premature mobilization alters the maturity-distribution of differentiating cells in both the bone marrow and the blood. However, in this simulation, less than 1% of blood cells were in the myeloblast phase. Because BCR-ABL does not inhibit differentiation, fully mature cells are abundant in the system as well, and this tissue remains in what would be classified as the chronic phase of CML. This implies that although deregulated mobilization may occur during the progression of CML due to overcrowding in the bone marrow, another mutation is needed that promotes self-renewal in progenitors if the percentage of blasts is to significantly increase.

8.2.4 Discussion

The results of this section demonstrate that a maturity-structured model incorporating regulatory mechanisms provides a mathematical framework that accurately captures the growth dynamics involved in CML. In particular, the maturity structure facilitates the incorporation of maturity-dependent mutations, such as the acquisition

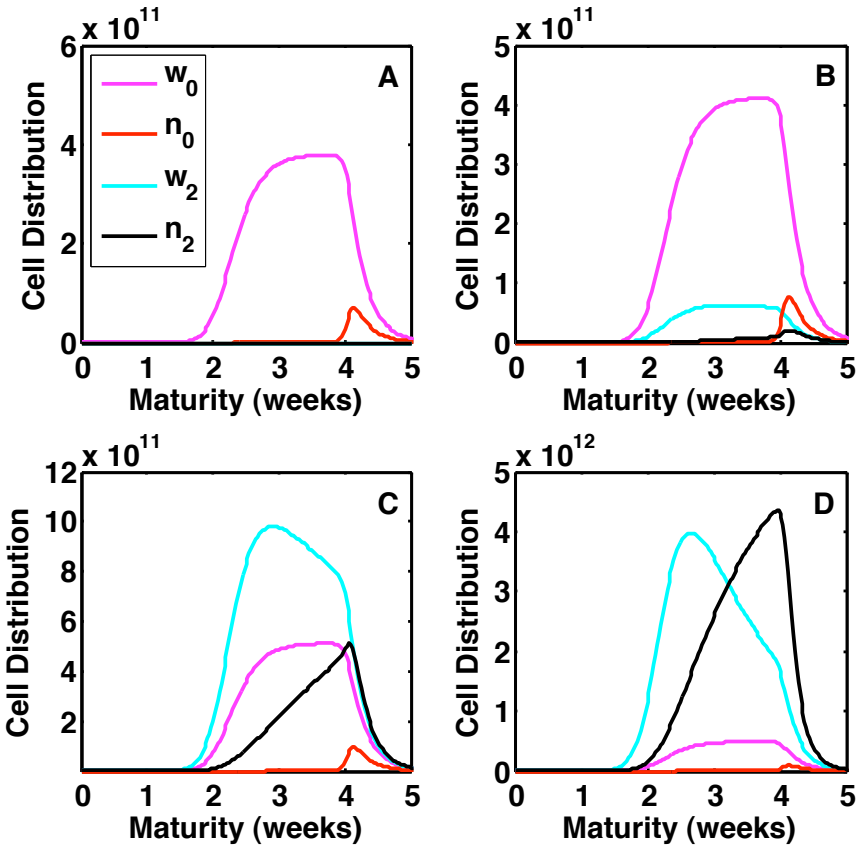

Figure 8.10: **The maturity distribution of cells in the bone marrow and blood changes as a result of premature cell release due to bone marrow hypercellularity.** (A) The initial healthy distribution of cells. (B) At 60 years, there is little change in the maturity distribution of cells in the bone marrow and blood. (C) At 70 years, cells with two mutations surpass non-mutated cells in both the bone marrow and the blood and immature cells appear in the blood as they are forced out of the bone marrow. (D) At 80 years, more mutated cells are in the blood than the bone marrow due to crowding. Furthermore, many cells have been released prematurely from the bone marrow into the blood.

of self-renewal capability in early progenitors, and is useful in simulating the accumulation of immature blast cells that promote disease progression. Although CML is better characterized than many other forms of cancer, there are still unanswered questions, and model predictions were made to address these issues.

It is believed that BCR-ABL endows cells with a proliferative advantage, though there is disagreement in how it is conveyed. Recent experimental data recorded that BCR-ABL-expressing cells had an increased rate of division in comparison to normal counterparts [125]. The other opinion is that progenitors with BCR-ABL do not divide faster but can complete extra rounds of division [19, 27, 48, 122]. The model predicts that both cases are feasible, though the former requires certain conditions. If BCR-ABL acts to increase the proliferation rate, then it cannot merely act in differentiating cells. That is, if the rate of division is increases in progenitors but not stem cells, then the resulting dynamics do not reflect those of CML.

While both scenarios generate CML-like diseases, the contrasts in tissue dynamics imply that the second more accurately portrays CML. In particular, doubling the proliferation rate causes mutated stem cells to displace healthy stem cells, which may not be consistent with scientific observations. For instance, when the disease is in chronic phase, with blasts comprising only 1% of the bone marrow or blood, Ph-positive stem cells outnumber Ph-negative cells three to one. This does not agree with the belief that a small number of BCR-ABL expressing stem cells are responsible for initiating the chronic phase [103, 48]. However, it cannot be discounted that an increased rate of proliferation does cause hypercellularity in differentiating cells expressing BCR-ABL, which is often the indicator of a myeloproliferative disorder, such as CML.

Several parameters influence model predictions for the time it takes to develop

CML and progress to blast phase. In the case where the rate of proliferation is increased, the magnitude of change affects the time in which normal granulopoiesis is displaced and determines the amount of hypercellularity, which is due to quickened rounds of stem-cell division. In the case where increased survival enables additional progenitor divisions, the degree of expansion in the mutated clone depends on how many extra divisions are completed. In both cases, the net rate of growth in the blast population controls the rate at which the disease progresses from chronic to blast phase. If the blast population expands faster than Ph-positive differentiating cells, then blasts are the cause of hypercellularity and the resulting disease is more aggressive. In addition, the model predicts that the blast population grows more quickly when cells of all maturity are capable of acquiring self-renewal capability.

Finally, model predictions agree with the the general consensus that BCR-ABL alone is insufficient to cause malignancy. Assuming that BCR-ABL does not completely transform the mechanisms governing stem cell division or enable self-renewal in progenitors, there is no cell population in which self-renewal is deregulated to allow unlimited expansion. Furthermore, model results suggest the mutation creating BCR-ABL originates in stem cells, otherwise, there is no expansion of Ph-positive cells.

8.3 Conclusions

The research of this dissertation is culminated in the mathematical models of tissue homeostasis and mutation acquisition that are presented in this chapter. Maturity structure captures the dynamics of tissue cells of all maturity-levels, namely, stem cells, progenitors, and differentiated cells. Regulatory mechanisms governing stem-cell division adapt to promote or inhibit self-renewal and differentiation, which

mediates homeostasis in healthy tissue or can contribute to malignancy when erroneously transformed. Lastly, the sequential acquisition of somatic mutations allows investigation of the pathways that contribute in tumorigenesis. To our knowledge, this is the first mathematical model that incorporates all of these aspects in its framework.

In this chapter, the developed mathematical model was specifically applied to simulate Chronic Myelogenous Leukemia in order to demonstrate the model's potential contributions to the scientific community. In particular, the general framework of this model can be utilized to investigate mutation acquisition in any hierarchically structured tissue. By using appropriate parameters for the tissue in question, it is possible to predict the emergence of cancer stem cells, quantify cellularity, and determine tissue composition. Although many details regarding cancer stem cells remain unknown, the model provides a useful tool for predicting tissue dynamics in tumorigenesis. As stem cell research advances, new discoveries will only increase the model's effectiveness.

CHAPTER IX

Summary

Several factors make it difficult to study human cancers *in vivo*. For example, it is particularly challenging to investigate the pathways that lead to cancer. Mutations are often identified in cancer cells long after a patient has developed cancer. As a result, the sequential acquisition of mutations initiating tumorigenesis is tough to accurately determine. Furthermore, tumors are composed with cells of different phenotypes, even among patients diagnosed with the same type of cancer. Consequently, it is impossible to generate a prototype that characterizes all tumors. In addition to these difficulties, there are also experimental limitations to overcome. For instance, human stem cells are not easily isolated for experimental study, particularly those in solid tissues. Since various forms of cancer are believed to originate in mutated stem cells, the inability to monitor stem cells over long periods is an obstacle that prevents further understanding of how these cells behave.

Although many mathematical models of tumorigenesis have generated insightful conclusions pertaining to cancer dynamics, none, to our knowledge, have investigated mutation acquisition within the confines of a hierarchically structured tissue governed by regulatory mechanisms. The modeling approach used in this dissertation addresses this need and has several novel features. First, it accurately captures the

unique dynamics of heterogeneous cellular populations, as opposed to other models that simulate tumor growth in homogeneous tissues. Second, it follows the chronological order in which mutations accumulate and can predict which sequences initiate cancer fastest under various assumptions. Third, it incorporates all three modes of stem-cell division while also including governing mechanisms that mediate homeostasis in healthy tissue and contribute to malignancy when altered.

The presented mathematical model provides a general framework that can be employed in future cancer investigations. The explicit consideration of tissue hierarchy reveals useful insight into tumor composition and heterogeneity. As a result, the incorporation of maturity structure is an important feature that provides more detailed and comprehensive information concerning cancer growth in hierarchical tissues. In addition, the inclusion of regulatory mechanisms more accurately models tissue in homeostasis. With governing mechanisms intact, mutation does not necessarily result in exponential growth, a nuance that could be missed in a model that does not incorporate these regulating factors.

The battle against cancer continues, but there are various ways in which this modeling approach can supplement experimental research. Two of the obstacles in cancer research are determining the order in which mutations are acquired and establishing which transformations are most tumorigenic. If certain mutations are known to occur in cancer cells of a particular tissue, model simulations of potential pathways can be compared and contrasted with scientific data in order to predict which sequences generate the type of tumor that is clinically observed. Moreover, the model may be used to test hypotheses concerning the cell of origin for specific types of mutations.

Model simulations can also predict the *in vivo* dynamics of tumor growth based on

experimental data. This could benefit clinical research in several ways. If it is known that a current treatment regimen specifically targets cells of a particular phenotype but not others, then analysis of the tumor composition may dictate whether that specific treatment is appropriate. For instance, if the tissue is primarily composed of mutated cells that are known to respond to chemotherapy, then treatment may successfully decrease the tumor and prolong survival. On the on the other hand, if the tissue is dominated by mutated cells that will not be targeted, then the administration of chemotherapy will be futile, and may even cause greater damage by causing unnecessary toxicity to any healthy cells that may be in the tissue.

There are various directions for future research. The most immediate is to incorporate treatment and investigate the effects on tumor burden and composition. In particular, imatinib is the first-line of treatment for CML patients in chronic phase. This drug specifically kills cells expressing BCR-ABL, which makes it successful in decreasing hypercellarity. Once patients discontinue therapy, however, disease re-emerges, thereby suggesting that stem cells expressing BCR-ABL are not effectively targeted [83]. A maturity-structured mathematical model can predict response to this treatment and determine the maturity-distribution persistent cells. In addition, the development of drug resistance can be simulated, which may be of clinical assistance.

Since many current methods of chemotherapy are dependent on the cycling status of cells, it may be appropriate to segregate cycling and quiescent stem cells when modeling treatment. Stem-cell quiescence is problematic because it prevents mutated cells from being targeted. It would be interesting to examine the composition of cancer stem cell population to determine the proportions that are quiescent versus cycling. If the majority are quiescent, this may suggest that cell-cycle specific

drugs will not effectively eliminate cancer stem cells, and other forms of treatment should be considered. Furthermore, the effects of therapies that promote stem-cell differentiation could be investigated to determine if this method of treatment can successfully eradicate cancer stem cells without sacrificing healthy tissue.

In studying mutation acquisition in this dissertation, various sequential mutation pathways were considered, but not simultaneously in the same tissue. In reality, tissue cells may accumulate various mutations concurrently. For instance, three mutations were previously discussed, namely D, G, and R, that affected apoptosis, genetic instability, and proliferation, respectively. Suppose tissue cells could acquire any of the mutations at any time. One cell may first acquire G, while another first acquires D. The cell with G could then acquire either D or R, whereas the cell with D could acquire G or R, and so forth. All of these clones would co-exist and compete with each other, which may impact tumor composition and disease progression.

The general framework of the maturity-structured mathematical model could easily be applied to any type of cancer that evolves in hierarchical tissue. Further complexity could be added by incorporating space variables when modeling solid tumors. The location of cells within the tissue may also influence cellular behavior, particularly for stem cells in the niche. For example, in the colon, stem cells reside in the base of the crypt, whereas progenitors and differentiated cells rise to the top as they differentiate. The inclusion of a space variable would allow one to determine where mutated cells are within the colon crypt. Additionally, the incorporation of space to simulate tumor masses, such as lumps found in the breast, may enable predictions for tumor aggressiveness, based on the location of cancer stem cells within the mass.

The modeling results presented in this dissertation highlight potential areas of further research for experimentalists. For instance, even for the well studied hematopoi-

etic system, there is a wide range of suggested values that can be used for model parameters. Better quantification of stem-cell kinetics will improve the accuracy of model predictions concerning the time required for cancer stem cell emergence and disease progression. Due to the significance of unbalanced symmetric self-renewal and genetic instability in promoting tumorigenesis, it would also be useful to classify any one-hit mutations that advantageously transform cells.

The unique features of the presented mathematical models, particularly the inclusion of regulatory mechanisms and maturity structure, have enabled investigation of various aspects of tumorigenesis, which in turn has generated additional questions. For example, in simulating the dynamics of Chronic Myelogenous Leukemia, model results suggest that under certain assumptions, BCR-ABL may impart advantage differently in stem and differentiating cells. In order to effectively treat this disease, it will be important to determine if BCR-ABL affects stem, progenitor, and differentiated cells in the same manner. In addition, model results predict that the extent to which progenitors and downstream progeny acquire self-renewal capability influences the tempo of disease progression. Consequently, it would be of great interest to determine the extent to which progenitors can limitlessly self-renew. For example, how many mutations, if any, must first be acquired in progenitors before they have the ability to stop maturation? Is there a threshold maturity after which differentiated cells are incapable of reacquiring stem cell properties?

Unfortunately, at this time there is relatively little quantified data of cancer stem cells for several reasons. In general, stem cells are difficult to identify, isolate and maintain *in vitro*. Furthermore, it is hard to monitor them *in vivo* because they are rare within the tissue and reside in stem-cell niches that offer protection. There has been some success in studying malignant cells of the hematopoietic system due to

the relative ease of accessing blood and bone marrow. Solid cancer stem cells, on the other hand, are particularly challenging to study *in vivo*, and difficult to monitor *in vitro* due to the difficulty of experimentally reconstructing the niche. As more discoveries are made and cancer stem cells are better understood, the mathematical models developed in this dissertation can be used to investigate tumors arising in any hierarchical tissue.

BIBLIOGRAPHY

BIBLIOGRAPHY

[1] JL Abkowitz, SN Catlin, MT McCallie, and P Guttorp. Evidence that the number of hematopoietic stem cells per animal is conserved in mammals. *Blood*, 100:2665–2667, 2002.

[2] GB Adams and DT Scadden. The hematopoietic stem cell in its place. *Nature Immunology*, 7:333–337, 2006.

[3] M Al-Hajj, MW Becker, M Wicha, I Wessman, and MF Clarke. Therapeutic implications of cancer stem cells. *Current Opinion in Genetics and Development*, 14:43–47, 2004.

[4] M Al-Hajj and MF Clarke. Self-renewal and solid tumor stem cells. *Oncogene*, 23:7274–7282, 2004.

[5] LK Andersen and MC Mackey. Resonance in periodic chemotherapy: a case study of acute myelogenous leukemia. *Journal of Theoretical Biology*, 209:113–130, 2001.

[6] DJ Araten, DW Golde, RH Zhang, HT Thaler, L Gargiulo, R Notaro, and L Luzzatto. A quantitative measurement of the human somatic mutation rate. *Cancer Research*, 65:8111–8117, 2005.

[7] R Ashkenazi, SN Gentry, and TL Jackson. Pathways to tumorigenesis - modeling mutation acquisition in stem cells and their progeny. *Neoplasia (Accepted)*, 2008.

[8] N Barker, van Es JH, J Kuipers, P Kujala, M van den Born, M Cozijnsen, A Haegebarth, J Korving, H Begthel, PJ Peters, and H Clevers. Identification of stem cells in small intestine and colon by marker gene *Lgr5*. *Nature*, 449:1003–1007, 2007.

[9] DR Barreda, PC Hanington, and M Belosevic. Regulation of myeloid development and function by colony stimulating factors. *Developmental and Comparative Immunology*, 28:509–554, 2004.

[10] JC Barrett. Mechanisms of multistep carcinogenesis and carcinogen risk assessment. *Environmental Health Perspectives*, 100:9–20, 1993.

[11] RA Beckman and LA Loeb. Efficiency of carcinogenesis with and without a mutator mutation. *Proceedings of the National Academy of Science*, 103:14140–14145, 2006.

[12] F Behbod and JM Rosen. Will cancer stem cells provide new therapeutic targets? (Review). *Carcinogenesis*, 26:703–711, 2004.

[13] S Bernard, J Bélair, and MC Mackey. Oscillations in cyclical neutropenia: new evidence based on mathematical modeling. *Journal of Theoretical Biology*, 223:283–298, 2003.

[14] S Bernard, L Pujo-Menjouet, and MC Mackey. Analysis of cell kinetics using a cell division marker: mathematical modeling of experimental data. *Biophysical Journal*, 84:3414–3424, 2003.

[15] JH Bielas, KR Loeb, BP Rubin, LD True, and LA Loeb. Human cancers express a mutator phenotype. *Proceedings of the National Academy of Science*, 103:18238–18242, 2006.

[16] MJ Bissell and MA LaBarge. Context, tissue plasticity, and cancer: are tumor stem cells also regulated by the microenvironment? *Cancer Cell*, 7:17–23, 2005.

[17] D Bonnet. Normal and leukaemic stem cells. *British Journal of Haematology*, 130:469–479, 2005.

[18] DM Bortz and PW Nelson. Sensitivity analysis of a nonlinear lumped parameter model of hiv infection dynamics. *Bulletin of Mathematical Biology*, 66:1009–1026, 2004.

[19] AM Buckle, R Mottram, A Pierce, GS Lucas, N Russell, JA Miyan, and AD Whetton. The effect of bcr-abl protein tyrosine kinase on maturation and proliferation of primitive hematopoietic cells. *Molecular Medicine*, 6:892–902, 2000.

[20] E Caussinus and C Gonzalez. Induction of tumor growth by altered stem-cell asymmetric division in *Drosophila melanogaster*. *Nature Genetics*, 37:1125–1129, 2005.

[21] SH Cheshier, SJ Morrison, X Liao, and IL Weissman. *In vivo* proliferation and cell cycle kinetics of long-term self-renewing hematopoietic stem cells. *Proceedings of the National Academy of Science*, 96:3120–3125, 1999.

[22] MF Clarke. Chronic myelogenous leukemia – identifying the hydra's heads. *New England Journal of Medicine*, 351:634–636, 2004.

[23] MF Clarke. A self-renewal assay for cancer stem cells. *Cancer Chemotherapy and Pharmacology*, 56 (Supp I):s64–s68, 2005.

[24] C Colijn and MC Mackey. A mathematical model of hematopoiesis – i. periodic chronic myelogenous leukemia. *Journal of Theoretical Biology*, 237:117–132, 2005.

[25] MJ Conboy, AO Karasov, and TA Rando. High incidence of non-random template strand segregation and asymmetric fate determination in dividing stem cells and their progeny. *PLoS Biology*, 5:1120–1126, 2007.

[26] J Cortes, S O'Brien, and H Kantarjian. Discontinuation of imatinib therapy after achieving a molecular response. *Blood*, 104:2204–2205, 2004.

[27] D Cortez, G Reuther, and AM Pendergrast. The bcr-abl tyrosine kinase activates mitogenic signaling pathways and stiimulates g1-to-s phase transition in hematopoietic stem cells. *Oncogene*, 15:2333–2342, 1997.

[28] DL Crowe, B Parsa, and UK Sinha. Relationships between stem cells and cancer stem cells (Review). *Histology and Histopathology*, 19:505–509, 2004.

[29] M Dean, T Fojo, and S Bates. Tumour stem cells and drug resistance. *Nature Reviews Cancer*, 5:275–284, 2005.

[30] GD Demetri and JD Griffin. Granulocyte colony-stimulating factor and its receptor. *Blood*, 78:2791–2808, 1991.

[31] D Dingli and F Michor. Successful therapy must eradicate cancer stem cells. *Stem Cells*, 2006:2603–2610, 2006.

[32] J Domen. The role of apoptosis in regulating hematopoietic stem cell numbers. *Apoptosis*, 2001:239–252, 2001.

[33] J Domen, SH Cheshier, and IL Weissman. The role of apoptosis in the regulation of hematopoietic stem cells: overexpression of bcl-2 increases both their number and repopulation potential. *Journal of Experimental Medicine*, 191:253–263, 2000.

[34] J Domen and IL Weissman. Self-renewal, differentiation or death: regulation and manipulation of hematopoietic stem cell fate. *Molecular Medicine Today*, 5:201–208, 1999.

[35] J Domen and IL Weissman. Hematopoietic stem cells need two signals to prevent apoptosis; bcl-2 can provide one of these, kitl/c-kit signaling the other. *Journal of Experimental Medicine*, 192:1707–1718, 2000.

[36] L Edelstein-Keshet, A Israel, and P Lansdorp. Modelling perspectives on aging: can mathematics help us stay young? *Journal of Theoretical Biology*, 213:509–525, 2001.

[37] EA Eklund. The role of *HOX* genes in malignant myeloid disease. *Current Opinion in Hematology*, 14:85–89, 2007.

[38] H Enderling, MAJ Chaplain, ARA Anderson, and JS Vaidya. A mathematical model of breast cancer development, local treatment and recurrence. *Journal of Theoretical Biology*, 246:245–259, 2007.

[39] TM Fliedner, D Graessle, C Paulsen, and K Reimers. Structure and function of bone marrow hemopoiesis: mechanisms of response to ionizing radiation exposure. *Cancer Biotherapy and Radiopharmaceuticals*, 17:405–426, 2002.

[40] CM Flynn and DS Kaufman. Donor cell leukemia: insight into cancer stem cells and the stem cell niche. *Blood*, 109:2688–2692, 2007.

[41] F Frassoni, M Podestà, and G Piaggio. Normal and leukaemic haematopoiesis in bone marrow and peripheral blood of patients with chronic myeloid leukaemia. *Baillière's Clinical Haematology*, 12:199–208, 1999.

[42] E Fuchs, T Tumbar, and G Guasch. Socializing with the neighbors: stem cells and their niche (Review). *Cell*, 116:769–778, 2004.

[43] U Galderisi, M Cippollaro, and A Giordano. Stem cells and brain cancer. *Cell Death and Differentiation*, pages 1–7, 2005.

[44] R Ganguly and IK Puri. Mathematical model for the cancer stem cell hypothesis. *Cell Proliferation*, 39:3–14, 2006.

[45] G Garcia-Manero, S Faderl, S O'Brien, J Cortes, M Talpaz, and HM Kantarjian. Chronic myelogenous leukemia: a review and update of therapeutic strategies. *Cancer*, 98:437–457, 2003.

[46] DG Gilliland, CT Jordan, and CA Felix. The molecular basis of leukemia. *Hematology*, pages 80–97, 2004.

[47] JM Goldman and JV Melo. Chronic myeloid leukemia – advances in biology and new approaches to treatment. *The New England Journal of Medicine*, 349:1451–1464, 2003.

[48] MY Gordon, F Dazzi, SB Marley, JL Lewis, D Nguyen, and FH Grand. Cell biology of cml cells. *Leukemia*, 13:S65–S71, 1999.

[49] K Haapala, T Kuukasjarvi, E Hyytinen, I Rantala, HJ Helin, and PA Koivisto. Androgen receptor amplification is associated with increased cell proliferation in prostate cancer. *Human Pathology*, 38:474–478, 2007.

[50] D Hanahan and RA Weinberg. The hallmarks of cancer (Review). *Cell*, 100:57–70, 2000.

[51] K Hardy and J Stark. Mathematical models of the balance between apoptosis and proliferation. *Apoptosis*, 7:373–381, 2002.

[52] WJ Harrison. The total cellularity of the bone marrow in man. *Journal of Clinical Pathology*, 15:254–259, 1962.

[53] Y He, OE Franco, M Jiang, K Williams, HD Love, IM Coleman, PS Nelson, and SW Hayward. Tissue-specific consequences of cyclin d1 overexpression in prostate cancer progression. *Cancer Resesarch*, 67:8188–8197, 2007.

[54] RP Hill. Identifying cancer stem cells in solid tumors: case not proven. *Cancer Research*, 66:1891–1896, 2006.

[55] MS Holtz and R Bhatia. Effect of imatinib mesylate on chronic myelogenous leukemia hematopoietic progenitor cells. *Leukemia and Lymphoma*, 45:237–245, 2004.

[56] KJ Hope, L Jin, and JE Dick. Human acute myeloid leukemia stem cells. *Archives of Medical Research*, 34:507–514, 2003.

[57] BJP Huntly and DG Gilliland. Leukaemia stem cells and the evolution of cancer-stem-cell research. *Nature Reviews Cancer*, 5:311–321, 2005.

[58] AL Jackson and LA Loeb. The mutation rate and cancer. *Genetics*, 148:1483–1490, 1998.

[59] S Jaiswal, D Traver, T Miyamoto, K Akashi, E Lagasse, and IL Weissman. Expression of bcr/abl and bcl-2 in myeloid progenitors leads to myeloid leukemias. *Proceedings of the National Academy of Science*, 100:10002–10007, 2003.

[60] CHM Jamieson, LE Ailles, SJ Dylla, M Muijtjens, C Jones, JL Zehnder, J Gotlib, K Li, MG Manz, A Keatling, CL Sawyers, and IL Weissman. Granulocyte-macrophage progenitors as candidate leukemic stem cells in blast-crisis cml. *The New England Journal of Medicine*, 351:657–667, 2004.

[61] CA Jr. Janeway, P Travers, M Walport, and MJ Shlomchik. *Immunobiology*. Garland Science, sixth edition, 2005.

[62] CT Jordan and ML Guzman. Mechanisms controlling pathogenesis and survival of leukemic stem cells. *Oncogene*, 23:7178–7187, 2004.

[63] NM Joseph and SJ Morrison. Toward an understanding of the physiological function of mammalian stem cells. *Developmental Cell*, 9:173–183, 2005.

[64] P Karpowicz, D Morshead, A Kam, E Jervis, J Ramunas, V Cheng, and D van der Kooy. Support for the immortal strand hypothesis: neural stem cells partition dna asymmetrically *in vitro*. *The Journal of Cell Biology*, 170:721–732, 2005.

[65] MJ Kiel, S He, R Ashkenazi, SN Gentry, M Teta, JA Kushner, TL Jackson, and SJ Morrison. Haematopoietic stem cells do not asymmetrically segregate chromosomes or retain brdu. *Nature*, 449:238–242, 2007.

[66] MJ Kiel and SJ Morrison. Uncertainty in the niches that maintain haematopoietic stems cells. *Nature Reviews Immunology*, 8:290–301, 2008.

[67] MJ Kiel, GL Radice, and SJ Morrison. Lack of evidence that hematopoietic stem cells depend on n-cadherin-mediated adhesion to osteoblasts for their maintenance. *Cell Stem Cell*, 1:204–217, 2007.

[68] MJ Kiel, OH Yilmaz, T Iwashita, OH Yilmaz, C Terhorst, and SJ Morrison. Slam family receptors distinguish hematopoietic stem and progenitor cells and reveal endothelial niches for stem cells. *Cell*, 121:1109–1121, 2005.

[69] NL Komarova and D Wodarz. Evolutionary dynamics of mutator phenotypes in cancer: implications for chemotherapy. *Cancer Research*, 63:6635–6642, 2003.

[70] HG Kopp, ST Avecilla, AT Hooper, and S Rafii. The bone marrow vascular niche: home of hsc differentiation and mobilization. *Physiology*, 20:349–356, 2005.

[71] T Lapidot, A Dar, and O Kollet. How do stem cells find their way home? *Blood*, 106:1901–1910, 2005.

[72] L Laterveer, IJ Lindley, MS Hamilton, R Willemze, and WE Fibbe. Interleukin-8 induces rapid mobilization of hematopoietic stem cells with radioprotective capacity and long-term myelolymphoid repopulating ability. *Blood*, 85:2269–2275, 1995.

[73] Leukemia and Lymphoma Society. Chronic myelogenous leukemia, June 2008. www.leukemia-lymphoma.org.

[74] L Li and WB Neaves. Normal stem cells and cancer stem cells: the niche matters. *Cancer Research*, 66:4553–4557, 2006.

[75] L Li and T Xie. Stem cell niche: structure and function. *Annual Review of Cell and Developmental Biology*, 21:605–631, 2005.

[76] Z Li and L Li. Understanding hematopoietic stem-cell microenvironments. *Trends in Biochemical Sciences*, 31:589–595, 2006.

[77] MC Mackey. Unified hypothesis for the origin of aplastic anemia and periodic hematopoiesis. *Blood*, 51:941–956, 1978.

[78] MC Mackey. Cell kinetic status of haematopoietic stem cells. *Cell Proliferation*, 34:71–83, 2001.

[79] N Mahmud, SM Devine, KP Weller, S Parmar, C Sturgeon, MC Nelson, T Hewett, and R Hoffman. The relative quiescence of hematopoietic stem cells in nonhuman primates. *Blood*, 97:3061–3068, 2001.

[80] WJ McKinstry, CL Li, JEJ Rasko, NA Nicola, GR Johnson, and D Metcalf. Cytokine receptor expression on hematopoietic stem and progenitor cells. *Blood*, 89:65–71, 1997.

[81] JR Merok, JA Lansita, JR Tunstead, and JL Sherley. Cosegregation of chromosomes containing immortal dna strands in cells that cycle with asymmetric stem cell kinetics. *Cancer Research*, 62:6791–6795, 2002.

[82] F Michor. Chronic myeloid leukemia blast crisis arises from progenitors. *Stem Cells*, 25:1114–1118, 2007.

[83] F Michor, TP Hughes, Y Iwasa, S Branford, NP Shah, CL Sawyers, and MA Nowak. Dynamics of chronic myeloid leukaemia. *Nature*, 435:1267–1270, 2005.

[84] F Michor, I Iwasa, H Rajagopalan, C Lengauer, and MA Nowak. Linear model of colon cancer initiation. *Cell Cycle*, 3:358–362, 2004.

[85] F Michor, Y Iwasa, C Lengauer, and MA Nowak. Dynamics of colorectal cancer. *Seminars in Cancer Biology*, 15:484–493, 2005.

[86] R Möhle and L Kanz. Hematopoietic growth factors for hematopoietic stem cell mobilization and expansion. *Seminars in Hematology*, 44:193–202, 2007.

[87] KA Moore. Recent advances in defining the hematopoietic stem cell niche. *Current Opinion in Hematology*, 11:107–111, 2004.

[88] MAS Moore, KY Chung, M Plasilova, JJ Schuringa, JH Shieh, P Zhou, and G Morrone. Nup98 dysregulation in myeloid leukemogenesis. *Annals of the New York Academy of Sciences*, 1106:114–142, 2007.

[89] SJ Morrison and J Kimble. Asymmetric and symmetric stem-cell divisions in development and cancer. *Nature*, 441:1068–1074, 2006.

[90] SJ Morrison, NM Shah, and DJ Anderson. Regulatory mechanisms in stem cell biology. *Cell*, 88:287–298, 1997.

[91] SJ Morrison, M Uchida, and IL Weissman. The biology of hematopoietic stem cells. *Annual Review of Cell and Developmental Biology*, 11:35–71, 1995.

[92] JD Murray. *Mathematical Biology*. Springer, second edition, 1989.

[93] National Cancer Institute. Surveillance epidemiology and end results, June 2008. http://seer.cancer.gov/statfacts/.

[94] MJ Nemeth and DM Bodine. Regulation of hematopoiesis and the hematopoietic stem cell niche by wnt signaling pathways. *Cell Research*, 17:746–758, 2007.

[95] G Nikolova, B Strilic, and E Lammert. The vascular niche and its basement membrane. *Trends in Cell Biology*, 17:19–25, 2006.

[96] MA Nowak, F Michor, and Y Iwasa. The linear process of somatic evolution. *Proceedings of the National Academy of Science*, 100:14966–14969, 2003.

[97] B Ohlstein, T Kai, E Decotto, and A Spradling. The stem cell niche: theme and variations. *Current Opinion in Cell Biology*, 16:693–699, 2004.

[98] A O'Neill and DV Schaffer. The biology and engineering of stem-cell control. *Biotechnology and Applied Biochemistry*, 40:5–16, 2004.

[99] C Orelio and E Dzierzak. Bcl-2 expression and apoptosis in the regulation of hematopoietic stem cells. *Leukemia and Lymphoma*, 48:16–24, 2007.

[100] I Ostby, HB Benestad, and P Grottum. Mathematical modeling of human granulopoiesis: the possible importance of regulated apoptosis. *Mathematical Biosciences*, 186:1–27, 2003.

[101] OG Ottmann, A Ganser, G Seipelt, M Eder, G Schulz, and D Hoelzer. Effects of recombinant human interleukin-3 on human hematopoietic progenitor and precursor cells in vivo. *Blood*, pages 1494–1502, 1990.

[102] R Pardal, MF Clarke, and SJ Morrison. Applying the principles of stem-cell biology to cancer. *Nature Reviews Cancer*, 3:895–902, 2003.

[103] E Passagué, CHM Jamieson, LE Ailles, and IL Weissman. Normal and leukemic hematopoiesis: are leukemias a stem cell disorder or a reacquisition of stem cell characteristics? *Proceedings of the National Academy of Science*, 100:11842–11849, 2003.

[104] E Passagué, AJ Wagers, S Giurato, WC Anderson, and IL Weissman. Global analysis of proliferation and cell cycle gene expression in the regulation of hematopoietic stem and progenitor cell fates. *Journal of Experimental Medicine*, 202:1599–1611, 2005.

[105] K Polyak and WC Hahn. Roots and stems: stem cells in cancer. *Nature Medicine*, 12:296–300, 2006.

[106] CS Potten, WJ Hume, P Reid, and J Cairns. The segregation of dna in epithelial stem cells. *Cell*, 15:899–906, 1978.

[107] L Rambhatla, S Ram-Mohan, JJ Cheng, and JL Sherley. Immortal dna strand cosegregation requires p53/impdh-dependent asymmetric self-renewal associated with adult stem cells. *Cancer Research*, 65:3155–3161, 2005.

[108] FM Rattis, C Voermans, and T Reya. Wnt signaling in the stem cell niche. *Current Opinion in Hematology*, 11:88–94, 2004.

[109] P Reizenstein. Growth of normal and malignant bone marrow cells. *Leukemia Research*, 14:679–681, 1990.

[110] T Reya, SJ Morrison, MF Clarke, and IL Weissman. Stem cells, cancer, and cancer stem cells. *Nature*, 414:105–111, 2001.

[111] NJ Savill. Mathematical models of hierarchically structured cell populations under equilibrium with application to the epidermis. *Cell Proliferation*, 2003:1–26, 2003.

[112] CL Sawyers. Chronic myeloid leukemia. *The New England Journal of Medicine*, 340:1330–1340, 1999.

[113] BE Shepherd, h Kiem, PM Lansdorp, CE Dunbar, G Aubert, A LaRochelle, R Seggewiss, P Guttorp, and JL Abkowitz. Hematopoietic stem-cell behavior in nonhuman primates. *Blood*, 110:1806–1813, 2007.

[114] V Shinin, B Gayraud-Morel, D Gomèz, and S Tajbakhsh. Asymmetric division and cosegregation of template dna strands in adult muscle satellite cells. *Nature Cell Biology*, 8:677–687, 2006.

[115] GH Smith. Label-retaining epithelial cells in mouse mammary gland divide asymmetrically and retain their template dna strands. *Development*, 132:681–687, 2005.

[116] SL Spencer, MJ Berryman, JA García, and D Abbott. An ordinary differential equation model for the multistep transformation to cancer. *Journal of Theoretical Biology*, 231:515–524, 2004.

[117] E Stochat, SM Stemmer, and L Segel. Human hematopoiesis in steady state and following intense perturbations. *Bulletin of Mathematical Biology*, 64:861–886, 2002.

[118] IPM Tomlinson and WF Bodmer. Failure of programmed cell death and differentiation as causes of tumors: Some simple mathematical models. *Proceedings of the National Academy of Science*, 92:11130–11134, 1995.

[119] C Udomsakdi, CJ Eaves, B Swolin, DS Reid, MJ Barnett, and AJ Eaves. Rapid decline of chronic myeloid leukemic cells in long-term culture due to a defect at the leukemic stem cell level. *Proceedings of the National Academy of Science*, 89:6192–6196, 1992.

[120] JW Vardiman, NL Harris, and Brunning RD. The world health organization (who) classification of the myeloid neoplasms. *Blood*, 100:2292–2302, 2002.

[121] I Voloshyna, A Besana, M Castillo, T Matos, IB Weinstein, M Mansukhani, RB Robinson, C Cordon-Cardo, and SJ Feinmark. Trek-1 is a novel molecular target in prostate cancer. *Cancer Research*, 68:1197–2003, 2008.

[122] M Warmuth, S Danhauser-Riedl, and M Hallek. Molecular pathogenesis of chronic myeloid leukemia: implications for new therapeutic strategies. *Annals of Hematology*, 78:49–64, 1999.

[123] MS Wicha, S Liu, and G Dontu. Cancer stem cells: an old idea–a paradigm shift. *Cancer Research*, 66:1883–1890, 2006.

[124] D Wodarz. Effect of stem cell turnover rates on protection against cancer and aging. *Journal of Theoretical Biology*, 245:449–458, 2007.

[125] M Wu, HY Kwon, F Rattis, J Blum, C Zhao, R Ashkenazi, TL Jackson, N Gaiano, T Oliver, and T Reya. Imaging hematopoietic precursor division in real time. *Cell Stem Cell*, 1:541–554, 2007.

[126] T Yin and L Li. The stem cell niches in bone. *Journal of Clinical Investigation*, 116:1195–1201, 2006.